Multi-terminal HVDC Grids: Control Strategies for Ancillary Services Provision in Interconnected Transmission Systems with Offshore Wind Farms

Bernardo Marques Amaral Silva

PhD Program in Sustainable Energy Systems - MIT/Portugal

Faculty of Engineering of University of Porto

Supervisor: Dr. Hélder Filipe Duarte Leite

Co-supervisor: Dr. Carlos Coelho Leal Monteiro Moreira

Thesis submitted to the Faculty of Engineering of University of Porto in partial fulfilment of the requirements for the degree

PhilosophiæDoctor (PhD)

December 2013

This work was supported by FCT Fundação para a Ciência e a Tecnologia (Portuguese Foundation for Science and Technology) under the grant SFRH/BD/61600/2009 (co-funded by the European Social Fund through the POPH program), by the ERDF European Regional Development Fund through the COMPETE Program (operational program for competitiveness) and by National Funds through the FCT within project COMUTE-DC: Control and Operation of Offshore Multi-Terminal DC grids, PTDC/EEI-EEL/2053/2012 and by INESCPorto-Laboratório Associado.

Abstract

Wind Energy (WE) has largely contributed to the de-carbonisation of the energy sector and consequently to the definition of the European Commission (EC) targets on renewable-based electricity generation. During the last decade, massive investment has culminated in the substantial installation of Wind Farms (WF). Moreover, the ambitious plans for increasing these targets on renewable-based electricity generation demand the deployment of more WF. To tackle this challenge, a large amount of offshore WF is envisioned to be built during the next decade. From the technical perspective, the adoption of HVDC becomes crucial to allow the installation far from coast and large power WF. Most recent plans point for the adoption of DC-grids as the mean of interconnecting offshore WF and also inter-AC area, allowing further renewable integration and the development of a common European electricity market.

This thesis presents control strategies based on a communication-free framework that were developed in order to allow DC grid-connected offshore WF and interconnected AC areas on providing advanced system services such as: a) primary frequency regulation, b) inertial behaviour emulation, c) Fault Ride-through (FRT) capability. The association of the control strategies for primary frequency regulation and FRT has culminated in the design of the coordinated approach for increasing the DC grid reliability by allowing its operation following the disconnection of one onshore HVDC converter. The presented control strategies rely on local controllers to be housed in offshore and onshore High Voltage Direct Current - Voltage Source Converter (HVDC-VSC) as well as on WT. The local controllers operate autonomously providing the adequate regulation based on quantity variations.

The main outcomes of this thesis consist on the development of communication-free control strategies for MTDC grid with offshore WF participating in the mainland systems frequency regulation, the capability of remaining connected to the mainland grids during voltage sags, thus mitigating the problems resulting from the disconnection of a large amount of wind power. Finally, a control scheme to guarantee the operation of the DC grid following the disconnection of one evacuation node (onshore HVDC-VSC) is presented.

Resumo

A Energia Eólica contribuiu largamente para o descarbonização do setor de energia no cumprimento das metas para geração de eletricidade com base renovável. Durante a última década, o investimento avultado culminou na instalação substancial de Parques Eólicos (PE). Para responder às novas metas, espera-se uma contribuição proveniente de parques *offshore* (no mar). Do ponto de vista técnico, a adoção de ligações em corrente contínua de alta tensão (CCAT) torna-se crucial para permitir a instalação de PE de grande potência e longe da costa. Planos mais recentes apontam para a adoção de redes em corrente contínua como forma de interligar os parques eólicos no mar e também para promover a interligação entre áreas de corrente alternada continental, permitindo uma maior integração de energia renovável e o desenvolvimento de um mercado Europeu comum de energia elétrica.

Esta tese apresenta estratégias de controlo desenvolvidas num contexto sem comunicações para permitir o fornecimento de serviços de suporte às redes AC em terra, por parte do PE *offshore*, através da ligação em CCAT. As estratégias de controlo desenvolvidas visam o fornecimento de: a) regulação primária de frequência, b) emulação de inércia, c) capacidade de sobrevivência a cavas de tensão. A associação das estratégias de controlo culminou na conceção da abordagem coordenada, permitindo seu funcionamento após a desligação de um conversor CCAT em terra. As estratégias apresentadas são passíveis de serem implementadas em controladores locais, instalados nos conversores CCAT, do tipo fonte de tensão e ao nível dos aerogeradores, permitindo a operação autónoma.

Os principais resultados desta tese consistem no desenvolvimento e avaliação de estratégias de controlo sem necessidade de comunicações para que redes de corrente contínua, multi-terminal com presença PE *offshore*, possam participar na regulação de frequência dos sistemas continentais, na capacidade de permanecer ligado à rede continental durante cavas de tensão, mitigando os problemas resultantes da desligação de uma grande quantidade de energia eólica. Finalmente é apresentado um esquema de controlo para garantir a operação da rede de corrente contínua após a desligação de um nó de evacuação (conversores CCAT interligado a uma rede continental).

Acknowledgements

During the development of this thesis I have received the contribution ans support that I would like to acknowledge here. First of all, I would like to acknowledge my host institution, INESCPorto for providing the means to develop my work and give always support to disseminate the achievements of this thesis in international conferences. I must also acknowledge the person that introduced me to INESCPorto, the Prof. João Abel Peças Lopes who believed in my work and potential to perform this PhD research.

The amazing and friendly atmosphere that helped me on the development of this thesis is of responsibility of Power Systems Unit (USE) leader, Prof. Manuel Matos and also of my colleagues: Luís Seca, Filipe Joel Soares, André Madureira, Pedro Almeida, Jorge Pereira, Ricardo Ferreira, Miguel Heleno, Iván Franschin, David Rua, Clara Gouveia, Miguel Miranda, Pedro Barbeiro, Justino Rodrigues, Jorge Alves, Rute Miriam Ferreira and Paula Castro.

I would like to specially gratify the Prof. Carlos Moreira, Power System Unit leader of Smart Grids Research Area and the responsible for the project TWENTIES and COMUTE-DC. His help and guidance were crucial to the accomplishment of this theses. His support and motivation have helped me on persisting the research and development even during the less fruitful phases.

A special thanks to my classmates Ricardo Bessa and Leonardo Bremermann for the friendship and delightful discussions (not always about work), during this four-year period.

To my family, my mother Norvinda, my step father Flórido, my brother Guilherme and my grand-mother Maria Rosa, I would like to thank the understanding and support and also apologize for the moments of absence during this four year period. I would also like to thank to my family living in Brazil, Lúcia, Manuel, Adriana e Raphael for the hospitality and support during the time I spent there to disseminate part this thesis work in a conference.

To my beloved wife Sara, I would like to thank a lot for all the affection, companionship and support and also apologize the absence and stress during this four-year period.

At last but not least, I would like to thank to Prof. Hélder Filipe Duarte Leite, my PhD supervisor for inviting me to this challenge and for sticking with me during the whole process. His wise words gave me motivation during the research and writing phase.

To the memory of my father William and
my grandfather Adriano.

"I have not failed. I've just found 10,000 ways that won't work."
Thomas A. Edison

Contents

List of Figures

LIST OF FIGURES

List of Tables

Glossary

AC Alternate Current

AGC Automatic Generation Control

CSP Concentrated Solar Power

DFIG Doubly-fed Induction Generator

DVR Dynamic Voltage Restorer

ENTSO-E European Network of Transmission System Operators for Electricity

EU European Union

EUNEMA Europe, Middle East and North Africa

FACTS Flexible AC Transmission System

FRT Fault Ride-through

FSIG Fixed Speed Induction Generator

GHG Green House Gases

GSC Grid-side Converter

HVAC High Voltage Alternate Current

HVDC High Voltage Direct Current

IGBT Insulated-gate Bipolar Transistor

KE Kinetic Energy

LCC Line Commuted Converter

LVRT Low Voltage Ride-through

MMC Modular Multi-level Converter

MSC Machine-side Converter

MTDC Multi-terminal Direct Current

OVPS Over Voltage Protection System

PI Proportional-Integral

PMSG Permanent Magnet Synchronous Generator

RES Renewable Energy System

RES-E Renewable Energy Source in Electricity

RSC Rotor-side Converter

SO System Operator

STATCOM Static Synchronous Compensator

TMC Transient Control Mode

TMF Temporary Minimum Frequency

TSO Transmission System Operator

UK United Kingdom

VSC Voltage Source Converter

WF Wind Farm

WT Wind Turbine

WTG Wind Turbine Generator

1

Introduction

1.1 Background and Thesis Motivation

The modernization of electrical power systems is walking toward the adoption of endogenous energy resources for electricity generation. The wherefores for that approach are based on economical and environmental aspects. Strategically, it is necessary to create alternatives to walk in the direction of external energy independence (namely from oil gas and coal suppliers) and to reduce the Green House Gases (GHG) emissions in the electric power sector. The recent statistics from EREC (see Figure 1.1), the European Union is progressing towards the imposed goals of 20% for renewable-based electricity generation, also called as Renewable Energy Source in Electricity (RES-E).

However, the goal of 20% of renewables share in electricity generation, first proposed by 2008 European Commission Climate and Energy Package, has been raised to 30% [14]. To attain such ambitious target, an increment in the adoption of carbon-free electric energy resources must be considered by the EU-member countries in the next decade. In continuation, the EU Energy Roadmap 2050, envisions *"A secure, competitive and fully de-carbonised power sector"* with specific targets of 54% to 68% CO_2 reduction by 2030 increasing to 93% to 99% in 2050 [15]. Regarding the energy framework, wind power has been a strong resource to comply with the renewable energy share in electricity generation [1].

According to the results presented in Figure 1.2, it is expected that by 2020 wind energy together with hydro energy are going to be the most used RES in the electric-

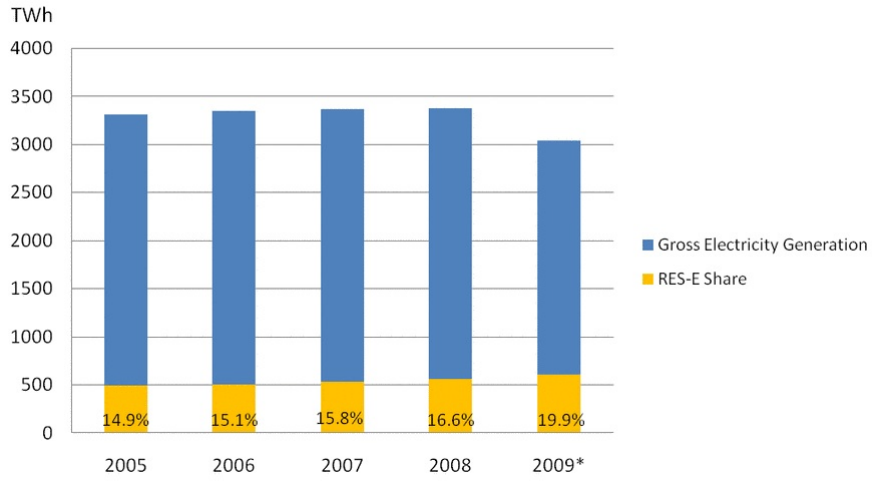

Figure 1.1: RES-E share in gross electricity generation in Europe [1]

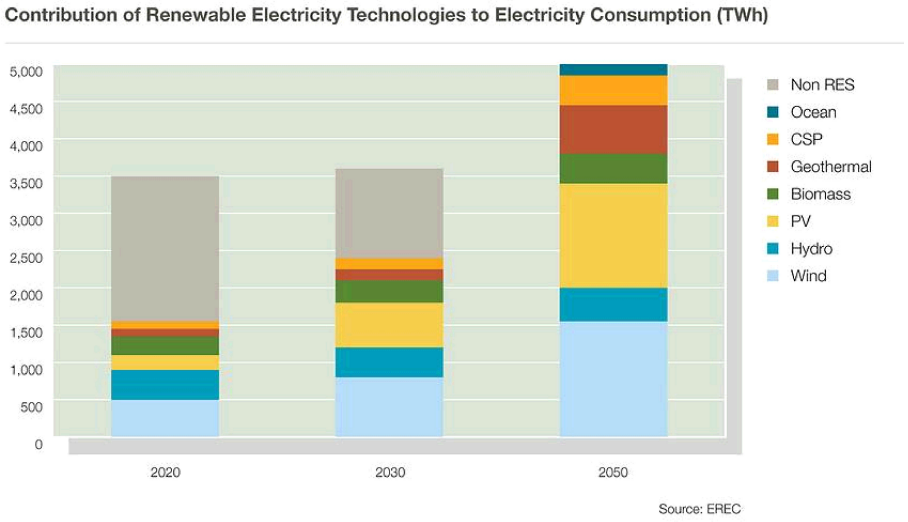

Figure 1.2: Renewable technologies contribution electricity generation in Europe [1]

ity mix. By 2030, it is predicted that wind power will assume the biggest share on what regards RES contribution and by 2050, besides maintaining the biggest share, wind power will provide a significant contribution to the electricity mix considering the non-RES power plant (fossil fuel-based power) should not be adopted for electricity generation.

The envisioned wind energy contribution, can only be attained with the adop-

tion of offshore Wind Farms (WF). Aware of that necessity, European Commission has published a communication [16] defining a set of action to foster offshore wind integration. A key motivation topic for this thesis is already mentioned in this document as a challenge on *"Dealing with bottlenecks and power balancing in the onshore electricity grids"* [16].

To overcome the costs associated to the offshore WF infrastructure, the European Network of Transmission System Operators for Electricity (ENTSO-E) [17], envision an electrical infrastructure - the offshore grid - which should allow not only the connection of offshore Wind Power but also increase the flexibility of operation of interconnected mainland countries through the creation of additional channels for active power flows thus, allowing further electricity market expansion. That way, the costs of deployment of connection infrastructures should be shared among the stakeholders (offshore WF owners and electricity markets).

The predicted massive offshore Wind power integration through HVDC technology as well as the inter-AC onshore areas power exchange through the DC grid infrastructure, is potentially dangerous from the AC mainland grid dynamic security perspective. The main reason for that is related to the fact that offshore WF connected through the HVDC technology are de-coupled from the AC grid in terms of voltage and frequency. So, they are not able to sense AC onshore grid disturbances and consequently are unable to provide adequate response. Some studies have investigated the possibility of equipping offshore WF with point-to-point fast communication channels to transmit onshore grid AC voltage and frequency measurements. However, the transposition of this concept to a DC grid becomes challenging due to the number of offshore WF and AC onshore grid connections requiring several point-to-point connections (between all the intervenients).

On contrast, the work developed in this thesis proposes the adoption of local controllers, to be housed in the HVDC-VSC. The overall control scheme has been designed to operate in a cascade philosophy, using the DC grid as the mean of artificially communicating the AC onshore grid voltage or frequency disturbance.

The developed control schemes should allow the offshore WF and the DC grid

to autonomously provide support services to the AC onshore systems, assuring no deterioration of the dynamic security level.

1.2 Objectives of the Thesis

The work conducted on this thesis intended to answer a set of research questions formulated on the early stage of the PhD research. The research questions were:

- **RQ 1:** *What are the impacts on AC system dynamics from the integration of offshore wind power interconnected by MTDC grids?*
- **RQ 2:** *Is there the possibility of allowing offshore WF (connected through a MTDC grid) on participating in AC primary frequency control in a communication-free framework?*
- **RQ 3:** *How can the DC voltage be controlled in a MTDC with offshore incoming wind power during a mainland AC grid fault event?*

The first phase of the research has the objective of identifying barriers from an operational perspective for the deployment of offshore MTDC grids that serve as mean for interconnecting offshore wind power. This identification aimed at addressing the research question RQ 1 and was performed based on the study of the state-of-the-art publications that had already identified the major barriers for point-to-point HVDC connections. The validation of the identified barriers to the MTDC case has been performed in the process of the research, fully addressing the RQ 1.

The second phase consisted on developing a dynamic simulation tool to evaluate the behaviour and validate the identified barriers for the MTDC grid with offshore incoming power. The development of this simulation platform was crucial to the thesis advancement, since it also allowed to assess the performance of the proposed control schemes and to provide answers to RQ 2 and RQ 3.

The third phase consisted on developing control schemes in a communication-free framework, to autonomously deal with specifics challenges previously identified. These challenges consisted on overcoming the lack of primary frequency support and

inertia capability overcoming from the adoption of HVDC technology and also on the DC voltage control during mainland AC-mainland fault event and the FRT.

The ultimate contribution of this thesis is to provide means to mitigate the concerns related to the massive integration of offshore WF in AC grid dynamic security indexes and demonstrate, that in fact, the whole system can actively contribute to the enhancement of AC power system dynamic security indexes. To achieve such fulfilment appropriate control schemes were designed to endow offshore WF and the DC grid to:

- Participate in the primary frequency control;
- Emulate the inertia behaviour;
- Withstand onshore AC voltage sags, complying with the Fault Ride-through requirement;
- Remain operating after the disconnection of an onshore HVDC-VSC.

1.3 Structure of the Thesis

This thesis is divided in six chapters which are organized as follows:

Chapter 1 introduces the topic of research and the motivation of this thesis, as well as the research questions established in the early-stage of the research process. The thesis objectives, structure and the list of scientific publications that disseminates the research performed are also presented.

Chapter 2 aims at presenting the main drivers and challenges for the deployment of MTDC grids for offshore wind power interconnection. It intends to range from background overview to the state-of-the-art research work performed in the topics covered in this thesis. It is divided among wind power technologies and its integration on the power system, HVDC technology, from the first projects to current converters technology and afterwards, the HVDC used as mean of interconnecting wind power. An overview on the actual practice and advanced services requirements at onshore-level is presented to enable a further extent of some concepts to offshore

MTDC-connected WF.

In Chapter 3 the simulation platform is presented. The general considerations regarding the model development are introduced followed by the description of models adopted for each component (Wind turbine, HVDC-VSC, MTDC grid, AC system). The interaction between the models and the HVDC-VSC operational strategy are also highlighted. Finally, simulation tests are conducted to assess the performance of the developed model framework for different DC grid topologies, as well as to several combinations of HVDC-VSC control parameters.

In Chapter 4, the control strategies developed in this thesis for enabling the DC grid and offshore WF on contributing to the onshore AC system support are presented. First, it is introduced the cascaded control scheme to allow the participation of offshore WF and inter-AC frequency support. Together with the presentation of the control loops for primary frequency support, the control enhancements to allow inertia emulation provided by offshore WF are also presented. This chapter also focus on presenting strategies to control DC grid voltage during a fault event in an AC mainland grid. Fast power reduction control schemes are introduced to be located at offshore or onshore-level, allowing the DC grid to remain connected to an AC mainland system during a fault event without dangerous overvoltage development in the DC grid. Finally, a hybrid control (exploiting concepts developed for the primary frequency control and FRT provision) strategy is presented to guarantee the operation of the DC grid during the sudden disconnection of an onshore HVDC-VSC.

In Chapter 5, performance of the proposed control schemes (presented in Chapter 4) is evaluated through an extensive set of simulations. The chapter is divided concerning the major topics, being: primary frequency control, FRT provision and the associated DC voltage control and the operation of the DC grid following the disconnection of an onshore HVDC-VSC.

In Chapter 6 the main contribution of the thesis are highlighted followed by the perspectives for future work.

1.4 Contributions of the Thesis

The contributions of this thesis consisted on developing:

- A dynamic simulation platform to assess the interactions between the offshore WF, the DC grid and the AC systems. The simulation platform with re-configuration capabilities allows the simulation of a varied set of DC grid topologies with different number of offshore WF and AC mainland grid (or grids) connection points and also the development of user-defined control schemes.

- A cascaded control scheme to allow the autonomous deployment of offshore WF and inter-AC area frequency support services such as the primary frequency control and the inertia emulation.

- A set of control schemes and strategies to assure FRT complianceby not disconnecting the whole DC grid during AC-side fault events. This thesis proposes different approaches to cope with the requirements for the safe operation of the DC grid.

- A cascaded control scheme to endow the offshore WF and the DC grid to remain operating after the disconnection of one onshore HVDC-VSC (loss of active power extraction).

1.4.1 Research Projects

Part of the work developed within the framework of this thesis has been submitted as part of INESCPorto contribution in Work Package 5 of the 7^{th} Framework EU Research Project - TWENTIES.

The achievements of this thesis serve also as input to the FCT national funding project COMUTE-DC, which aims at demonstrating the proposed control strategies for providing frequency support by WF and DC grids, on a scaled-size laboratory test-rig.

1.4.2 Publications

International Journals

- Silva, B. ; Moreira, C.L. ; Seca, L. ; Phulpin, Y. ; Peças Lopes, J.A., "Provision of Inertial and Primary Frequency Control Services Using Offshore Multiterminal HVDC Networks," *Sustainable Energy, IEEE Transactions on* , vol.3, no.4, pp.800,808, Oct. 2012 doi: 10.1109/TSTE.2012.2199774

- Bessa R.J. ; Moreira, C.L. ; Silva, B. ; Matos, M., "Handling Renewable Energy Variability and Uncertainty in Power Systems Operation", *Wiley Interdisciplinary Reviews: Energy and Environment*, 2013.

- Silva, B.; Moreira, C.L.; Leite, H.; Peças Lopes, J.A., "Control Strategies for AC Fault Ride-Through in Multi-terminal HVDC Grids," *Power Delivery, Transactions on* - (*accepted for publication in September 2013*)

Conferences

- Moreira, C.L. ; Silva, B. ; Soares, F.J. ; Seca, L. ; Peças Lopes, J.A., "Inertial Control in Offshore Wind Farms Connected to AC Networks through Multiterminal HVDC grids with VSC," *CIGRÉ SYMPOSIUM - Cigré International Symposium* , Bologna, Italy, September, 2011.

- Ciapessoni, E.; Cirio, D.; Gatti, A.; Pitto, A.; Denis, A.M.; Despouys, O.; He, L.; Moreira, C.L.; Silva, B., "Dynamics and control of multi-terminal high voltage direct current networks for integration of large offshore wind parks into AC grids," *44th CIGRÉ - CIGRÉ Session 2012 (44th ed.)*, Paris, France, August, 2012.

- Silva, B.; Moreira, C.L. ; Leite,H.; Peças Lopes, J.A., "Barriers and solutions for AC low voltage fault ride-through on Multi-terminal HVDC grids," *11th WIW - 11th Wind Integration Workshop*, Lisbon, Portugal, November, 2012.

- Silva, B. ; Moreira, C.L. ; Leite, H., "Operation and control of multiterminal HVDC grids following the loss of an onshore converter," *Innovative Smart Grid Technologies Latin America (ISGT LA), 2013 IEEE PES Conference On* , vol., no., pp.1,8, 15-17 April 2013 doi: 10.1109/ISGT-LA.2013.6554464

2

Offshore Wind Generation

2.1 Introduction

This Chapter describes the most relevant research work in the topics tackled in this thesis. It gives an overview from the background to the state-of-the-art of different topics such as: wind power, wind generator technologies and its integration in electric power systems. After presenting these concepts, an introduction to wind power at offshore-level is performed. Here, the topics regarding the offshore WF point-to-point and DC grid connection are highlighted.

2.2 Wind Generation

The concept of using wind power consists on the process of transforming the kinetic energy available in the wind into another form of energy to be adopted on a given process. This concept dates back to 200 B.C. when Persian-Afghan adopted vertical-axis windmills [18]. Much later, between 1300-1875 A.C., horizontal-axis windmills were used in Netherlands mainly for water pumping applications. The first Wind Turbine (WT) for electricity generation, a 12 kW generator ,was installed in Cleveland (Ohio - USA) in 1888. In Europe, during the late stages of World War I, 25 kW generators were widespread throughout Denmark [18].
The basics of a WT for electricity generation consists on taking advantage of kinetic energy available in the wind through the use of an aerodynamic body (the WT blades), converting it into mechanical energy in a rotating axis that is further

coupled to a generator to be transformed in electric power. The aforementioned aerodynamic aspect in wind power is of extreme importance. In fact, the WT blades development was related with aeronautical propellers design. Simultaneously the concept of WT for large-scale applications was proved when a 20 kW three-bladed horizontal-axis WT was installed in Denmark in early 1960s [19].

One driver for the huge development of wind energy industry was the oil crises of 1973. Several research and development was made, aiming at finding alternative energy sources for electricity generation [20]. In the following years, WT market shifted from domestic and agricultural use (1-25kW), to grid-connected applications (50-600kW) [18]. Between 1981 and 1990 United States (US) government gave incentives for wind power development.As a result, about 16.000 WT ranging 20-350 kW were installed in California, achieving a total of 1.7 GW of installed capacity. Simultaneously, in Europe, the development of wind energy industry suffered from the lack of incentives and consequently presented a smaller growth. However, after 1990 most of the market moved to Europe.

The 1990 and 2000 decades were very important for the wind energy industry in Europe. Environmental and economic drivers together with R&D have turned Europe as the major player in the WE industry, gathering most of the wind manufacturing industry, technological advances and installed capacity in the world. The results on wind energy capacity presented by European Wind Energy Association (EWEA) in [2] are illustrated on Fig. 2.1 for the years between 1995 and 2011.

The graphic on Fig.2.1 shows that the wind power installation in Europe is exponentially growing from mid-1990s until present days. Behind this growth there are several driving factors that are going to be further discussed in the next topic.

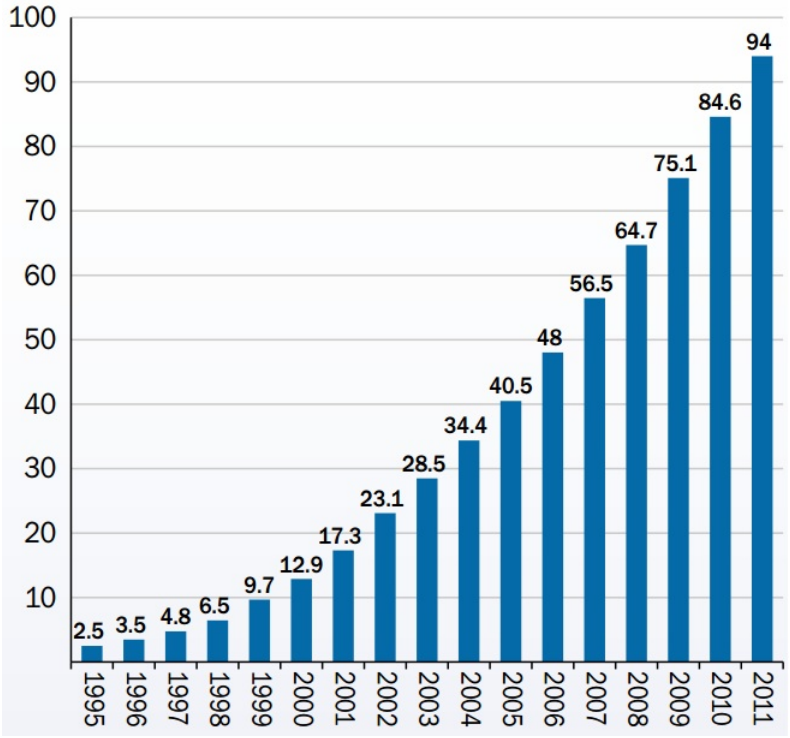

Figure 2.1: Cumulative Wind Power installations in the EU (GW) [2]

2.2.1 Drivers for Wind Power Deployment

During the last decades, there have been several drivers for the adoption of Renewable Energy Systems (RES) on electricity generation. The most significant drivers are:

- Environmental;
- Economical;
- Social.

The climate change associated with Green House Gases (GHG) emission has led Governments to change the paradigm for electricity from a purely fossil fuel-based system to a mixed system containing the exploration of endogenous resources such as the water, wind and sun. Together with the need of acting on the change of primary energy resource, it also came the need of developing technologies for electricity generation based on RES. Since hydro technology (for electricity generation) has a

quite considerable level of maturity (having been adopted for some decades), the current efforts lie now on Wind and Solar power.

The wind power industry has highly evolved over the past two decades. Associated with the industry development are the wind turbine size and increase in power capacity. According with Figure 2.2, the wind turbine size and power have been increasing. Nowadays, wind turbines have 8-10 times bigger diameter and are able to generate 14-20 times more power compared with the end 1980's and early 1990s predecessor models.

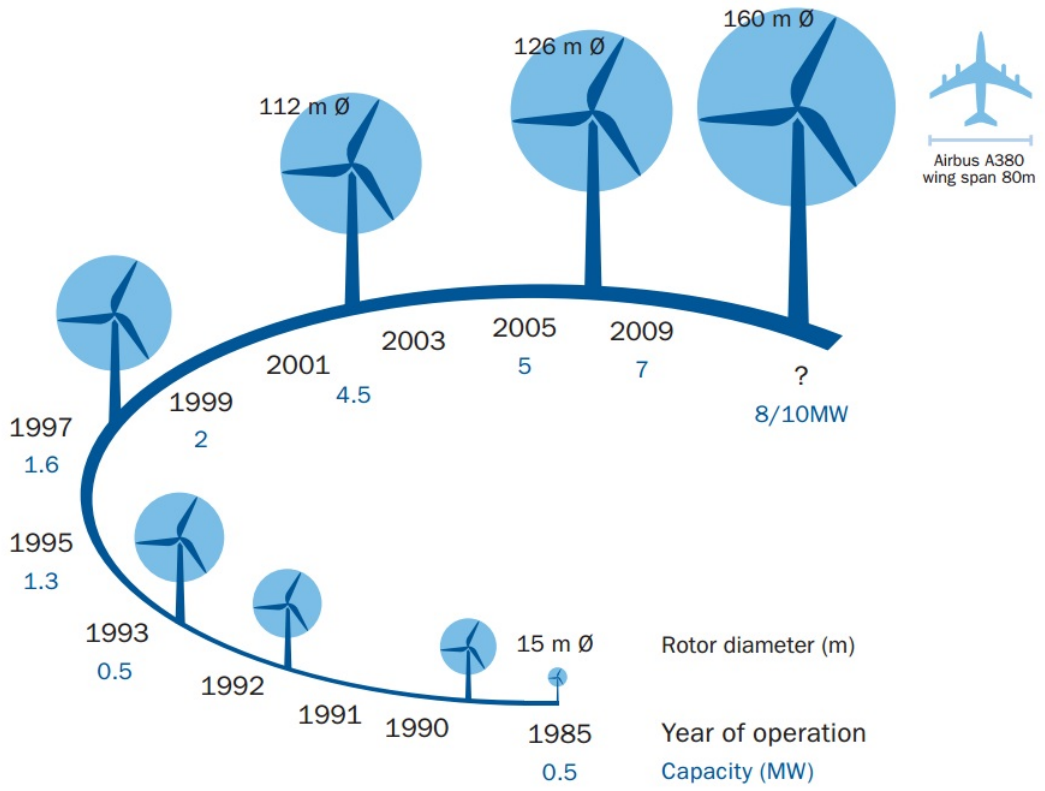

Figure 2.2: Wind turbine size and power growth [3]

The fast development and growth in the wind power industry is being supported by policies that stimulates the adoption of RES for electricity generation. European

Commission (EU) has launched the 20-20-20 program envisioning 20% of electricity based on RES, 20% of green-house gases reduction and 20% increase on energy efficiency (in comparison to 1990 values) [21]). Member state governments are responsible by complying with the targets. Thus, each country has its own stimulus scheme to foster renewable energy adoption.

2.2.2 Wind Power Integration on Power Systems

The Electrical Power System has been under constant evolution through the years. The population growth, regional development and demand increase have been putting challenges to power Systems Operators (SO) in the past decades on guaranteeing system adequacy at generation and transmission infrastructures to cope with the consumers needs. Currently, these challenges on electrical power systems still remain. However, from the end of the last century, a new era in power system is being actively growing. Nowadays, the power system generation setup (or electricity generation mix) is getting more diversified with new generation technologies emerging. Wind power is among the new renewable-based technologies. The modernization of the power systems brings additional challenges for its planning and operation. Despite bringing benefits to the environment and reducing fossil fuel dependency, the renewable-based units are responsible for increasing the challenges on the Power Systems planning and operation [22].

In the early stages of wind power integration, the WT used to have small capacity (hundreds of kW – see Fig. 2.2). Thus, the Wind Farms (WF) usually had a small installed power. Additionally, the ratio of conventional versus the wind power plants was very high. Thus, the wind power integration on the electrical power systems was not seen as a matter of concern from the operational perspective. Nevertheless, the WT size have grown (up to 1-2MW) and simultaneously the WF size (ranging from tens to hundreds of MW). Consequently, the ratio between conventional units and wind power plants decreases, bringing some concerns for the power systems operation due to the lack of inertia response and primary frequency support capabilities. Many authors have investigated the integration of wind power on power system operation and control regarding frequency-related aspects [22, 23, 24, 25, 26, 27, 28].

A detailed analysis on this topic is presented on Section 2.2.2.

Besides the frequency control, which is related with load/generation balance, another aspect that has been object of investigation consists on the capability of WF on remaining connected to the grid during fault events, performing similarly to synchronous generators. As a matter of fact, due to the small size and the technology, wind generators were originally not able to remain connected to the grid, having specific protections to trip facing voltage sags. From the power system stability perspective, losing a small amount of wind generation may not be relevant. Nevertheless, the increase of wind power penetration led that the amount of power loss aftermath a fault occurrence could be significant, leading to dynamic instability on the power systems. To avoid that, Transmission System Operators (TSO) have started requiring wind generators to comply with specific requirements, established in grid-codes. From a variety of services (that differs from country to country), the grid codes for wind power integration commonly requires to WF the Fault Ride-through (FRT) capability. The FRT is usually expressed as voltage versus time characteristic curve that a wind generator or, a wind farm should withstand connected to the grid. In addition to the voltage versus time requirement, FRT compliant WF are sometimes requested to inject reactive current according to specified values. The rationale of this requirement is to provide AC voltage support during the fault occurrence, on attempting to avoid non-FRT compliant wind farm trip. The techniques for FRT provision on the different Wind generator technologies are going to be discussed in Section 2.2.2.

Primary Frequency Control Performed by Wind Farms

In [29] authors assessed the effects of increased wind generation on system frequency and the system dynamic security following disturbances. The study allowed concluding that in high wind penetration scenarios, especially during valley hours, the system inertia and primary frequency control capability was reduced since less conventional generation units were connected to the system and consequently the ratio between plants with and without frequency control capability became very low. These specific situations were reported as problematic from the power system operation and dynamic security perspective. To overcome the encountered bottleneck,

authors have proposed that a reserve margin should be created at the wind generator (by operating the generators below the maximum extraction capability) thus, allowing a deployment of an extra active power output whenever necessary (namely when power system frequency gets bellow nominal). Nevertheless, authors have concluded that despite having additional primary reserve, the system inertia will remain reduced since wind generators are not able to naturally deploy the inertia contribution (only present on synchronous generation units). As conclusion, this work recommends the adoption of additional mechanisms such as the parallel connection of flywheel devices or the requirement for wind turbines to provide an inertia response in order not to degrade the frequency rate-of-change and to avoid curtailing wind power.

Following the previous studies, authors assessed in [23] the impacts on frequency control with different wind turbine technologies, namely Fixed Speed Induction Generator (FSIG) and Doubly-fed Induction Generators (DFIG) wind turbines. They have have concluded that FSIG were able to slightly contribute to the frequency support since a small inertia response was deployed following the loss of generation. On the other hand, DFIG-based WT could not provide any support to the system frequency control as it does not contributes with inertia response. As conclusion, authors suggested the adoption of supplementary control loop to enable the DFIG on providing the inertia response to the system.

The massive wind power integration begun to be pointed as a matter of concern in what regards the power systems security margins. SO became skeptical to operate power systems with reduced reserve margins to guarantee further wind power integration. In this context, several studies have been published with proposals for wind generators to participate on the primary frequency control [30], [31], [32], [33], [34], [35], [36]. The consensual aspects beyond the publications consist in the fact that to provide primary frequency regulation the generators should be able to increase/decrease their active power output. The concept of providing downward reserve is quite simple to understand. In the limit, it can be attained by the disconnection of some generators within a WF. However, the questions that emerged are:

- How are the WT going to provide upwards regulation?
- How is it possible to increase the power output in a wind generator?

In fact, contrary to conventional units, the WT does not have any primary energy intake regulator to increase the wind speed according to the frequency negative deviation. In fact, the wind, as natural resource, is not even controllable. Nevertheless, WT are able to extract less power than its maximum capability by taking advantage of aerodynamic effects of the blades, namely the pitch angle. Operating WT below its maximum capability (through pitch angle adjustment) creates a reserve margin that can be further deployed for primary frequency control through appropriate blades pitch regulation.

The work conducted by *Holdsworth et al.* in [37] identifies that the high level of wind power penetration resulted in the revision of TSO grid codes for the connection of large WF. The grid codes require large-MW capacity WF to assist the power system with some control services that used to be traditionally carried out by conventional synchronous generation units. Frequency control is one of the control services that is required by some grid codes. In order to provide this capability in WT, these authors have investigated additional control-loops to enhance DFIG on synthesizing inertia behaviour. In addition, the investigation of primary frequency control by de-loading the wind generators through blade pitch angle control, was carried out for both DFIG and FSIG. According to the authors, synchronous and asynchronous generators directly connected to the power system can release kinetic energy proportionally to the square of the speed and machine inertia, facing grid frequency deviation. However, according to authors, generators with electronic converters (such as the DFIG WT, between rotor and the AC grid) are not able to do so, since torque control is applied to the rotor (through electronic converters control), decoupling it from the power system frequency. This is a point of controversy since the inertia response is only naturally achieved in synchronous generators. So, the presence of electronic converter is not the reason for disabling the DFIG (or only the IG) on providing fast frequency response as inertia response. In fact, the induction generators cannot naturally provide the inertia contribution similarly to synchronous

units. Nonetheless, according to [38] proper control-loops can be designed to synthesize the inertia behaviour. The papers' results show that this approach impacts on the reduction of frequency drop following the loss of a conventional generation unit or due to a step load increase. To assess the primary frequency control capability, a full modelling of wind turbine aerodynamics and electrical generator was performed on BLADED software. The frequency control loops were implemented as an external controller. The results show that FSIG and DFIG wind turbines have the ability of providing frequency regulation services according to the requirements defined by the TSO. Regarding the contractual framework for this service provision authors suggest that appropriate agreement between the WF operator and the TSO must be set since generators are going to operate below its maximum capacity (de-loaded) to create the previously mentioned reserve margin.

An alternative study focusing on control schemes for synthetic inertia response in DFIG is presented in [4]. Authors are able to achieve inertia response contribution by extracting kinetic energy from the DFIG rotor through the control of rotor-side controller and allowing the reduction of machine speed. The main contribution of the paper consists on defining a strategy for primary frequency control by changing the electric torque set-point based on the grid frequency error. This factor impacts by changing the generator speed. Thus the idea is to transitorily increase the maximum power limit P_{max} (see Figure 2.3) by 20% in order to take advantage of the rotor's kinetic energy, emulating the inertia contribution. Authors have concluded that despite having a good contribution to frequency support, the extraction of kinetic energy to provide the inertial contribution negatively impacts on the rotors' speed (few moments aftermath the disturbance). Thus, the output power, and consequently frequency support suffers a small reduction in comparison to a pure primary frequency support scheme.

In [36], authors propose an enhanced methodology to enable DFIG wind turbines providing primary frequency support to the grid. The methodology consists on the previously mentioned de-loaded generator operation to create a reserve margin combined with control-loops implemented at DFIG power electronic converters. Due to pitch control relative slow response-time, the additional controllers cope with the

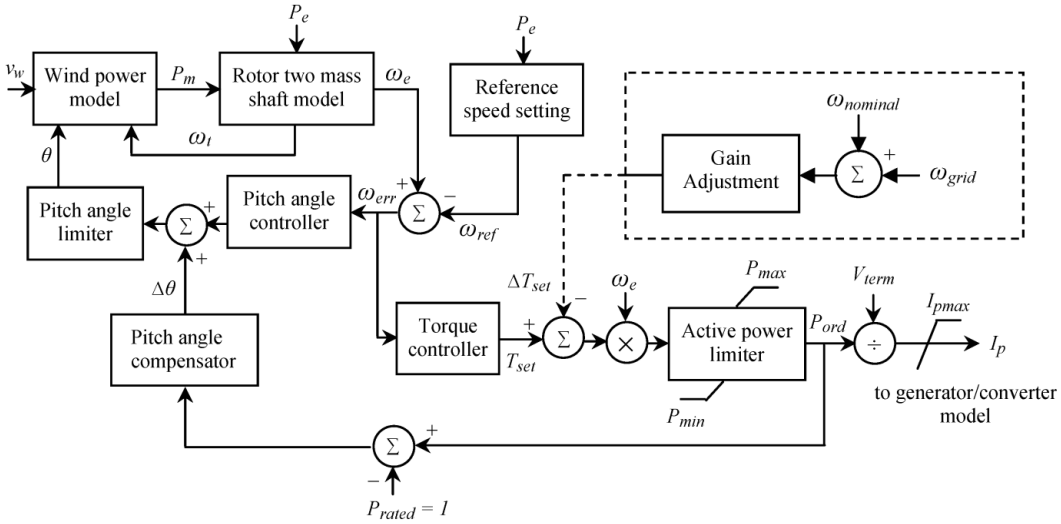

Figure 2.3: DFIG frequency control scheme adopted in [4].

moments subsequent to the frequency disturbance by controlling the active power output through the generator speed control. Then, pitch control action defines a new operational point for the DFIG. This paper presents results for a small isolated power system case where the control scheme implementation enhances the frequency behaviour of the system facing a load imbalance when compared to the case where the DFIG had not the aforementioned control scheme implemented.

The research conducted in [39] discusses the drawbacks of previously proposed methods. The paper establishes a comparison between pitch and speed-based mechanisms for the creation of the reserve margin. In fact the mechanism for the creation of power reserve margin in a wind turbine can be achieved by two approaches: (1) Changing the aerodynamic power coefficient C_p through the pitch angle adjustment or (2) increasing the generators rotational speed ω_r. Hence, by controlling one or both variables, the reserve margin can be achieved. Authors' have concluded that both approaches are effective regarding the primary frequency support. However, a robust controller design must be performed for the speed-based frequency/active power control.

According to [40], adopting under-speed de-load can be problematic since it can

result in detrimental behaviour of the wind generator regarding the load frequency control, on treating the balance within the mechanical system. Regarding the over-speed de-load technique, authors find that a 10% de-load operation can require up to 150% of over speed representing a heavy burden for DFIG converters. On the other hand, Permanent Magnet Synchronous Generator (PMSG) wind turbines, which are fully interfaced by electronic converters, do not present this kind of problem since the generator can theoretically rotate at any speed. Additionally, it is concluded that the de-loading through pitch control may present slow response. In order to enhance the frequency support authors propose to endow pitch controlled generators with inertia emulation, guaranteeing a global satisfactory response.

In [31], a methodology for endowing variable-speed wind turbines with inertia emulation and primary frequency control control capability is presented. Authors do not present any de-load technique as the previously presented communications refer. In contrast, authors' proposal is based on the kinetic energy stored at the wind turbine rotor. According to the paper, a PMSG wind turbine with integral interface converter is adopted. Thus, the generator is fully de-coupled from the grid and consequently does not respond to any grid disturbance. Nevertheless, the frequency measurement at WF grid-side terminals is provided to the generator converters' control. So, for a frequency deviation the generator controller housed in the converters will be able to generate an additional mechanical torque set-point. For emulating inertia behaviour, the letter proposes to generate an additional generator torque reference based on the frequency rate-of-change (derivative of the frequency). It is important to stress that unlike the previously presented primary frequency control approaches, in this paper authors promote a limited-time frequency support (only during 20 seconds) Simulation results show that an effective frequency support has been attained. The generator rotational speed decreased due to the extra power generation during the frequency support. This fact impacts on an active power reduction after some period, mainly in the moments subsequent to the disturbance. However, this control approach has a limited time of deployment serving only to promote some support after the disturbance. After a period (15-20 seconds), the stored kinetic energy is fully deployed and consequently the generator loses the ability of remaining on contributing to frequency support. Then the generator accelerates,

reducing the active power injection, provoking a smaller frequency decrease. The proposed control approach can be beneficial for supporting the frequency while conventional units with larger time constant do not deploy active power for providing frequency support. Additionally, has the advantage of not requiring additional pitch controller and the associated blades' angle control mechanism.

Ullah et al. in [30] quantify the capability of frequency support of a commercially available variable speed WT and make a generalization of the results for different WT technologies. Authors also stress that wind energy has an important contribution to the primary frequency support in hydro predominant systems. The primary frequency support provided by hydro units is affected by the hydraulic time delay existing between the water intake and the turbine, known as water starting time [12]. The presence of wind turbines with the capability of fast release of short-term active power presents to be beneficial for the frequency support. Authors consider this feature as an improvement in the system Temporary Minimum Frequency (TMF), which is the minimum transitory frequency value during a disturbance. The simulations results present higher improvements in the TMF (lower TMF) when the WF support is higher. Authors concluded that the inertia emulation can be attractive for small isolated systems and for providing frequency support in islanding operation.

Chang-Chien and Yin have presented in [25] a set of strategies to operate wind power in a similar manner to a conventional power plant. Authors have presented control approaches to tackle issues related with wind variability and further active power variability, by controlling the active power of a DFIG-based WF. The presented control strategies rely on rotational generator speed control and on WT pitch control. An approach of setting individual WT set-points has been addressed to attain an homogeneous WF power output. Power reserve issue has also been presented through the conventional pitch de-load techniques. Additionally, this paper provides a comprehensive analysis on development of strategies for enabling WF on participating in the secondary frequency control, responding to Automatic Generation Control (AGC) set-points. The results allowed verifying that modern WF equipped with DFIG have the flexibility of operate similarly to a conventional plant with adequate control schemes. The reserve margin can be successfully deployed according to

the AC grid frequency imbalance or AGC set-points. The homogenization of active power injection has also been achieved through individual WT set-point.

Keung *et al.* have presented in [41] a strategy to emulate inertia behaviour from WT aiming at contribution to the AC system frequency support, taking advantage of the kinetic energy stored on the WT rotors'. A supplementary control-loop has been proposed. These enhancements are meant to be implemented at DFIG rotor-side converter. The control consists on generating active power references according to the wind turbine rotational speed and an active power increment. The active power increment is a power versus time profile named as KE (from Kinetic Energy) and overrides the converter basic PI controllers for a small period (of about 3 seconds according with the authors). That way, the existing energy store in the generator is transformed into active power and delivered to the grid. The results show that a quick active power output is achieved for the small time duration period, followed by a slow reduction towards the nominal power. The generator speed is hardly reduced. However, generators are able recover since the inertia emulation has a small deployment time and consequently the impacts on the generator speed are afterwards recovered.
This paper also assesses the under existence of delay on acquiring the measurement, impacting on the provision of the inertia contribution. Bearing in mind that the synthetic inertia behaviour can be characterized as a fast power deployment during AC frequency decrease, the existence of delay distorts the concept. Different delays of 0.2, 1 and 2 seconds were considered. The delay impacts consisted in the increase on the frequency rate of decrease which increased with the delay duration.

The research work conducted in the topics of the provision primary frequency control and emulation of inertia behaviour by WT demonstrate the feasibility of their implementation through WT control-loop design, enabling an autonomous deployment. Generally, primary frequency support is achieved through the creation of a reserve margin through the degradation of the WT aerodynamics by acting on the blades' pitch angle. Proper control schemes associated to mechanical pitch angle adjustment are able to endow WT with primary frequency support capability. However, the work developed in [31], does not rely on the creation of reserve margin

through pitch adjustment. In contrast, author proposes a PMSG speed control to increase the injected power proportionally to the frequency disturbance by taking advantage of the kinetic energy of generator rotor. Nevertheless this strategy has the drawback of not allowing extended primary frequency support due to the excessive reduction of the generator speed. Regarding the inertia emulation, the analysed papers are consensual stating that it can be achieved through the exploitation of the stored kinetic energy available on the generator rotor. To synthesize the inertia behaviour, adequate control schemes were presented, responding proportionally to the AC system frequency derivative.

Fault Ride-through Capability

In the last years, TSO have published grid codes with specific requirements for wind power integration. Among them, a common aspect consists on the provision of the FRT capability or also known as the Low Voltage Ride-through (LVRT). The FRT objective consists on guaranteeing the WF are able to withstand low voltage periods often provoked by fault occurrence. Bearing in mind that nowadays WF have large installed capacity (ranging from tens to hundreds MW), they present a significant amount on the electricity generation mix. From the TSO point of view it is extremely important to prevent that during a fault event, a huge amount of wind power disconnects to the grid, creating a load/generation imbalance event. Depending on the transmission system, a voltage versus time characteristic curve is set, defining the minimum time that a generator (or WF) should withstand connected to the grid according to a voltage sag at it terminals. FRT voltage-time curves assume different shapes. A summary of some FRT curves is presented on Figure 2.4 and Table 2.1.

On the attempt of supporting the AC voltage profile on the WF neighbouring area, some grid codes also require to WF to inject reactive current during the voltage sag. The example of a reactive current injection requirement, for the Portuguese grid code defined at [42], is depicted in 2.5.

The curve depicted in Figure 2.5 represents the Portuguese grid code requirement for reactive current injection during voltage sags. It is composed by two main zones. Zone (1) consists on the reactive current requirement in function of pre-fault active current injection, according to the AC voltage profile measured at the wind turbine terminals. This zone is effective for voltage profiles below a threshold value

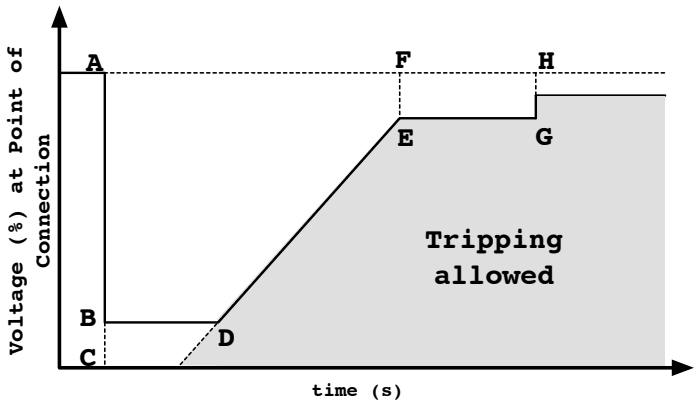

Figure 2.4: Example curve of FRT voltage-time requirements (adaptable for several grid codes)

Grid Code	BC	BD	AF	FE	AH	HG
Denmark	25%	0.1s	0.75s	25%	10s	N.A.
Germany	0%	0.15s	0.15s	30%	0.7s	10%
Ireland	15%	0.625s	3s	10%	N.A.	N.A.
Spain	20%	0.5s	1s	20%	15s	5%
Spain (Canary Islands)	0%	0.5s	1s	20%	15s	5%
United Kingdom	0%	0.14s	1.2s	20%	2.5s	15%
Portugal	20%	0.5s	1.5s	20%	10s	N.A.

Table 2.1: Wind power grid code FRT voltage versus time characteristics

(0.9 p.u. for this case). Zone (2) is related with the reactive current injection in normal operation.

The introduction of this requirement has brought challenges for the wind turbine manufactures to design generators and control strategies coping with the specified requests. During the last decade several research work have been conducted on this specific topic, presenting several approaches for FRT compliance over the most dominant wind generators technologies. It can be stated that nowadays wind turbines, independently of the generator technology, are able to be FRT compliant. Nonetheless, some may require the presence of external devices such as Flexible AC Transmission Systems (FACTS) to fully comply with grid code requirements

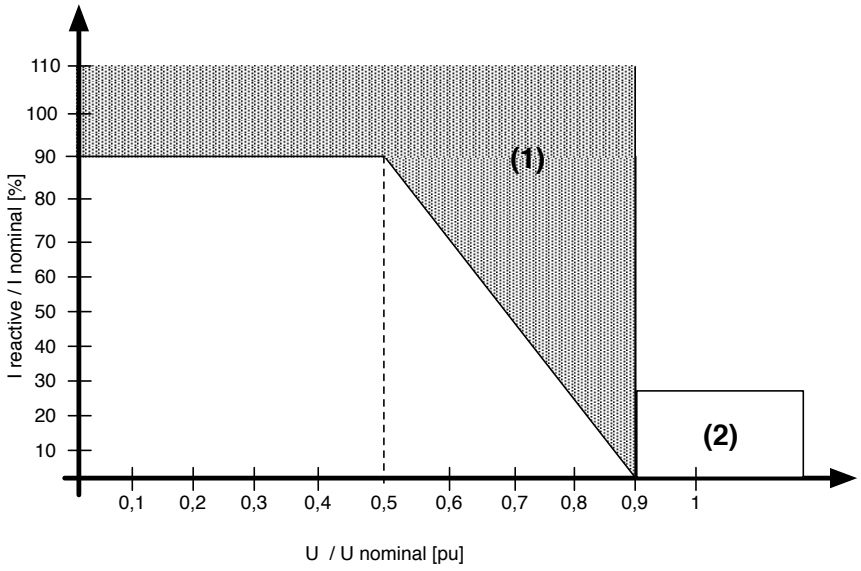

Figure 2.5: Portuguese FRT reactive Current injection requirement

[43, 44, 45].

The investigation conducted by *M*orren et al. in [46] developed a solution to make possible for DFIG on remaining connected to the grid during grid faults, without losing the synchronism. The proposed strategy consisted on bypassing the rotor converter during the fault event. In addition, during the fault event the rotor is connected to a thyristor controlled resistance which dissipates the rotors' power. The inclusion of external thyristor-controlled braking resistors' reduces the rotor currents and simultaneously guarantees the operation of the machine within acceptable slip range This method also reduces the induced rotor current by increasing the rotor resistance (being the total resistance defined by the sum of the rotor winding resistance plus the external thyristor controlled resistance. The simulation set-up to assess the performance of the proposed control scheme consisted was achieved by modelling a DFIG generator in Matlab Simulink in the *d-q* reference frame. The power electronic converters between the machine rotor and the grid were represented by their control-loops. To evaluate the performance of the strategy,authors tested the base case DFIG (without power electronic converters protection) facing a 85% voltage dip. The results presented a high increase on the rotor currents achieving

the magnitude above 3 p.u. which is above the converter limits. Authors assessed that this specific situation could provoke severe damage to the DFIG converters. To overcome the high inrush currents, authors have evaluated the performance of the generator, facing the same fault event but with the inclusion of the proposed control approach. The results highlight that the DFIG was able to remain connected to the grid. The rotor current was reduced being kept bellow the nominal current. Despite speed drift has been also observed during the fault event, the generator was able to recover the active power injection and pre-disturbance speed aftermath.

In [5], authors have implemented a time-domain model for the DFIG to assess the validity and feasibility of a proposed control scheme regarding the generator FRT capability. Similarly to the approach aforementioned in [46], this investigation also adopts a electronic interfaced resistor that is connected to the DFIG rotor during the fault. The set composed by resistor and the electronic interface converter is denominates as crowbar (see Figure 2.6) ans is used to restrain the induced current on the DFIG rotors' winding. The objective of the proposed FRT strategy consists on:

1. Protect the switches of the converters against overcurrent and overvoltage stress and the DC bus capacitor against overvoltage;

2. Fulfil the grid code requirements by feeding reactive current during the fault and resuming active generation after fault clearing;

3. Optimize the hardware added to the generator and the mathematical processing of control techniques.

The operation of the proposed FRT control is activated when the voltage fall below a given pre-defined undervoltage level. The FRT control is responsible for disconnecting the Rotor Side Converter (RSC) from the rotors' windings (through S2, connection a in the Figure 2.6). As aforementioned the rotors' windings are then connected to the crowbar resistance to limit the induced rotor current (through S1 in Figure 2.6). The RSC operation mode is then changed from Normal to Transient Control Mode (TMC). Since the RSC does not operate at the same frequency as the Grid Side Converter (GSC), a small delay time is given to the converter guaranteeing

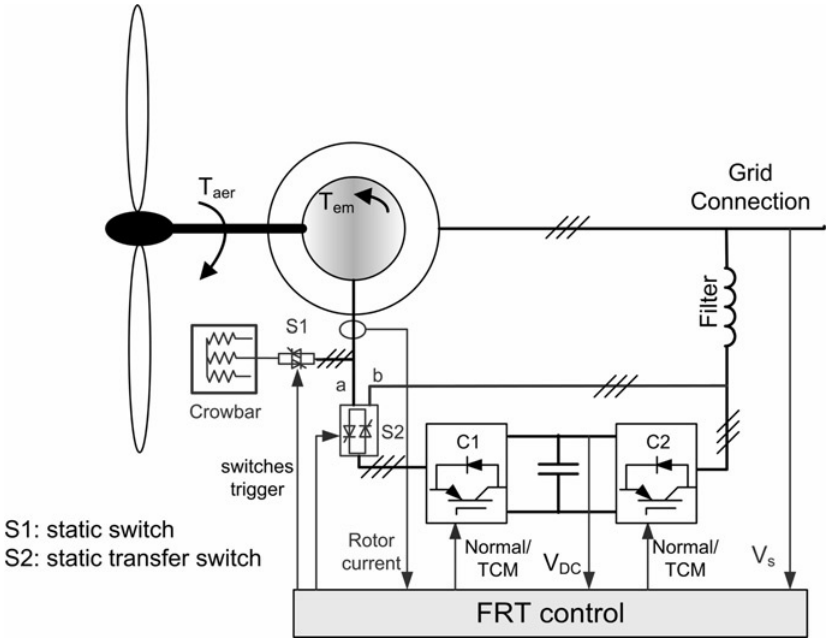

Figure 2.6: Overview of FRT control approach on DFIG [5]

that the operational mode change is effective on the converter behaviour. Then the RSC is connected in parallel to the GSC (through S2, connection b - see Figure 2.6). The GSC and RSC will provide reactive current injection to the AC grid, performing similarly to a STATCOM using the energy stored in the capacitor. When the fault is cleared and the voltage rise above the minimum voltage detection threshold the opposite strategy will take place. The RSC will be disconnected from the GSC and followed by the control operation change from TMC to normal mode. Also a small delay time will be given to let the converter operate with the new set points and then, the converter will be connected to the DFIG rotors' windings and simultaneously the crowbar will be disconnected. This strategy allows the DFIG to remain connected to the grid without facing high current magnitudes in the rotor. The synchronism is not lost and simultaneously the connection of both converters in parallel allow a maximized reactive current injection without requiring hardware over-sizing.

The FRT capability on PMSG wind turbines has been investigated by *Muyeen et al.* in [47]. This particular type of generator is fully de-coupled from the grid since its interface is performed by back-to-back electronic converters. Hence, the

Machine Side Converter (MSC) is responsible by injecting the Generator AC power into the DC busbar after being rectified. The Grid Side Converter (GSC) is responsible by delivering the generated power to the AC grid while controlling the DC voltage. During an AC fault, the generator will not sense any voltage sag at its terminals thus will remain generating the pre-fault power and no problems regarding synchronism loss will occur. Nevertheless, the GSC will sense the fault event and will commute its operation mode from normal to FRT mode. In the FRT control mode, is priority is given to the reactive current injection to meet the grid code requirements. Consequently the generated active power will not be totally delivered to the grid, provoking a power imbalance on the DC-Busbar. The DC capacitor will then experience an overvoltage that can damage the capacitor as well as the power electronic converters. To avoid the overvoltage, a fast voltage control strategies are adopted. Authors proposed that during the voltage sag an Overvoltage Protection System (OVPS) should be connected to the DC-link busbar. The OVPS consists on an electronically controlled resistor that is connected in parallel with the DC capacitor, dissipating the active power surplus of the DC-link. By doing this, the control strategy is able to maintain the DC voltage within admissible. Additionally, the PMSG will deliver a constant active power amount, avoiding any power imbalance. The GSC will be able to deliver reactive current to the AC grid. To assess the effectiveness of the proposed control strategy a full modelling of the wind turbine, including power electronic switching, has been performed in PSCAD/EMTDC software. The results allow concluding that the strategy is effective since the PMSG wind turbine remain connected to the grid facing a fault event. Also reactive current injection is successfully achieved. The DC link voltage is kept within the admissible values.

Regarding the FRT capability on PMSG wind turbines another study presented in [48], assesses the DC overvoltage that overcome from this service provision. Similarly to the reviewed by *Muyeen et al* in [47], the major bottleneck for FRT provision in PMSG wind turbines interfaced by back-to-back converter, consists on the existence of a DC overvoltage in the DC busbar, led by the power imbalance during the fault event. In this particular study authors investigated three possible mechanisms for power balance promotion being:

- Active power reduction through blade pitch control;
- Sizing bigger DC-bus capacitor;
- Dissipate the exceeding active power on the DC bus through braking resistor.

Regarding the active power reduction through blades' pitch control, authors ascertained that the time for effective operation is not in-line with the fast dynamics DC voltage rise. In fact, according to [49], modern wind turbines are able to achieve pitching rates in the range of $5^\circ - 10^\circ$ per second, in normal operation and $10^\circ - 20^\circ$ per second in emergency operation. Authors have concluded through simulation tests that even the maximum pitching rate of 20° per second, do not mitigate the DC overvoltage effect.

The second proposed strategy consisted on increasing the capacitor size in the attempt of achieving a smaller DC overvoltage. Calculations performed allowed to conclude that for a severe fault that leads the AC voltage to 0 p.u., during 150 ms, would require a capacitor to withstand $1.15MJ$ energy storage capacity that is equivalent to have an capacitor size of $C \approx 11F$, which is impractical.

The third approach consisted on the adoption of electronic interfaced braking resistor to be installed in parallel with the DC capacitor. This approach is similar to the proposed in [47]. During the fault event the non-delivered active power should be dissipated on the braking resistor thus promoting the DC power balance on the DC busbar. Authors have calculated that for a severe fault leading to the loss of full power delivery capacity, the braking resistor should have $R_b = 0.5\Omega$ to dissipate $2MW$ at the rated DC voltage of $1kV$. Another relevant aspect is the maximum energy that the resistor can dissipate, defining the resistor thermal limit. The simulations performed to assess the performance of this strategy demonstrates its feasibility and effectiveness regarding the DC voltage rise mitigation.

The work conducted by Amutha and Kumar in [50] presents an approach for allowing non-FRT compliant WF on remaining connected to the grid during voltage sags. According to the previously described, FRT capability is extremely important from the power system dynamics perspective, since it reduces the amount of wind

power disconnect after a fault event, mitigating load/generation imbalance after grid fault clearance. The proposed approach consists on equipping WF with an external additional device called Dynamic Voltage Restorer (DVR). This device decouples the WF from the grid during the fault and transitory assures the AC voltage profile at the WT terminals mitigating the induction generators accelerating. The adoption of this approach present promising results by allowing induction generator based WF on remaining connected to the grid during voltage sags, thus mitigating the stability effects after fault clearing.

2.3 Wind Turbine Technologies

A significant evolution on wind turbine technologies have been taking place on the last two decades with a high contribution on constructive aspects, design and control enhancements. On the attempt of achieving better performance, wind turbine aerodynamic design as well as the materials for wind blades' construction has experienced quite remarkable development on the last decades. Simultaneously, the electrical generators have also been facing modifications to meet the connection requirements. The flexibility of operation and the efficiency over a wide set of wind speed are the key concerns for the research and development on this specific topic.

Three major wind generator technologies equips nowadays wind turbines. The first generation, which equips the oldest WF are the fixed speed WT based on Fixed Speed Induction Generators(FSIG). These turbines are less flexible from the wind speed operation range and also from the grid connection perspective [51]. The second generation, are variable speed WT which are equipped by an induction generator with accessible wounded rotor that is interfaced to the grid through a power electronic converter. This technology is named as Doubly-fed Induction Generators (DFIG). It is nowadays most spread wind turbine technology and have been adopted in several projects due to its wider operation range and the capacity of providing support services to the power grid. The third wind turbine technology is also a variable-speed WT equipped by Synchronous Generators (SG) with auto excitation provided by a proper auxiliary circuit or by permanent magnets. These generators are normally multi-pole machines, don't requiring gearbox to adapt the rotors' speed

to the generator speed. The interface between the generator and the electric grid is performed via an integral converter. In the literature this technology is know as full or integral converter WT or Permanent Magnet Synchronous Generator (PMSG).

2.3.1 Fixed Speed Wind Turbine

The fixed speed wind turbine is composed by an induction generator connected to the WT through a gearbox. The gearbox is an essential part of this generator since adapts the blades' shaft speed to the operation speed range of the induction generator. Also, it is the most delicate part of the WT on what regards maintenance needs. The induction generator is not able to generate reactive power autonomously and requires reactive power for magnetizing [51]. Thus, capacitor banks are usually installed in this type of wind turbines. This generator is not able to autonomously deal with the recent grid code requirements, namely on the fault ride-through capability. Often, external devices can be set in a FSIG-based WF to guarantee the flexibility required be the nowadays grid-codes [52].

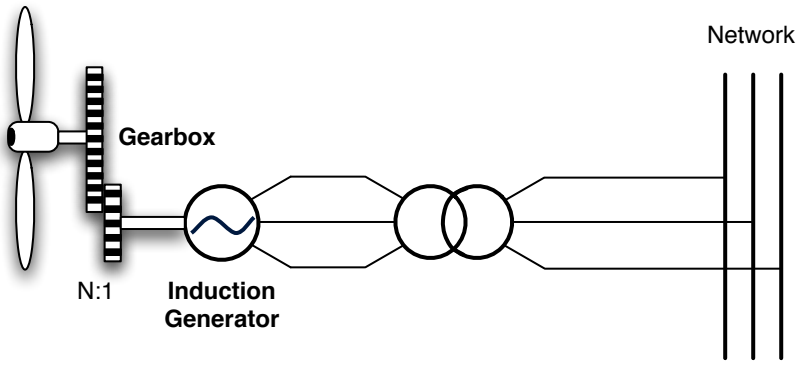

Figure 2.7: Scheme of Wind Turbine based on Induction Generator

This technology was widely spread during 1990's decade. By 2000, manufacturers have enhanced the induction generators with power electronic converter interface between the rotor and the AC grid. This fact enhances the operational flexibility as well as allows the provision of novel ancillary services to the AC grid.

2.3.2 Doubly-fed Induction Generator – DFIG

The DFIG is currently the most spread WT technology over the world. It consists on an induction generator with accessible rotor windings. The rotor is interfaced with the grid by a back-to-back converter (as illustrated in Figure 2.8) with reduced size (ranging from 20-35% of the generator rated power) [26]. Despite requiring the adoption of a gearbox to adapt the turbine rotational speed to the generators' speed, this generator can operate in a wider speed range being more flexible than the predecessor conventional induction generator. Additionally, it is capable of coping with grid code requirements by providing effective primary frequency control [36], [26] and even withstanding voltage sags and provide reactive current injection during these events [5].

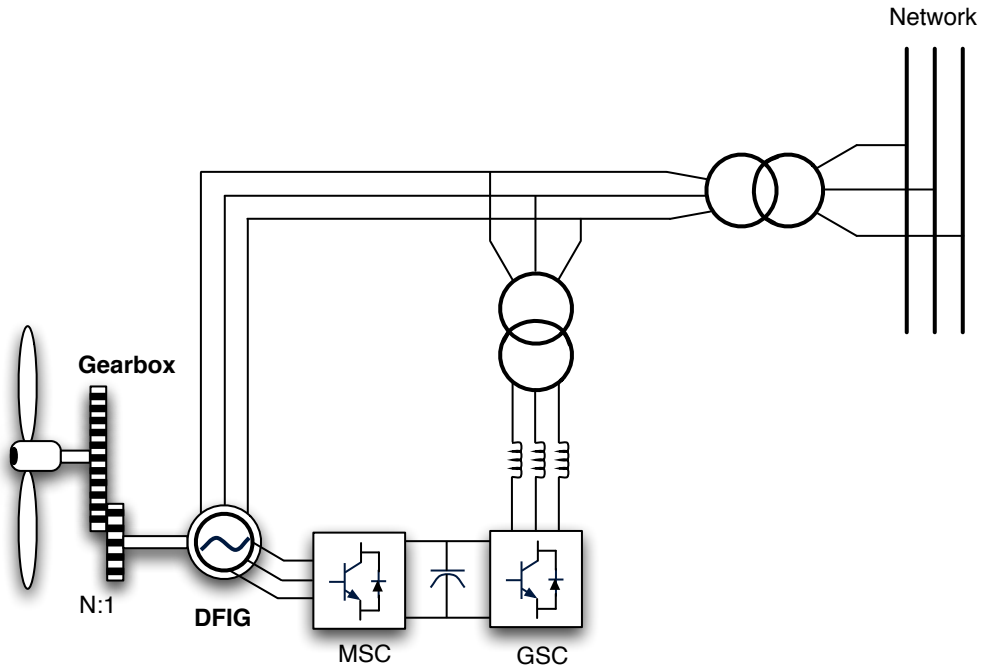

Figure 2.8: Scheme of Wind Turbine based on Doubly-fed Induction Generator

2.3.3 Permanent Magnet Synchronous Generator

The PMSG is connected to the grid via an back-to-back converter. The general connection scheme is illustrated in Figure 2.9. The adoption of integral converter connection allows the generator to operate at any non-fixed frequency. The PMSG

are multi-pole generators that rotates at low speed, close to the WT hub speed, not requiring gearbox for speed adaptation. This factor is very beneficial since reduces the maintenance requirements associated with the gearbox, turning it in an attractive solution for offshore applications. The generated power is rectified to DC by the Machine-Side Converter (MSC). The power is stored at a DC capacitor installed at the DC busbar and the Grid-Side converter (GSC) inverts the power into AC at the nominal grid frequency, enabling its delivery. Normally, the control associated to the GSC controls the active power delivery based on the DC voltage value. The interface made through power electronic converter is advantageous since smooth the power delivery by reducing the impacts from wind variations. Additionally, the converters cascade decouples the generator from the grid, mitigating the impacts of voltage sags. In fact, this technology of WT is able to withstand AC voltage sags and simultaneously provide voltage support by injecting reactive power.

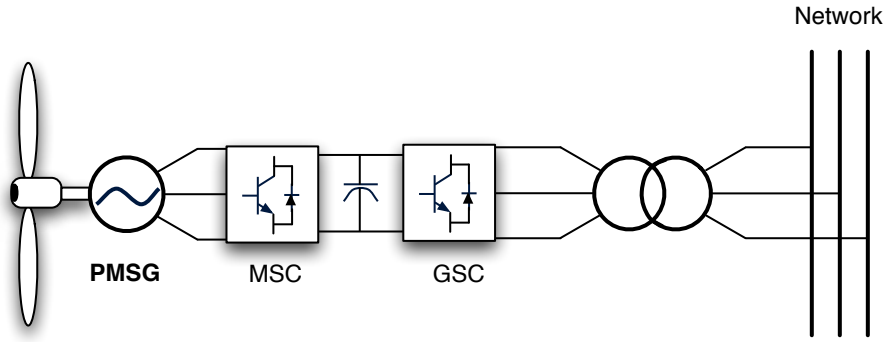

Figure 2.9: Scheme of Wind Turbine based on Permanent Magnet Synchronous Generator

2.4 Offshore Wind Power

Recent trends points toward to the adoption of wind power generation at offshore level. Nevertheless, several challenges arise for the deployment of these WF. From the electrical perspective the major challenges related with offshore wind power deployment are related with the connection infrastructure, control of wind power injection and also the participation of offshore WF on grid services similarly to what is nowadays required to onshore WF. Several projects and studies have been carried

out, mainly in the last decade, over several aspects inherent to offshore wind power integration. The sub-topics of this section try to highlight some of the challenges that are addresses in this thesis, as well as gives an overview of what are the main existing contributions.

2.4.1 Offshore Wind Farm Grid Connection

Offshore WF are electrically connected to the mainland grid by a cable circuit. The adoption of cable circuits in AC has some implications on the power transmission. In fact, the cable circuits also known as insulated or shielded cable circuits are composed by a conducting core isolated by a non-conducting material as depicted in Figure 2.10.

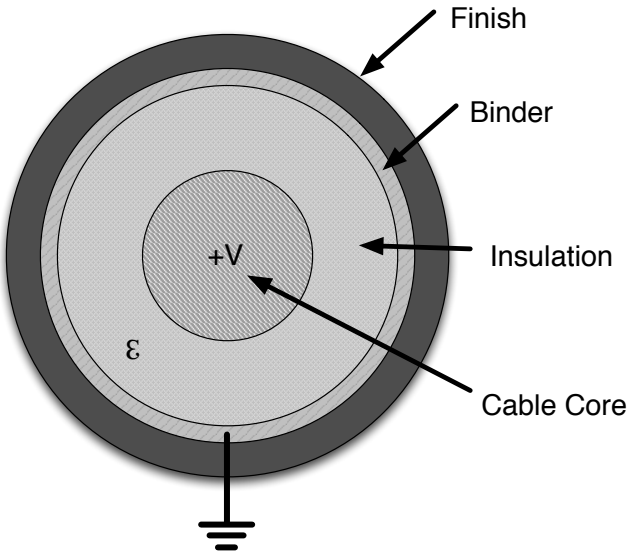

Figure 2.10: Power Transmission Cable Cross-section

The cross-section illustration on Figure 2.10 shows that the cable core will operate on a given voltage and it is separated through a non-conducting medium from the outer shield that is ground connected. Thus, a cable circuit behaves as a capacitor, whose capacity is distributed over the cable length. In sum, the interconnection cable circuit will generate a massive capacitive reactive power which reduces the overall active power transmission capability and also hempers the cable voltage control. To avoid this effect, a high inductive compensation should be required. The issue is that over a certain amount of power and length it becomes impractical the adoption

of AC cable circuits. According to *K*im et al., the High Voltage AC (HVAC) should not be adopted for connections over 300 MW 200 km or 200MW-250 km [6]. Above these power rates and lengths the HVDC adoption is more adequate to establish the power transmission from technical and economical perspective.

The HVDC technology has been gaining importance on the last decade as the way to tackle many of the power system problems. Nevertheless, this technology begun being investigated on the mid-20^{th} century. In 1954 the first commercial HVDC system was placed in Gotland (Sweden), consisting in a 10 MW unidirectional point-to-point connection between mainland Sweden and Gotland Island. Additionally to cable circuit connections, HVDC has been used for long length, high power links. The advantages of HVDC in comparison to HVAC systems are [6]:

- No technical limit to the length of submarine cable circuit;
- No synchronism required between AC interconnected grids;
- Immunity from phase angle, frequency or voltage fluctuations;
- Interconnection of AC systems running on different frequencies (50-60 Hz);
- Controllability of power injection (not a power flow angle and voltage-based solution);
- Capability of independent control of active and reactive power (on VSC);
- Uses only two conductors (one if the return path is established by the ground).

The range of application of HVDC system is very broad. The scheme on Figure 2.11 illustrates possible utilization of HVDC technology.

According to the illustration of Figure 2.11, HVDC technology is adopted to handle particular applications which cannot be established by HVDC. It can promote the interconnection between non-synchronous areas (operating with different frequencies) in a back-to-back configuration, interconnection between distant bulk power generation and load consumption spots (like Itaipu connection in Brazil, Cahora-Bassa in Mozambique) and also, cable circuit power transmission for Island or offshore WF connection (Gotland- mainland Sweden). Several plans and studies

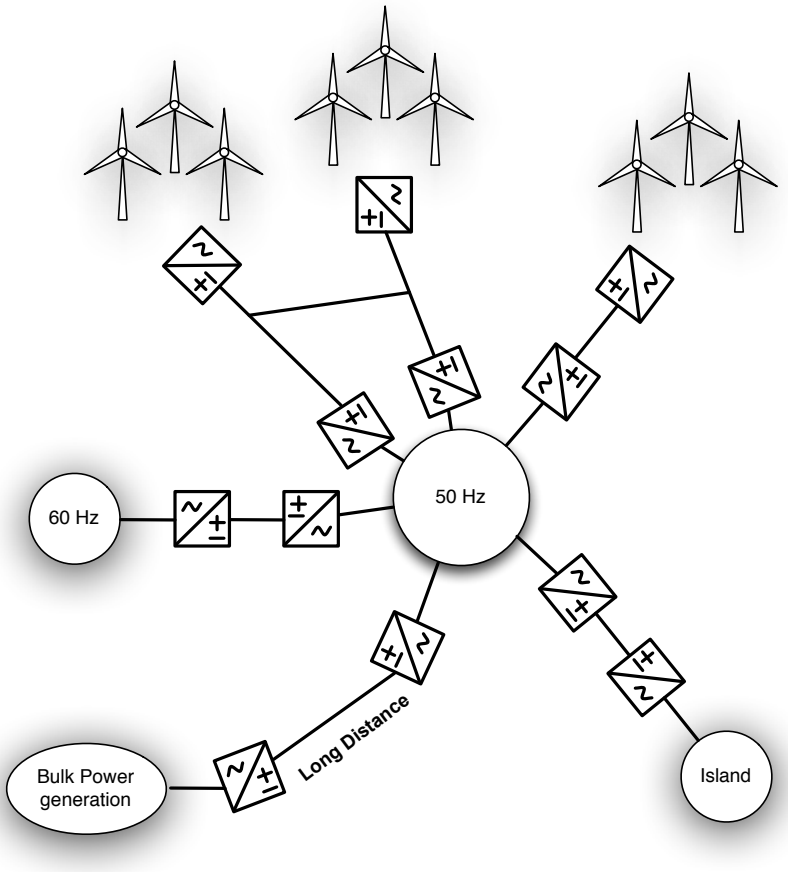

Figure 2.11: Possible applications of HVDC technology adapted from [6]

envision the adoption of offshore wind power to tackle the electrical green-energy needs on the next decades. The deployment of WF at offshore level is surrounded by technical challenges that go from the structural, logistic to electrical connection scope. From the electrical perspective the connection should:

- Be economically viable;
- Provide operational flexibility;
- Allow ancillary service provision;
- Be reliable.

Several works that have been recently performed are consensual pointing the HVDC as connection the technology to allow a massive offshore WF penetration [53], [54], [55]. Nevertheless, beyond installing wind turbines at offshore level being very expensive, the HVDC connection increases the investment by still being a quite expensive technology. Several studies have assessed the economic impacts of the HVDC adoption for offshore WF deployment and concluded that HVDC is not competitive technology from the economic perspective. Nonetheless, is the only technology able to promote the interconnection for certain power amount as well as distance from shore. The study conducted by The Crown State in [56] concluded that HVDC is crucial for the far from shore offshore wind power deployment and forecasts that the technology cost will decrease within the next years with the increase of its adoption.

Simultaneously, the HVDC technology has been widely adopted in several projects over the world by diversified reasons. Long distance power transmission has been the major responsible for HVDC deployment. Examples such as the 2500km, 3500MW connection between Madeira River and Araraquara, Brazil [57] and the 890km 3000MW connection between Three Gorges and Changzhou in China [58] are helping on the development of HVDC technology. According to Buijs *et al.* in [59], HVDC has been also being investigated to tackle challenges in metropolitan areas over Europe where the need of transmission capacity assured by underground cable circuits is highly increasing. In [59] authors give specific examples over several European cities in diverse countries such as Spain, UK, Denmark, Italy, Germany, Netherlands and Austria.

2.4.2 Multi-terminal DC Grids for Interconnecting Offshore Wind Power

The HVDC technology has been envisioned to help on creating a common European grid infrastructure commonly named as the SuperGrid [60]. The Super Grid concept consists on a network infrastructure with hybrid AC and DC connections. The DC connections need is related with offshore WF collection, promote power exchange between non-interconnected areas and foster the long distance renewable energy connection. The report found in [60] refers to the possibility of having a common

electricity market between several distinct electricity markets in Europe. The lack of interconnectivity or limited interconnections, constraint the power exchanges between countries. According to [60], the existence of additional connectivity can also help on increasing the renewable energy penetration and extend the network share of renewable power by allowing storage on hydro dams located on Scandinavian area. Research projects such as the Offshore Grid and TWENTIES have investigate the deployment of DC grids in Europe. The works presented in [61] and in [62] proposes the DC grid as an overlay to the existent European grid, allowing to increase the Renewable Energy Sources in Electricity (RES-E) penetration as well as fostering electricity market development.

The Offshore Grid final report [63] presents the DC grid as an advantageous solution by being the way to achieve:

- Security of Supply
- Competition and Markets
- Integration of Renewables

From the security of supply perspective, the DC grid should improve connection between big electricity consumption centres around North Sea, reduce fossil fuel dependency, transmit offshore renewable electricity and bypass onshore electricity transmission bottlenecks. From an electricity market perspective the DC grid can create or improve connections, fostering the trades and improving competition. The DC grid also promotes the renewable energy integration through the collection of offshore Wind Power generation. Several offshore WF can be interconnected to the grid smoothing the wind power variability. Also, the DC grid promote connection between non-interconnected AC areas which is advantageous since facilitate the accommodation of renewable energy in Scandinavian hydro dam reservoirs. These factors simultaneously contributes to the Europe's 2020 targets for renewable share and CO_2 emission reduction [63].

The project DESERTEC also envisions the HVDC grids for enabling the creation of a Super Grid among Europe, Middle East and North Africa denominated

as EUMENA [7]. The objective of this initiative is to promote massive renewable power integration and promote power exchanges between the intervenient areas. The DESERTEC supergrid conceptual layout is depicted in Figure 2.12. It consists on

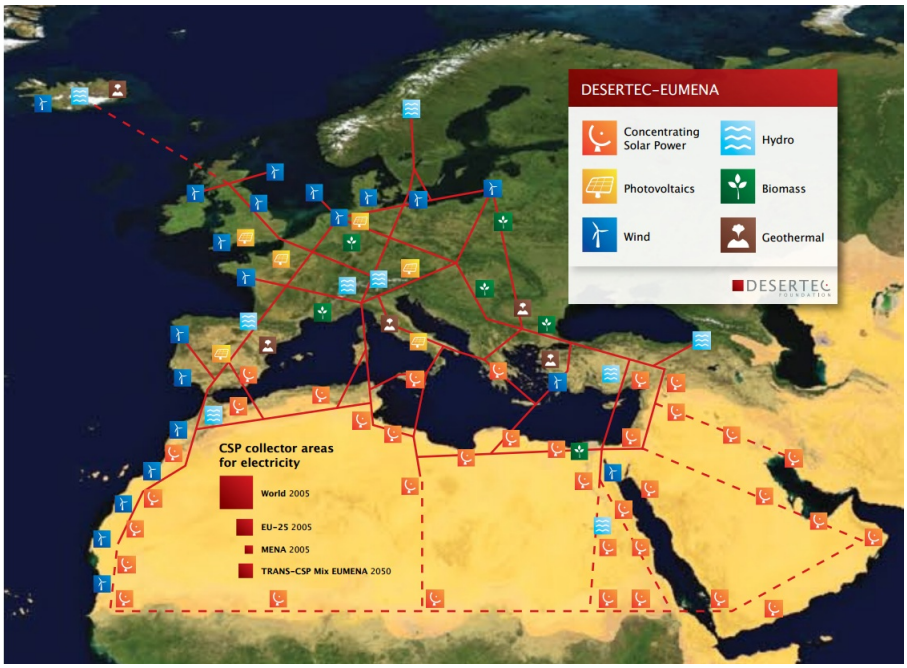

Figure 2.12: DESERTEC Super Grid concept [7]

taking advantage of the existing ENTSO-E power grid and extends it to the renewable generation location. This extension in many cases must be HVDC-based due to the power and distances at stake. One of the projects vision is noticeable by the illustration in the Figure 2.12 and consists on collecting a massive amount of solar power at North Africa and Middle East regions through Concentrated Solar Power (CSP) plants. MTDC grid is expected to interconnect the several distant CSP plants as well as wind farms into the European ENTSO-E AC grid [7]. The DC grid can also perform as a backbone for the existing AC grid by allowing the power flow, for instance from Iberian Peninsula to France or Greece to Italy or Iberian Peninsula to Italy.

The development of Multi-terminal DC grids has been also addressed in [64]. According to authors, the (Multi-terminal DC) MTDC grids will start being installed for onshore applications and further will be adopted for offshore and pan-continental

connections. In fact, India has recently announced a four terminal HVDC ±800-kV grid to be placed in operation by 2015. The system will be rated to 8.000 MW and should promote the connection of hydropower-based electricity to 90 million people. Several point-to-point connection projects for offshore wind power transmission in Europe have been required to be grid-enabled allowing future expansion via connection to other DC systems [64].
This fact is a clearly intention on building a MTDC infrastructure at the North Sea. According to authors, the projects for offshore point-to-point connections will play the role of primary blocks and in a further phase, these blocks are going to be connected building a DC grid infrastructure.

Regarding the plans for DC grid deployment, there have also place for discussion on what regards the DC grids topology. In theory, DC grids can have unlimited connections as well as injection and extraction points. However, in practice it is need to define an appropriate topology allowing on reducing the implantation costs, creating a flexible and reliable grid and assuring security of supply and reasonable interconnection capability to foster electricity markets competitiveness. The work conducted by Gomis-Bellmunt *et al.* presented in [8] analysis several DC grid topologies based on varied criteria such as the loss of power in-feed aftermath fault occurrence and economic aspects as well. The analysed topologies consisted on ring topology, star topology, star with a central switching ring topology, wind farms ring topology and substation ring topology. For illustrative purposes, the MTDC grid topologies are depicted in Figure 2.13. From reliability and reconfiguration purposes some of the presented topologies may be more interesting than others. However, the results of this work shows that the optimum topology does not depend only on operational and robustness requirements but also on geographical dispersion of substations and WF. Circuit breakers and cables price are also important factors that must be weighted. Authors have also stated that based on the current price of solid-state breakers the most appropriate configuration should be the WFRT (c) in the Figure 2.13) since it meets all the criteria's with reduced price. However this fact is not strict and depending on the project specifications an analysis should be performed and other topologies might be more suitable [8].

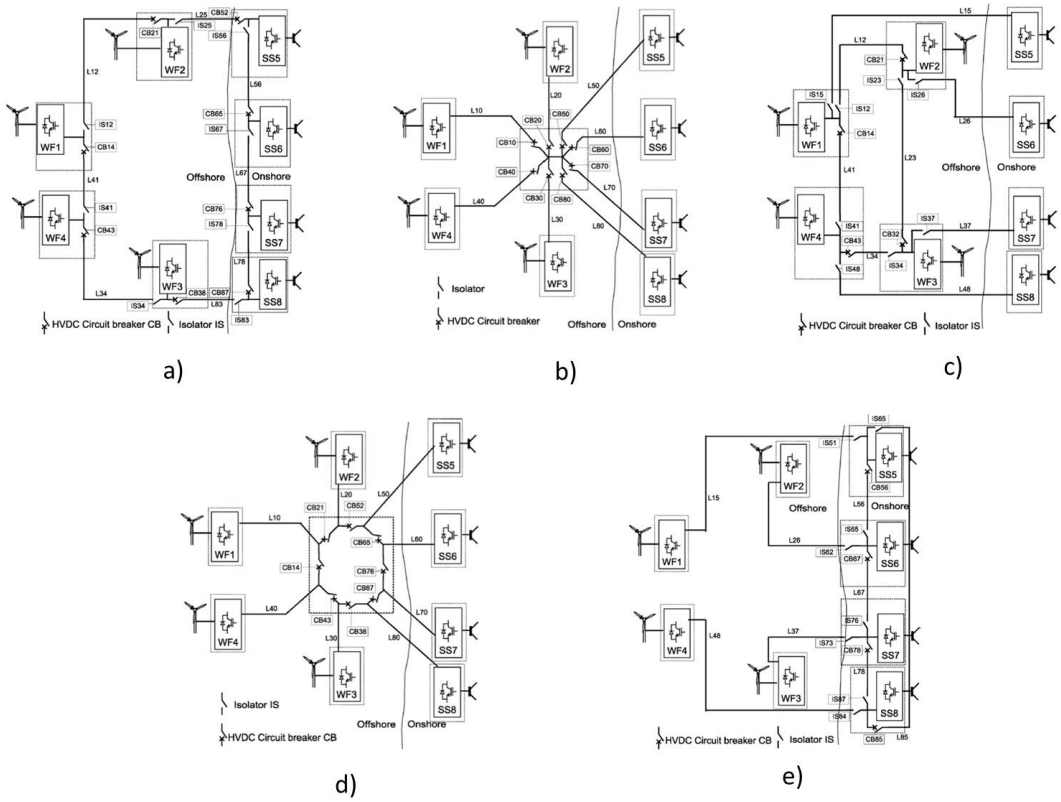

Figure 2.13: MTDC grid topologies: a) General Ring Topology (GRT); b) Star Topology (ST); c) Wind Farms Ring Topology (WFRT); d) Star with central switching ring topology (SGRT); e) Substation Ring Topology (SRT) [8]

The European Project TradeWind, which behaviour developing Europes electricity power market for large scale integration of Wind Power, points in its final report [65], that HVDC is essential for creating the connection infrastructures for electricity markets development. Regarding the wind power integration, the same report envision a massive integration at North Sea and affirms that multi-terminal HVDC meshed grids are essential for the interconnection and more research and development should be performed in this specific topic.

The North Seas Countries' Offshore Grid Initiative (NSCOGI) is a ENTSO-E committee responsible to evaluate and facilitate the development an offshore grid to meet the EU renewable targets up to 2020 [66]. Aspects such as efficiency and economic use of RES and grid investments are taken into the consideration. To

cover all the topics within the DC grid deployment, three Work Groups (WG) were created:

- WG1 - grid implementation;
- WG2 - market and regulation;
- WG3 - permissions and planning.

The WG 1 final report [66] addresses several scenarios and some considerations leads to the adoption of DC grids the mean of achieving the better goals.

2.4.3 HVDC Technologies

The transmission in HVDC is accomplished by the transformation of AC into DC and further the transformation from DC to AC. These processes involving AC transformation into DC is called rectification. To achieve this transformation usually a rectifier is adopted. The opposite process, the transformation of DC into AC is known as inversion and is accomplished by an inverter. The inverter recomposes an AC sine wave using the DC power.

The technology of HVDC converters has evolved along with the development of power electronic devices. Nowadays the HVDC converters are divided between two main technologies. The older, Line Commuted Converter (LCC) and the more recent Voltage Source Converters (VSC).

The LCC was introduced using mercury-arc valves. Nowadays they are composed by solid-state thyristor valves [6]. This specific type of converter relies on the AC system voltage for establishing the commutation (naturally commuted converter) and have been being adopted for bulk power transmission through long distances, back-to-back converters and even for offshore applications providing a point-to-point connection. This technology was in fact adopted in several commercial projects and nowadays still being commercialized for high power applications (over 1000 MW). However, the development in power electronics and the requirement for enhanced flexibility has culminated on the development of the HVDC-VSC technology. This HVDC technology is able to handle the same application field of HVDC-LCC however limited to 1000 MW due to the power electronic switch devices (Insulated

Gate Bipolar Transistor IGBT and Gate Turn-off thyristor - GTO) and converters topology limitations. Additionally, the HVDC-VSC technology allows independent control of active and reactive power, bi-directionality (without requiring blocking the transmission for power flow inversion). Since HVDC-VSC uses forced commuted switches also allows the operation with AC low-voltage profile, operation under weak AC systems and black-start capability [67]. The flexibility of control inherent to the converter technology and control also allows the formation of Multi-terminal DC (MTDC) grids [67], [68]. Lead power systems manufacturers are presently commercializing HVDC-VSC technology for the most varied field of applications. Siemens has a specific product line called HVDC-Plus [69] and ABB has the similar technology named as HVDC-Light [70].

In [69], author presents the state-of-the-art Siemens technology in HVDC converters for power transmission. It consists on a HVDC-VSC composed by a Modular Multi-level Converter (MMC). The MMC converter is achieved by associating series of IGBT switches to reconstruct the AC voltage sine-wave based on the DC voltage magnitude (further details on this converter topology are addressed in Section 2.4.4). The adoption of MMC topology allows the HVDC-VSC system operation under AC system phase imbalance without having issues related with DC voltage ripple since no common DC capacitor is shared by all phases. In fact, according to the paper [69], the MMC HVDC-VSC can operate with a continuous voltage imbalance (during AC imbalanced faults for instance). In these situations the converter can remain delivering the pre-fault power on healthy phases. Thus, on the limit, only one third of the pre-disturbance power will be lost in the case of a phase-to-ground fault. This feature is very advantageous for the AC power system since can reduce load/generation imbalance problems. However, can simultaneously increase the imbalance on AC voltages if not properly operated.

In line with the aforementioned aspect of the possibility of operation in AC phase imbalance, the HVDC-VSC can also operate with DC half circuit. Normally, HVDC-VSC technology is designed to transmit power in DC circuits with symmetrical DC voltages (+VDC/2 and -VDC/2). The scheme depicted in Figure 2.14 was included for illustrative purposes to depict the basic VSC structure. For instance, a 400 kVDC

link is obtained by having one terminal operated between null voltage (medium point) and +200 kVDC and symmetrically the other terminal operated between the medium point and -200 kVDC. Facing a situation of loss of one terminal, (DC cable terminal fault or VSC malfunction) the system can remain being operated using the healthy DC terminal, carrying half of the pre-disturbance power. This functionality is attained by the design of the HVDC converter that normally is separated for each DC cable pole.

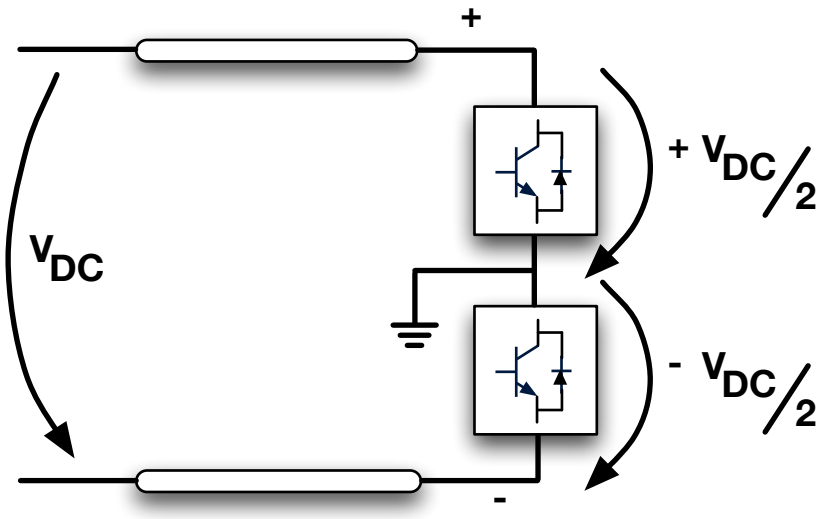

Figure 2.14: Conceptual scheme of HVDC-VSC bipolar link

The HVDC-VSC technology has also evolved on what regards the converters topology. This theme is related with power electronic development and requirements for enhanced operation, mainly from the DC-side perspective. From the AC perspective, the converter topology is important to guarantee the quality of the sine-wave reconstruction. The basic HVDC-VSC functionalities are shared among the topologies. However, an overview of the latest developments is hereafter briefly addressed.

2.4.4 HVDC Voltage Source Converter Topologies

According to the paper published by Andersen *et* al., in [71] the VSC topologies for power transmission are divided in three main categories:

- The two-level topology;
- The multilevel diode-clamped topology;
- The multilevel floating capacitor topology.

In fact, as reported by Flourentzou *et* al. in [9] there are several topologies of multilevel VSC thus, they are based on the principles of the previously mentioned diode-clamped and floating (or commonly mentioned, flying) capacitor technologies.

Two-level VSC

The two-level VSC topology has been widely adopted in power applications. This converter topology can basically output a square wave form which, despite being alternate signal, is far from the sine-wave output standards. Nevertheless for low quality demanding applications it presents to be sufficient and economically viable. According to [71], in order to improve the output, Pulse-Width Modulation (PWM) can be used as trigger for the power electronic valves, producing a waveform with a dominant fundamental component nonetheless, with a significant amount of high-order harmonics. The scheme depicted in Figure 2.15 depicts the two-level VSC electrical configuration as well as its output waveform. The advantages of the two-level topology are:

- Simple circuitry;
- Small DC capacitors;
- Small footprint;
- Semiconductor switches have equal duties.

Enhanced AC wave quality can be attained with the adoption of this topology. However, the number of switch devices doubles in comparison of the previously presented 2-level VSC topology. The main disadvantages of this topology are:

- Large Blocking voltage of semiconductor switches;
- Crude basic AC waveforms;
- High converter switching loss due to high switching frequencies.

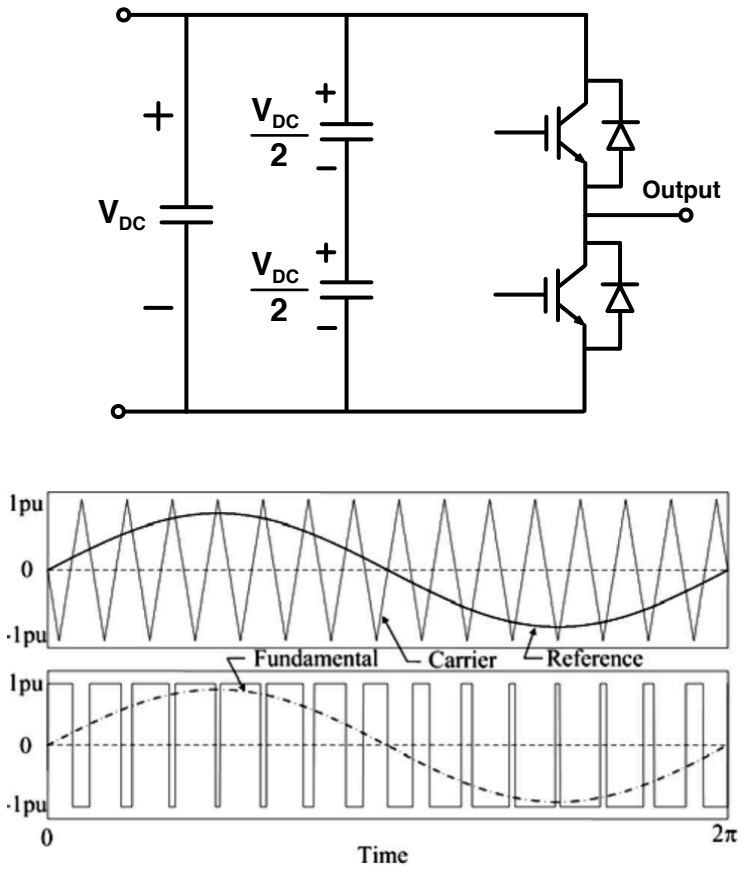

Figure 2.15: Two-level VSC scheme *top*. Converter output *bottom* [9]

Since this topology produces high-order harmonic components, filtering is commonly required to improve the output AC wave quality.

Multilevel Diode-clamped - VSC

The multilevel diode-clamped VSC is attained by using a number of DC capacitor in series and diodes. The AC-side voltage output should then vary between $+V_{dc}$, 0 and $-V_{dc}$.The scheme depicted in Figure 2.16 illustrates the connection layout for a three-level single phase diode-clamped VSC.

According to [71], the diode-clamped VSC advantages are:

- Reasonable small DC capacitors;
- Lower switch blocking voltage;

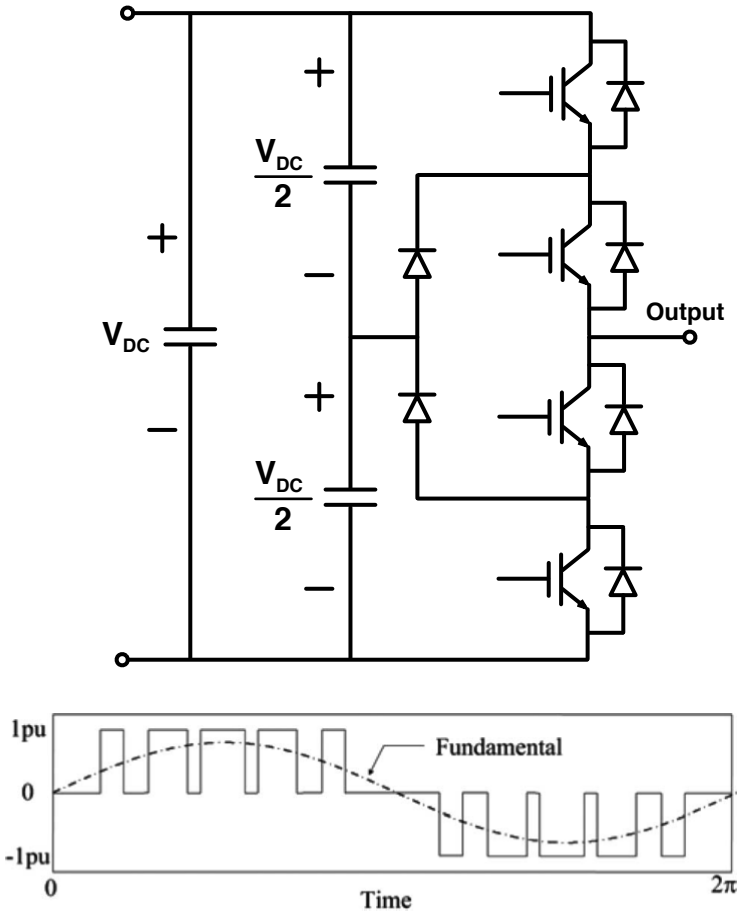

Figure 2.16: Multilevel diode-clamped VSC scheme *top*. Converter output *bottom* [9]

- Good basic AC waveform;
- Small footprint;
- Relatively low converter switching loss.

Regarding the main disadvantages the same paper presents:

- Inherent difficulty in keeping DC capacitor voltage levels constant;
- Complex circuitry for large number of levels;
- Semiconductor switches have different duties.

Multilevel Floating Capacitor (MFC) VSC

The Multilevel floating capacitor VSC produces the same output AC waveform as the previously presented Multilevel diode-clamped VSC topology. However, this topology does not use additional diodes. Instead, additional capacitors are adopted. For illustrative purpose a five level converter and the output signal are depicted in the Figure 2.17.

These capacitors are normally known as floating capacitors. The main advantages of this topology are:

- Semiconductor switches have the same duty;
- Lower switch blocking voltage;
- Good AC waveform representation;
- Low Converter switching loss.

The main disadvantage of this topology is the number of capacitors which increases proportionally to the square of their nominal voltages thus, increasing the converter footprint [71]. Also, as can be observed on the AC power output illustration depicted on Figure 2.17, the increase of converter level impacts by enhancing the quality of the AC output wave.

Modular Multilevel Converter - MMC

As mentioned in Section 2.4.3, HVDC manufactures are adopting the modular multilevel converter. This concept consists on having a so-called IGBT's module or cell that has in the interior two series IGBT and a capacitor as depicted in Figure 2.18. The adoption of modules is advantageous since allows re-configuration or electrical re-arrangement of the HVDC converter, allows the fast substitution of a damaged module and also progressive upgrading by the increase of sub-modules number. The upgrade aspect may be divided in voltage level increase or converter capability increase. If for any reason is necessary to increase the converter voltage level, more sub-modules should be associated in series and the converter control must be re-programmed. However, if the objective is to increase the converter power transfer

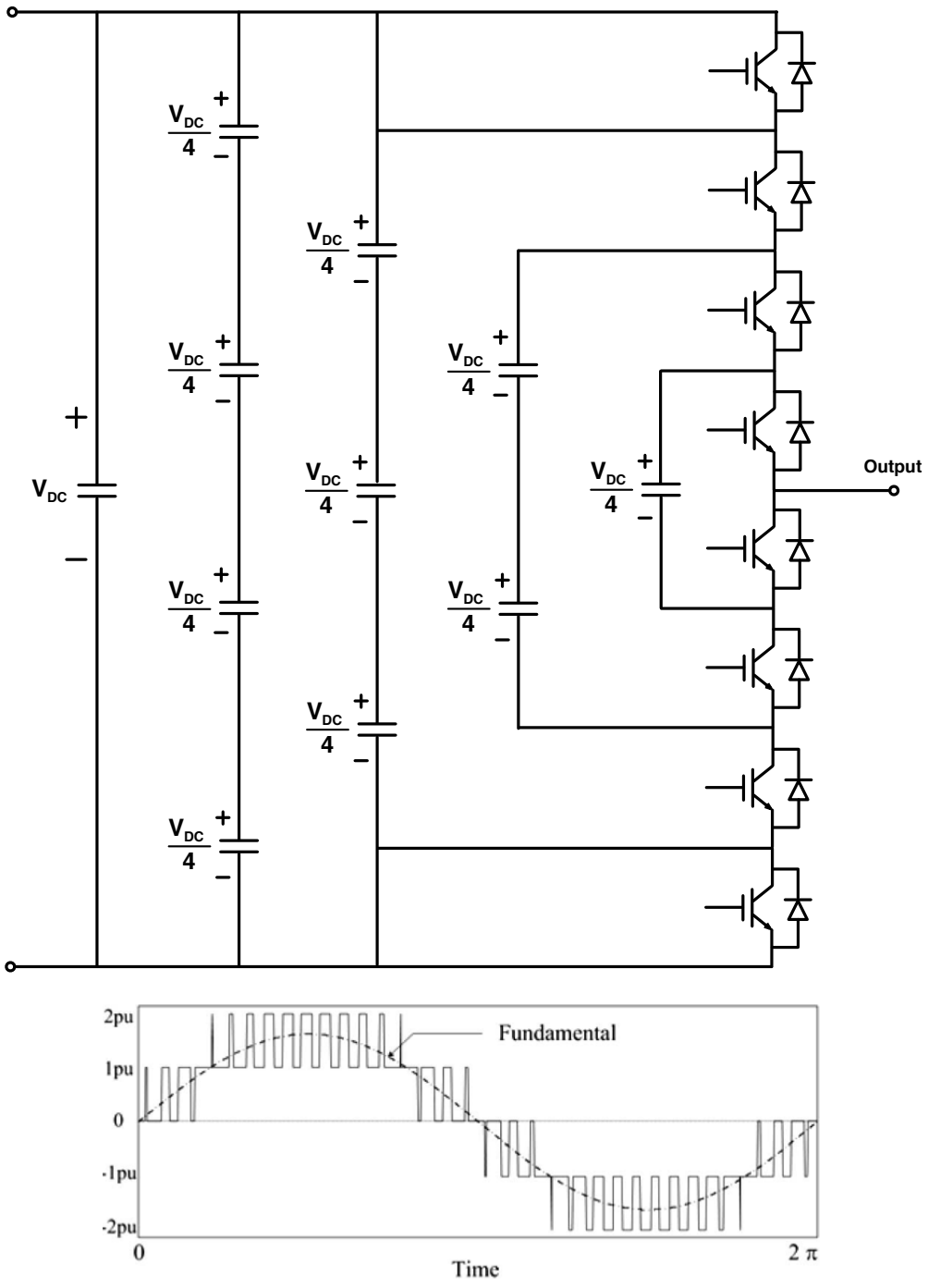

Figure 2.17: Five level multilevel floating capacitor VSC scheme *top*. Converter output waveform *bottom* [9]

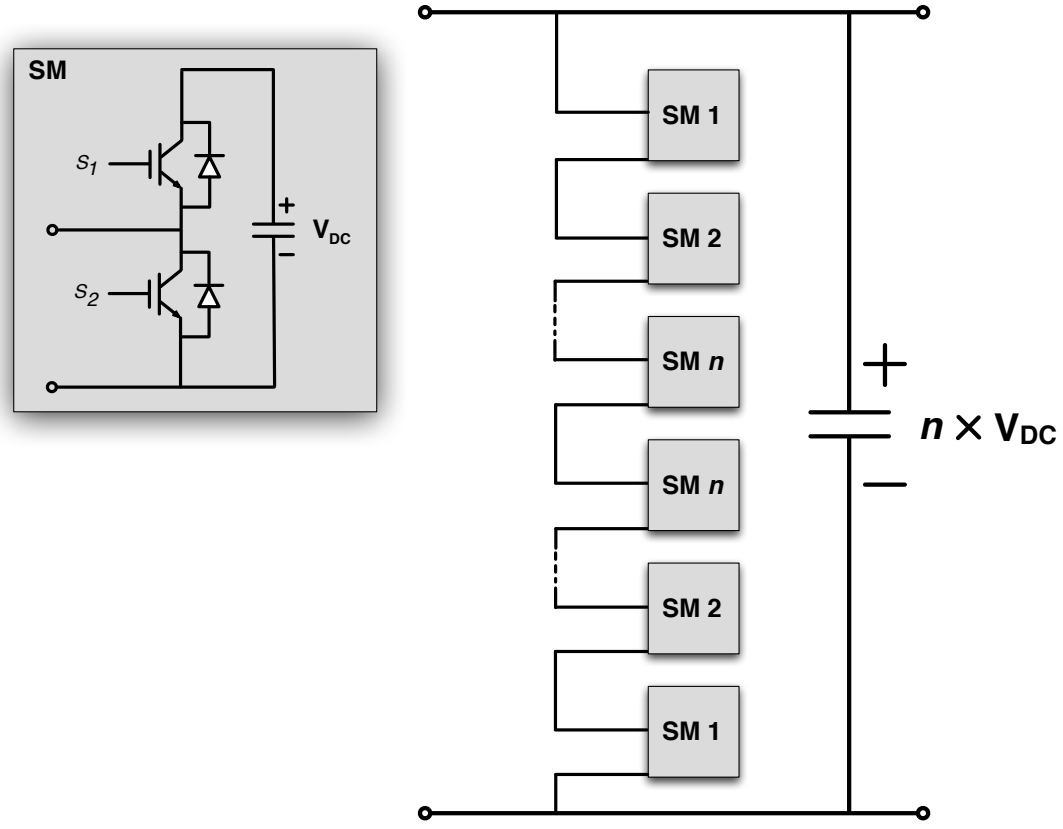

Figure 2.18: Modular Multilevel VSC converter topology and submodule configuration - adapted from [9]

capability, additional sub-modules may be associated in parallel, constructing a twin HVDC converter leg, sharing the sub-module triggering signals.

Modern HVDC-VSC applications adopt multilevel converters that are able to guarantee the quality standards specified by network operators. Power quality issues such as constrained harmonic distortion levels and high to ultra-high voltage connections requirements have been helping the VSC development and real-world application.

2.4.5 Grid Support Services from Offshore Wind Farms

Similarly to the requirements to onshore WF, it is expected that offshore WF should provide ancillary services to the AC grid. Several works have been conducted in this specific field for offshore point-to-point HVDC connected WF. The main support

services identified in the literature were the primary frequency control and the fault ride-through capability. An overview of the most important contributions in these specific fields has been performed and is presented in the following sub-sections.

Primary Frequency Control on Offshore Wind Farms

As described in 2.2.2, WF are able to provide primary frequency control service by increasing or decreasing its generation according to the AC network frequency needs. Normally, due to the tight time-frame, this service is autonomously deployed based on the frequency measurement at the wind turbine terminals. For a HVDC-connected offshore WF, despite WT having primary frequency support capability and being also AC-based, a barrier related with the frequency de-coupling is introduced by the HVDC connection. In fact, the HVDC interconnected areas does not share the frequency behaviour thus, frequency deviation in the onshore AC area will not be sensed at offshore AC network. Nevertheless, some studies have presented alternative mechanisms to deal with primary frequency control deployment on offshore WF connected by a point-to-point link.

In [72], authors have investigate the feasibility of having primary frequency control provided by offshore wind farms connected through a point-to-point HVDC-LCC technology. For this specific case where HVDC-LCC was adopted, the power balance in the AC offshore network is important since will dictate its frequency deviation. Thus, a proper coordination between the generated and delivered power must exist. The HVDC-LCC power delivery is assured by the inverter firing angle which basically determines the amount of power to be transmitted. Authors have implemented a coordinated controller between onshore AC frequency measurement and the offshore AC frequency. So, during a AC onshore frequency disturbance, the offshore converter changes the active power output (through the firing angle adjustment), to mimic a similar frequency disturbance in the AC offshore grid. The tests conducted were just for the case where positive frequency drifts take place on the AC onshore grid (no de-load mechanism was implemented on the DFIG wind generators). So, this specific configuration is only able to respond to AC onshore overfrequency disturbances meaning that; when the frequency signal increases the HVDC link should

reduce the active power. The results highlight the achievement of frequency support contribution by presenting a reduction on the offshore generated power for a overfrequency event. This paper serves mostly as a proof of concept. Further challenging aspects could also be addressed namely the transmission of the AC onshore frequency measurement as well as the implementation of de-loading mechanisms.

A similar research has been conducted by Miao *et al.* in [10]. In this paper authors have also studied the coordination between a DFIG-based offshore WF and the HVDC-LCC rectifier converter firing angle. However, in this research authors propose a droop-based approach for the offshore frequency control. The authors assume that offshore HVDC-LCC has access to the onshore freaquency measurement. The HVDC-LCC firing angle is controlled based on the scheme presented bt Figure 2.19.

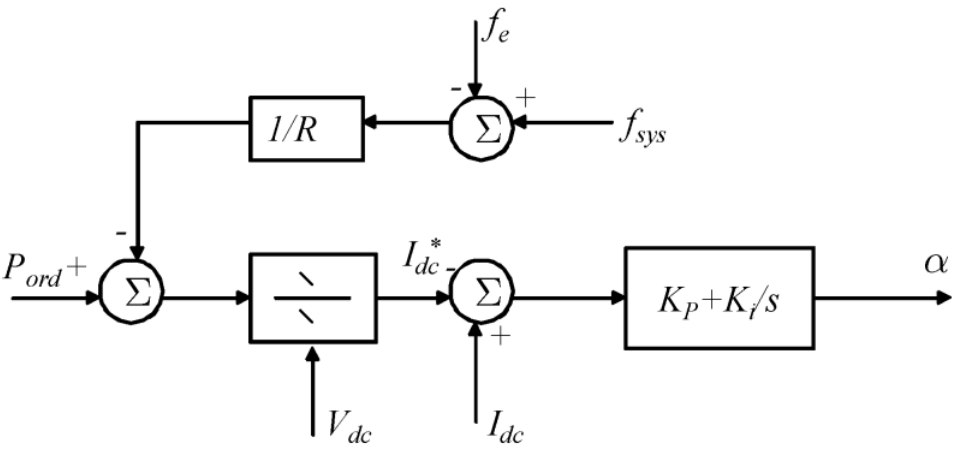

Figure 2.19: HVDC-LCC firing angle control proposed in [10]

The converts' power is defined by the steady-state active power setpoint (P_{ord}) and an additional power set-point that is result of the onshore AC frequency deviation, after being adapted by the frequency/active power droop, defined by $1/R$ in the Figure 2.19. Then, based on the DC voltage the control loop is able to set a new current set-point (I_{dc}^*). The error existing between the current set-point (I_{dc}^*) and the actual converter current (I_{dc}) feeds a Proportional-Integral (PI) controller that defines the accurate HVDC-LCC firing angle α. Similarly to [72], the power

imbalance in the offshore AC grid will provoke a frequency deviation. For this specific case, authors have endowed offshore WF with DFIG with capability to provide primary frequency support as presented in Section 2.2.2. Results highlight effective frequency reproduction at offshore level and deployment of active power at WF-level, contributing to the frequency support. Authors have also tested the proposed control for a set of frequency/active power droop values. The main conclusion is that the contribution is greater with higher droops values since it corresponds to a higher induced offshore frequency disturbance.

In the work conducted by Li it et al. in [73], authors had assessed the feasibility of deployment of primary frequency control facing an under-frequency deviation. To achieve such fulfilment the DFIG-based wind farm has been set to operate in a de-load regime through the previously presented in Section 2.2.2, pitch de-load mechanism. Additionally authors have investigated the feasibility of emulating the inertia behaviour in the DFIG wind turbines testing also the performance of this service deployment in the chain system composed also by the HVDC-LCC onshore and offshore converters, as well as the DC cable circuit. The control mechanism for inertia emulation is in-line with the proposed in [37], where the rotor's kinetic energy is delivered as active power increase through an additional proportional control loop based on the frequency derivative. Results allowed verifying that both primary frequency control and inertia emulation are successfully accomplished and bringing benefits to the AC onshore grid frequency recovery.

Recently, this topic of primary frequency control provision by offshore WF has been addressed by Chaudhary in [74]. In this work, author has studies the provision of primary frequency control by offshore WF connected by HVDC-VSC in a point-to-point configuration. Three strategies were assessed:

- Dedicated Communication channel between onshore and offshore HVDC-VSC plus additional control to replicate the onshore frequency at offshore level: The AC onshore frequency measurement is transmitted to the offshore HVDC-VSC that is able to place a proportional offshore frequency.

- Dedicated Communication channel between onshore HVDC-VSC and each Wind Turbine: A communication link transmits the onshore AC frequency measurement to the offshore HVDC-VSC that is responsible to transmit the signal to each offshore WT.

- Cascaded control scheme (implemented at offshore VSC level) based on the DC voltage/Offshore frequency droop: The onshore AC frequency disturbance is translated as a DC voltage variation (imposed by the onshore HVDC-VSC). At the other cable ending, the offshore HVDC-VSC is able to detect the voltage variation and set a proportional AC offshore frequency value.

The three proposed approaches were able to cope with the frequency regulation services. The offshore WF responded to AC grid frequency increase and decrease. Author have also considered the existence of delays in the communication channels and concluded that a $100ms$ delay (which is a reasonable latency for dedicated communication channels), did not significantly impact on the global response regarding frequency support services. However, an important issue regarding the adoption of communication infrastructure for this kind of service provision is the communication reliability, which was not tackled. In fact, relaying in te communication channels brings additional complexity for system operation, which may contribute to global system availability in case of failures occurring in the communication system.

Regarding the application of primary frequency control in MTDC grids, recent work conducted by Chaudhuri *et al.* has been published in [75]. The test system consisted on a MTDC grid interconnecting synchronous AC areas. The approach followed consisted on enhancing the the active power control, which originally was only composed by DC voltage/Active power droop, with an extra control rule dictated by an AC frequency/Active power droop. This enhancement behaviour minimizing the frequency deviation on each correspondent AC area. Authors have concluded that the MTDC interconnected DC areas are able to cooperate towards the frequency control provision of a given disturbed area. In fact, the converters autonomously re-dispatch the power extraction/delivery amount to minimize the DC voltage error, culminating in a successful Active power/frequency control. With this approach authors also have demonstrated that for primary frequency control provision, there

is no need of creating communication channels between the HVDC-VSC. Also, the adoption of local controllers presents satisfactory results thus not requiring the settlement of a centralized control infrastructure that increases the costs and decreases the overall system reliability. However, the primary frequency contribution is achieved by the re-dispatch of active power within the DC grid. So, the lack of active support from the AC generators is enhancement not performed in this paper.

The recent work presented by Zhu *et al.* in [76] exploits the topic of inertia response provision by a HVDC-link. Authors emulate the AC onshore frequency deviation as a DC voltage variation. The system gives the responsive active power injection symmetrically to the DC voltage variation. Authors claim that the same approach can be adopted on MTDC systems. However, the significant inertia response is achieved by extracting stored energy at the HVDC-VSC capacitor bank and consequently the results show a its impacts on the AC onshore system frequency rate-of-change and support. However, authors have adopted a 7.5 mF HVDC-VSC capacitor which is typically 100 times greater than the common practice value for the same power and voltage application [77], [78].

Fault Ride-through Provision by HVDC-connected Offshore Wind Farms

The FRT, as described in Section 2.2.2 is one of grid codes requirements and basically consists on the ability of a given generation facility have on remaining connected to the grid during voltage sags typically resulting from AC grid faults. As highlighted in Section 2.4.3, HVDC-VSC technology is able to operate under low AC voltage since the commutation of the electronic valves is forced and does not rely on the grid voltage to be induced. Nevertheless, according to several studies, additional challenges arise on HVDC links in case of AC network faults.

The work conducted by Ramtharan *et al.* presented in [79], assess the provision of FRT by wind farms connected through DC transmission systems. The adopted with wind farms were based on fully rated converter wind turbines.

The aforementioned challenge consists on a DC voltage rise during the AC-side voltage sag, led by the reduction of active power extraction capability at the onshore HVDC-VSC with low AC voltage. In order to deliver the pre-disturbance

active power, the converter will increase the current output during the voltage sag. However, the current excursion is limited by the maximum current that the onshore HVDC-VSC has been designed to deal with (physical limitation of the converter). As referred, the active power delivered by the converter will be limited. Within the DC grid, this active power will be accommodated at the HVDC-VSC capacitors, leading to a DC voltage rise. DC voltage mechanisms are then required to quickly mitigate the DC overvoltage magnitude. The maximum time to promote the DC voltage control can be expressed by equation 2.1.

$$T = \frac{C}{(P_{Grid} - P_{Grid-f})} \times (V_{dc-max}^2 - V_{dc-th}^2) \tag{2.1}$$

Where C is the capacitance value, P_{Grid} is pre-fault power injected to the grid, P_{Grid-f} is the power injected to the grid during the fault V_{dc-max} is the maximum admissible DC voltage and V_{dc-th} is the DC voltage threshold for operation of DC voltage regulation mechanism. Authors were able to calculate the maximum time for providing effective DC control for a HVDC link at 140 kV interconnecting a 50 MW wind farm with an equivalent capacitance of 50 μF and a threshold voltage of 145 kV. For a severe fault occurring on the onshore HVDC-VSC terminals leading to null power output and to guarantee that the DC voltage does not overpass 170 kV, the dissipation mechanism must act within 24ms. This short time for effective DC voltage control is crucial when choosing between the conventional methods. Authors have studied the effects of communication and the inherent delays and have concluded that a small delay of about $10ms$ can lead the failure on succeeding with the DC voltage control. Alternatively, authors have proposed the adoption of the DC overvoltage as the trigger for the DC voltage control scheme installed at offshore converter level. The DC voltage control can be achieve through three schemes using the DC voltage rise as trigger:

- **De-loading**: The offshore HVDC-VSC detects the DC overvoltage and sends a signal to every WT through fast communication channel. During the fault the WT rotor speed increases, the excess power is converter into kinetic energy at WT-level.
- **Short circuting**: The offshore HVDC-VSC places a null voltage at the AC-side. The WT, with fault ride-through capability are able to withstand the

voltage sag and reduces the active power injection. For this specific case, it is required offshore HVDC-VSC to have a high current rating to deal with the transients (from setting the AC voltage to null to the WT detect it and reduce the power injection).

- **Chopper resistor**: Connecting a chopper resistor in the DC link, responding to the DC voltage rise by dissipating power as heat. This strategy has the drawback of requiring a chopper breaking resistor equal to the WF rating.

The achieved results illustrate an effective DC voltage control on the three proposed DC voltage control approaches.

A similar study was conducted by Feltes *et al.* in [80]. Authors have highlighted the previously mentioned DC overvoltage during onshore AC fault and presented solutions to control the DC voltage. The first approach consisted on installing a DC chopper at the offshore converter DC terminal. This device is controlled by a DC voltage/Active power droop: DC voltages above a given threshold should trigger the control of power dissipation proportionally to the DC voltage. This scheme allows reducing the excess power on the capacitors, reducing the overvoltage magnitude. Despite presenting satisfactory results, this scheme may not be attractive from the economic perspective since it requires a full-scale DC chopper with at least the same installed power as the offshore WF (to cope with severe AC faults leading full power reduction). Alternatively, authors have presented a scheme to reduce the power injected by offshore HVDC-VSC through a power reduction control scheme installed at its level, while maintaining the AC offshore frequency constant. To do so, a communication channel was considered (between onshore converter and offshore converter) to transmit the onshore AC voltage to the offshore HVDC-VSC. Despite being presented, authors do not emphasize this approach since it may cause AC overvoltage at offshore WF grid and mechanical stress on the offshore WT. As solution for communication-based approach, authors have suggested a control scheme based on a communication channel between onshore and offshore converters and an additional communication channel between the offshore converter and each WT. That way, during fault the onshore converter should be responsible by calculating the maximum power transfer capability, transmit it to the offshore converter

that have to calculate the power reduction share to be transmit to each WT. Authors concluded that such complex communication channel and the inherent delays could not cope with the fast time requirements for controlling the DC voltage rise. Authors decided then to eliminate the communication channel between the onshore and offshore HVDC-VSC and instead, similarly to the approach adopted in [79], use the DC overvoltage as triggering signal to the offshore converter. Additionally, the adoption of communication between the offshore converter and the offshore WT was also abandoned since is not effective for fixed-speed wind generators. Authors have proposed a new control approach that rely on the DC voltage (without communications between HVDC-VSC), consisting on a DC voltage/AC offshore frequency droop control. This control scheme requires some modifications at WT-level to ensure the frequency/power response. Results presented that offshore WF were able to reduce the injected power contributing towards the DC voltage control. Alternately, authors have presented a AC voltage-based approach. This control scheme consists on endowing the offshore HVDC-VSC with a DC voltage/AC voltage. So, a DC overvoltage should be reproduced as a AC undervoltage. It is stated that by adopting this control approach, FRT-compliant WT are able to reduce the active power injection, contributing to the DC voltage control. This paper gives a quite extensive overview of methodologies for endowing a point-to-point HVDC-VSC connected WF with FRT capability. However it fails on analysing the proposed control approaches for the different WT technologies and the extendibility of the concept of DC grids.

The work conducted by Vrionis *et al.* in [81] proposes a fuzzy control mechanism to deal with the FRT provision in a point-to-point offshore WF connected by HVDC-VSC. The proposed approach consists on reducing the power injected at the offshore level by acting on the offshore HVDC-VSC. A fuzzy controller is responsible by quantifying the AC onshore-side fault magnitude according to the DC voltage rise magnitude and acts on the offshore HVDC-VSC control, reducing the injected power to the DC grid. From the offshore WF AC grid a power imbalance takes place. However, the offshore WF was composed by induction generators that experienced frequency variations and were able to continue operating since the time fault duration is relatively small. In this section several research studies regarding FRT

capability on HVDC-VSC links. The gap of research works conducted in HVDC-LCC technology is related its lack of capability on complying with such requirement. In fact, HVDC-LCC are composed by naturally commuted power electronic valves (eg:. thyristors), which rely on the AC voltage amplitude to provide the valve triggering. Thus, an AC voltage sag culminates in the disconnection of the converters. The works presented are consensual on the aspect of development of a DC voltage rise during the low voltage sag. The challenge for the compliance of FRT requirement is not directly connected to the HVDC-VSC technology (which is able to remain connected during an AC voltage sag) but with the DC voltage control within the DC link. Several approaches for DC voltage control are proposed on the analysed literature. The contributions are coordinated on defining control strategies to reduce the offshore incoming active power or dissipate it, in order to reduce the capacitor power that provoke the overvoltage.

2.4.6 Operation of DC Grids Following the Loss of a Converter

The loss of a converter is a situation that can occur due to an AC-side fault and consequent associated converter AC breaker tripping due to protective relay functions, an internal converter fault leading to the converter disconnection due to converter fault or malfunction or a DC-side fault.
From the offshore HVDC-connected WF perspective, the loss of an offshore converter (i.e.:. Converter that connects the WF to the DC grid) will culminate in the loss of WF power injection and on a transitory DC voltage reduction. Nevertheless, no potential dangerous situation will occur for the DC grid and the remaining connected converters. However, the disconnection of an onshore converter, assuming that this is a power evacuation point from the DC grid to the AC system can compromise the whole DC grid operation as well as components. This topic has a strong similarity to the FRT provision since is also a situation of DC power imbalance. Nevertheless on contrary to FRT, the loss of a converter has a wider time range characteristic and can even be a permanent situation that may require human intervention and repair actions. The effects on the DC voltage rise will be also permanent and if no corrective mechanism acts promoting the DC power balance an uncontrollable DC voltage rise will take place.

This specific situation in a point-to-point connection may be amended by the disconnection of offshore HVDC-VSC and consequently offshore WF injection. Despite the connection link is lost, no dangerous DC voltages will be induced on the link, capacitor banks and HVDC-VSC.
For the case of a MTDC grid, the loss of a converter brings more challenge requiring the adoption of enhanced control strategies. In fact the procedure of disconnecting converters may bring additional problems for the interconnected AC systems related with stability aspects.

The work conducted by Lu *et al.* presented in [82], presents an approach for dealing with DC overvoltage during the loss of a converter in a MTDC grid. The DC grid considered in the paper aimed on providing connection between onshore AC areas. So, two situations may occur: (1) if the lost converter was importing power to the DC grid, a negative power imbalance will take place thus; a DC voltage reduction will also take place not putting in danger the operation of the DC grid as well as any component. (2) If the lost converter was exporting power from the grid then, a positive power imbalance will take place leading to DC overvoltage occurrence. For the case suited in the paper, authors have considered one of the HVDC-VSC as DC voltage Regulator consists on provide a fixed DC voltage and supply an amount of power to maintain the power balance as a slack bus on AC systems. The additional converters will collect/inject power according to specific set-points. The proposed control schemes are implemented at the DC voltage regulator HVDC-VSC and can be divided in two approaches:

1. ΔP_n control: The DC voltage feeds a PI controller that determines a given ΔP_n, active power amount to be reduced.

2. ΔU_{ref} control: The DC voltage rise will provoke the reference voltage to drift. Thus a PI controller is responsible to generate a transitory DC voltage value to guarantee the operation of the DC grid.

The title of this paper suggests that the control approaches are valid for the permanent loss of a converter. However, on the paper authors explain that the cases evaluated are based on a loss of a converter followed by a quick recovery (typically $100ms$ was considered). This fact turns this paper into another approach for FRT

provision.

At the moment there is a gap in the literature related with the operation of DC grids facing a permanent loss of power export capability due to the loss of one of extracting converters (commonly onshore converters on offshore WF connection cases). This topic has been focused in this thesis and is further detailed on Chapter 4.

2.5 Summary

The literature analysis performed in this chapter allows to conclude that the adoption of offshore WF is inevitable to achieve the targets of RES-E share in Europe. Along to the integration of offshore WF, comes the adoption of HVDC technology as the mean of providing large amount of offshore WF power through longer distances.

Modern WT are able to provide a set of advanced services to the AC grids. As reported in this chapter, those services started being required by TSO to maintain the power system stability levels with high level of wind power penetration. However, the adoption of HVDC technology as the mean of interconnection of offshore wind power, disables offshore-located WTG on participating in the AC mainland grid support.

Some research works have tackled specific issues regarding the provision of advanced services to the AC system, aiming at increasing the credit on the adoption of HVDC technology as the mean of interconnection of offshore WF. The most emphasized ones were related with primary frequency support and FRT capability.

Simultaneously, several initiatives points towards the adoption of DC grids, namely on Northern Sea, in Europe, as the mean of establishing a sustainable infrastructure for offshore and RES-E integration. The integration of massive amount of offshore wind power will require HVDC technology as the mean of connection. The adoption of HVDC brigs challenges for the provision of primary frequency control, inertia emulation and FRT capability. The literature review performed in this

chapter identifies the major contribution on these topics. However, there is a gap regarding advances related to the aforementioned topics, applied to DC grids.

3

Modelling of Multi-terminal HVDC Grid for Offshore Wind Power Transmission

3.1 Introduction

This chapter aims to present the models adopted for each component followed by the presentation of Multi-terminal HVDC (MTDC) grid simulation platform, developed in Matlab/*Simulink*, which served as the simulation framework for the developments of this thesis. A comprehensive description of each constituent model (from the offshore wind turbine to the AC onshore network) and the interactions among them are performed in this chapter. Finally, a set of simulation tests has been performed to assess the simulation platform performance, its operation under different DC grid topologies and the proposed base-case HVDC-VSC control philosophies.

3.2 Modelling Objectives and General Considerations

The Multi-terminal HVDC grid is a DC cable circuit that interconnects N offshore facilities to M onshore mainland AC grids, as it is depicted in Figure 3.1. The DC grid topology may vary according to factors such as interconnection and reliability requirements. Normally, the interconnected grids are AC-based (at offshore and

onshore level) so, there is the need of having an interface converter associated to each DC grid terminal.

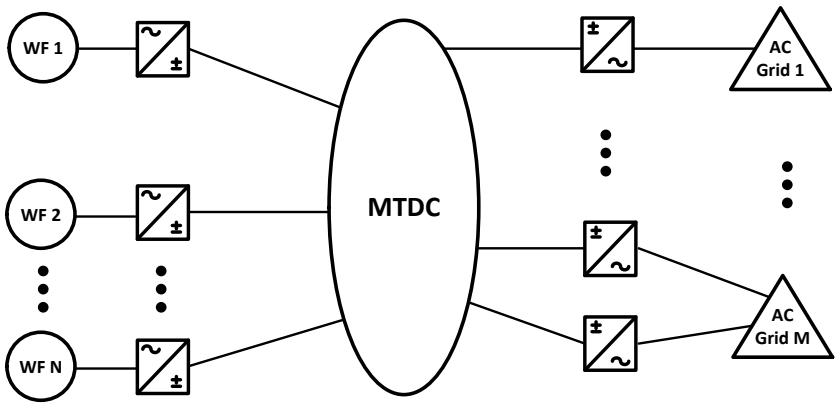

Figure 3.1: Conceptual architecture of MTDC grid

Thus, each onshore DC terminal may perform as a power injection or collection node, allowing the DC grid to interconnect the AC mainland systems. Also, the promotion of power exchange between onshore mainland AC areas can be performed allowing the DC grid to act as a backbone for the AC mainland grids.

Simulation models of the MTDC grids are fundamental to evaluate their impacts on the AC grid dynamics, as well as for the development of advanced control schemes regarding the implementation of system services, which is the main objective of this thesis. The rationale of the developed MTDC model consists on representing the dynamics inherent to the DC grid and the associated converters in a time frame of mili-seconds [80]. Thus, detailed models of HVDC converters representing the switching of converter valves (IGBT or GTO) are not necessary for the analysis performed in this work. In fact their inclusion would represent an additional computational burden, limiting the simulation time range.

The approach followed in the modelling process consisted on representing the power system in the dq reference frame. The quantities such as voltage and currents were represented by the average value, also called as Root Mean Square (RMS)

value. This approach neglects the fast transients but on the other hand, allow representing more complex systems and performing simulations with increased time (from mili-seconds to thousand seconds). Several commercial software for power system dynamic analysis adopt the same computational model representation (e.g.:. PSS/E, Eurostag). Nevertheless, none has the particular MTDC grid models for the purpose of this study. So, the development of this simulation platform has been fundamental for the accomplishment of the research topics proposed within this thesis.

The setup of the whole platform was based on the development of user-defined models in MATLAB/*Simulink* without relying on library models. The MATLAB/ *Simulink* served as the calculation engine to solve the mathematical models, namely the differential equation system, through its dedicated solvers. The models were fully represented by mathematical equations (state and algebraic) in block diagram following the per unit representation. To allow further re-configuration, each component has been implemented as a single block, allowing the interconnection and reconfiguration of the blocks to build DC grids with different topologies (e.g.:. varying the number of HVDC-VSC).

The per unit representation is very common in AC power systems. Nevertheless, its application to DC systems presents some specificity. According to [83], the following bases are used for computing DC per unit quantities:

$$V_{base}^{DC} = V_{base}^{AC} \tag{3.1}$$

$$I_{base}^{DC} = I_{rate}^{DC} = I_{n}^{DC} \tag{3.2}$$

$$S_{base}^{DC} = V_{base}^{DC} \times I_{base}^{DC} \tag{3.3}$$

$$Z_{base}^{DC} = \frac{V_{base}^{DC}}{I_{base}^{DC}} \tag{3.4}$$

3.3 Modelling HVDC Voltage Source Converters

The HVDC-VSC are responsible for interfacing the offshore AC wind farm grid to the DC grid, as well as for interfacing the DC grid and the AC onshore grid. These

converters were considered to be bi-directional meaning that direct and reverse powerflows can occur from and into the DC grid. The representation of HVDC-VSC for transient stability studies followed the general approach presented in the literature [84][85], where the converters are represented by the control transfer functions.

3.3.1 Offshore HVDC-VSC

The offshore converters interface the offshore WF AC grid and the MTDC grid (as previously stated in Section 3.2). The offshore WF grids were assumed to be operated in AC. Usually, offshore WT are organized in rows and are interconnected to a central collection point through different feeders. For this specific case, a lumped model has been adopted, to represent the whole offshore WF. The adoption of lumped model is a common practice in dynamic models for transient stability studies [12]. The rationale of this approach is to reduce the computational burden inherent to the representation of all generators, replacing it by an equivalent generator that represents the general dynamics of all the generators.

The offshore converter station is responsible for controlling the voltage magnitude and frequency of the AC wind farm network and allows the transfer of all the generated wind power to the HVDC grid. Following the considerations proposed in the literature, the offshore HVDC-VSC has been modelled in the dq frame by its control loops [85]. The d frame is responsible by setting the d axis voltage while the q frame is responsible by controlling the q axis voltage. This fact turns the offshore HVDC-VSC into a grid forming converter. Regarding this definition, according to the literature, there are two major converter types [86]:

- Grid forming VSC: the grid forming VSC defines the grid voltage and frequency reference by assuring a fast response in order to balance power generation and loads;
- Grid-tied VSC: The grid-tied VSC is responsible by controlling the active and reactive power injection towards an existing AC grid.

The general overview of the control scheme is depicted in Figure 3.2. The controllers were considered to be proportional-integral (PI), following the general consideration

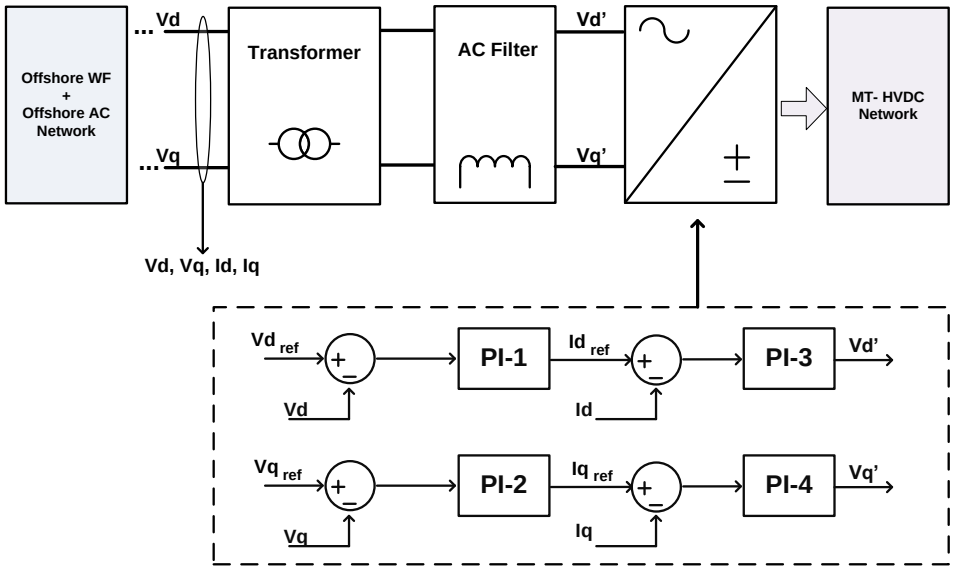

Figure 3.2: Offshore HVDC Voltage Source Converter control loops

that can be found in the literature [85],[67], [80]. The proportional section aims at stabilizing the input signal while the integral section aims at offsetting the permanent error. PI controllers were implemented following the Matlab/*Simulink* mask blocks' concept. The controller structure, located inside the PI blocks are composed by the two aforementioned gains organized as depicted in the Figure 3.3. The out-

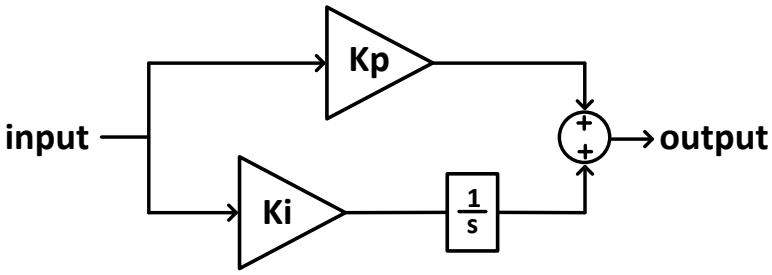

Figure 3.3: Proportional Integral controller

put signal is obtained by the sum of the input signal after being affected by the proportional gain K_p and the integral gain K_i. Generally the input signal is the error signal obtained by the difference between an actual value (measured) and the

set-point (target) value.

From the dynamic modelling perspective, the converter is a voltage source ($V^{'}d+ jV^{'}q$) behind an impedance (impedance defined by the AC filter and the coupling transformer, according to the scheme depicted in the Figure 3.2). The objective of the control loops consists on defining the voltage on the dq frame at the converter level to obtain the pre-defined voltage (in dq frame) at the impedance opposite terminal. To determine the voltage at the converters terminal, namely $V^{'}d$ and $V^{'}q$, the control loops need to acquire the voltage profile at the impedance opposite terminal, Vd and Vq, as well as the current along the impedance Id and Iq. Based on the error existing between the Vd, Vq and their correspondent reference value, Vd_{ref}, Vq_{ref}, the first PI controllers (PI-1 and PI-2 according to scheme depicted on Figure 3.2), usually named as outer control loop, generate the Id_{ref} and Iq_{ref} current reference values. These current values corresponds to the current that should be flowing in the coupling impedance, in order to produce the target Vd_{ref} and Vq_{ref} voltage references. The second PI group (PI-3 and PI-4 according to scheme depicted on Figure 3.2), also named in the literature as inner current control loop, are responsible by controlling and offsetting the error existing between the id and iq actual current values and the previously generated current references, by imposing the $V^{'}d$ and $V^{'}q$ voltage values at the converter internal terminal. This cascaded scheme is able to control the internal converter output voltage in order to obtain the respective current that will lead a voltage drop on the impedance which then give origin to the targeted voltage profile at the AC network slack busbar. By controlling the internal converter voltage based on the flowing current, this converter is able to guarantee that all the generated power is delivered to the DC grid and simultaneously maintain the AC voltage profile on the AC offshore grid on the specified value.

Regarding the AC grid offshore frequency, its value can be defined as fixed (e.g.:.50Hz) or otherwise, may be defined by additional control-loops that are going to be further presented and discussed in Chapter 4 and Chapter 5.

3.3.2 Onshore HVDC-VSC

The onshore converter is responsible for interfacing the MTDC grid to the respective AC mainland grid. Similarly to the previously presented converter, the onshore converter is also a HVDC-VSC with bidirectional powerflow capability. For this specific case the bi-directionality is a crucial factor that enables the MTDC grid not only on establishing power flows from the incoming power from offshore WF to the AC mainland grids, but also performing as backbone for the AC interconnected mainland grids by allowing inter/AC mainland areas power exchange through its infrastructure.

Once again, based in the literature of HVDC systems, the onshore HVDC-VSC was also modelled by its control loops in the dq frame. The overview of the control-loops is depicted in the Figure 3.4. On contrary to the offshore converter, the onshore HVDC-VSC controls the active and reactive power injection to the AC mainland grid. The converter relies on the DC grid voltage balance at the associated DC grid terminal in order to determine the active power extraction amount. Based on the proposed in the literature, there are two major control modes that can be set at the onshore HVDC-VSC [85].

- **Master Control:** Within a DC grid, one of the onshore HVDC-VSC is defined as master, being responsible for accommodating the DC power fluctuations while the others onshore HVDC-VSC inject or collect active power according to a pre-set, user-defined DC voltage value;

- **Distributed Control - Power Sharing:** DC power fluctuations are shared among the connected onshore HVDC-VSC through a DC voltage distributed control approach. The amount of active power extracted by each converter is based on a DC voltage/Active power droop-based control rule. Each onshore HVDC-VSC will assume a active power amount proportional to the DC voltage available at its associated DC-side terminal. That way, the effects arising from wind power fluctuations can be mitigated from the AC grids perspective, since they are shared among the interconnected AC mainland areas.

Details regarding the HVDC Onshore VSC are exploited on Section 3.7.2.

Similarly to the addressed to the offshore converters, in Section 3.3.1, the onshore HVDC-VSC behaviour was also characterized by four PI controllers following the scheme depicted in the Figure 3.4.

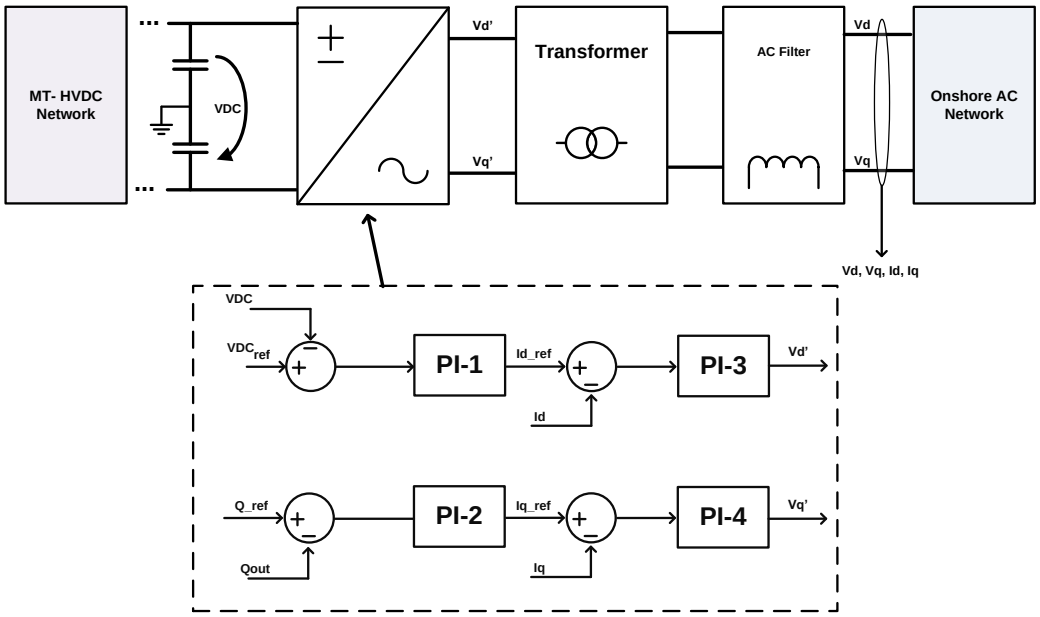

Figure 3.4: Onshore HVDC Voltage Source Converter control loops

For this converter, similarly to the previously presented offshore HVDC-VSC, PI-1 and PI-2 are the outer control-loop while PI-3 and PI-4 are the inner current control-loop. The PI-1 controller is responsible to set the Id_{ref} current reference based on the error between the associated HVDC-VSC DC voltage (VDC) and the reference specified DC voltage (VDC_{ref}). The PI-2 controller sets the Iq_{ref} current reference based on the error between the actual reactive power output Q_{out} and a reference pre-specified reactive power value Q_{ref}. The strategies to feed the PI-1 and PI-2 controllers may be enhanced according to the operational objectives. Nevertheless, this specific topic will be further detailed in the Section 3.7.2. The Vd and Vq values are respectively set by the PI-3 and PI-4. Based on the error between the Id_{ref} and the actual Id current, the PI-2 sets the respective Vd voltage.

Similarly, the PI-4 sets the Vq voltage based on the error between the Iq_{ref} and the actual Iq current measurement.

3.4 Multi-terminal DC Grid Model

The approach followed for the MTDC grid model intended to be as general as possible aiming at enabling an easy adaptation for several DC grid topologies. The development of the DC grid model is based on the general architecture depicted in Figure 3.1, MTDC is regarded as the infrastructure that provides the interconnection of N offshore WF with M mainland onshore AC grids.

Regarding the DC cable circuit, bipolar structure is often adopted. This means that the DC cable circuit is operated with symmetrical DC voltages, $\pm V_n$. The advantages of this adoption are related with the increase of the transmission capability and the reliability of the DC grid, by allowing to be operated with just one pole in case of fault or failure. For the studies developed in the framework of this thesis, the converter topology and DC-side faults are not going to be analysed. Thus, the DC cable circuit can be represented by a single pole incorporating the parameters of both poles. The schematic depicted in Figure 3.5 highlight the simplification which consists on summing the positive and negative pole resistance, inductance and the capacitance.

The approach adopted for the modelling process followed the proposed in [87], by considering the DC cable as a series resistance (R) and inductance (L) which represents the concentrated parameters of a given DC cable branch. In addition, the DC cable capacitance has also been considered enhancing the proposed in[87], following a Π section representation. Each cable branch or by other words, cable segment, was represented by a Π-section. For the particular case of the cable terminals connecting to the HVDC-VSC DC-side terminals, its capacitance gets physically connected in parallel to the HVDC-VSC capacitor banks as illustrated in Figure 3.5. Normally, the cable capacitance is much smaller than the converters' capacitor bank capacitance. However, both were summed, attaining the equivalent capacitance C_{eq}, generalizing the modelling approach for further applications. Since the HVDC-VSC capacitor banks have been modelled on the associated DC cable terminal, the DC

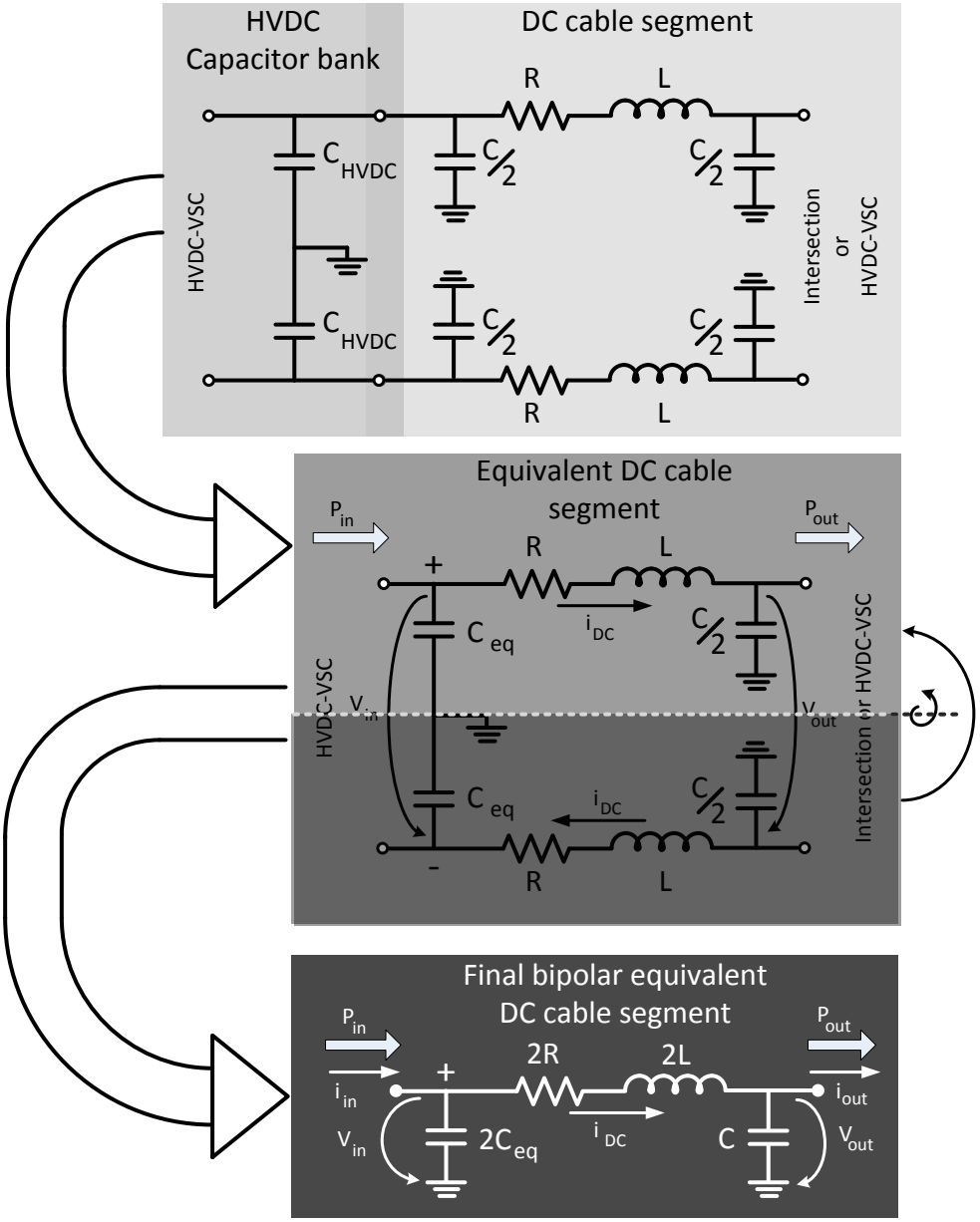

Figure 3.5: DC cable electrical parameters representation

cable model was implemented as a block with active power input and active power outputs. Inside the block, mathematical equations describes the cable circuit according to the given DC grid topology. Based on the schematic depicted in Figure 3.5, a set of algebraic and state equations can be obtained to determine the output

power according to the input power and the DC voltage profile, as follows:

$$i_{in} = \frac{P_{in}}{V_{in}} \tag{3.5}$$

$$i_{out} = \frac{P_{out}}{V_{out}} \tag{3.6}$$

$$\frac{\partial V_{in}}{\partial t} = \frac{i_{in} - i_{DC}}{2C_{eq}} \tag{3.7}$$

$$\frac{\partial V_{out}}{\partial t} = \frac{i_{DC} - i_{out}}{C} \tag{3.8}$$

$$\frac{\partial i_{DC}}{\partial t} = \frac{U_{in} - U_{out} - 2R \times i_{DC}}{2L} \tag{3.9}$$

Where i_{in}, P_{in} and V_{in} are respectively a DC current input, DC power, and the DC voltage at the respective node. Analogously, i_{out}, P_{out} and V_{out} are the output values for the output current, DC power and the DC voltage at the opposite DC cable segment node. The current i_{DC} is the effective DC current that flows in the DC cable segment, R and L are respectively the DC cable resistance and inductance. The state and algebraic equations system can be extended to model any MTDC grid topology. To do so, it is necessary to describe the DC grid infrastructure electrical representation branch by branch, respecting the Kirchhoff's law. It is also important to guarantee that the DC capacitor bank is included in the DC grid representation at each converters' interconnection terminal.

3.5 Offshore Wind Farm

The offshore WF were considered to be equipped with AC wind turbines, namely DFIG and PMSG wind turbine technologies which, as previously stated, are assumed to be the most promising technologies for offshore application. The offshore WT are connected through an AC cable circuit aggregated in feeders and further connected to the Medium Voltage (MV) to High Voltage (HV) substation, located at the offshore converter platform station. Due to relatively small distance between the wind turbines and the offshore HVDC-VSC, a typical AC voltage of 30 kV has been adopted. Regardless of the offshore WT technology, each wind farm was modelled by a lumped model, representing a set of wind turbines. In addition to the representation of the AC offshore grid, and equivalent cable circuit, a step-up transformer

and the offshore HVDC-VSC filter, have been considered. The general overview of the offshore WF components and its connections is illustrated in Figure 3.6.

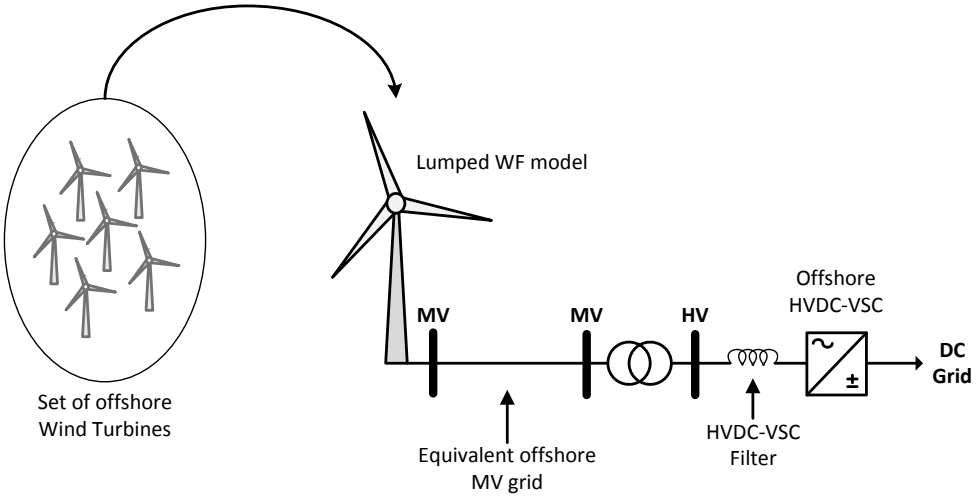

Figure 3.6: Schematic of offshore WF modelled components

3.5.1 Wind Turbine Aerodynamics

In order to test the proposed regulation schemes, the aspects of wind turbines aerodynamic behaviour were also considered. In this topic, a common representation has been shared among the DFIG and PMSG-based WT. Based on the literature of wind turbine modelling for dynamic studies, the extracted mechanical power (P_{mec}) can be determined based on the incoming wind speed P_{wind}, defined by the equation 3.10 [11].

$$P_{wind} = \frac{1}{2}\rho A V^3 (W) \tag{3.10}$$

where A is the swept area by the WT blades, ρ is the air density, P is the wind power and V is the wind speed. The wind turbine blades are not able to capture all the existing kinetic energy available on the wind. There is an aerodynamic relation which defines the amount of power that a given WT blade-set can transform into mechanical power. The denominated power coefficient C_p, defines that amount. According to the studies performed by Albert Betz in the $20th$ century, the maximum power that an airfoil-shaped body can extract from the wind occurs when the wind

speed that leaves the airfoil body is one third of the wind speed incoming to the same body. The theoretical maximum power that can be extracted from the wind is about 59.3% of the existing wind power. This coefficient as previously presented, the Betz coefficient, varies with the airfoil body characteristics. Modern wind turbine blades are able to capture about 40% - 50% of the existing wind power [88]. Nevertheless, the general expression to represent the mechanical power extracted from the wind by a WT can be expressed as presented in equation 3.11:

$$P_{mec} = \frac{1}{2}\rho \times C_p A V^3 \tag{3.11}$$

The equation 3.11 allows determining the mechanical power available at wind turbine generators shaft according to the existing wind speed, WT blade length, the air density and the WT aerodynamic power coefficient.
As previously described, the power coefficient C_p, has a maximum value which characterizes the maximum power that can be extracted from the wind by a given WT blade set. Nevertheless, this value can be reduced meaning that the WT blade-set becomes aerodynamically less efficient by capturing less power from the incoming wind. Since the WT blade is a non-deformable body, the reduction of the aerodynamic properties is achieved by acting on the angle between the blade cord and the incoming wind as depicted in Figure 3.7 and usually denominated a pitch angle (β). The pitch angle, can be modelled by rotating the wind turbine blades on the hub, over its own axis. In practice, a set of servo-motors are responsible by setting the position of the blades.

Another aspect that is extremely important to characterize the generated power at an electrical generator is the rotational speed ω. The rotational speed can be related with the wind turbine radius and the wind velocity. There is a factor that characterizes the relation between these two speeds, the tip-speed ratio λ which can be described by the equation 3.12.

$$\lambda = \frac{\omega \times R}{V_{wind}} \tag{3.12}$$

where λ is the tip-speed ratio, ω is the rotational speed, R is the wind turbine radius, or the wind turbine blade length and V_{wind} is the incoming wind speed.
According to the aerodynamic properties of a WT, the power coefficient varies with

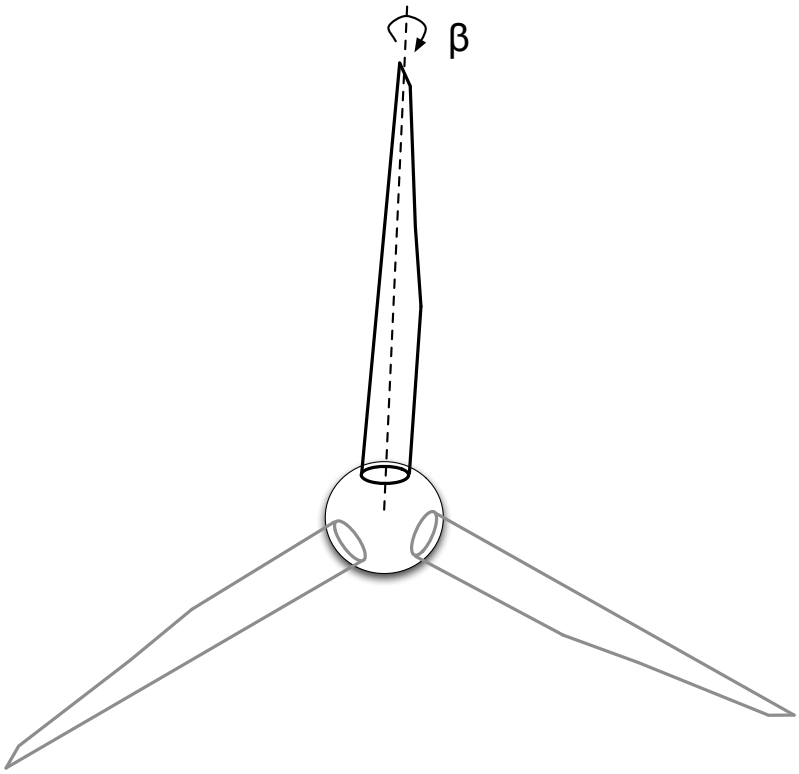

Figure 3.7: Wind turbine pitch angle mechanism

the pitch angle and the tip-speed ratio. Thus, the relation that describes the power coefficient variation for a variable speed WT can be described by the equation 3.13 [11]:

$$C_p(\lambda,\beta) = 0.22\left(\frac{116}{\lambda_i} - 0.4\times\beta - 5\right)e^{\frac{12.5}{\lambda_i}} \tag{3.13}$$

where λ_i can be defined by the equation 3.14:

$$\lambda_i = \frac{1}{\frac{1}{\lambda+0.08\times\beta} - \frac{0.035}{\beta^2+1}} \tag{3.14}$$

An example of the power coefficient under tip-speed ratio change for several pitch angles β is depicted in Figure 3.8.

Finally, the aerodynamic interactions of wind turbine can be represented by the mechanical form, through the mechanical torque available at the WT rotor according to the equation 3.15.

$$T_m = \frac{P_m}{\omega} = \frac{1}{2}\times\rho\times\frac{C_p(\lambda,\beta)}{\lambda}\times\pi R^2\times V^2(N.m) \tag{3.15}$$

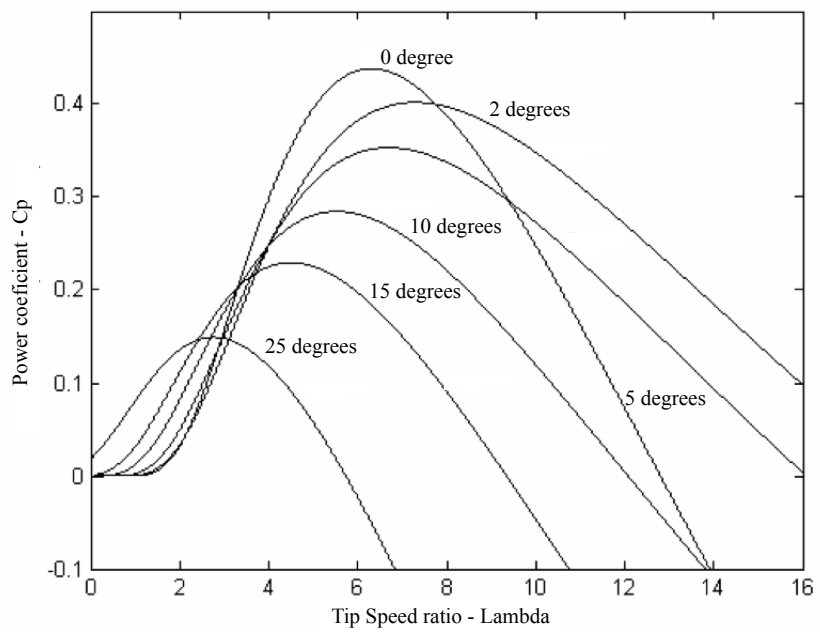

Figure 3.8: Power coefficient versus tip speed ratio for several WT blades' angle [11]

3.5.2 Wind Turbine Pitch-angle Controller

A pitch controller has been adopted in order to set the WT pitch angle and dynamically adjust its value. The control schematic is depicted in Figure 3.9. Based on the frequency error, determined between the frequency reference (f_{ref}) and the offshore frequency (f_{off}), a proportional active power reference(P_{ref}) is generated through an active power/frequency droop (K_{pf}). Then, the error between the P_{ref} and the actual generated power P_{gen} is set to a PI which determines the pitch position to be imposed to the actuator (modelled by a first order transfer function). Then, the pitch angle B rotation is limited by a rate limiter, limiting the maximum servo-motor excursion. Finally, the WT pitch blade is obtained and imposed on the WT blades through the adjustment of the aerodynamic equations.

3.5.3 Offshore WF Equipped with PMSG

The PMSG, as previously presented in Section 2.3.3, is a WT generator technology that is fully interfaced to the grid by a back-to-back AC/DC/AC converter. The generator has self-excitation promoted by permanent magnets placed in the generator rotor. The model for this generator comprises the mechanical and electrical

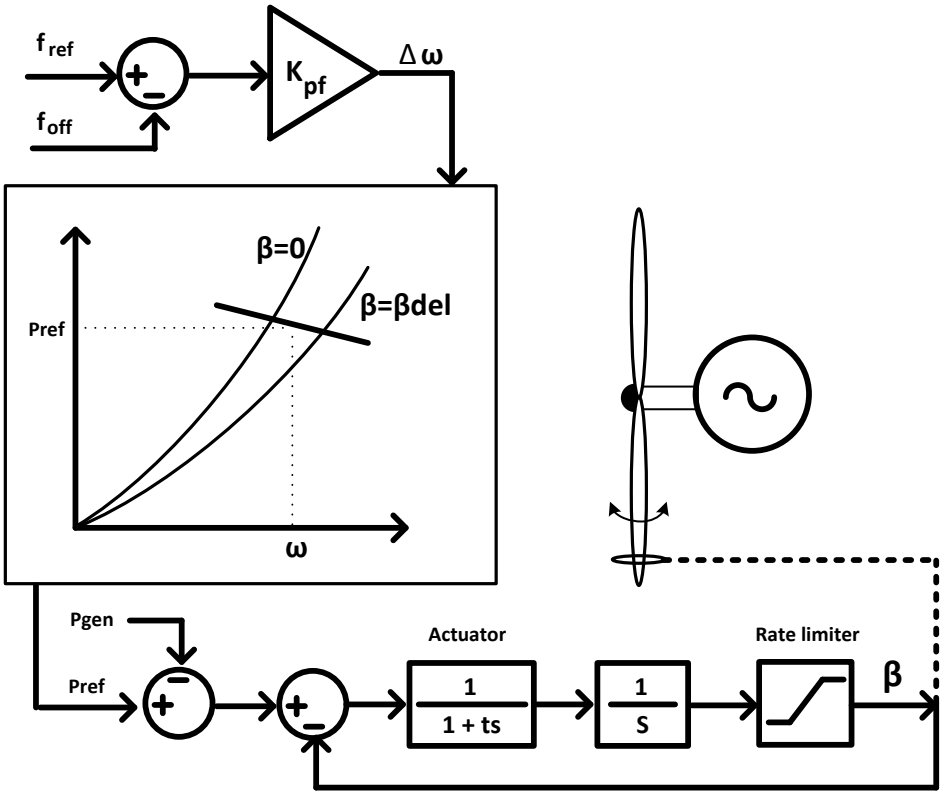

Figure 3.9: Wind turbine pitch angle controller

representation, interacted by the electrical and mechanical torque. The mechanical model was performed based on the equations that describe the mechanical behaviour of the generator. The electrical part was modelled taking into account the generator electrical equations and the integral converter control-loops both on the *dq* frame. It was considered that the distribution of the magnetizing rotor flux is sinusoidal. Thus, the voltage induced in the machine stator can be described by:

$$E = j \times \omega \times \psi = j \times 2\pi f \times \psi(V) \tag{3.16}$$

where:

- ω is the electric rotational generator speed (rad/s);
- f - electric frequency (Hz);

- ψ - excitation flux (Wb).

The voltages induced in the stator can be written in the dq frame according to the equations 3.17, 3.18 and 3.19.

$$u_{sd} = R_s i_{sd} - p\omega_r L_q i_{sq} + L_d \frac{di_{sd}}{dt} \tag{3.17}$$

$$u_{sq} = R_s i_{sq} - p\omega_r L_d i_{sd} + L_q \frac{di_{sq}}{dt} + p\omega_r \Psi_m \tag{3.18}$$

$$T_e = \frac{3}{2} p \left[\Psi_m i_q + (L_d - L_q)\, i_d i_q\right] \tag{3.19}$$

where:

- u_{sd} - stator voltage component referred to the d axis (V);
- u_{sq} - stator voltage component referred to the q axis (V);
- i_{sd} - stator current component referred to the d axis (A);
- i_{sq} - stator current component referred to the q axis (A);
- i_f - current in the field winding (A);
- L_d - stator inductance component in the d axis (H);
- L_q - stator inductance component in the q axis (H);
- p - number of pair of poles;
- ψ_m - excitation induced permanent magnets in the stator winding (Wb);
- T_e - electromagnetic torque (N.m).

In addition to the electromechanical model, the PMSG complete model also comprises the electronic interface converter model. Following the literature in [47], the power electronic converter has been represented by the control-loops of each converter together with the DC link representation as depicted in the Figure 3.10. The PMSG converters can be identified as Machine-side Converter (MSC) and the Grid-side Converter (GSC). Since the PMSG converters are VSC, independent control of active and reactive component was implemented in the dq reference frame. Besides the characterization of the converter control, it is also important to define

the control strategy to be adopted. According to the schematic depicted in Figure 3.10, it can be highlighted that the MSC extracts the generated power according to the machine speed. This particularity guarantees that the electrical is similar to the mechanical torque, preventing the generator instability due to over or under-speed.

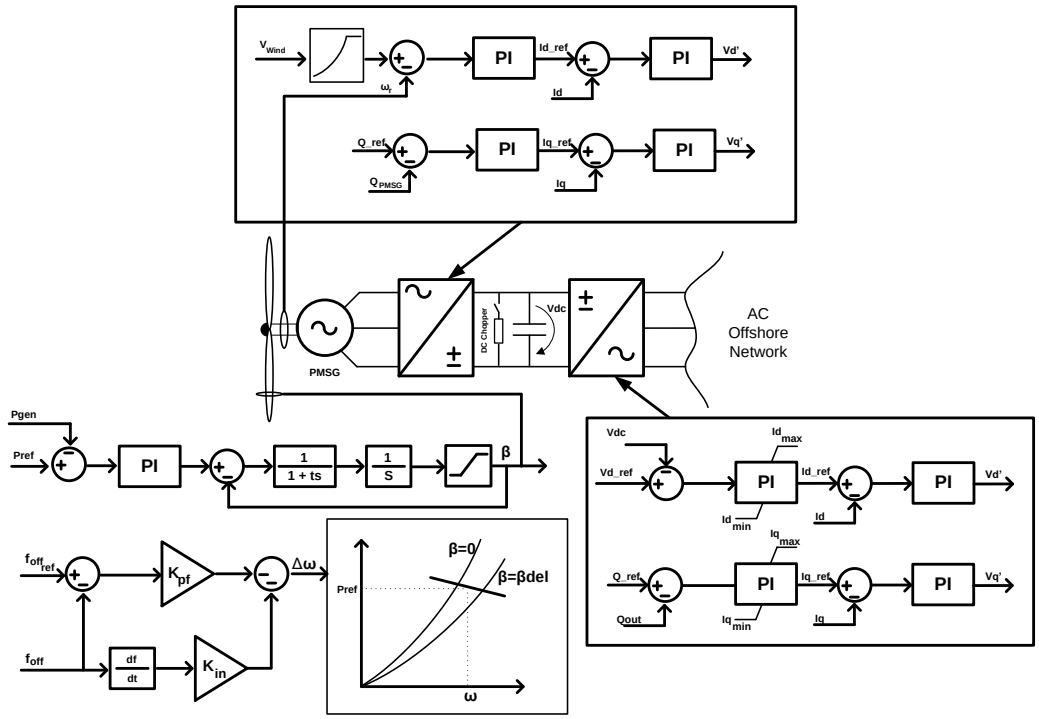

Figure 3.10: Control overview of the PMSG wind turbine dynamic model

The GSC is responsible by interfacing the DC link and the offshore AC grid. The control philosophy of this converter consists on extracting active power from the DC link in order to maintain a fixed predefined DC voltage value. In this specific task, two situations may occur. (1) the incoming wind power may increase leading to an additional power delivery from the MSC to the DC link. The DC link voltage will transiently rise being counteracted by power delivery increase at the GSC (from the DC link to the AC offshore grid). The other situation (2) can occur if suddenly the active power delivery at the PMSG is reduced. This fact will cause a DC link voltage reduction, being analogously counteracted by an active power delivery reduction performed by the GSC. As previously mentioned, the GSC is also able to

set independent active and reactive power control. So, the reactive power component control was set by the q frame to follow a predefined value Q_{ref}. Regarding the protection of the PMSG, current limiters are installed in the GSC (according to the illustrated in Figure 3.10). These limiters guarantee that the maximum converter current is not overreached during AC-side voltage sags. Additionally, a chopper resistor is incorporated in the DC-link (in parallel with the capacitor), to provide DC voltage control during AC-side voltage sag occurrence. The aspects related to the FRT and its control, are highlighted in Section 4.4.4.

3.5.4 Offshore WF Equipped with DFIG

In the process of definition of the offshore WF technologies to be adopted, the DFIG was also taken into consideration since is the most spread technology over the world for onshore application. Thus, it is expected that some offshore WF may be equipped with this type of wind generator. Similarly to the approach considered for the PMSG, the model developed for the DFIG shares the common aspects of the wind turbine aerodynamics, differing mostly in the electro-mechanical model.

As previously mentioned in Section 2.3.2 the DFIG is an induction generator with accessible rotor windings. The generator stator is directly connected to the AC grid while the back-to-back AC/DC/AC converter interfaces the rotor and the AC grid (as depicted in Figure 2.8).
Following the described in the literature, the mean adopted for establishing the DFIG model follows the common approach on transient stability studies, consisting on representing the generator in the dq frame as a voltage source behind a transient impedance ($3^{rd} ordermodel$). Assuming that there is no flux variation in the stator, the voltage source can be defined by:

$$v_{ds} = -R_s i_{ds} + X' i_{qs} + e_d \tag{3.20}$$

$$v_{qs} = -R_s i_{qs} - X' i_{ds} + e_q \tag{3.21}$$

$$\frac{de_d}{dt} = -\frac{1}{T_0} \times \left[e_d - (X - X')i_{qs}\right] + s\omega_s e_q - \omega_s \frac{L_m}{L_{rr}} v_{qr} \tag{3.22}$$

$$\frac{de_q}{dt} = -\frac{1}{T_0} \times \left[e_q - (X - X')i_{ds}\right] + s\omega_s e_d - \omega_s \frac{L_m}{L_{rr}} v_{dr} \tag{3.23}$$

where:

- v_{ds} and v_{qs} are the direct and quadrature stator voltages (p.u.);
- i_{qs} and i_{ds} are the direct and quadrature stator current (p.u.);
- v_{dr} and v_{qr} are the direct and quadrature rotor voltages (p.u.);
- i_{qr} and i_{dr} are the direct and quadrature rotor current (p.u.);
- e_q and e_d are the direct and quadrature e.m.f. (p.u.);
- X' is the transient reactance of the generator (p.u.);
- X is the open-circuit reactance of the generator (p.u.);
- ω_s can be defined as $\omega_s = 2\pi f_s$ where f_s is the system frequency;
- T_0 is the generator open circuit transient time constant (seconds);
- L_m is the magnetizing inductance (p.u.);
- L_m is the rotor windings inductance (p.u.).

The rotor currents can be determined in function of the stator current and the e.m.f. as described in the following equations:

$$i_{dr} = \frac{L_m}{L_{rr}} i_{ds} + \frac{e_q}{L_m} \tag{3.24}$$

$$i_{qr} = \frac{L_m}{L_{rr}} i_{qs} - \frac{e_d}{L_m} \tag{3.25}$$

The voltages and currents previously obtained by the algebraic and state equations are further combined with the rotor swing equation, which is defined by:

$$\frac{d\omega_r}{dt} = \frac{1}{2H}(T_m - T_e - D\omega_r) \tag{3.26}$$

Where T_m is the mechanical torque produced by the primer mover (in this case, the wind turbine as previously defined in Section 3.5.1), T_e is the electrical torque, D is the damping factor and H is the inertia constant that can be defined by the system composed by aggregation of the wind turbine inertia and the generator inertia (in seconds) and ω_r is the generator rotational speed. According to [12], the electrical torque can be attained by the equation 3.27.

$$T_e = e_d i_{ds} + e_q i_{qs} \tag{3.27}$$

The electrical and mechanical power can be defined as:

- For the Stator:

$$\text{ActivePower} : P_s = T_e\omega_r = v_{ds}i_{ds} + v_{qs}i_{qs} \tag{3.28}$$

$$\text{ReactivePower} : Q_s = v_{qs}i_{ds} - v_{ds}i_{qs} \tag{3.29}$$

- For the Rotor:

$$\text{ActivePower} : P_r = -sP_s = v_{dr}i_{dr} + v_{qr}i_{qr} \tag{3.30}$$

$$\text{ReactivePower} : Q_r = v_{qr}i_{dr} - v_{dr}i_{qr} \tag{3.31}$$

The mechanical power can be determined by the equation 3.32,neglecting the mechanical losses.

- Mechanical Power:

$$P_m = T_m\omega_r = (1-s)P_s \tag{3.32}$$

Regarding the signal convention, the machine is operating as generator whenever T_m, P_m and T_e are positive.

DFIG Control Strategy

In order to establish the model for the DFIG, it is extremely important to define the DFIG control aiming at obtaining the proper generator response. There are several approaches regarding the DFIG control strategies [89],[90],[91]. The one adopted in this modelling process consisted on controlling the generator rotational speed and the active power generation following the proposed in [90]. The rationale of this approach comprises the matching of the mechanical and electrical torque, obtaining a steady speed for the generator. According to the swing equation expressed by the equation 3.26, the torque equilibrium can be attained whenever the speed drift is null, $\frac{d\omega_r}{dt} = 0$. For this particular situation the electrical torque can be defined by:

$$T_e = T_m - D\omega_r \tag{3.33}$$

The relation described by equation 3.33 means that the electrical power (related with the electrical torque) is determined by the difference between the

mechanical power and mechanical losses (modelled by the damping and varying with the generator speed). In order to achieve this, the rotor voltages must be set by the machine-side converter (MSC) (see Figure 3.11) accordingly.

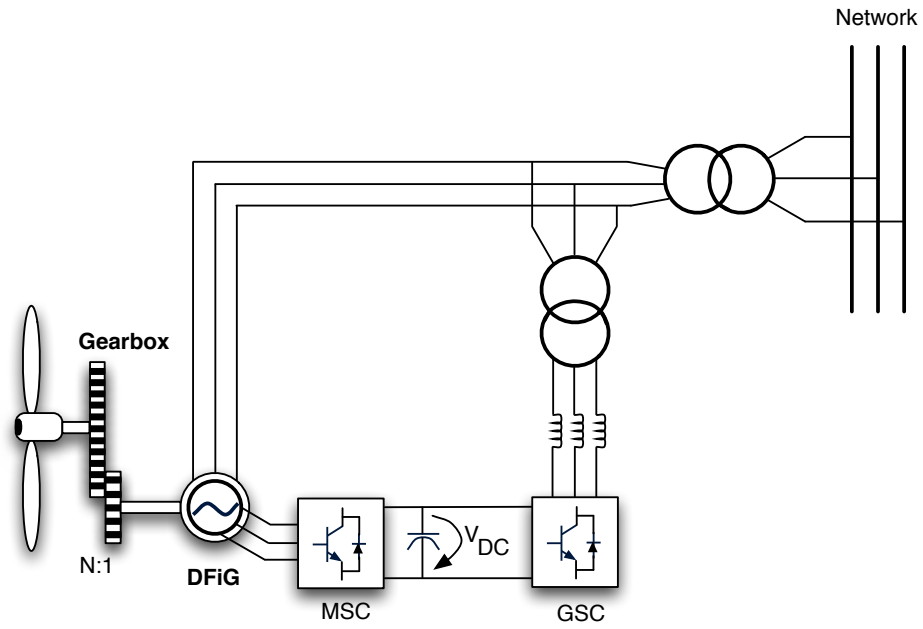

Figure 3.11: DFIG

On the other hand, the GSC is responsible by setting the current grid delivery and is also able to dispatch reactive power. Additionally, this converter is responsible for controlling the DC link voltage, imposing the DC power balance [90].
Since the dq frame approach was considered, the control loops are independent and can be divided. It was also considered that the rotors' dq frame was synchronized with the stator flux aligned by the d axis component. So, the stator voltage in the d component, v_{ds} will be null. The electromagnetic torque and the stator active power will depend on the rotors' q component i_{qr} as indicated in the equation3.34:

$$T_e = \frac{L_m}{L_s + L_m} \times \frac{|V_s|}{\omega_s} \times i_{qr} \tag{3.34}$$

where:

- T_e is the electromagnetic torque (p.u.);
- L_m is the magnetizing inductance (p.u.);

- L_s is the stator windings inductance (p.u.);
- $|V_s|$ is the voltage absolute value at the stator terminals (p.u.);
- ω_s is the synchronous angular frequency (rad/s);
- i_{qr} is quadrature rotor current (p.u.).

So, the active and reactive power in the generator stator can be re-written in order of the rotor current:

$$P_s = |V_s| \times \frac{L_m}{L_{ss}} \times i_{qr} \tag{3.35}$$

$$Q_s = \frac{L_m\,|V_s|}{L_{ss}} \times i_{dr} - \frac{|V_s|^2}{\omega_s L_{ss}} \tag{3.36}$$

Having defined the set of equations that describes the electrical behaviour of the DFIG, the values for the rotor voltages v_{dr} and v_{qr} can be imposed by the converter control-loops depicted in the Figure 3.12.

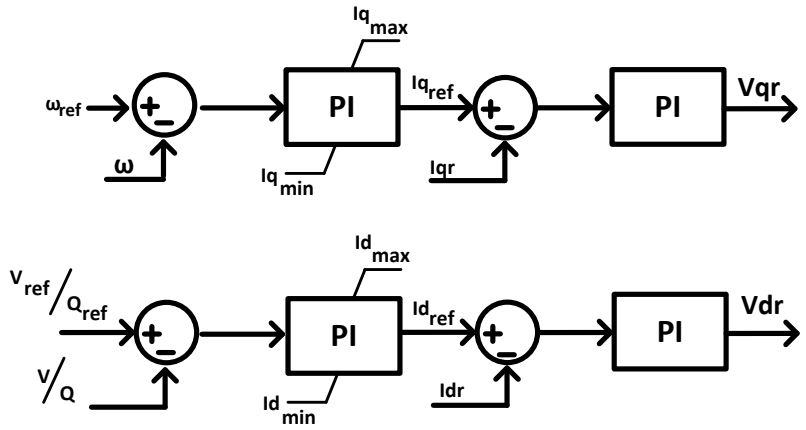

Figure 3.12: DFIG MSC control-loops

The generator speed drift (defined by the error between the ω and its reference ω_r) will feed a PI controller that will imposed the quadrature current ref iq_{ref}. The error existing between iq_{ref} and the quadrature current i_{qr} will feed the second PI that will set the v_{qr} voltage.

Analogously, the error existing between the voltage reference V_{ref} and the actual voltage V will feed a PI controller that will impose the direct axis current reference, id_{ref}. The error existing between the id_{ref} and the direct current i_d will feed a PI that will define the v_{qr} voltage. The d axis control loop can control the reactive power, alternatively to voltage.

Regarding the GSC, the control loops to set the v_{da} and v_{qa} (see Figure 3.11) are defined on the schematic illustrated in Figure 3.13.

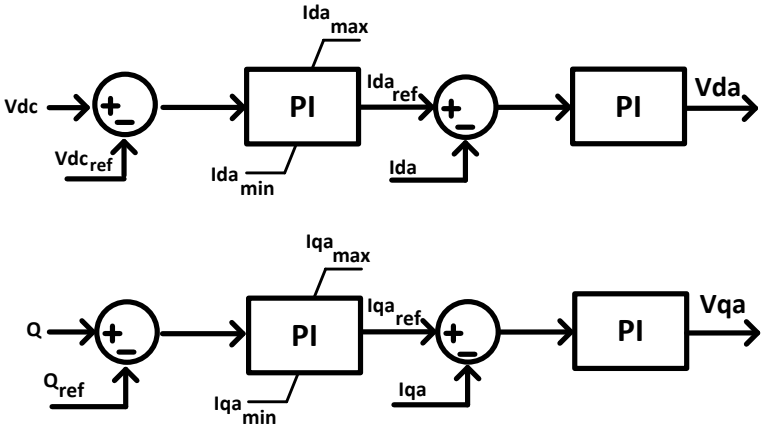

Figure 3.13: DFIG GSC control-loops

As aforementioned, the GSC will be responsible by imposing a reactive power value. In order to define the currents that leads to the target reactive power amount, a control based on the instantaneous power theory has been implemented following the suggestions presented by [11]. Additionally, the GSC is also responsible by controlling the DC voltage value by promoting the active power balance on the DC link. The DC voltage that appears in the DC link capacitor can be determined through the relation presented in the equation 3.37:

$$E_c = \int_{-\infty}^{t} \left(v_{dc}(t) \times i_{dc}(t) - p_{dc}(t)\right) dt = \frac{1}{2} C_{dc} v_{dc}^2(t) \tag{3.37}$$

where: E_c is the capacitor stored energy, v_{dc} is the DC capacitor voltage, i_{dc} is the DC link current, p_{dc} is the GSC power flow and C_{dc} is the capacitor value. The capacitor stored energy depends on the power balance existing between the incoming

power (from the MSC to the DC link) and the delivered power (flowing from the DC link to the AC grid through the GSC). So, to avoid high DC voltage variations the active power delivery must be balanced with the active incoming power.

3.6 Mainland AC System

A representation of the AC onshore system was necessary for the validation of the models and the further control strategies that are going to be developed over this simulation platform. Thus, instead of representing the AC system by an equivalent infinite power busbar, a single equivalent machine representation was considered and modelled in the *dq* frame. This generator is an equivalent machine that aims at representing the conventional generation system existing in the AC area. Following this approach, the HVDC onshore converter terminals are interconnected to an AC system. The AC electric network comprising lines, transformers and shunts, were represented by an admittance matrix.

3.6.1 Synchronous Generator

Following the suggestion of [12], the equivalent synchronous generator was considered to be round rotor type ($X''d = X''q$) and was represented by its electro-mechanical equations, neglecting fast rotor and stator transitory effects. The generators were then represented by the 6^{th} order mathematical model. The differential and algebraic equations in the *dq* frame followed the presented in [12]. Once again, similarly to the approach considered in the modelling of wind generators, the synchronous generator representation follows also the principle of being represented by an e.m.f. behind a sub-transient impedance.

Stator algebraic equations (in p.u.):

$$v_{ds} = E_d + X''_q i_{qs} - r_s i_{ds} \tag{3.38}$$

$$v_{qs} = E_q - X''_d i_{ds} - r_s i_{qs} \tag{3.39}$$

Transient and sub-transient rotor's differential equations (in p.u./s):

$$\frac{dE''_d}{dt} = -\frac{1}{T'_{q0}} \left[E''_d + i_{qs}(X'_q - X''_q) \right] \tag{3.40}$$

$$\frac{dE''_q}{dt} = -\frac{1}{T''_{d0}}\left[E''_q - E'_q - i_{ds}(X'_d - X''_d)\right] \tag{3.41}$$

$$\frac{dE'_q}{dt} = -\frac{1}{T'_{d0}}\left[E'_q - E_f - i_{ds}(X_d - X'_d)\right] \tag{3.42}$$

$$\frac{dE'_d}{dt} = -\frac{1}{T'_{q0}}\left[E'_d - i_{qs}(X_q - X'_q)\right] \tag{3.43}$$

Swing equation (p.u./s)

$$\frac{d\omega_s}{dt} = \frac{1}{2H}(T_m - T_e - D_s\delta\omega) \tag{3.44}$$

Rotor electrical angle equation (rad)

$$\frac{d\delta_s}{dt} = \omega_s - \omega_0 \tag{3.45}$$

Electromagnetic Torque equation (in p.u.)

$$T_e = E''_q i_{qs} + E''_d i_{ds} + (X''_d - X''_q) i_{ds} i_{qs} \tag{3.46}$$

Where:

- v_{ds} and v_{qs} are synchronous generator stator voltages in the respective d and q coordinates;
- i_{ds} and i_{qs} are synchronous generator stator currents in the respective d and q coordinates;
- R_s is the synchronous generator stator resistance;
- X_d and X_q are the synchronous generator stator reactance in the d and q axis, respectively;
- X'_d and X'_q are the synchronous generator stator transient reactance respectively in the d and q axis;
- X''_d and X''_q are the synchronous generator stator sub-transient reactance respectively in the d and q axis;

- E''_d and E''_q are the synchronous generator voltages behind the sub-transient reactance respectively in the d and q axis;
- E'_q is the synchronous generator voltage behind the sub-transient reactance in the q axis;
- E_f is the synchronous generator field voltage;
- T''_{q0} is the synchronous generator open-circuit sub-transient time constant in the q axis;
- T'_{d0} and T''_{d0} are respectively the synchronous generator transitory and sub-transient open-circuit time constant in the d axis;
- T_m and T_e are respectively the mechanical and electrical torque developed by the synchronous generator;
- ωs is the generator rotor's angular speed (being the synchronous angular speed $\omega_0 = 1$p.u.) and D_s is the damping factor associated to the rotors' mechanical losses.

3.6.2 Synchronous Generator Excitation System

The excitation system is commonly associated with the synchronous generators and aims at providing the field excitation voltage that allows the synchronous machine to perform as a generator, controlling the terminal voltage and the reactive power generation. For these reasons this system is also denominate in the literature as Automatic Voltage Regulator (AVR). Among the existing AVR types, the one adopted in this work is known as AVR IEEE type I and its control plant is depicted in Figure 3.14.

The differential equations related with the voltage regulator can be defined as:

$$\frac{dV_R}{dt} = -\frac{1}{T_R}V_R + \frac{k_r}{T_R}V_t \tag{3.47}$$

$$\frac{dV_A}{dt} = -\frac{k_A}{T_A}V_R - \frac{1}{T_A}V_A - \frac{k_A}{T_A}V_F + \frac{k_A}{T_A}V_{ref} \tag{3.48}$$

$$\frac{dV_F}{dt} = \frac{k_F}{T_E T_F}V_A - \frac{k_E}{k_F}T_E T_F E_f - \frac{1}{T_F}V_F - \frac{k_f}{T_E T_F}V_x \tag{3.49}$$

$$\frac{dE_f}{dt} = -\frac{k_E}{T_E}E_f + \frac{1}{T_E}V_A - \frac{1}{T_E}V_x \tag{3.50}$$

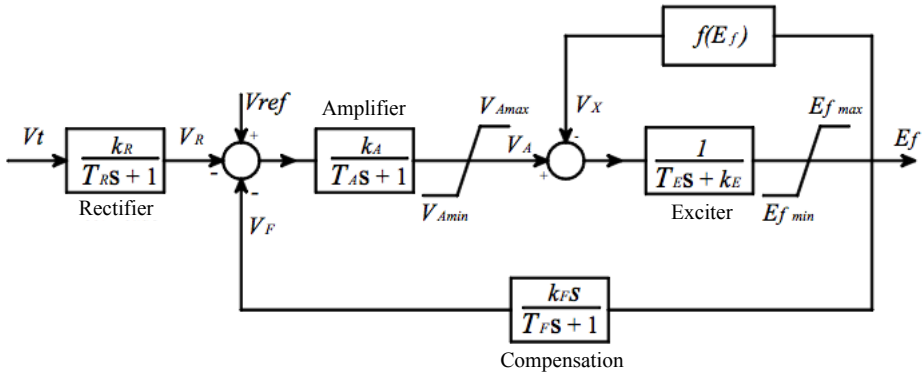

Figure 3.14: Automatic Voltage Regulator control-loop [12]

where:

- V_R, V_A, V_F and V_E are the voltage output of each control subsystem (p.u.);
- k_R, k_A, k_F and k_E are the gains associated to each control subsystem (p.u.);
- T_R, T_A, T_F and T_E are the time constants relative to each control subsystems (s);
- V_{ref} is the reference voltage value(p.u.);
- E_f is the field voltage(p.u.).

The saturation effect has been neglected thus, the sub-block associated with the $f(E_f)$ in the scheme depicted in the Figure 3.14 has not been considered.

3.6.3 Prime Mover

Every synchronous generator requires a prime mover that delivers the mechanical rotational movement to the generator rotor. In the process of development of this simulation platform, thermal units (steam and diesel) have been considered. The steam and diesel turbines were modelled through the first order simplified model, following the suggested in [12]. The block diagrams depicted in the Figure 3.15 illustrates the thermal turbine model.

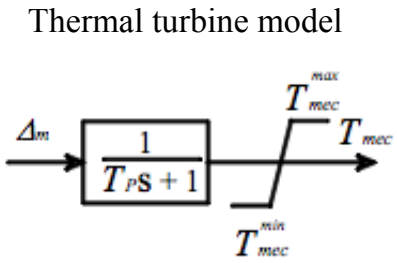

Figure 3.15: Thermal turbine model

The aforementioned model can be described by differential equations which are based on the scheme depicted in Figure 3.15 and can be written as:

- Steam and Diesel turbines:

$$\frac{dT_{mec}}{dt} = -\frac{1}{T_p}T_{mec} + \frac{1}{T_p}\Delta_m \tag{3.51}$$

where:

- T_{mec} is the mechanical torque delivered by the primary machine to the synchronous generator (p.u.);
- T_P is the first order time constant that represents the steam and diesel turbines (s);
- Δ_m is the intake fuel variations consumed by the thermal turbine (p.u.).

3.6.4 Power-Speed Regulator

The power/speed regulator is a controller that comes often associated with synchronous generator and the turbine set. It aims at balancing the active power generation by relying on the frequency deviation and controlling the primary machine fuel intake. The power speed regulator adopted in this work is composed by a proportional control commonly named as droop (primary control) and an integral control (secondary control) as depicted in the Figure 3.16. The presented control

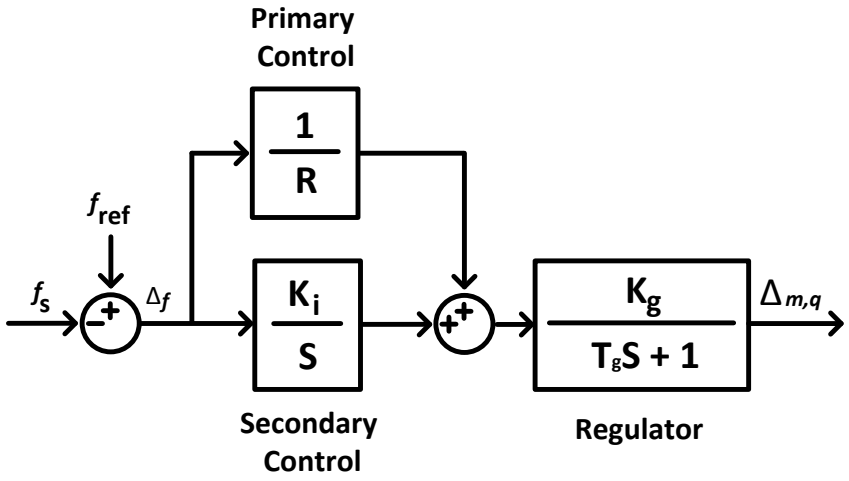

Figure 3.16: Synchronous generator and turbine speed control

scheme can be described by the following set of differential equations:

$$\frac{dP_C}{dt} = k_I \Delta f \tag{3.52}$$

$$\frac{d\Delta_{m,q}}{dt} = \frac{k_g}{T_g} P_c - \frac{1}{T_g} \Delta_m - \frac{k_g}{T_g R} \Delta f \tag{3.53}$$

where:

- f_{ref} is the frequency reference value (p.u.);
- f_s is the system frequency (p.u.);
- k_i is the integral gain (Hz(p.u.)/MW(p.u.));
- $1/R$ is the droop gain (Hz(p.u.)/MW(p.u.));
- k_g is the regulator gain (p.u.);
- T_g is the regulator time constant (s);
- Δf is the frequency deviation (p.u.);
- $\Delta m, q$ is the fuel quantity that will originate a given power.

The proportional and integral controller (primary and secondary control) forms a PI controller that will determine the active power set-point based on the frequency deviation measurement. Then, the active power set-point will be an input for another block called regulator, that will determine the fuel intake variations.

3.7 The Operation of HVDC Converter Stations

The definition of the operation of HVDC-VSC is crucial for the evaluation of the behaviour and performance of the overall MTDC grid model. Without lack of completeness, it has been defined that each onshore and offshore HVDC-VSC will operate within the same specification on what regards the control and operation philosophy approach, which are going to be highlighted independently for the offshore and onshore HVDC-VSC.

3.7.1 Offshore HVDC-VSC Operation

The offshore HVDC-VSC will perform as a slack bus for the AC offshore WF internal grid. It will be responsible by collecting all generated power and delivering it into DC form to the MTDC grid. Thus, it can impose AC-side voltage and frequency. For the standard operation of the DC grid, the AC offshore frequency will be a fixed value and the offshore AC voltage profile will depend of the pre-defined AC voltage value (defined at offshore HVDC-VSC level) and on the reactive power control implemented at the offshore HVDC-VSC control as explained in Section 3.3.1. It was also defined that offshore WT will inject a fixed or null reactive power amount in order to do not interfere with the offshore HVDC-VSC control.

3.7.2 Onshore HVDC-VSC Operation

Following the described in the literature by [85], [8], [67] and previously mentioned in the Section 3.3.2, the onshore HVDC-VSC connected to a MTDC grid can be explored under two operation principles. Nevertheless, there is a common aspect shared between the control principles that consists on controlling the DC voltage level at its terminal. Therefore, appropriated DC voltage magnitudes should be maintained at each onshore converter station in order to allow proper power sharing

among converters in case of power variations such as the ones occurring at the offshore WF level. Regarding these control issues, two approaches can be followed [85] [67]:

1. **Master onshore VSC control** - This strategy consists on maintaining a constant DC voltage at a single onshore converter station, which acts as a DC slack bus, while the other offshore converter stations are controlled in order to inject a pre-defined active power into the AC grid. The main drawback of this approach is related with the impossibility of the system to continue operation in case of losing the DC slack bus converter station. In case of using such modelling option, the slack bus converter is controlled according to scheme presented on Figure 3.4. In the other converter stations, the i_d current reference is calculated based on the corresponding active power reference and actual injected power into the AC system.

2. **Shared onshore VSC Control (droop control)** - This strategy consists on using a droop control approach in order to determine the DC voltage reference at each onshore converter station as a function of the injected power in the AC system (or DC current flowing to the converter station). In this case, DC power variations are shared among all onshore converter stations. Additionally, the loss of any onshore converter potentially allows the DC grid to continue its operation. Therefore, it was considered that each onshore converter sets the terminal DC voltage V_{DC} as a function of the converter active power injection P_{out} into the AC grid, and of a target V_{DCset}, according to the flowing control rule which is defined based on the active power/ DC voltage droop coefficient k_{pv} [85]:

$$V_{DC} = V_{DCset} + k_{pv} \times P_{out} \tag{3.54}$$

V_{DCset} and k_{pv} are configurable values that can be parametrized in the onshore HVDC-VSC by an upstream supervision and control system, according to a specific operational strategy envisioned for the onshore AC grid.

In the development of the work presented in this thesis, the droop-control approach was considered on onshore HVDC-VSC.

3.8 Overview of Overall Simulation Platform

The previously described models were implemented in Matlab/*Simulink* in order to develop a MTDC grid simulation platform. The models were implemented based on user-defined functions and exploiting the "look under mask" functionalities available in the simulation environment.

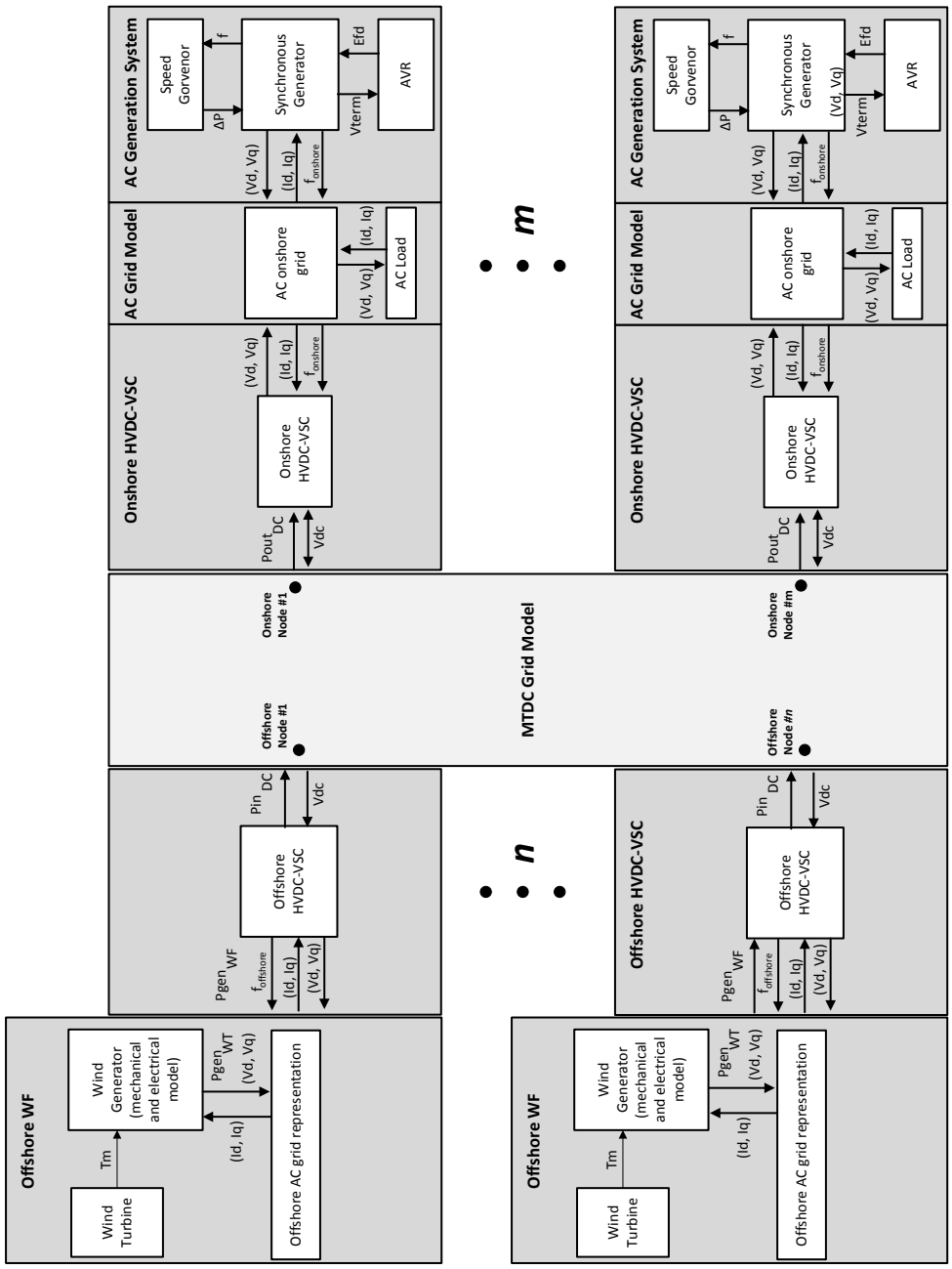

Figure 3.17: Schematic of models interaction

The incoming wind power is transformed into a mechanical torque at the wind turbine level (wind turbine block) based on the aerodynamic equations described in Section 3.5.1. The mechanical torque feeds the wind generator model that comprises the mechanical and electrical modelling. The principles used in the modelling of the wind generators are presented in Section 2.3.3 and Section 3.5.4 depending whereas the offshore WF is is equipped with PMSG or DFIG, respectively. The generator outputs are the dq voltage values that are inputs to the AC offshore grid model. Depending on the offshore AC grid topology, several offshore wind generators may be interconnected to different AC nodes thorough its corresponding dq voltage. Without lack of generality, the approach considered for this thesis consisted in representing the offshore WF by a single equivalent generator model. Thus, the AC offshore grid was composed by two accessible nodes, one connected to offshore WF and the other to the offshore HVDC-VSC. In between the AC step-up transformer, the AC equivalent cable circuit and the offshore HVDC-VSC filter have been considered (modelled by an admittance matrix).

The MTDC grid model block contains the algebraic and state equations that describe the DC grid according to its topology as introduced in Section 3.4. At the opposite DC grid terminal endings, the onshore converter blocks modelled according to the description presented in Section 3.3.2, are responsible for interconnecting the DC grid to the AC mainland grid. The AC mainland grid is represented by the AC grid model block in a similar manner of the AC offshore grid (by an admittance matrix). So, it contains the modelling of the Onshore HVDC-VSC filter, transformer (step-down or step-up depending on the AC mainland grid voltage profile) and the representation of the AC interconnection network which serves to interconnect the DC system to the equivalent representation of the AC mainland grid.

The AC generation system is a block which intends to represent the equivalent AC generators within an AC grid by a single equivalent generator. This specific block gathers the AVR model block, the Generator mechanical and electrical model block and the speed governor block, following the modelling principles presented in Section 3.6.

The implementation approach consisting on adopting model blocks allows to change the simulation platform according to the specifications of a given case. The DC grid can be redefined based on the set of state and algebraic equations derived in Section 3.4. Thus, combinations of N offshore WF and M onshore mainland AC connectors can be easily implemented within the simulation platform.

3.9 Evaluation of Multi-terminal DC Grid Simulation Platform

After having defined the MTDC grid simulation platform, as well as the basic control philosophies an illustration of the main operation characteristics is now presented and discussed. In order to avoid the overlapping of the aspects to be assessed, the assessment test-set has been divided in two phases. The first phase aimed at testing the flexibility and scalability of the simulation platform and consisted on testing the model performance over several DC grid topologies. The second phase aimed at assessing the power sharing mechanisms and the droop control behaviour over the MTDC grid. Two DC grid topologies have been adopted and active power variations at offshore WF level were performed having defined different active power/DC voltage droop gain k_{pv} and DC voltage setpoint VDC_{set} values at the onshore HVDC-VSC.

3.9.1 Evaluation of the Multi-terminal DC Grid Simulation Platform for Different DC Grid Topologies

In order to test the flexibility and scalability of the developed simulation platform, several tests consisting on changing the DC grid topology have been performed and are presented in the following sub-sections. In order to establish a comparative analysis between the performances of the model over the tested DC grid topologies, the wind farm power variation profile remained the same and consisted on a ramp down power reduction, a stabilization period and finally an active power ramp up. The sequence of events of the offshore wind farm active power injection variation is depicted in Figure 3.18. To simulate these events, instead of acting in the wind speed, active power ramps where set directly in the offshore HVDC-VSC.

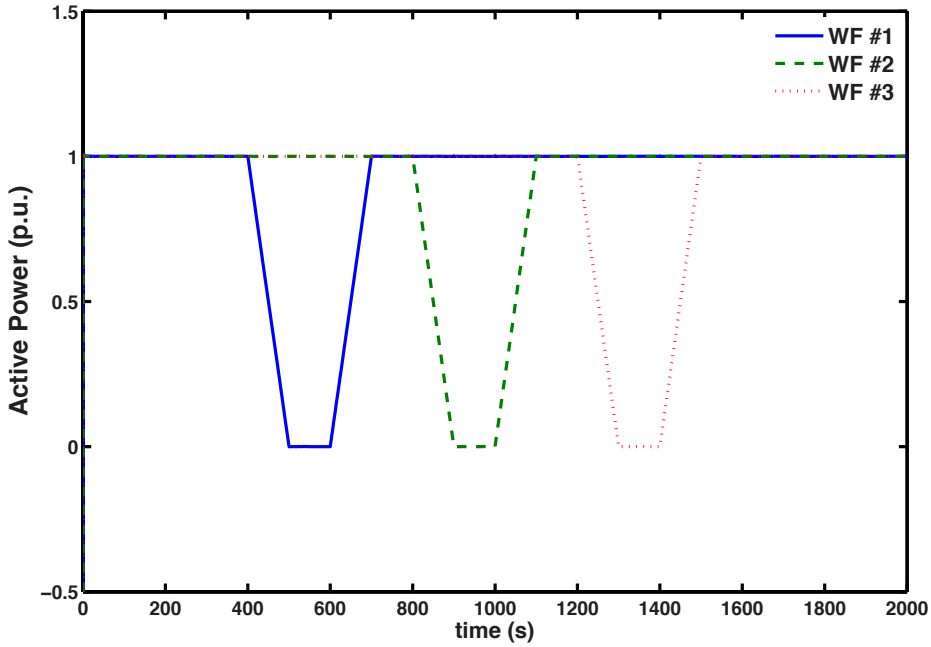

Figure 3.18: Active power output at each offshore Wind Farm

Star topology

The DC grid star topology is composed by three WF injection points and two onshore HVDC-VSC collection/injection points that connects the DC grid to two independent AC mainland grids, as depicted in Figure 3.19.

The results show active power variation at the offshore injection points power has been shared by the Onshore HVDC-VSC, as depicted in Figure 3.20 and Figure 3.21. Despite the difference in the cable circuit length the onshore HVDC-VSC are able to share the active power reduction and increase independently of its origin. The equality on the active power delivery at the onshore HVDC-VSC is related with the assumption of the same k_{pv} and V_{DCset} values. Regarding the DC voltage profile, the results are depicted in Figure 3.21 and shows that as expected the DC voltage profile at the generation ends (offshore WF DC grid terminals) are higher than at the receiving ends (onshore HVDC-VSC). Despite the DC voltage have presented small variations with the active power fluctuation, adequate active power sharing has been successfully accomplished at the onshore HVDC-VSC.

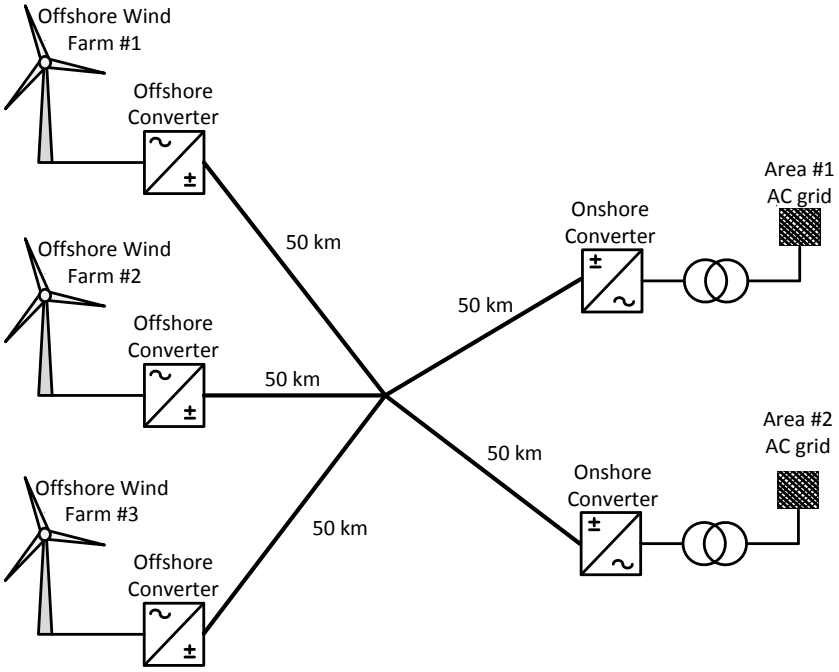

Figure 3.19: Multi-terminal HVDC grid — Star topology

U Topology

The DC grid U topology consists on a connection path that interconnects two offshore WF to two mainland onshore AC grids. The Figure 3.22 illustrates the network topology.

The previously considered active power variations were performed on the wind farms (for WF ♯1 and ♯2). The active power delivered by onshore HVDC-VSC are depicted on Figure 3.23. From the simulation results it is possible to conclude that both onshore VSC identically share the active power variations. In addition, it is also possible to verify that the active power at onshore VSC ♯2 is slightly smaller than the active power delivery at onshore HVDC-VSC ♯1. The reason for the existence of this power delivery difference is related with the DC grid topology and can be proven by the DC voltage profile results depicted at Figure 3.24. In fact, according with the results, the most distant wind farm (WF ♯2, electrically connected by a higher impedance path) presents the highest DC voltage level in the DC terminal of the associated HVDC-VSC. Bearing in mind that the k_{pv} droop gain was assume to

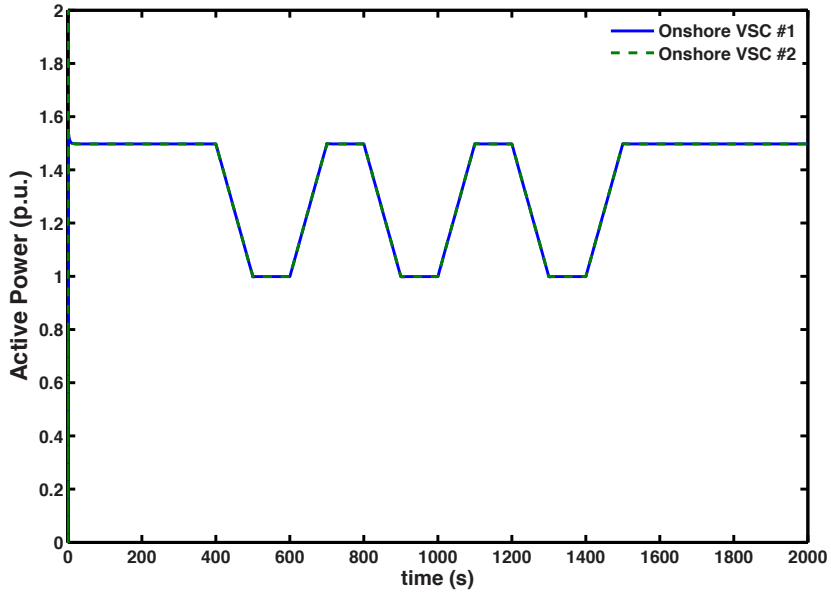

Figure 3.20: Active power flow at each star topology DC grid onshore terminals

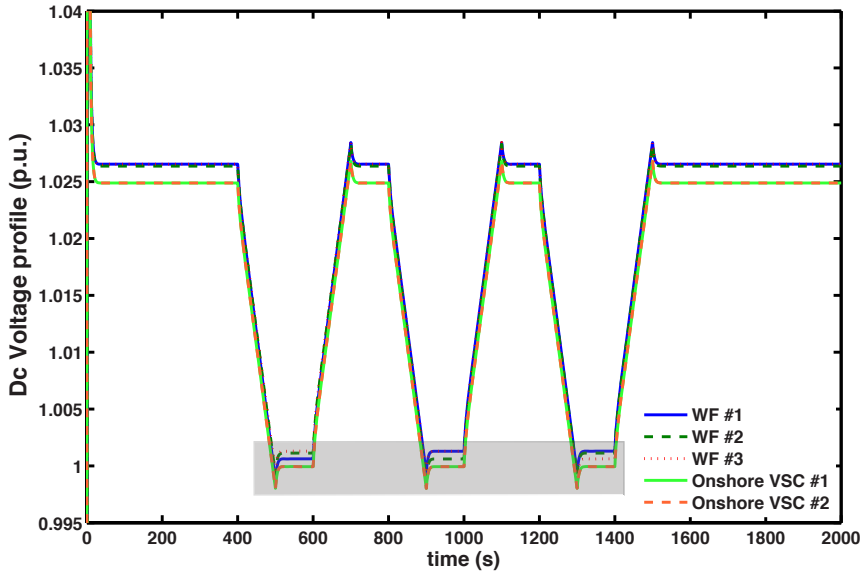

Figure 3.21: DC voltage at each star topology DC grid onshore terminals

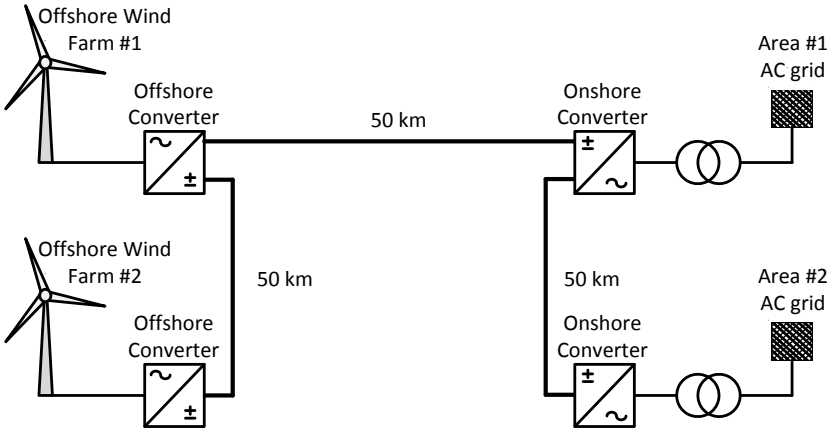

Figure 3.22: Multi-terminal HVDC grid — U topology

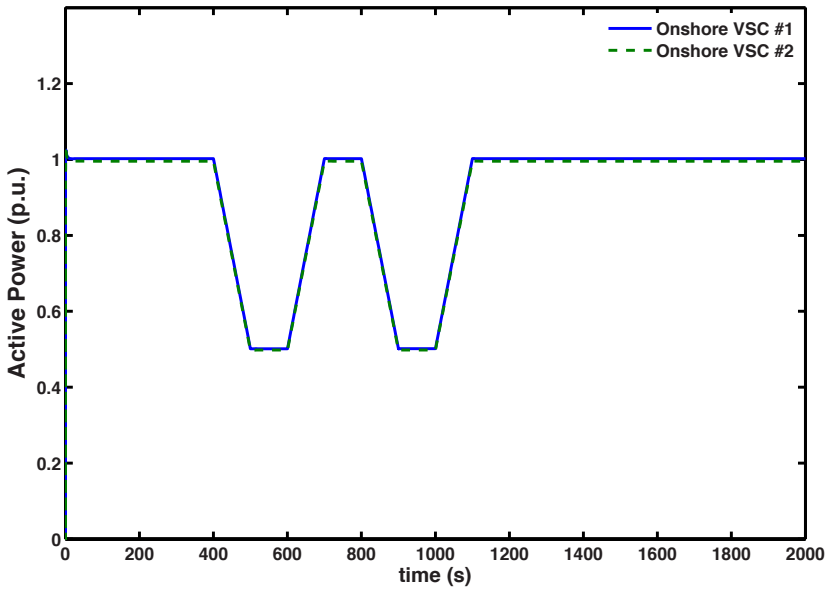

Figure 3.23: Active power flow at each DC grid onshore terminals — U topology

be equal at both onshore HVDC-VSC, then a small active power difference will also exist between both HVDC-VSC power delivery that can be justified by the higher voltage drop existing in relation to the HVDC-VSC ♯2, which results by the DC grid topology.

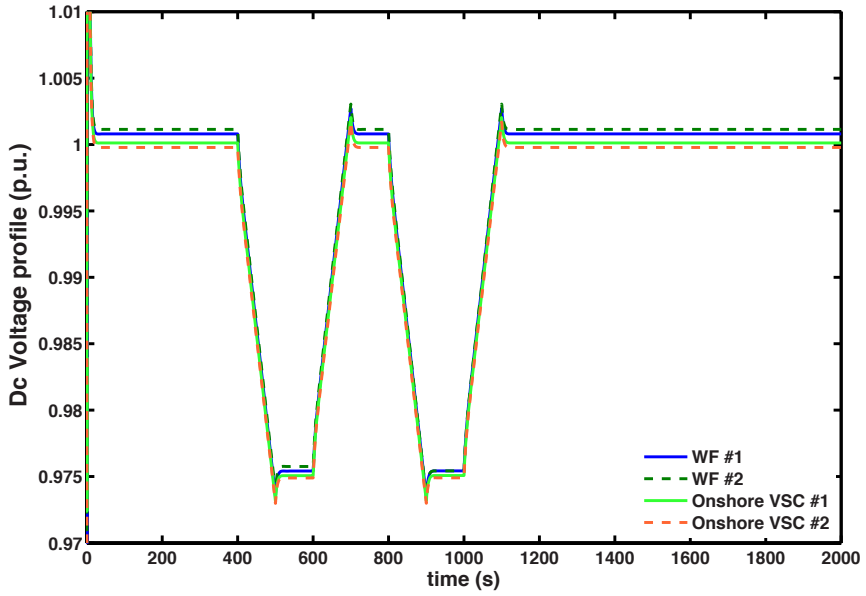

Figure 3.24: DC voltage at each DC grid onshore terminals — U topology

H Topology

The H topology connects two offshore WF to two onshore AC collection points as depicted Figure 3.25. The schematic also allows identifying that the DC cable infrastructure is composed by two point-to-point connections that are interconnected by a middle cable section. This simple connection enhances the previous independent links to a grid infrastructure, allowing the power sharing between the AC mainland areas and also increasing the infrastructure reliability. This kind of topologies may be very common as an upgrade to previously existing point-to-point connections.
The same set of simulations were carried out under this topology to test the performance of the implemented control strategies facing resource variations. The results are presented in the Figure 3.26 and Figure 3.25.
From the results depicted in Figure 3.26 it is possible to verify that the active power is equally shared among the onshore HVDC-VSC for the pre and post-disturbance periods. The reason for that equal active power splitting are related with the specific DC grid topology homogeneity which for an equal active power generation and equal onshore HVDC-VSC parameters leads to a null current in the middle section

H topology cable. On contrary, facing a resource variation, to attain equal active power delivery at onshore HVDC-VSC, an amount of power must flow in the middle section cable circuit giving origin to an extra voltage drop. The results related with the DC voltage at each DC grid terminal are depicted in Figure 3.27.

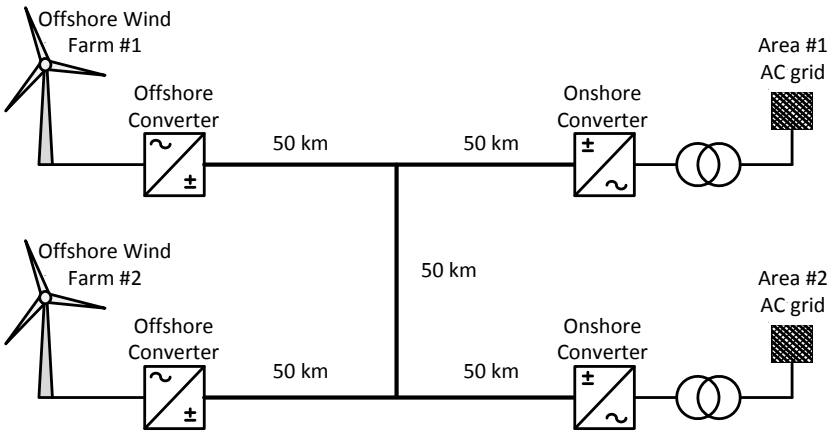

Figure 3.25: Multi-terminal HVDC grid — H topology

On the pre and post-disturbance periods it can be seen that the offshore WF ♯1 and ♯2 are identical and greater the onshore VSC ♯1 and ♯2 that will be also identical. Facing the disturbance it is noticeable that the DC voltage gets stable, however will not be equal among the offshore WF and onshore converters. For the first disturbance case located at offshore WF ♯1, the offshore WF♯2 voltage will be the higher (since offshore WF ♯1 is not generating any power). The onshore converter voltages are not exactly the same. Since active power will have to be directed from offshore WF ♯2 to the onshore VSC ♯1 overcoming the loss of WF ♯1 power, as previously mentioned, an extra voltage drop will exist on the middle cable section, impacting as a DC voltage reduction at the onshore VSC ♯1. For the second disturbance (active power reduction at offshore WF ♯2), an analogous process takes place on the onshore VSC ♯2. Despite the minor DC voltages changes and the consequent impact on minor differences on active power flows on the onshore HVDC-VSC, the methodology for power sharing presented a very satisfactory response.

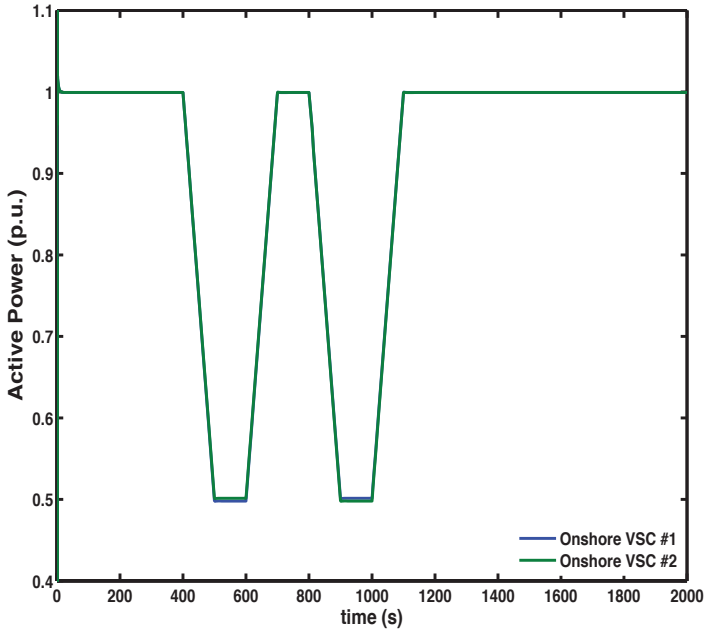

Figure 3.26: Active power flow at each H topology DC grid onshore terminals

Double H Topology

The Double H topology is an extension of previously presented H topology, being the layout presented in Figure 3.28. It consists on a DC grid infrastructure with six terminals connecting three offshore WF to three onshore AC grid nodes. The simulation of resource variation has been also performed for this DC grid topology and the results are presented in Figure 3.29 and Figure 3.30.

The active power flows at each DC grid terminal are presented on Figure 3.29 shows that during the pre and post-disturbance periods the onshore HVDC-VSC were able to share the incoming wind power. Again, some minor variations on active power injection on the onshore grids occur due the asymmetry loss during resource variations. The same effect is noticeable on the DC voltage results depicted in Figure 3.30.

In fact, analysing the DC voltage results, it can be concluded that whenever the active power injection are equal (at offshore level), the active power flows at

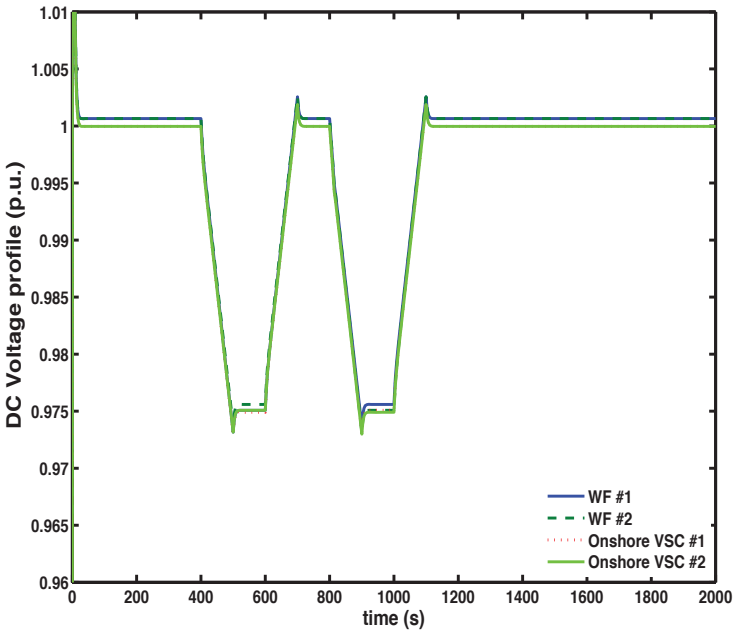

Figure 3.27: DC voltage at each H topology DC grid onshore terminals

onshore-level are also equal. The justification for this consists on the fact that in this pseudo-equilibrium, no power flow in the two mid-section cable branches. However, the asymmetrical power injection leads to the occurrence of current on the mid-section cable branches, increasing the lenght and consequently the voltage drop. Despite slight differences, adequate power share has been also verified for this DC grid topology.

Meshed Topology

The meshed DC grid topology has been included in this analysis with the objective of illustrating how the active power/DC voltage droop control performs on meshed DC networks. Additionally, on contrary of the previous examples, where the same length has been considered for each branch, for this case the cable segments have different lengths (see Figure 3.31). The scheme depicted on Figure 3.31 presents the topology adopted for the meshed DC grid as well as the length of each DC cable segment. The adopted meshed DC grid consists in an infrastructure to interconnect two offshore WF to two mainland AC grids.

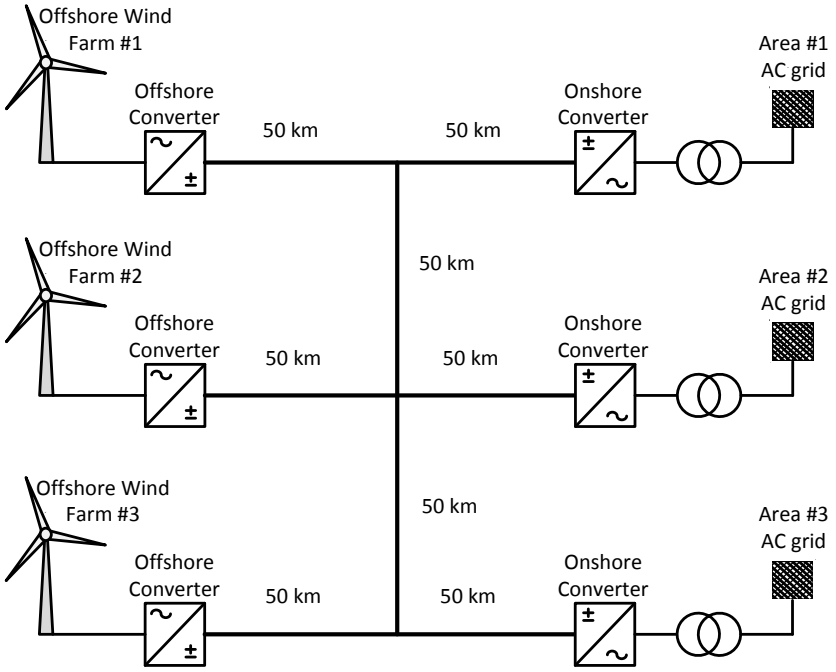

Figure 3.28: Multi-terminal HVDC grid — Double H topology

The results containing the active power flows to the onshore grids as well as the DC voltage profile at each MTDC grid terminal are depicted in Figure 3.32 and Figure 3.33, respectively.

The active power flows are identical on both converters for the pre and post-disturbance periods. A small (almost unnoticeable) difference exists between the onshore converter Area ♯1 and ♯2 (being the Area ♯1 power slightly higher than Area ♯2) due to the higher cable length interconnecting the offshore WF and area ♯2 converter in comparison to the cable that interconnects the offshore WF and area ♯1 converter.

The same trend is noticeable in the DC voltage profile at each onshore converter as depicted by the DC voltage profile results illustrated in the Figure 3.33. Regarding the DC voltage profile at offshore level, as expected, its value is higher than the onshore HVDC-VSC DC busbars. A clear difference between offshore WF ♯1 and

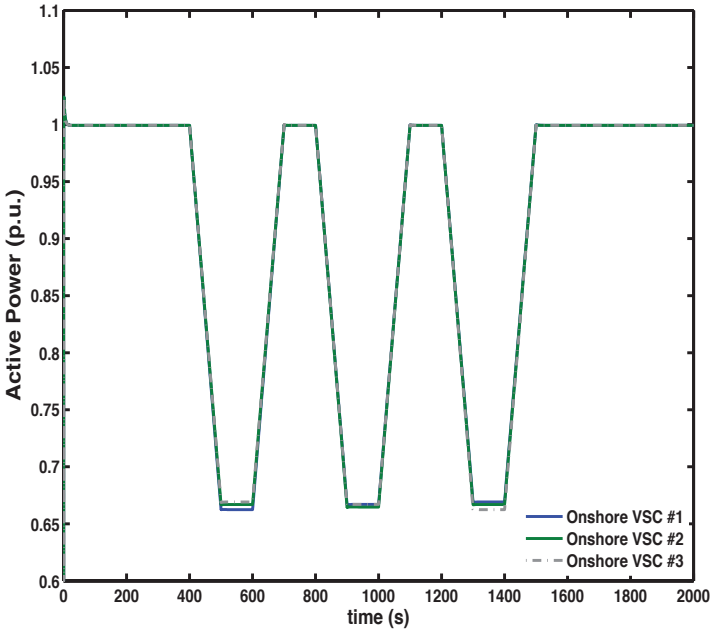

Figure 3.29: Active power flow at each Double H DC grid onshore terminals

♯2 is noticeable. In fact the offshore WF ♯2 voltage profile is higher to compensate the voltage drop across long radial connection that interconnects the offshore WF ♯2 to the DC grid. Despite having a meshed DC grid topology infrastructure, the droop control also provides the capability of controlling the power sharing among HVDC-VSC connected to mainland areas when the DC grid has a meshed topology.

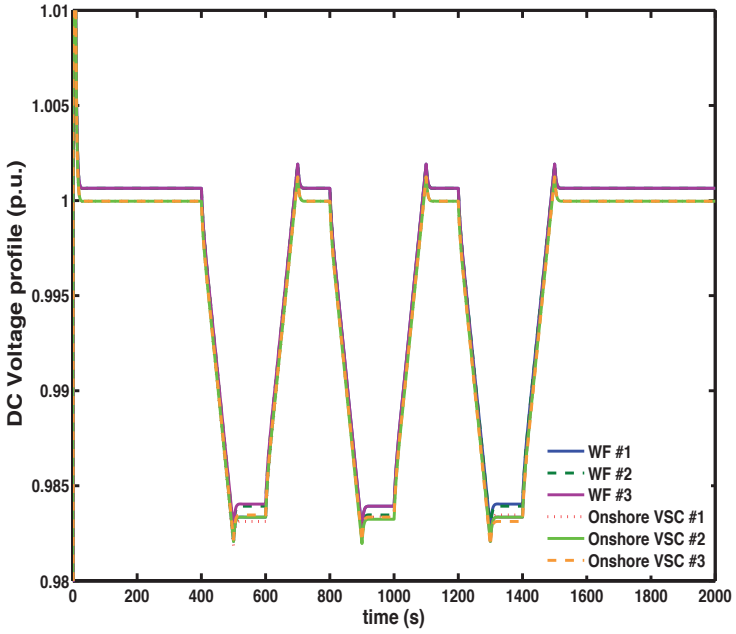

Figure 3.30: DC voltage at each Double H topology DC grid onshore terminals

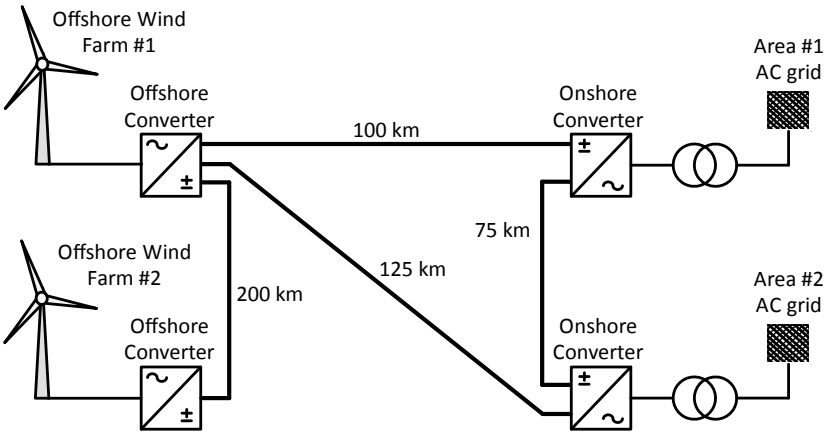

Figure 3.31: Multi-terminal HVDC grid — Meshed topology

3.9.2 Droop Control Sensitivity Analysis

This section aims to illustrate the behaviour of the droop control approach regarding variation of its parameters, namely the VDC_{set} and the droop gain K_{pv}.

For this specific case, the double H DC grid topology (depicted at Figure 3.30) and

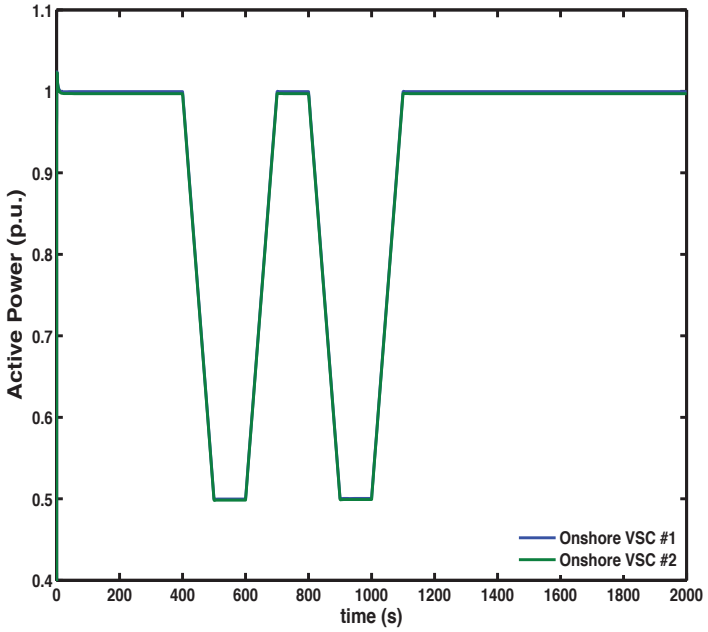

Figure 3.32: Active power flow at each Meshed topology DC grid onshore terminals

the meshed DC grid topology (depicted at Figure 3.31) have been chosen to test different combinations of onshore HVDC-VSC control parameters and to assess its implication regarding offshore active power variations. Without lack of generality, the disturbances adopted in the assessment were the same used to assess the DC grid behaviour under different topologies, presented in Figure 3.18.
The simulations were divided in cases which are presented in Table 1. The cases differ in terms of DC voltage setpoint V_{DCset}, Active Power/DC Voltage droop gain and the DC network topology.

The first cases - case A and case B - intend to test the impact of the DC voltage profile setpoint V_{DCset} in the DC voltage and Active power sharing among the onshore HVDC-VSC. Thus, for these specific cases the droop gains k_{pv} were kept constant. The case A has been performed under the H topology DC grid while case B has been carried out using the previously presented meshed DC grid topology.

The results for the case A are depicted in the Figure 3.34. The result analysis

[1]Represented in (p.u.)
[2]Represented in (V(p.u.)/W(p.u.))

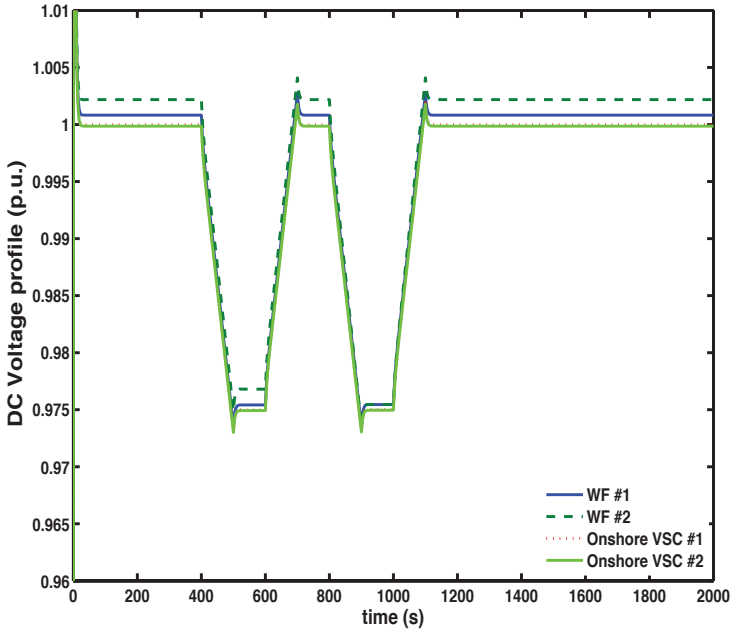

Figure 3.33: DC voltage at each Meshed topology DC grid onshore terminals

Table 3.1: Summary of droop control parameters and DC grid topology for each analysed case

	Case A	Case B	Case C	Case D	Case E
Onshore Converter ♯1 VDC_{set} [1]	1.00	0.90	0.95	0.95	0.95
Onshore Converter ♯2 VDC_{set} [1]	0.97	0.95	0.95	0.95	0.95
Onshore Converter ♯3 VDC_{set} [1]	0.95	N/A	0.95	0.95	N/A
Onshore Converter ♯1 K_{pv} [2]	0.05	0.05	0.2	0.4	0.05
Onshore Converter ♯2 K_{pv} [2]	0.05	0.05	0.1	0.2	0.1
Onshore Converter ♯3 K_{pv} [2]	0.05	N/A	0.05	0.1	N/A
DC grid topology	Double H	Meshed	Double H	Double H	Meshed

allows to conclude that the V_{DCset} has a noticeable impact on the steady-state power sharing. Comparing the steady-state power with the steady-state DC voltage, it is possible to observe that the DC node with higher specified DC voltage (VDC_{set}) corresponds to the converter that is extracting less active power.

Regarding the case B, where results are depicted in Figure 3.35, a similar steady-state behaviour is verified. The higher V_{DCset} onshore HVDC-VSC, corresponds to

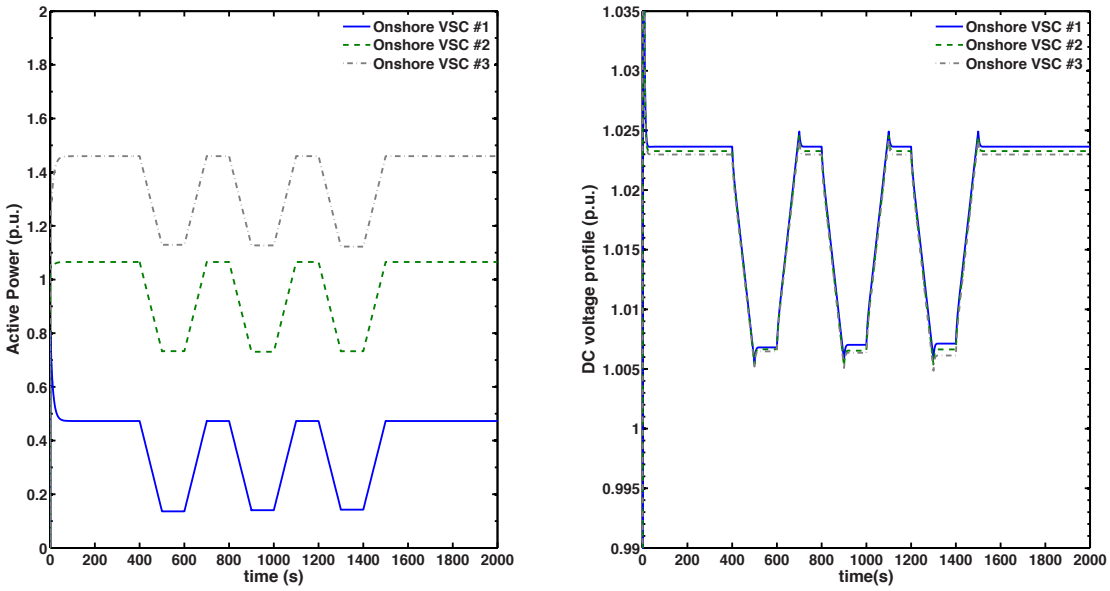

Figure 3.34: Onshore HVDC-VSC Active Power and DC voltage profile - Case A

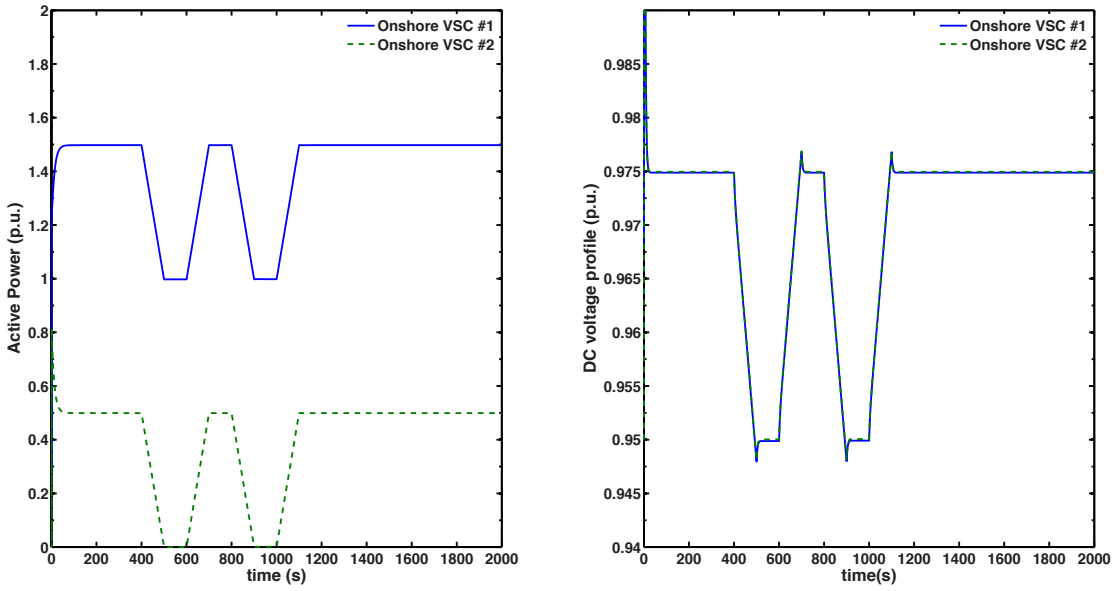

Figure 3.35: Onshore HVDC-VSC Active Power and DC voltage profile - Case B

the converter absorbing less active power. Due to the network topology the DC voltage difference between the onshore HVDC-VSC are not very high. Nevertheless, for steady operation, onshore HVDC-VSC ♯1 presents higher DC voltage profile in

comparison to onshore HVDC-VSC ♯2. Once again, the active power variations at WF level have been equally shared among the onshore HVDC-VSC.

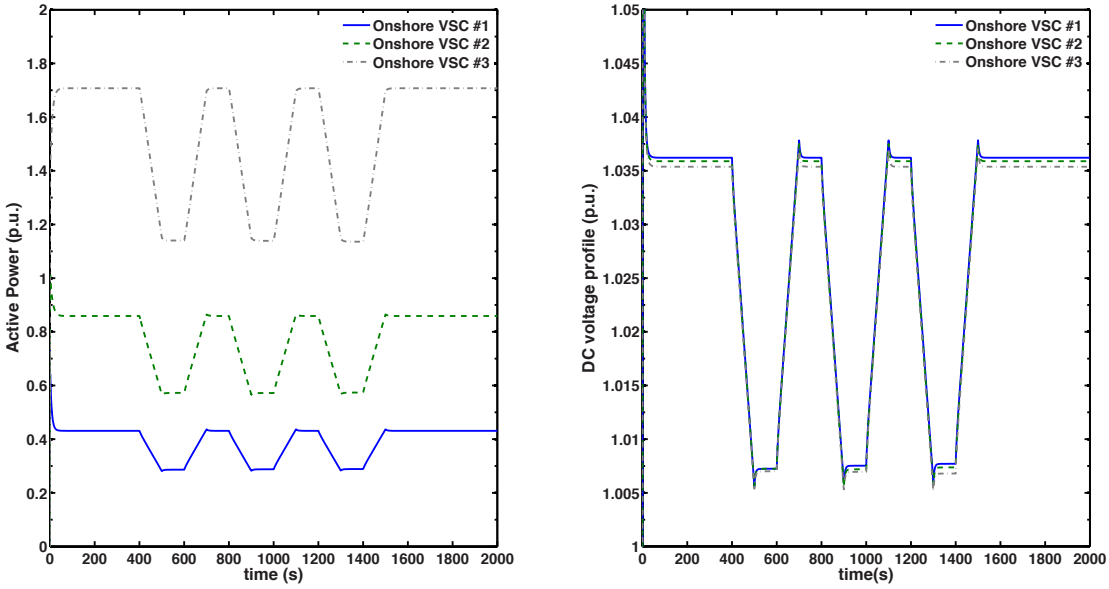

Figure 3.36: Onshore HVDC-VSC Active Power and DC voltage profile - Case C

In case C, the double H DC grid topology has been considered and the DC voltage references are the same in all onshore HVDC-VSC. On contrary, the active power/DC voltage droops were imposed with different values, aiming at assessing its impacts on the DC grid. The case C results are depicted in the Figure 3.37. Despite having the same V_{DCset} values, the steady state power sharing for this case were not equal. Onshore HVDC-VSC with higher k_{pv} has a smaller participation regarding the sharing of active power variations. During the offshore power variations, each onshore HVDC-VSC modifies the active power injection in the inverse proportion to k_{pv} gain. Converters with higher k_{pv} values accommodate less active power variations. Regarding the DC voltages, for equilibrium situations (where all the offshore WF are generating the same power), the DC voltage profile decreases inversely to the active power extraction. This behaviour is expectable since the DC voltage difference between two cable endings culminates in a higher power flow.

The case D is similar to the previously presented case C. In fact the V_{DCset} values are the same and the k_{pv} are the double of the ones adopted in case C example. The results for this case are illustrated in Figure 3.37. At a first sight the active power

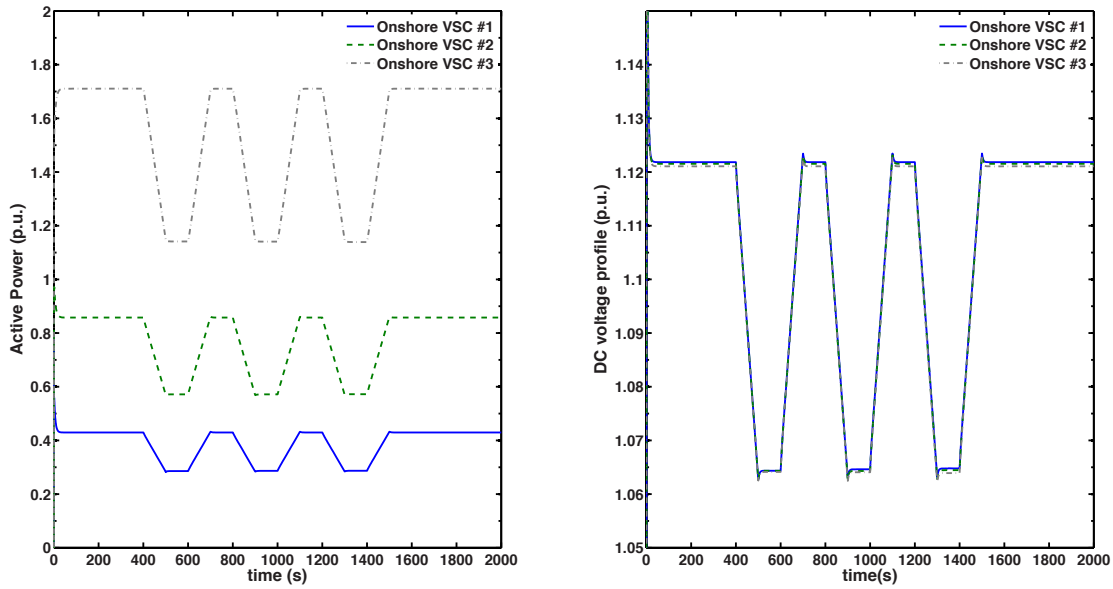

Figure 3.37: Onshore HVDC-VSC Active Power and DC voltage profile - Case D

flows for this case are the identical to the ones obtained for the previous case. This fact indicates that the active power share is not dependent on the droop value but mainly on the relation between the droop values among a given DC grid. Regarding the DC voltage, the increase on the k_{pv} gain significantly increases the DC voltage profile. Nevertheless, the case D DC voltage profile follows the evolution observed in the case C.

Finally, in the case C, a scenario with equal V_{DCset} parameters and different k_{pv} values has been assessed on the meshed DC grid topology. The steady state operation reveals that the power share has been properly achieved, accounting that the small deviation from the expected values are due to the losses existing in the DC grid cable circuits. Regarding the DC voltage profile, for this specific case both onshore VSC ♯1 and ♯2 present a similar value.

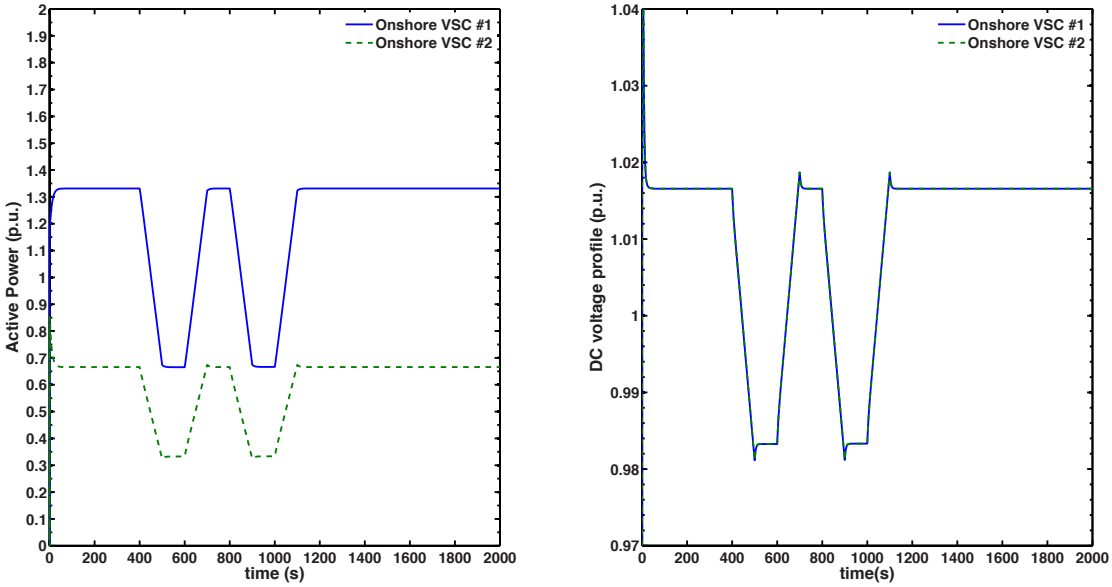

Figure 3.38: Onshore HVDC-VSC Active Power and DC voltage profile - Case E

3.10 Summary

This chapter has described models adopted for the several components of the DC grid for offshore WF interconnection. The models presented indented to represent the dynamic aspect of the several components in a time scale from mili-seconds to hundred of seconds. Thus, the modelling followed the RMS representation and neglecting the fast transients. Each component model has been solely presented, followed by the description of the interactions among each model, obtaining the overview of the simulation platform. The developed platform is an important tool to understand the interactions between each component, as well as the interactions between the AC and DC sides. Additionally, the block-to-block implementation of user-defined models allows the development of additional controllers, enabling to develop innovative control strategies that ultimately aims at enhancing the operation of the DC grid towards the AC grid support.

The operation of HVDC-VDC has also been described followed by some simulations aiming at assessing the performance of the simulation platform under a varied set of DC grid topologies as well as under different onshore HVDC-VSC control

parameters.

4

Control Schemes for Advanced Service Provision from MTDC Grids to Mainland AC Systems

4.1 Introduction

This chapter aims at presenting the contribution of this thesis in terms of the developed control schemes to allow the provision of advanced services to support AC mainland grids operation. In Section 4.2 it is introduced the developed control scheme to allow MTDC grids with offshore WF on contributing to the AC mainland system primary frequency regulation. In Section 4.4, an assessment for the provision of FRT by MTDC grids is performed. It has been identified a major challenges, precluding the FRT provision. First, the de-coupling introduced by the adoption of DC that disables the offshore-located WT on detecting mainland AC voltage sags. Then, the development of DC voltage raise during the AC-side voltage sag. In order to overcome these barriers, several control strategies are proposed and evaluated in this chapter. Finally, in Section 4.6 a control strategy to assure the operation of the DC grid following the permanent disconnection of an onshore HVDC-VSC is proposed.

The control schemes presented in this chapter share the aspects of being local, not relying in communication infrastructure and operating autonomously.

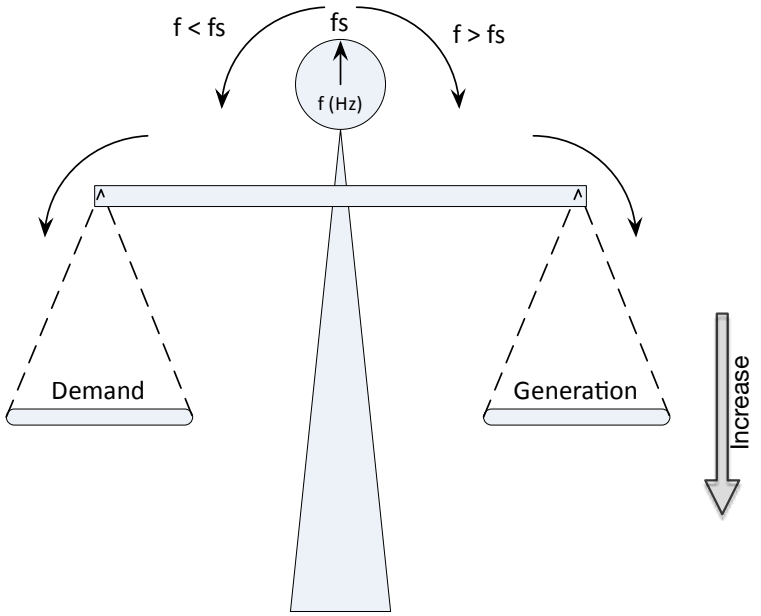

Figure 4.1: Frequency equilibrium conceptual principle

4.2 Provision of Frequency Control Services by MTDC Grids with Offshore Wind Farm Presence

4.2.1 The Primary Frequency Control in Power Systems

The power system frequency is the quantity that contains the information of the system equilibrium between the generation and the demand. When the power equilibrium is attained, the generation copes with the demand and consequently the frequency assumes the nominal value. The illustrative scheme depicted in Figure 4.1 has been included to help understanding the power system frequency principle. The scheme consists on an old-fashioned weighing-machine which symbolically contains the generation and demand quantities at each plate. An equilibrium situation, as aforementioned, leads to a null frequency drift. Nevertheless, around the power equilibrium two situations of disturbance may occur:

- Overfrequency - The generation increases or the demand decreases.
- Underfrequency - The generation decreases or the demand increases.

In a classical power system the frequency regulation is provided by synchronous generation units. Two distinct frequency regulation actions co-exists (primary and

secondary frequency regulation) [92]. The primary frequency regulation is based on local controllers installed at each synchronous generator and has a quick deployment characteristic and aims at stabilizing the AC network frequency aftermath a disturbance. The secondary frequency regulation has a larger deployment time and aims at offsetting the frequency error (bringing the frequency back to the nominal value through the power equilibrium promotion). Therefore, secondary frequency regulation mechanisms are centralized over the well known Automatic Generation Control (AGC) System.
A power system can be operated without secondary frequency regulation assuming that the frequency can have permanent drifts from the nominal value, (for example in islanding operation). However, a power system cannot operate without primary frequency control. In fact, the primary frequency control, as aforementioned, is responsible to guarantee the power system stabilization after load/generation disturbance and without it, generation or load disturbances would lead to instability. The classical vision of electrical power systems also defines that generators are responsible for providing the primary frequency regulation. Nevertheless, some authors defend that future power systems may have frequency regulation capability at the demand-side through responsive loads [93], [94].

The first requirement for a generator to provide frequency regulation consists on the guarantee of the existence of a reserve power margin. This means that the generator should not be operating close to the minimum technical power, guaranteeing that an effective active power reduction will be performed in case of over-frequency disturbance. At the limit the generator can be disconnected however, the re-connection process may take some time. Similarly, the generator should not be operated near the maximum technical power guaranteeing that an effective active power increase can be performed in case of an under-frequency disturbance. The generator increases or decreases the active power generation through the control of the intake of the associated turbine (steam, diesel, water). So, a local controller is required to quickly determine the accurate turbine intake based on the generator speed mechanism or frequency at generator terminals. The fast characteristic determines that local controllers must be installed at the generator level allowing an autonomous operation. These devices make a constant monitoring of the frequency

at the generators' terminals and constantly adjust the valve that governs the turbine intake controlling the exact fuel quantity to origin the accurate active power delivery amount.
The primary frequency regulation fundamental controller is also called power-speed controller and consists on a droop control (proportional gain) that defines the generator power based on the frequency or generator speed deviations. A detailed description of this controller can be found in Section 3.6.4.

At the early stage of wind power integration on power systems, the generators used to be small and without primary frequency regulation capability. From the power systems dynamic security perspective , a small set of small induction generators with no frequency regulation capability did not represent a potential problem for the system stability. However, the rapid increase of generators size and the massive integration levels are now a matter of concern. Simultaneously, to accommodate the wind power, several conventional generation units needed to be set offline [29]. Consequently the share of generators with primary frequency control capabilities became reduced, contributing to making the system prone to instability in case of severe disturbance. At the time the challenge consisted on determining how to operate the electrical power systems with a significant amount of wind power, guaranteeing its dynamic security [29]. The previously mentioned challenge on how to operate a power system with a significant amount of wind power without degrading the dynamic security indexes has opened a new line of research. In order to avoid undermining the wind power reputation in terms of reliability and capability of control, the research focused on how to endow wind turbines with capability of contributing to the primary frequency regulation [11], [36], [95].
Nowadays, from the power system stability perspective, wind power is not seen as a passive technology but as an active player on the system frequency regulation.

4.2.2 Primary Frequency Control Provided by Wind Farms

As previously described, the primary frequency regulation is achieved through an output power injection control according to the frequency deviation. Over-frequency disturbances, related with demand decrease or generation excess, can be performed by the quick disconnection of some wind turbines or by reducing the generated

power and does not represent a significant implementation challenge. However, the opposite control capability, when the power systems experience an under-frequency disturbance, represents an enormous challenge. The under-frequency disturbances are related with demand increase or generation decrease. Thus the countermeasure to assure system stability consists on increasing the generated power. As previously addressed, conventional generation units can support the system through the operation of the primary frequency controller, increasing the generated power. However, the WT resource (the wind) is not controllable. Similarly to conventional generation units, to exploit primary frequency control in WT, the wind generators must have a reserve margin to be quickly deployed. To achieve this capability, several authors have proposed advanced control schemes that share a common characteristic, which consists on de-loading the generator. The wind turbine de-loading consists on operating it below its maximum wind power extraction capability. As discussed in Section 3.5, de-load operation can be achieved by degrading the aerodynamic performance of the wind turbine blade-set by acting on the blades' pitch angle β. In order to provide an adequate regulation, servo-motors are connected in the turbine hub, enabling the continuous adjustment of the turbines' blade pitch angle. A new active power/wind speed curve can be determined with a given de-loading margin as depicted in Figure 4.2

It is important to clarify that the pitch de-load at wind turbines is not a permanent condition and may be required for some situations where the network operator foresees a reduced primary frequency control capability margin (normally during valley hours where less conventional units are connected).

Several studies have been conducted on the topic of primary frequency regulation performed by wind turbines [30], [36] [96]. Nowadays, WT manufacturers provide this functionality in commercial WT. In line with the aforementioned concerns and aiming at achieving a larger and secure wind power penetration, ENTSO-E has recently published a grid-code draft version which tackles the primary frequency control aspects by requiring the frequency control regulation capability for type C units connected to the grid [13]. The details on type C units are defined by the installed active power and the grid zone where it is connected according to the Table 4.1 in order to participate in primary frequency regulation.

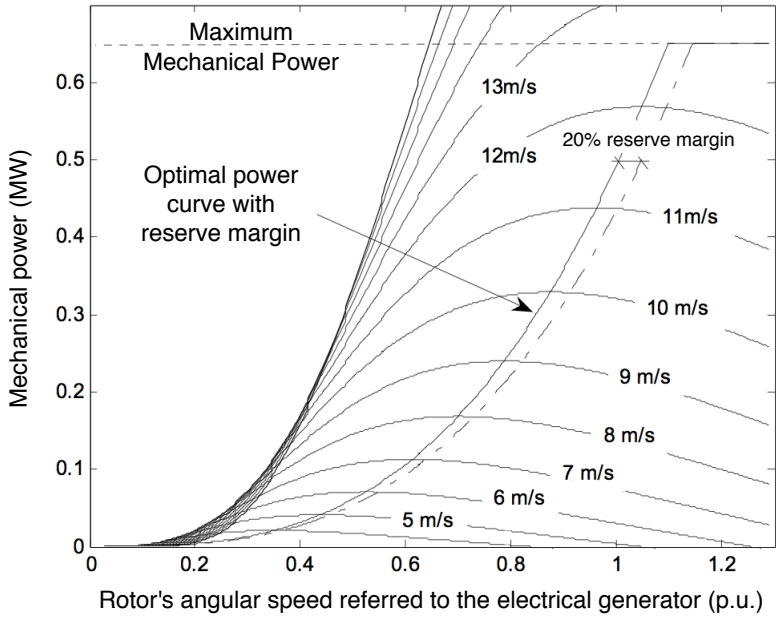

Figure 4.2: Example of wind turbine mechanical power/speed curve for a de-loaded operation (adapted from [11])

Table 4.1: ENTSO-Type C generation units minimum power threshold for different European Grid Areas [13]

Synchronous Area	Maximum capacity threshold from which a Generating Unit is of Type C participate in primary frequency regulation
Continental Europe	50 MW
Nordic	10 MW
Great Britain	10 MW
Ireland	5 MW
Baltic	5 MW

4.2.3 Inertia Emulation Provided by Wind Farms

The inertial response is an intrinsic characteristic of synchronous generators and consists in the fast active power response following an under-frequency disturbance. This behaviour avoids the frequency from assuming high decay rates. Some studies have concluded that the inertia behaviour is important to the power system frequency regulation by avoiding the loss of wind generation due to the tripping of rate-of-change-of-frequency (ROCOF) relays and consequently jeopardizing the frequency support capability [23]. A deep assessment of this topic was made in the Chapter 2 where several studies related with the topic of the inertia emulation by wind generators have been presented.

Since the wind generators are not synchronous machines, the inertia contribution has to be emulated and it is attained through a specific control-loop which commands the deployment of an additional power output proportionally to the frequency rate of change. The active power surplus is attained by converting the kinetic energy existing in the generators rotor, into active power that is quickly delivered to the grid.

4.2.4 Challenges for Primary Frequency Control Provided by Offshore MTDC-connected Wind Farms

The provision of frequency control services in offshore WF has been investigated for point-to-point connection as reported in Chapter 2. This type of service can be achieved through the adoption of wind turbines with primary frequency control capability. However, offshore located WT do not have physical access to onshore frequency. The existence of a DC connection fully decouples the frequency between the AC interconnected nodes. So, instead of acquiring the frequency measurement at their terminal, they receive the onshore frequency measurement through a dedicated fast communication channel [97]. The transposition of this approach to the MTDC grid is not direct. In fact, in a MTDC grid several AC mainland grids may be interconnected without a single AC frequency measurement. Instead, to directly apply the approach considered for point-to-point connections, several communication links must be deployed between offshore WF and all the interconnected AC

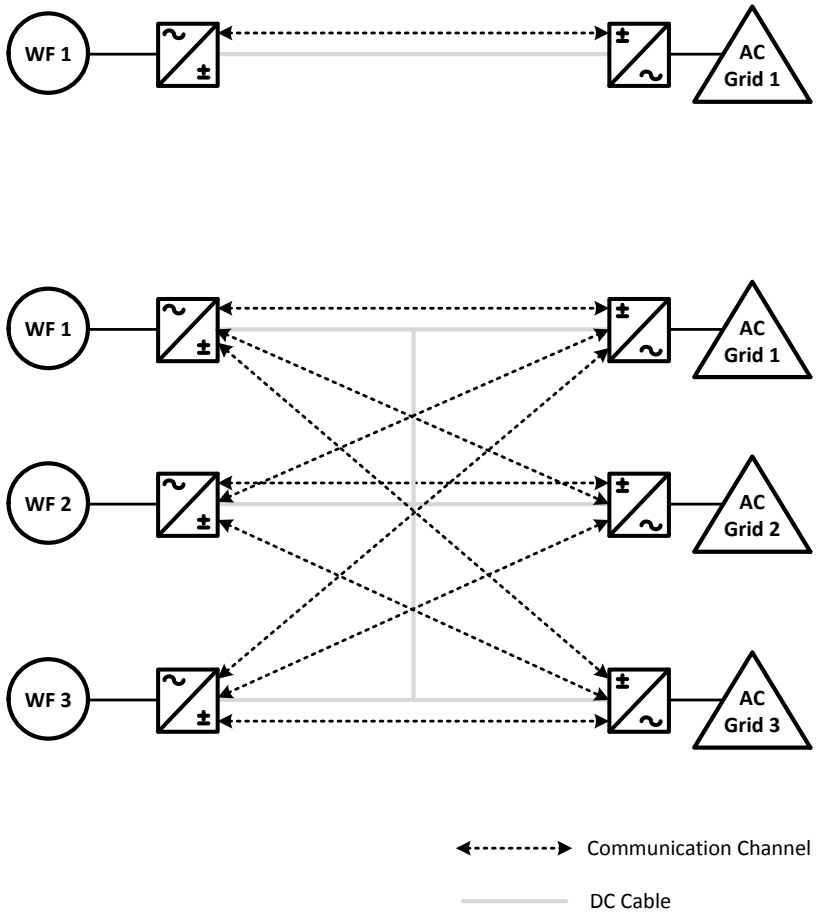

Figure 4.3: Communication infrastructure for offshore WF frequency regulation in point-to-point and Multi-terminal DC connections

mainland grids as illustrated in Figure 4.3. That way, offshore WF would be able to have access to the frequency measurement on every interconnected AC mainland grid .

However, from economical and technical perspective, the deployment of point-to-point communication in MTDC grids is not feasible. As depicted in Figure 4.3, the bi-directional interconnection between the offshore HVDC-VSC and all the onshore HVDC-VSC are required, increasing the cost and reducing the reliability (due to the increase of number of connection links and the associated length). In contrast, an option consisting on adopting a centralized controller, as illustrated in Figure

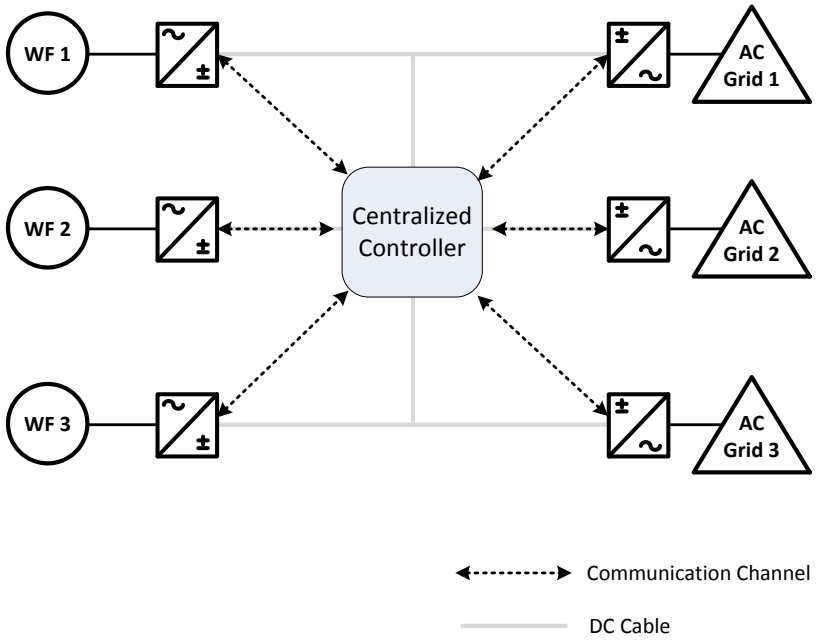

Figure 4.4: Centralized controller at Multi-terminal DC grid

4.4, can theoretically cope with the requirements for the primary frequency control provision.

The centralized controller performs as a concentrator that receives the AC mainland grids frequency measurements as well as the offshore WF active power delivery and respective reserve margins. Facing an AC mainland disturbance, the centralized controller must determine the offshore AC grids frequency set-point to transmit to the offshore HVDC-VSC of each offshore WF. That way the offshore WF are able to actively participate in the AC mainland frequency regulation.

However, as previously discussed, depending on the operation philosophy and on the associated control parameters, the active power regulation provided by the offshore WF will be shared through the onshore HVDC-VSC instead of being channelled to the most demanding AC area (the area there the frequency disturbance have occurred). Additionally, fast phenomena such as inertia emulation provided by offshore WF, may not be successfully deployed due to the communications and

calculations delay performed at the centralized controller.

In an attempt of avoid the aforementioned bottlenecks and overcoming reliability issues related to the communication channels and the centralized controller, the strategy proposed in this thesis consists on adopting local controllers to be housed both in onshore and offshore HVDC-VSC as well as at WT level in offshore WF. The major goal is to derive a communication-free control strategy that enables the MTDC grid to provide frequency regulation services to mainland AC grids. The control rules to be embedded in the onshore, offshore and WT level constitute a cascade control mechanism that is able to deploy the defined functionality.

4.3 Advanced Control Strategies for Primary Frequency Control Provision by Offshore Wind Farms

The control methodology developed in the framework of this thesis consists a communication-free cascade of local controllers. The common aspect among the offshore and onshore HVDC-VSC is the DC grid which serves as interconnection infrastructure between them. Thus, the proposed methodology relies on the DC grid infrastructure to perform as a virtual communication medium among the interconnected HVDC-VSC. Bearing in mind that the onshore HVDC-VSC (as discussed in Section 3.7.2) is responsible by controlling the DC voltage at its terminals, the frequency variations at onshore mainland AC grid can be transposed to DC voltage variations at the onshore HVDC-VSC terminal. Then, the DC voltage variation will be reflected at all the DC grid terminals. At offshore-level, offshore HVDC-VSC will measure the DC voltage variation and will be responsible to control the AC offshore frequency proportionally to the DC voltage variation. Offshore wind turbines with primary frequency control capability are then expected to respond accordingly.

In order to attain this cascade control scheme, several modification must be conducted at onshore and offshore converter-level. These modifications are highlighted in the following topics. An overview of the cascaded control operation is illustrated in Figure 4.5.

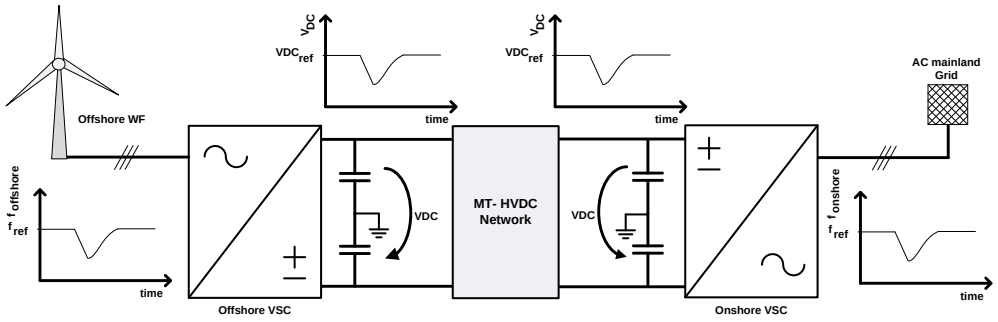

Figure 4.5: Frequency and DC voltage variations in the cascaded frequency regulation scheme

4.3.1 Onshore HVDC-VSC Advanced Control Scheme for the Provision of Primary Frequency Regulation

The onshore HVDC-VSC are the devices that have access to the respective AC mainland frequency and simultaneously to the DC grid. So, rationale of the proposed approach consists on transposing the AC mainland frequency deviation to a DC voltage deviation at each onshore HVDC-VSC. To perform this control strategy, some enhancements over the basic control of the onshore HVDC-VSC were performed, creating two operational modes:

- **Normal operation mode** - The frequency deviations are within an admissible range: the onshore HVDC-VSC DC voltage is governed by the previously mentioned K_{pv} droop control. The admissible frequency deviation range can be defined by the Transmission System Operator (TSO) according to the characteristics of the AC mainland network where the onshore HVDC-VSC is connected to.

- **Disturbance operation mode** - The AC grid frequency to which the HVDC-VSC converter station is connected drops below a certain margin due to any load/generation imbalance. In such situations, primary frequency regulation services are requested to be autonomously deployed in the MTDC grid in order to help stabilizing the AC grid frequency. Regarding the mode of deploying the offshore WF reserves, it firstly requires an additional control mechanism

that translates onshore AC grid frequency grid variations to MTDC voltage profile variations. In this case, the onshore HVDSC-VSC converter station measures the terminal frequency and whenever it drops below the referred margin, the active power/DC voltage droop control mechanism is held and a new droop control relating onshore AC grid frequency and MTDC voltage enters in operation, according to the following equation:

$$V_{DC} = V_{DC}^{0} - k_{fv} \times f_{grid} \tag{4.1}$$

where V_{DC} is the reference value for the DC voltage at the onshore HVDC-VSC, V_{DC}^{0} is the pre-disturbance DC voltage resulting from the operation of the converter in the normal mode governed by the k_{pv} droop, k_{fv} is the frequency/DC voltage droop and f_{grid} is the frequency of the onshore AC grid to which the converter is connected.

The control rule schematic illustrated in Figure 4.6 depicts the operation of the grid on both normal and disturbance modes.The DC voltage variations resulting from at a given onshore HVDC-VSC impacts on the MTDC grid DC voltage mainland AC grid. This cascade event is then used as a virtual communication medium in order to implement active power control strategies at the offshore converter level as it is described in the next section.

4.3.2 Offshore HVDC-VSC Advanced Control Scheme for the Provision of Primary Frequency Regulation

As presented on Section 4.2.2, modern WT are able to deploy frequency regulation services based on the frequency measurements at their terminals. Additionally, offshore HVDC-VSC, performing as a slack-bus for the AC offshore grid, are responsible by controlling the AC offshore voltage and frequency. Based on the control approaches previously discussed for the onshore HVDC-VSC, the rationale to derive the control scheme for primary frequency provision at offshore HVDC-VSC level consists on controlling the offshore AC grid frequency proportionally to the DC voltage variations. To do so, an additional control-loop for the offshore frequency has been added at the offshore HVDC-VSC. The schematic of this additional frequency control-loop is illustrated in the Figure4.7.

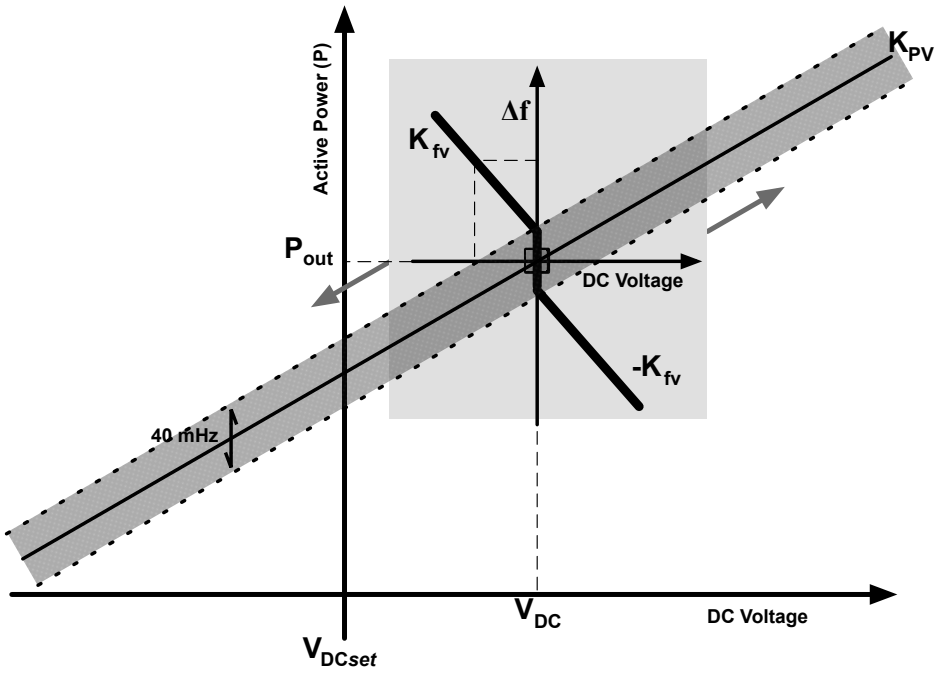

Figure 4.6: Onshore HVDC-VSC droop control for normal and disturbed operation

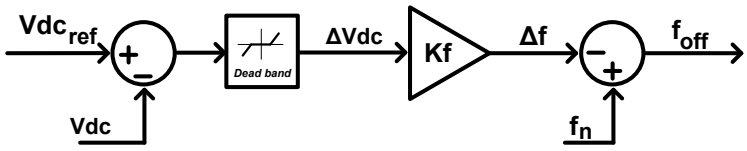

Figure 4.7: Offshore HVDC-VSC AC grid frequency control-loop

The additional control loop basically imposes a frequency variation proportionally to the DC voltage variation, determined by the difference between the actual DC voltage VDC and the steady-state DC voltage VDC_{ref} (the steady-state DC voltage may be determined with a few minutes base average) through a proportionality factor defined by the droop k_{vf} ($puHZ/puVdc$). So the offshore AC grid frequency is controlled according to the DC voltage variation which changes according to the AC mainland grid frequency variation. Offshore WT are then able to provide active power control based on the AC offshore frequency variation. This contribution is not going to have a direct impact on the offshore frequency variation (since it is synthetic and depends on the DC voltage profile variations). On contrary, it is expected the the active power contribution at offshore level will impact on the AC mainland grid frequency support. Thus, the positive effects on the mainland AC grid frequency will be translated as smaller DC voltage variations and consequently in smaller AC offshore grid frequency variations.

4.3.3 Offshore Wind Turbine Primary Frequency Support and Inertial Emulation Capabilities

The rationale of the presented cascaded control scheme is to allow offshore WT responding to onshore mainland AC grid primary frequency regulation in the same manner of the existing onshore WT. So, offshore WT were considered to be similar to onshore WT with primary frequency regulation capabilities. The concept of WT providing frequency support has been extensively described in the literature. Section 2.2.2 analyses the methodologies to achieve this type of behaviour. It is consensual that in order to provide frequency support, a reserve margin must exist at WT-level. The proposal consists on creating an operational power reserve margin through the WT de-loading, allowing afterwards its deployment when required. The reserve margin at WT is a topic that has already been addressed and is achieved through the WT pitch control.
Without lack of generality, for this specific evaluation case, PMSG-based WF with primary frequency regulation and inertial behaviour emulation have been considered. The overview of the whole WT blade's pitch control based on the AC offshore grid frequency is depicted in Figure 4.8

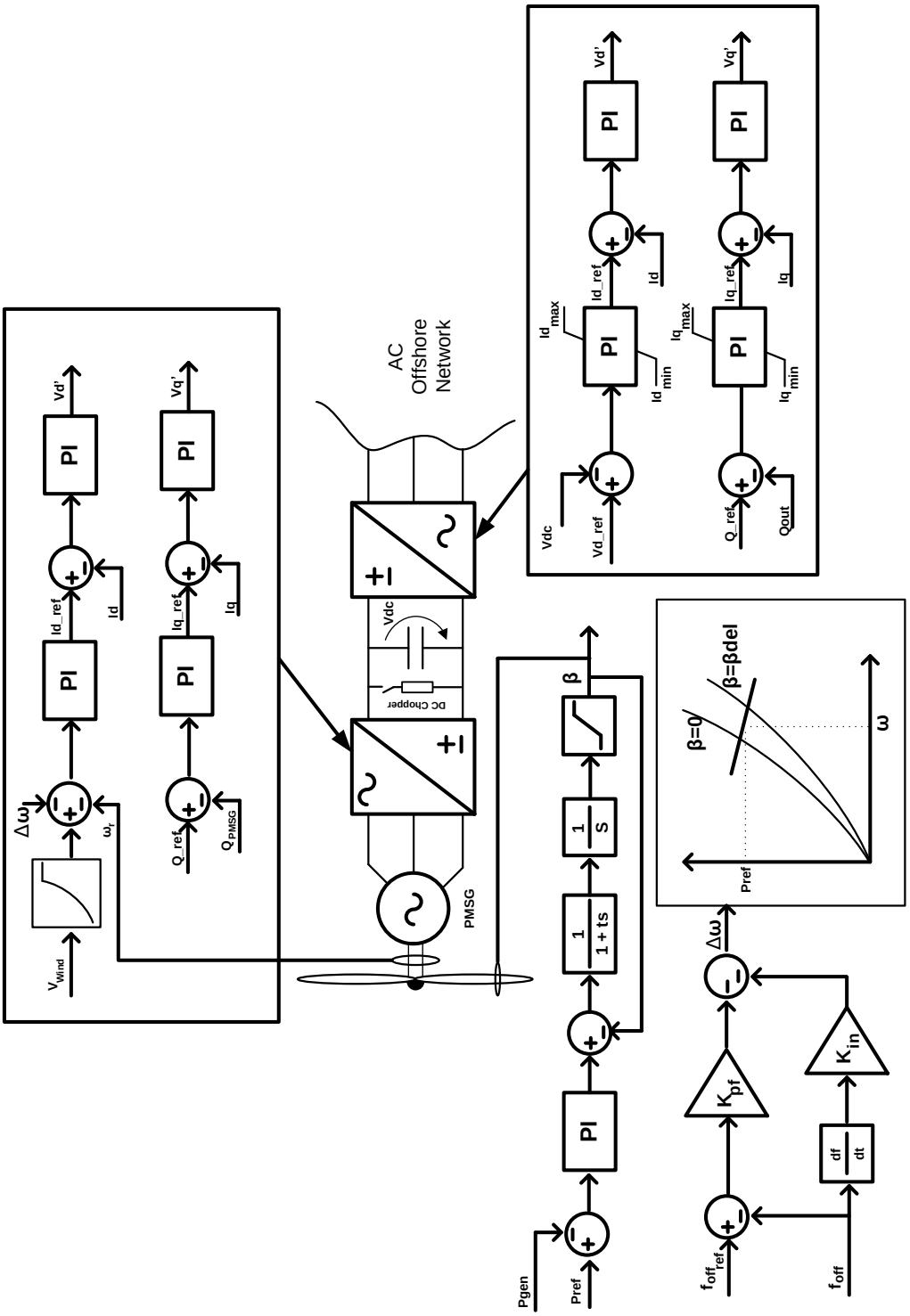

Figure 4.8: Control scheme of PMSG wind turbine with primary frequency control capability

The proposed control strategy relies on the AC offshore grid frequency measurement to determine the control of the generator active power output and the blade's pitch angle. The offshore frequency error is determined by the difference between the offshore frequency f_{off} and a frequency reference value f_{offref} ($50Hz$ by default). The frequency error is adapted to a rotational speed error which is further added to the nominal rotational speed ω_r obtaining a new reference speed. The new reference speed generates a new active power reference P_{ref} according to the generator characteristics. The active power reference P_{ref} serves as input to the WT blade's pitch controller. The P_{ref} is determined according to a linearised function (see Figure 4.8) around the generator operating point. To determine the linear relation, the generator characteristic curves were used, determining the extreme operating points: for $\beta = 0$ and β_{del}, where β_{del} is the β pitch angle for de-loaded operation. The β pitch angle is then controlled by comparing the actual generated active power P_{gen} and the reference active power P_{ref}. The obtained active power error serves as input to a PI controller which aims at determining the correct pitch blade's angle in order to achieve the new active power reference P_{ref}. The pitch blade's controller is also composed by a transfer function and a rate limiter that simulates the behaviour of the servo-motors responsible for acting on the blades rotation.

Regarding the inertial behaviour emulation, a frequency derivative, or in other words the frequency rate-of-change, is calculated and used to provide a fast active power control at the WT level in the moments subsequent to a mainland AC grid disturbance based on the k_{in} gain (see Figure 4.8). A fast active power injection from the WT is achieved through the transformation of rotor kinetic energy into electric power, implying generator speed reduction. As depicted in the Figure 4.8 the additional speed variation $\Delta\omega$ is provided to the GSC control-loop in order to allow the converter quick active power delivery related to the inertial response.

Primary Frequency Support Among Mainland AC Grids

Multiterminal DC grids are not envisioned for the single purpose of interconnecting offshore WF. As discussed, the MTDC grids can perform as backbone for AC systems providing inter AC area power flows. So, similarly to AC mainland control areas, it is expected that the interconnected AC mainland grids should be able to share

primary frequency regulation services for a disturbance on a given AC area. The control philosophy previously presented has been also designed to allow inter-AC area frequency support. In fact, the signal of the previously presented onshore HVDC-VSC droop gain k_{fv} is essential to achieve the inter-area frequency support since may cope with the remaining onshore HVDC-VSC k_{pv} droop control. For a under-frequency disturbance on a given AC area, the associated onshore HVDC-VSC will decrease the associated DC voltage in order to increase the active power extraction towards this AC Area. Simultaneously, the remaining onshore HVDC-VSC will decrease their active power extraction in the attempt of maintain the DC voltage, extracting less power from the DC grid, creating an active power reserve that can be channelled towards the affected HVDC-VSC converter.

4.4 Fault Ride-through Capability in Multi Terminal DC Grids

4.4.1 The Fault Ride-through Service in Modern Wind Turbines

The FRT can be defined as the ability of a given generator or a set of generators (a WF) have on remaining connected to the grid during voltage sags. Grid codes for WF connection often place an additional requirement for FRT capability, consisting on the injection of reactive current in order to leverage the neighbouring AC voltage profile in the attempt of avoiding the disconnection of non-FRT compliant WF. Voltage sags are commonly related to fault events in the grid. The disconnection of wind generators during the fault event could lead to significant power imbalance that might affect the system stability .

In Section 2.2.2, the main findings and approaches for FRT compliance for different WT technologies were addressed. The presented control approaches share a common aspect: they rely on the AC voltage as the triggering event for proper control schemes. Despite WT have the ability of withstanding voltage sags at their terminals, this characteristic is useless for offshore applications since the DC connection fully de-couples onshore and offshore AC grids.

4.4.2 Fault Ride-through Capability in HVDC-connected Offshore Wind Farms

On HVDC-connected WF, the capability to withstand the mainland AC grid voltage sags is associated to the onshore HVDC converter stations since they are the front-end for the interconnection between the DC-connected WF and the mainland grid. The classic HVDC-LCC are not able to fulfil the FRT requirements since it relies on the AC-side voltage to trigger the thyristor-based electronic valves [6]. On the other hand, HVDC-VSC, has the ability to remain connected to the AC grid during AC voltage sags. Additionally, the capability of independent control of active and reactive power, guarantees that the reactive current can be injected on the AC mainland grid during fault events. Nevertheless, the critical challenge regarding the FRT capability in HVDC-connected offshore WF consists in the loss of active power injection during the low voltage periods. Bearing in mind that the active power delivery can be defined as:

$$P_{AC} = I_{out} \times V_{AC} \times \cos\delta \tag{4.2}$$

where P_{AC} is the active power delivered by the onshore HVDC-VSC to the AC mainland grid, I_{out} is the current delivered by the onshore HVDC-VSC to the AC mainland, V_{AC} is the AC-side voltage profile and the $\cos\delta$ is the onshore HVDC-VSC power factor.

Following a mainland AC grid fault ($V_{AC} \approx 0$) assumes a low value, the onshore HVDC-VSC control loop will increase the current in the attempt of achieving the pre-fault active power delivery. However, the HVDC-VSC has a maximum current limit that cannot be exceeded. Therefore current injection will saturate at the maximum HVDC-VSC current rating. Consequently, the active power delivery will be significantly reduced. Without the adoption of dedicated control mechanisms, offshore WF will not detect the AC mainland fault event and will remain injecting the pre-fault active power. As reported in the literature and highlighted in Section 2.4.5, an active power imbalance will take place in the DC link. The resulting power imbalance impacts on the DC capacitors energy leading to a DC voltage rise effect that might culminate in a DC overvoltage [79]. The impacts of a AC voltage sag in the DC voltage rise can be quantified: it depends on the pre-fault power

injection into the mainland AC grid, the steady-state DC voltage, on the active power shortage during the fault event, the equivalent DC link capacitance and on the mainland AC grid voltage sag duration. However, the main objective does not consists on quantifying the maximum DC voltage level. On contrary, the most important issue consists on determining the maximum time interval to promote fast active power control actions in order to avoid DC voltage to overpass a maximum admissible value that may compromise the integrity of several components such as DC cable insulation, DC capacitors or even the HVDC-VSC, while precluding the accomplishment of the desired FRT functionality. According to equation 2.1, this time can be determined and for typical HVDC applications as reviewed in Section 2.4.5 it is around some tens of milliseconds.

The maximum time for DC voltage control (following a disturbance leading to an active power reduction on onshore HVDC-VSC) has been determined for the generic test case, the DC grid H topology. Since the amount of non-delivered power depends on the AC-side fault event, the time for deployment of DC voltage control strategy has been computed in function to its quantity. As stated in Section 2.4.5, according to the suggested in [79], the determination of the time for deployment of DC voltage control strategy can be computed according to the equation 2.1. For the sake of simplicity, the capacitance value C has been assumed as the equivalent capacitance of the whole circuit. Thus, considering that each HVDC-VSC has an associated DC capacitor bank (150 μF considering both terminal poles), the equivalent capacitance can be achieved by summing the capacitance of the 4 DC grid terminals. So, the equivalent capacitance C is of 600 μF. The total MTDC grid pre-fault active power delivery has been considered being 400 MW. The nominal DC voltage V_{dc-th} has been considered as being 300 kV while the maximum overvoltage V_{dc-max} has been considered as being 20%, consisting of 360 kV.

The maximum time for the effective deployment of DC voltage control strategy (aiming at avoiding overpassing 20% of the nominal voltage) has been computed for several levels of non-delivered active power. The results are depicted in Figure 4.9.

The results illustrated in Figure 4.9, show that the greater the non-delivered power, the faster the DC overvoltage avoidance mechanism must have an effective action. For example, a fault leading to 50% non delivered power (200 MW), requires

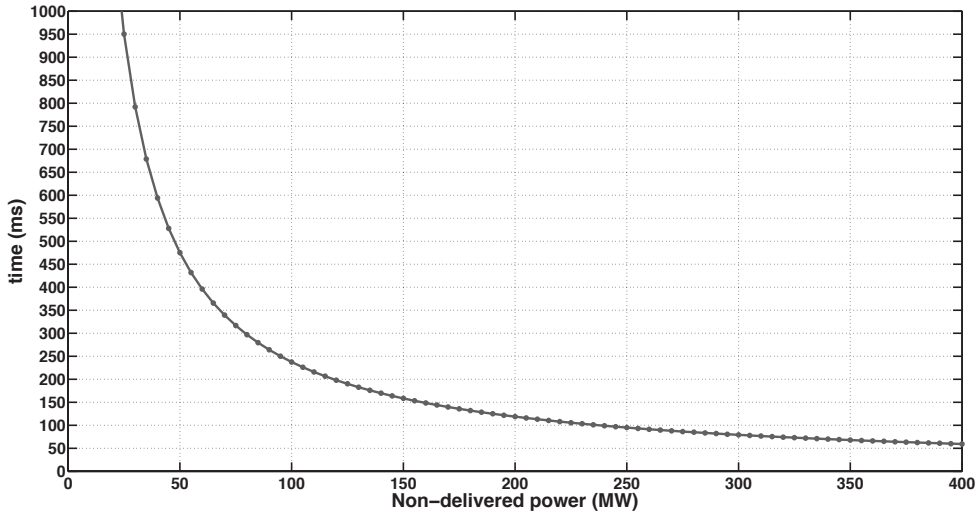

Figure 4.9: Time requirement for the deployment of DC voltage control strategy in function of non-delivered active

a control mechanism able to provide an effective DC voltage control on about 125 ms to avoid DC voltage on overpassing the maximum admissible value of 20% over the nominal.

4.4.3 Mechanisms for DC Overvoltage Control in MTDC Grids with Offshore Wind Farm During FRT Provision

FRT provision from MTDC grids relies on the ability of mitigating the DC voltage rise effect following a mainland AC grid fault. The DC voltage rise control requires mechanisms that are able to provide fast active power control. As presented in some papers [80] [79], the active power dissipation is a possible solution to control the DC voltage rise and can be achieved through the adoption of chopper resistors (usually denominated just as choppers [80]). This device consists on a power electronic interfaced resistor which is able to dissipate active power. The chopper can be characterized by the instantaneous power dissipation and maximum energy dissipation capacities [98]. Regarding the mechanisms for active power dissipation two approaches may be considered:

- **Onshore power dissipation:** Chopper Resistors are installed at onshore HVDC-VSC DC terminals and are set to dissipate power proportionally to

the DC voltage rise;

- **Fast active power control at WT level:** An auxiliary mechanism guarantees that offshore WF are able to reduce the active power inject to DC grid aiming to mitigate the DC voltage rise by:
  - **Dissipating active power at WT-located chopper resistors:** Fully electronic interfaced Wind Generators like PMSG with FRT capability have an internal DC chopper resistor mounted at the WT tower and connected to the back-to-back electronic converter DC link. The option consists on dissipating exceeding active power at this chopper resistor, reducing the injected power to the DC link or grid.
  - **Controlling active power injection through generator speed control:** In the case of DFIG, fast active power control can be achieved if a controlled acceleration of the WT id allowed while absorbing electric power in the form of kinetic energy.

The previously presented active power injection through generator speed control can be also applied to PMSG. However, the PMSG normally have a DC chopper resistor in the DC bus of the AC/DC/AC converter as a protective device.

It is important to stress that the active power reduction that have been mentioned so far does not have a definitive characteristic. The mainland AC voltage sags are normally associated to fault events that should be cleared by the AC protective system. So, depending on the grid code requirements (addressed in Section 2.2.2) the voltage sag should not least more than some hundreds of mili-seconds.

The previously introduced active power balance mechanism differ in terms of location, and thus control aspects. For a MTDC grid, dispersed power dissipation approaches does not rely on communication channels on contrary to what is proposed for point-to-point connections in [79] and [80]. The reason for that consideration consists to the fact that facing a more complex topology, a centralized control layer should be required to guarantee the proper coordination among the onshore and offshore HVDC-VSC. Nevertheless, the operational time frame of centralized is not adequate with the phenomena involved and the associated requirement for fast active power dissipation to guarantee the FRT provision. Thus on contrary, local

controllers operating in cascaded control scheme in a communication-free philosophy is here proposed. The aspects for the several controllers implementation are highlighted according to each case in the following sections.

4.4.4 Control Strategies for DC Voltage Rise Control at Onshore HVDC-VSC level

From the literature analysis, it becomes consensual that in order to avoid the DC voltage overpassing a pre-defined maximum admissible level, an active power equilibrium promotion mechanism must exist. For the specific case of onshore active power equilibrium mechanism it consists on the installation of DC chopper resistors at each onshore HVDC-VSC DC terminal. The control scheme for the onshore chopper device is robust and quite simple. According to the illustration on Figure 4.10 the chopper control consists on locally measuring the DC voltage profile (VDC) and determining the voltage variation through the comparison with a pre-defined reference value (VDC_{ref}) which corresponds to the steady-state DC voltage profile.

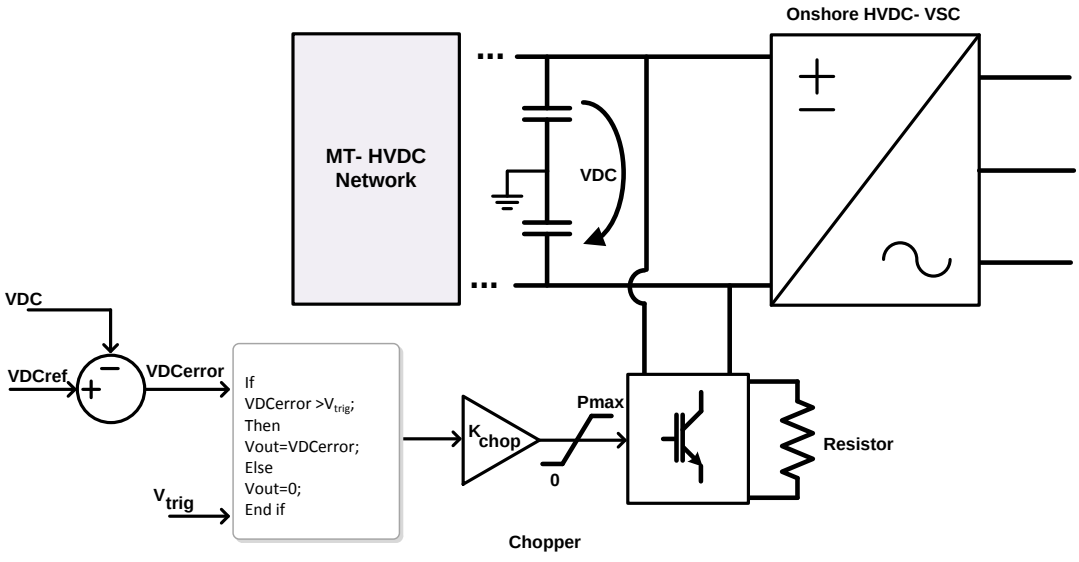

Figure 4.10: Onshore-located chopper and associated control-loop

The steady-state DC voltage profile can be determined by the mean DC voltage

profile value within an operation spectrum of a few minutes or, can be set through a supervisory control algorithm that refreshes its value with a given refresh rate of some second. Next, the DC voltage error is filtered by a dead-band block which eliminates small DC voltage fluctuations that may have origin on offshore wind power variations. Afterwards a proportional gain k_{chop} is set in order to adapt the DC voltage variations into an active power dissipation set-point (from null to the maximum DC chopper power dissipation capability P_{max}) that is further sent to the electronic converter which interfaces the chopper resistor and the DC grid. This approach allows an autonomous operation within the required time-frame. However, to guarantee the correct protection of the whole MTDC grid, a worst scenario approach must be followed, installing a chopper resistor at each onshore HVDC-VSC DC terminal with the same rate of the associated converter aiming at guaranteeing a proper DC voltage magnitude for the most severe situation which corresponds to the total loss of active power extraction capability . This fact bring an additional cost to the whole MTDC grid installation. In alternative, the dispersed power equilibrium promotion mechanisms may cope with the avoidance of DC voltage overreaching the maximum admissible value with a reasonable installation and deployment cost.

4.4.5 Control Strategies for DC Voltage Rise Control at Offshore HVDC-VSC level

As, previously discussed, mainland AC grid faults may lead to MTDC grid overvoltages due to the reduction of active power injection capability of the HVDC-VSC connected to the faulted area. Therefore, a possible approach consists on the development of advanced control mechanisms for fast active power control at WT-level to consequently mitigate the DC voltage rise effect, assuming the necessary conditions for the MTDC to provide FRT functionality.

The offshore WT are assumed to have FRT capability so, minor changes on the WT control are required. Nevertheless, the offshore WF are fully decoupled from the AC mainland grids. So, a cascaded control scheme has been designed to allow offshore WF reacting to the AC mainland fault events.

The proposed control scheme does not involve any modification to the onshore HVDC-VSC control-loops. In fact, it consists on taking advantage of the appearance

of the DC voltage rise effect in the MTDC grid (which will also appear at the offshore HVDC-VSC DC-side terminal) to control the offshore HVDC-VSC according to the main strategies (Figure 4.11) that share a common characteristic of achieving fast reduction of WT active power.

a) **Offshore AC grid voltage contreol:** - This control strategy consists on modulating the AC offshore grid voltage symmetrically to positive DC voltage profile variations. The control-loops of this specific strategy are depicted in Figure 4.11 and identified with the letter a). The AC offshore grid voltage (VAC) is set according to the equation 4.3:

$$VAC = VAC_{ref} + K_{DC/AC} \times (VDC_{ref} - VDC) \tag{4.3}$$

where, VAC_{ref} is the AC offshore grid voltage reference, $K_{DC/AC}$ is the DC voltage to AC voltage gain, VDC_{ref} is the offshore DC grid voltage reference and the VDC is the DC voltage at the associated offshore HVDC-VSC DC terminal. Through this control strategy, offshore WT are able to experience an AC voltage reduction at their terminals, which can be used to quickly reduce active power injection at WT-level.

b) **Proportional AC offshore frequency increase** - This control strategy consists on imposing AC offshore frequency variations proportionally to DC voltage profile variations. The control-loops of this specific strategy are depicted in Figure 4.11 and identified with the letter b). The AC offshore grid frequency ($f_{offshore}$) is set according to the equation 4.4:

$$f_{offshore} = f_{ref} - K_{DC/f} \times (VDC_{ref} - VDC) \tag{4.4}$$

where, f_{ref} is the offshore frequency reference ($50Hz$), $K_{DC/f}$ is the DC voltage/offshore frequency gain, VDC_{ref} is the offshore DC grid voltage reference and the VDC is the DC voltage at the associated offshore HVDC-VSC DC terminal. It is then expected that WT with frequency-dependant control are able to respond to the AC offshore overfrequency by reducing the injected power.

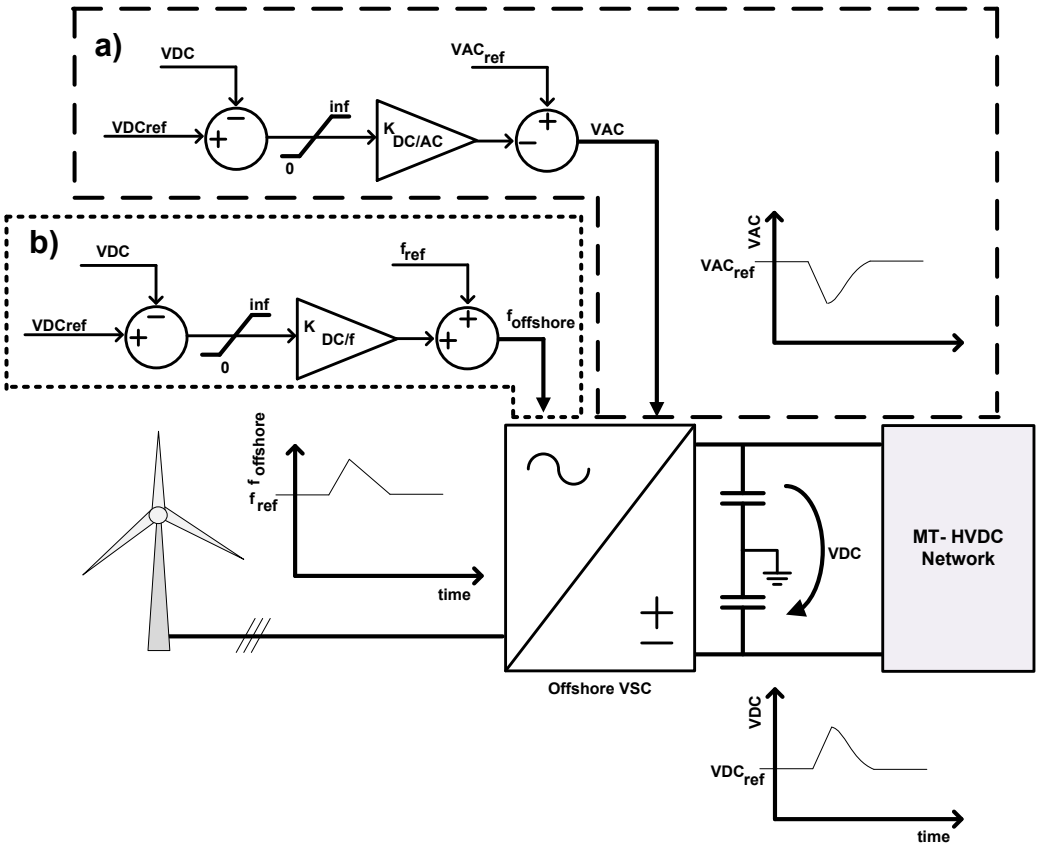

Figure 4.11: Possible control strategies of the offshore HVDC-VSC for fast active power reduction at offshore-level

4.5 Control Strategies for Offshore Wind Turbine FRT Response

The expected response for onshore WT applications during FRT situations consists on remaining connected to the grid and simultaneously inject a given reactive current according to the grid-code specifications. For the specific case of offshore WF with the previously mentioned offshore HVDC-VSC control schemes, it is expected that offshore WT do not inject any reactive current during a voltage sag, in order to avoid the resulting AC voltage profile leverage effect which may preclude the use of the previously discussed offshore AC grid voltage control. Additionally, it is expected that WT reduce the injected active power in order to contribute to the DC power

balance and consequently to the DC voltage rise effect mitigation. The modifications over WT control scheme for the FRT provision will depend on the WT technology as well as the offshore HVDC-VSC adopted control strategy (a) or b)).
Without lack of generality, two offshore WT technologies were considered in this research:

- Variable speed WT equipped with PMSG, which are interfaced with the grid through a AC/DC/AC back-to-back converter (including DC chopper at the DC-link);
- DFIG-generator.

4.5.1 Fast Active Power Control at Offshore WT-level based on the Terminal Voltage

For the cases where an offshore AC grid voltage control strategy is adopted, the PMSG-based WT must not inject reactive current during the resulting voltage sag. Thus, the reactive power component must be set to do not inject current during the low voltage.

In PMSG-based WF, the reduction of the active power injection at the WT-level will be achieved by a partial active power dissipation at DC chopper located at the back-to-back converter DC terminal. In order to achieve this , a DC chopper is installed inside the WT tower, being connected to the DC busbar as depicted in the scheme illustrated in Figure 4.12. The chopper resistor will not only promote the desired active power reduction but also will control the DC voltage rise magnitude at the DC busbar.

The control scheme of the chopper resistor is similar to the control scheme presented for onshore chopper application. The control-loop permanently measures the AC voltage at the generator's terminal (VAC) and determines the error existing between this actual AC voltage and the reference AC voltage profile (VAC_{ref} - 1 p.u. in normal operation) value. The error signal, ($VACerror$) feeds a comparison block implemented through a "IF" function which is also fed by a trigger value (V_{FRT}) which consists on the voltage profile error that should trigger the FRT service provision. So, if the AC voltage error ($VACerror$) is bigger then the FRT triggering voltage (V_{FRT}) then the block output voltage ($Vout$) is equal to the AC

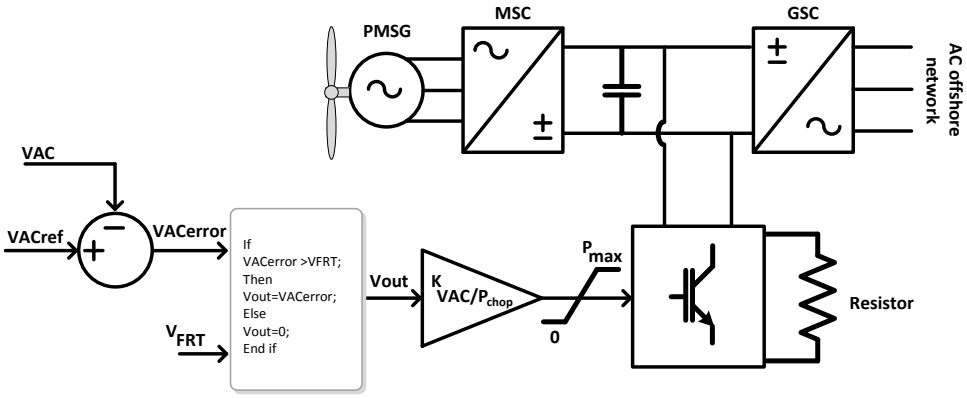

Figure 4.12: PMSG chopper resistor and associated control-loop for active power reduction based on AC undervoltage variations

voltage error ($VACerror$) else, the block output voltage ($Vout$) is null avoiding the chopper power dissipation. For the situations where the FRT functionality is active, the reference active power dissipation at the WT chopper is determined by equation 4.5:

$$P_{chopper} = K_{VAC/Pchop} \times (VAC_{ref} - VAC) \tag{4.5}$$

For DFIG-based WF the active power regulation is naturally achieved by the AC voltage regulation strategy (strategy a)). In fact, the undervoltage occurrence leads to the generator de-magnetization, slightly increasing its angular speed and consequently reducing the injected power. Recalling the DFIG electromagnetic torque (equation 3.34), it is directly proportional to the stator voltage $|V_s|$. As the electromagnetic torque is directly proportional to the active power, a stator voltage decrease will impact on the active power by decreasing it. However, following the proposals present in [99], some enhancements were made in the DFIG speed controller to avoid high speed variations and in-rush rotor currents.

Normally, on onshore-located applications, DFIG WT with FRT capability are set to inject reactive current through the reactive power control- loop in the attempt of providing support to the AC grid voltage. This functionality has been de-activated

in the offshore DFIG to avoid a counteraction over the offshore HVDC-VSC voltage control.

4.5.2 Fast Active Power Reduction at Offshore Wind Turbine Based on the Offshore AC Grid Frequency

The control schemes for frequency support have already been presented in Section 4.2.2 and involve the active participation of the pitch-angle regulation system. However, active power response through WT pitch-angle regulation does not cope with the FRT phenomena time requirements. In fact, the intrinsic WT pitch-angle response time is much higher than the active power regulation time-frame for DC grid voltage rise control. Nevertheless, fast active power regulation can also be performed on both PMSG and DFIG wind turbines with slight control-loops modifications in relation to offshore AC grid variations.

For the PMSG-based WF, the wind generator is fully de-coupled from the AC offshore grid by the back-to-back AC/DC/AC converter. Withal, the previously presented control scheme for active power reduction based on AC voltage reduction, can be adapted to respond to AC offshore grid frequency deviation. The control loop of the frequency responsive active power control is depicted in Figure 4.13 and can be described by the equation 4.6.

$$P_{chopper} = K_{freq/Pchop} \times (freq_{ref} - freq) \tag{4.6}$$

The measured AC offshore grid frequency ($freq$) will be compared to the reference value ($freq_{ref}$) which in normal operation is equal to 50Hz. For normal operation conditions the offshore frequency which is imposed by the offshore HVDC-VSC will remain constant at 50 Hz thus, the frequency error $freq_{error}$ will be null leading to no active power dissipation at WT chopper level. Following a frequency disturbance, the gain ($K_{freq/Pchop}$) define the power dissipation in the chopper proportionally to the frequency deviation. The power limiter included between the ($K_{freq/Pchop}$) and the chopper converter guarantees that the maximum chopper active power is not overpassed and also that underfrequency disturbances does not generate any set-point to the chopper converter.

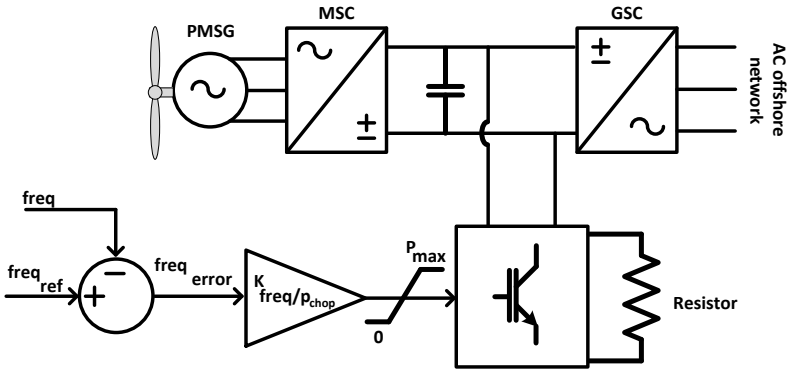

Figure 4.13: PMSG chopper resistor and associated control-loop for active power reduction based on overfrequency variations

For DFIG-based WT, the frequency increase at the wind generator terminals will impact on a natural active power reduction. Recalling the DFIG electromagnetic torque equation 3.34, it is inversely proportional to the grid frequency which is represented by the angular electrical speed ω_s. As the electromagnetic torque is directly proportional to the active power, an AC offshore grid frequency increase will have the impact on the active power decrease However, the frequency disturbance are meant to be small so, the natural DFIG response is not sufficient to achieve a proper DC voltage rise mitigation. So, an additional control-loop illustrated in Figure 4.14 has been add to the DFIG MSC converter. The rationale of this control loop is to provide to the DFIG a speed control proportionally to the AC offshore frequency variation according to the equation

$$\omega_{freq} = K_{f/\omega} \times (f_{ref} - f) \tag{4.7}$$

An additional speed reference (ω_{freq}) is determined based on the frequency deviation, between the frequency reference f_{ref} and the actual value f, after it is adapted by a proportional gain $K_{f/\omega}$. In case of an overfrequency event, the DFIG controller will increase the generator speed, reducing its active power injection.

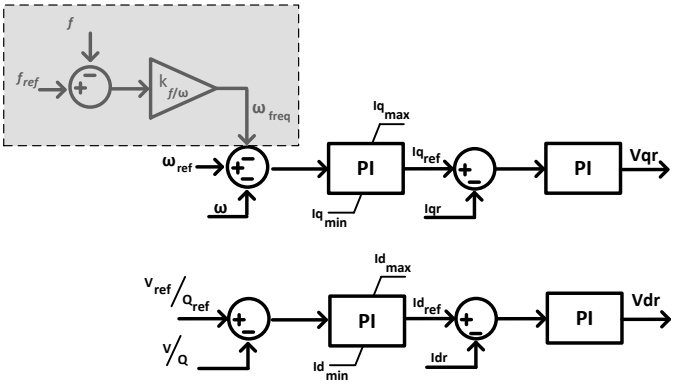

Figure 4.14: DFIG speed control based on grid frequency

4.6 Operation and Control of MTDC Grids Following the Loss of an Onshore Converter

The loss of an Onshore converter consists on the permanent disconnection of a given onshore HVDC-VSC due to internal or external causes. The phenomena that can cause the disconnection of onshore HVDC-VSC can be related to fault events on onshore mainland AC grid, at MTDC grid or internally on the onshore HVDC-VSC. n For the DC grid, the loss of an onshore converter can be regarded as the sudden loss of power injection from the MTDC grid to the mainland AC grid. The resulting effect, in terms of the MTDC grid voltage dynamics id expected to be equivalent to a fault in a mainland AC grid, thus affecting the DC grid power balance and leading to voltage rise phenomena. If the remaining onshore converter of the MTDC grid do not have capacity to accommodate all the power injection into the DC grid, additional control strategies need to be take to mitigate the resulting DC voltage rise effect.

The control strategies adopted for FRT voltage rise mitigation do not fully cope with the characteristics of permanent loss of an onshore HVDC-VSC. In fact, the permanent loss of an onshore HVDC-VSC has a high-time to permanent characteristic and so requires a DC voltage control mechanism able to be permanently deployed. The chopper based strategies adopted for FRT purposes, have a maximum active power energy dissipation capability. This maximum energy dissipation capability is associated to the chopper resistors thermal limits that once reached,

requires the immediate chopper resistor disconnection.
The DC voltage rise mitigation control with a permanent characteristic to deal with permanent loss of power extraction capability can be achieved by:

- Increase the active power injection into mainland AC grids in the remaining onshore HVDC-VSC;
- Active power reduction at offshore WF level.

The first option requires that the remaining onshore HVDC-VSC have enough margin to increase its power extraction before reaching its maximum rating. This situation may not be always guaranteed, culminating in the inability of providing an effective power equilibrium within the DC grid thus, not avoiding inadmissible DC voltage magnitudes. The second option consists on the fast reduction of the active power injection from the offshore WF. From a conceptual perceptive, this strategy is able to deal with the permanent characteristic of the loss of an onshore HVDC-VSC. The issue of reducing offshore WF active power injection is a new challenge to be addressed. Regarding FRT requirements, strategies for fast active power control have been presented for PMSG and DFIG-based offshore WF. Nevertheless, these strategies do not cope with larger time-frame that may be associated to the loss of a converter. On contrast, permanent active power reduction can be achieved through the pitch blade's angle adjustment however, its adjustment takes some time to turn effective since involves a mechanical adjustment through servo-motors, being not compatible with the fast active power reduction requirements presented for FRT as well as for the subsequent moments following an onshore HVDC-VSC disconnection. The solution for the operation of the DC grid facing the loss of an HVDC-VSC can be achieved an hybrid strategy that combines the two previously presented control approaches: (1) the fast active power dissipation and (2) the wind turbine pitch-angle adjustment used for the primary frequency support, according to the principle illustrated in Figure 4.15.

According to Figure 4.15, the process to handle the phenomena resulting from an onshore converter disconnection consists of two phases. Phase (1), after onshore HVDC-VSC disconnection, fast active power dissipation mechanism are deployed thus, avoiding massive overvoltages within the DC grid. Then, a second phase (2) is requires to guarantee the long-term active power equilibrium within the DC grid.

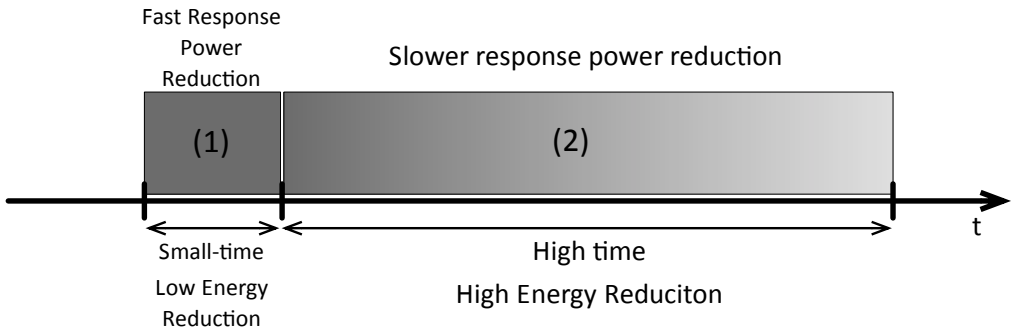

Figure 4.15: Energy dissipation requirements during the permanent loss of MTDC grid power evacuation capability

According to the work previously presented, the first phase (1) can be successfully assured by a chopper-based control scheme (with choppers at onshore or offshore-level).

Following the approach considered so far, the long-term active power regulation control scheme will be based on local controllers in a communication-free framework. So, it is important do define a common control scheme to allow both fast and long-term active power regulation schemes to be deployed. The WT blade's pitch angle regulation previously addressed relies on the frequency measurement at offshore AC grid. Moreover, the dispersed active power regulation schemes for FRT provision can also rely on the frequency deviation. The proposed strategy b) (see Section 4.5.2) the offshore HVDC-VSC takes advantage of the DC grid overvoltage occurrence to perform a proportional positive AC offshore grid frequency deviation. Further, WT-level control schemes are responsible by reducing the active power delivery proportionally to the AC offshore grid frequency deviation. The fast active power reduction based on AC voltage reduction strategy a) despite of being adequate for fast active power reduction, presents to be insufficient from the long-term active power reduction mechanism since the WT blade's pitch regulation scheme is based on frequency variation.

Regarding the adoption of onshore active power dissipation mechanism, it is independent of the control strategy applied at offshore HVDC-VSC level thus, it always feasible to be implemented and even work as a complement

4.7 Summary

In this chapter the advanced control schemes for the operation of MTDC grids have been presented. The control enhancements intended on allowing:

1. MTDC grid with offshore WF contributing to the mainland grids primary frequency regulation and inertial emulation.
2. MTDC withstand AC mainland voltage sags and remain operating during and aftermath fault events, complying with FRT requirements.
3. MTDC remain operating facing the loss of an onshore converter.

The control enhancements were based on local control rules, not requiring the adoption of fast communication channels. First, a control scheme for endowing MTDC grid and offshore WF on participating on primary frequency regulation and on emulating inertia behaviour, has been developed. The control scheme transposes the AC mainland frequency disturbances into DC voltage variations without colliding with the presented DC grid power sharing control approach. At offshore level, some modifications were introduced, namely on the offshore HVDC-VSC and on the offshore WT. The offshore HVDC-VSC control entails an additional control scheme to set the offshore frequency according to the DC voltage deviation. The inertia emulation has also been addressed by developing a control scheme to respond to frequency derivative as a fast active power injection.

Regarding the FRT provision, the contribution presented on this chapter is related with the control of the DC voltage rise magnitude through the promotion of active power equilibrium within the DC grid during the voltage sag at an AC mainland grid. The proposal of different DC voltage rise mitigation mechanisms been carried out. Basically, all the control strategies rely on the DC voltage rise appearance to promote proportional active power reduction or dissipation, controlling the DC voltage rise. The proposed schemes varies from onshore-located active power dissipation to offshore wind power injection reduction. That way, several WT technologies are covered and the FRT functionality can be provided by the whole MTDC grid.

Finally, during the assessment of the impacts overcoming from AC-side voltage sag and the consequent reduction of active power extraction, the operation of the DC grid following the sudden disconnection of an onshore HVDC-VSC was not guaranteed. Bearing in mind that this situation could preclude on transient stability problems, a coordinated control approach has been proposed. Taking advantage of the developments for the provision of primary frequency regulation and the FRT functionality, an hybrid control scheme was designed by adopting the fast characteristic from the FRT control strategies and the long-term aspects from the primary frequency control. That way, the DC grid voltage can be controlled during the moments subsequent to the onshore HVDC-VSC disconnection as well as with a long-term by the active power control through the WT pitch-angle control.

5

Evaluation of the Control Schemes for Advanced Services Provision from MTDC grids

5.1 Introduction

Following the discussion on the derivation of advanced control strategies for the provision of advanced services by the MTDC grid, through This chapter aims at demonstrate the feasibility of the proposed control approaches (presented in Chapter 4) through dynamic simulations using the simulation platform presented in the Chapter 3. The chapter is divided by the three major sections, each one corresponding to the advanced services whose control solutions were identified in chapter 4.

In Section 5.2, the primary frequency control scheme is evaluated for a mainland frequency disturbance. The inertial emulation performance is also analysed for the same case. Additionally, the frequency regulation scheme is evaluated for the situation of the sudden disconnection of an offshore WF.

In Section 5.3 exhaustive tests have been performed to assess the performance of fast power reduction mechanisms proposed in the Chapter 4 for the FRT provision and the associated DC overvoltage magnitude control. Different DC grid topologies with mixed offshore WF technologies and FRT control strategies have been also

tested, allowing to assess its performance for a varied set of control gains parameters.

In Section 5.3.5 the proposed control scheme to deal with the sudden disconnection of an onshore HVDC-VSC and provide the necessary conditions for the operation of the DC grid, has been tested.

5.2 Evaluation of Primary Frequency Control Capability by MTDC Grids with Offshore Wind Farms

5.2.1 Definition of the Case Study

In order to evaluate the effectiveness of the proposed control strategies to be applied at onshore and offshore converter stations, the test system shown in Figure 5.1 was used. It consists of two non-synchronous onshore AC Areas represented by a single machine equivalent that collects offshore power from a four terminal H-topology MTDC grid including two offshore WF. Regarding onshore AC grid, only primary frequency regulation capabilities are considered. To avoid distortion on the interpretation of frequency response results, the secondary frequency control capability of the AC generators connected at both AC systems have been de-activated through the disconnection of integral control-loop at the AC synchronous generator speed/power governor. The offshore WF are composed by PMSG, connected to the AC offshore network by an AC/DC/AC converter. Each offshore WF was modelled by a single equivalent machine of 250 MW. In order to promote a reserve margin at the offshore WF the simulations were carried out with a power output of 200 MW in each WF. The overall system modelling was performed using the simulation platform described in Chapter 3. It was also assumed that all DC branches have equal length. Additional data on the test system is provided in Appendix A.

The simulations carried out for the evaluation of the primary frequency regulation capability of the MTDC grid when using the proposed control approach, were performed in the presence of an under frequency disturbance. To achieve an onshore AC grid frequency reduction, a load increase of 150 MW has been performed in the Area ♯1 mainland AC grid. The equivalent AC generator was considered having adequate primary reserve to come with the load increase. It is important to stress that the objective of the simulation consisted on evaluating the capability of the

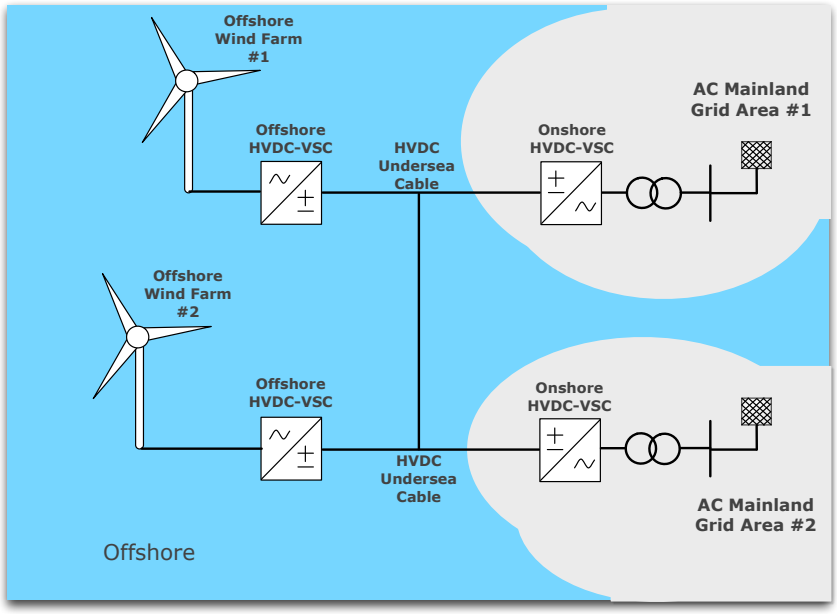

Figure 5.1: DC grid H topology layout

whole MTDC system on helping on the AC system frequency support instead of providing an integral primary frequency support.

5.2.2 Multi-terminal DC grid with Primary Frequency Support

The simulations results achieved for the evaluation of the performance of the control scheme for the provision of primary frequency regulation in MTDC grids are depicted in Figure 5.2, Figure 5.3 and Figure 5.4. Aiming at establishing a comparative analyses to assess the behaviour of the DC grid prior and after the inclusion of the proposed control scheme, two set of simulations were performed. The first, consisted on simulating a frequency disturbance (as aforementioned induced by a 150 MW load increase on AC grid Area ♯1) with the base case MTDC grid control scheme (ie:. without any frequency regulation capability). This case, where none of the previously presented primary frequency regulation schemes were implemented, is denominated as *without Primary Frequency Control Capability (PFCC)*. The other set of simulations were achieved by considering the same setup and the same disturbance but, with the primary frequency regulation scheme implemented in the MTDC grid, thus being entitled as *with PFCC*.

According to the results regarding the frequency at the onshore and offshore AC grids (depicted in Figure 5.2) it is noticeable that without any frequency regulation scheme the frequency disturbance only exists in the AC Area where the disturbance took place (dashed line). This fact is the ascertainment that the HVDC grid fully decouples the frequency and thus it disturbances among the interconnected AC grids. However, for the case where the proposed frequency regulation scheme is set (the case with PFCC), the interconnected AC Areas also experience frequency disturbances as it can be seen on the results illustrated on in Figure 5.2 (solid line). In overall terms, it is noticeable that the AC Area ♯1 frequency has a smaller deviation when the MTDC grid has the PFCC. this fact allows to conclude that the MTDC is able to actively contribute to the frequency support. Regarding the frequency variation a the offshore WF level imposed by the associated HVDC-VSC, it is possible to verify that it has also been successfully achieved, enabling the offshore WT with frequency control capability on deploying the proper regulation through an active power generation increase (see Figure 5.4).

Actually, the reduction on the active power delivery to the AC mainland Area ♯2 grid is beneficial by enabling an active power delivery increase towards the AC mainland Area ♯1 AC grid, helping on its frequency support. This behaviour suggests the possibility of providing primary frequency support among non-synchronous mainland AC Areas (inter-Area frequency support). Despite inter-AC Area frequency support led to a small frequency deviation in AC mainland Area ♯2 grid, the presence of the AC frequency/DC voltage droop in the associated onshore HVDC-VSC also supports the AC Area ♯2 frequency deviation by limiting the active power contribution. So, the DC voltage profile recovers, leading to an active power recovery. However, a new power dispatch and DC voltages are achieved within the DC grid, corresponding to a new operation point.

From the analyses of the DC grid voltage at the each DC grid terminal (see Figure 5.3), it is possible to verify that the DC voltage reduces. From the onshore-side DC grid terminals, the voltage reduction is set by the onshore AC frequency/ DC voltage droop control. This effect is then spread to the onshore converters and as illustrated on the same Figure. Also, it is possible to observe that the DC voltage

associated to the Area ♯2 onshore HVDC-VSC has a different behaviour when compared with the rest of the DC voltage on the others DC grid terminals. This fact is related with the frequency disturbance introduced on the mainland AC Area ♯2 due to the frequency support provided by a reduction of active power flow compared with the pre-disturbance value.This behaviour is evident on the results of active power flows at each DC grid terminal depicted in Figure 5.4.

Regarding the offshore WF frequency support, the previously mentioned offshore AC grid frequency decrease provides the necessary condition for an effective primary frequency support at each WT-level. The results illustrated on Figure 5.4 show that following the disturbance, the active power output at each offshore WF is increased, taking advantage of the power reserve available at WT-level. Due to the DC grid topological symmetry, the active power contribution on each offshore WF is identical, being proportional to the DC voltage variations which are also identical on each offshore WF DC-side terminal. Also, it is possible to highlight that WT pitch control response, responsible for the active power increase, is slower in comparison to the inter AC-Area frequency support, culminating in a slower response at WF-level comparing to the contribution of the healthy AC mainland grid. The wind turbine pitch angle evolution was also monitored during the simulation. Its response is illustrated in Figure 5.5. The results show that the wind turbine pitch angle are identical on both offshore WF and also show that a correct angle rotation has been achieved, leading the WT to the maximum angle position ($\beta = 0$), corresponding to the nominal power, as depicted in Figure 5.4, taking advantage of all available reserve margin.

After analysing all the variables, and as a concluding remark, the simulation set allows to observe that MTDC grid can provide primary frequency support from offshore WF (that have been previously de-loaded, having a reserve power margin) and also from the interconnected mainland AC-grids. The proposed control scheme is able to provide the necessary conditions for the autonomous deployment of primary frequency regulation in a communication-free framework.

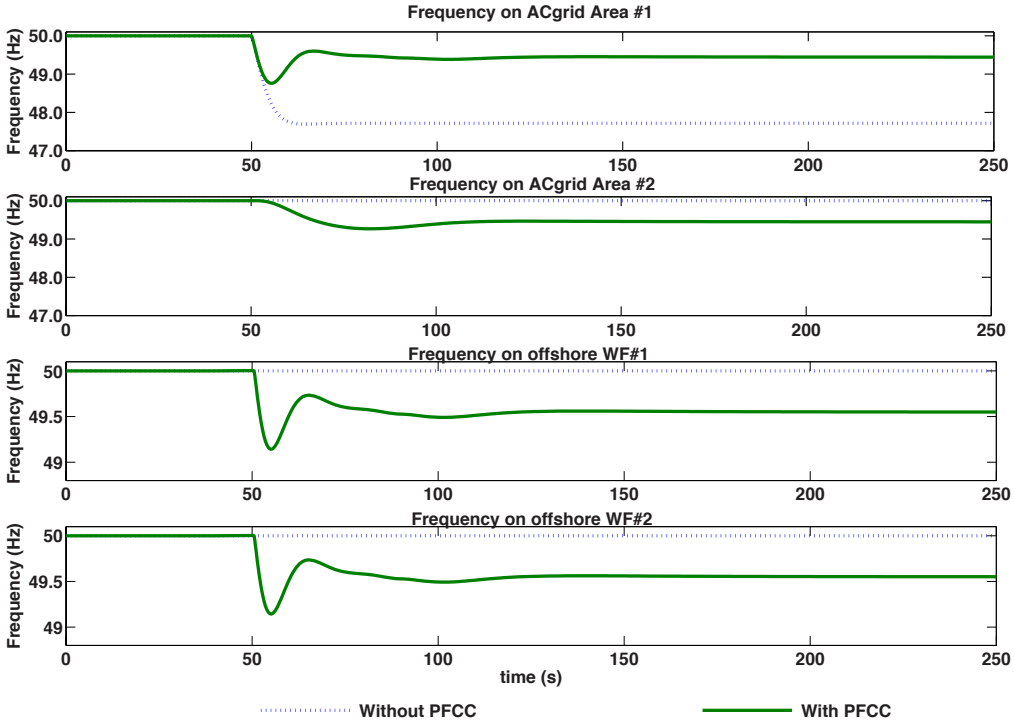

Figure 5.2: Frequency at MTDC grid terminals

5.2.3 Offshore Wind Farm Inertia Emulation

After evaluating the performance of primary frequency control schemes on MTDC grids, an additional set of simulation have been conducted. This set of tests consisted evaluation deployment of synthetic inertial behaviour. To assess the performance of the proposed control strategy, offshore WT were endowed with the inertial emulation control-loop as described in the Section 4.3.3. The control scheme for inertia emulation is similar to the previously presented control scheme for primary frequency regulation capability. The main difference consists on the WT control that is complemented with the inertia emulation term presented in Section 4.2.3. Basically, after implementing the inertial emulation control scheme, offshore WT are expected to be able to quickly deploy a fast active power injection which is determined based on the frequency rate-of-change, measured at WT terminals. The rationale of this simulation is to evaluate the whole cascaded control scheme regarding the inertia emulation response as well as the impacts that it may have on the mainland AC grid

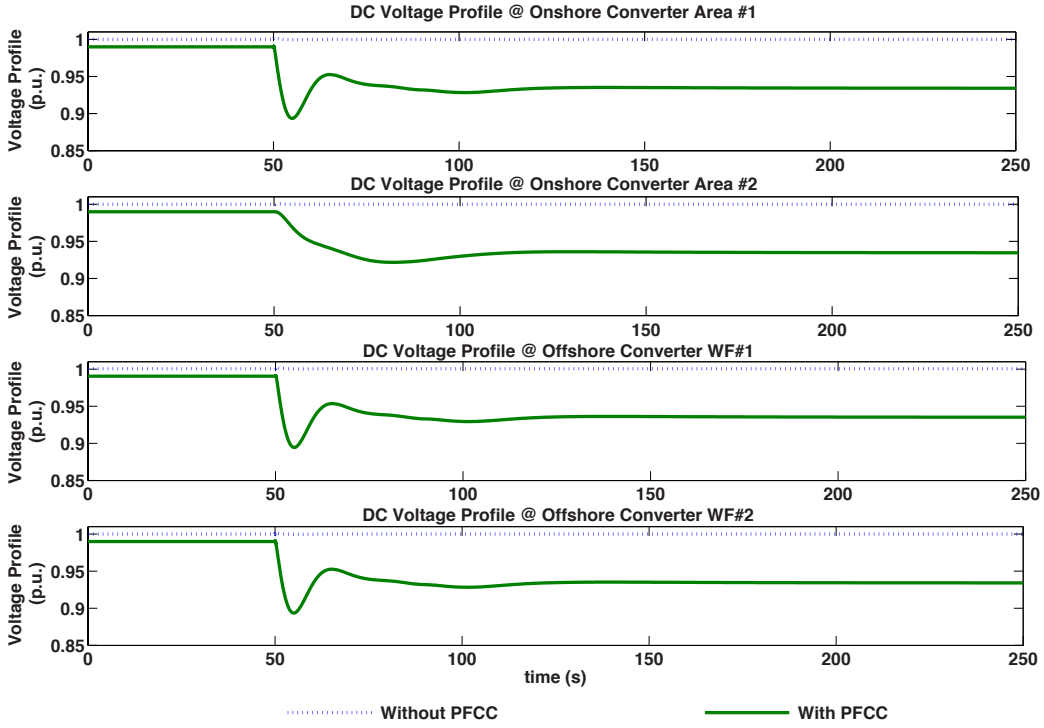

Figure 5.3: DC voltage profile at MTDC grid terminals

frequency support. The results for this set of simulations are presented together with the primary frequency support results (previously obtained and presented in Section 5.2.2, allowing to compare and evaluate the additional benefits resulting from the adoption of inertial emulation functionality. Since inertial contribution is characterized by a fast response, the results were focused on the moments subsequent to the disturbance (mainland AC Area ♯1 underfrequency event).

In Figure 5.6 the active power injection performed by offshore WF ♯1 is depicted. As previously stated, the DC grid topological symmetry leads to a similar response at both offshore WF. Thus, for the sake of simplicity, the offshore WF ♯2 results were not included in the following figures. The results show that a fast active power increase following the disturbance is achieved. However, the active power is lower than the case where the inertial emulation is deactivated. This fact is related with the deployment of inertial emulation that takes advantage of the kinetic energy in

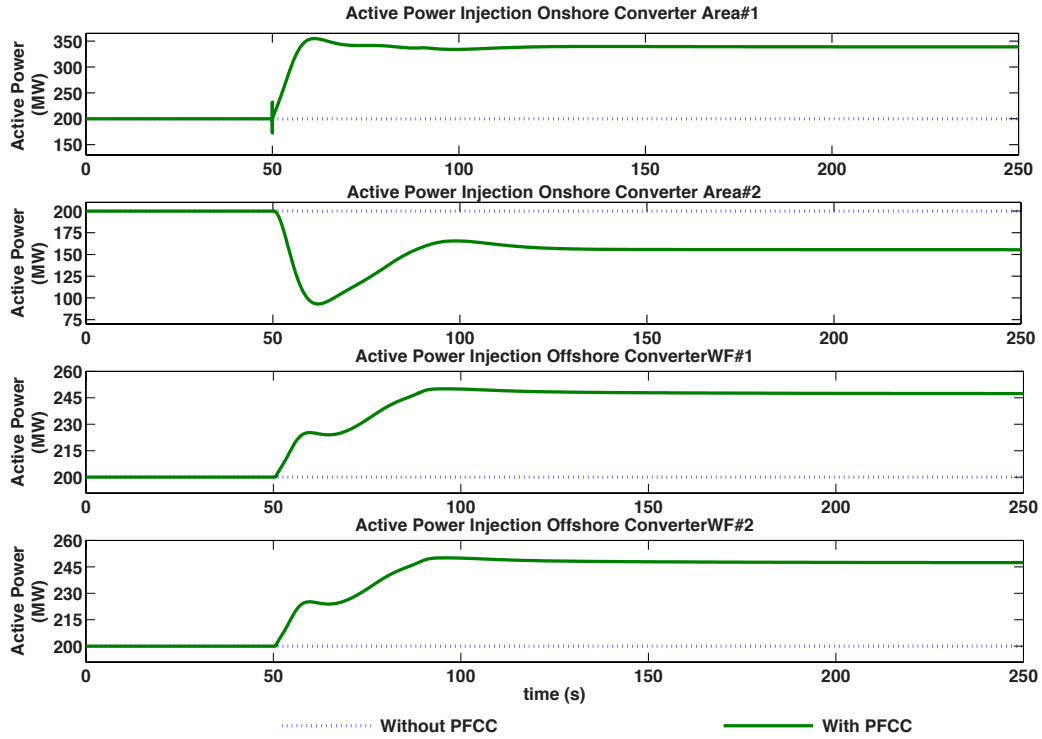

Figure 5.4: Active power-flow at MTDC grid terminals

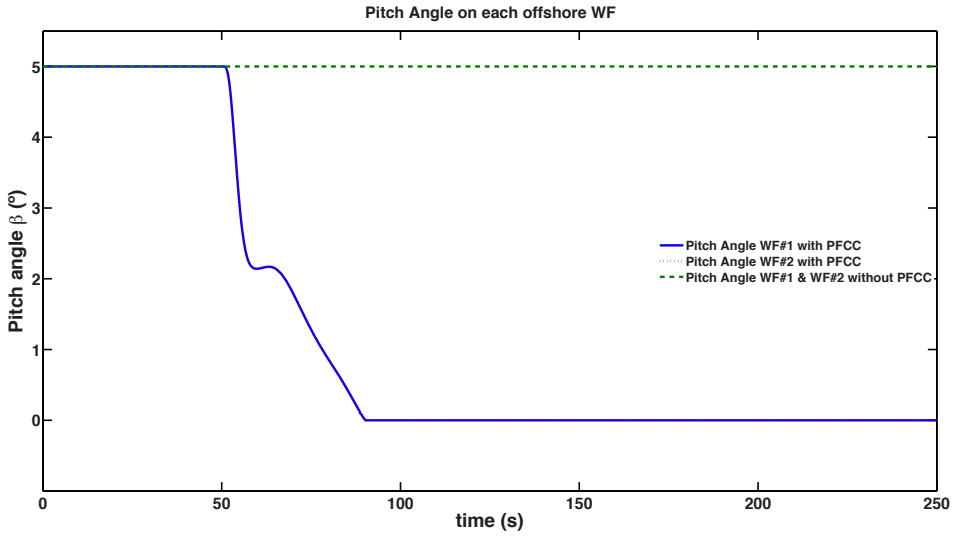

Figure 5.5: Pitch angle at WT-level on each offshore WF

the generators' rotor. So, after the fast inertial response, a speed decay takes place, reducing the injected active power. When the frequency transient stabilizes, it is observed that both responses (with and without inertial emulation) are coincident.

The results depicted in Figure 5.7 illustrates the active power injection from the DC grid towards the mainland AC Area ♯1 (the AC Area where the frequency disturbance took place). From the results analysis it can be verified that the active power increase inherent to the WF deployment of inertia response is directly channelled towards the mainland AC Area ♯1 grid (the one affected by the load increase) and has an effective impact on the frequency response (see Figure 5.8).

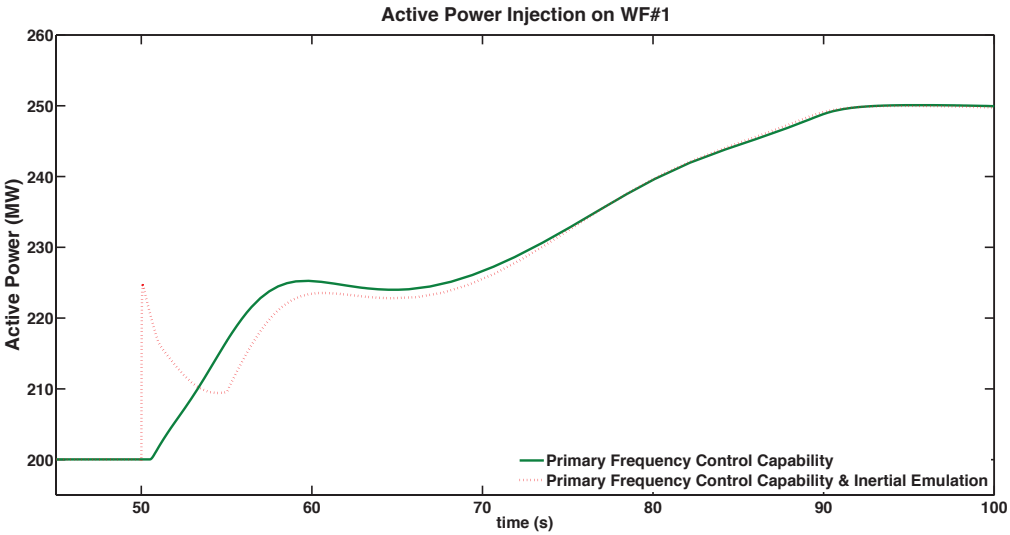

Figure 5.6: Active power delivery performed by offshore WF ♯1

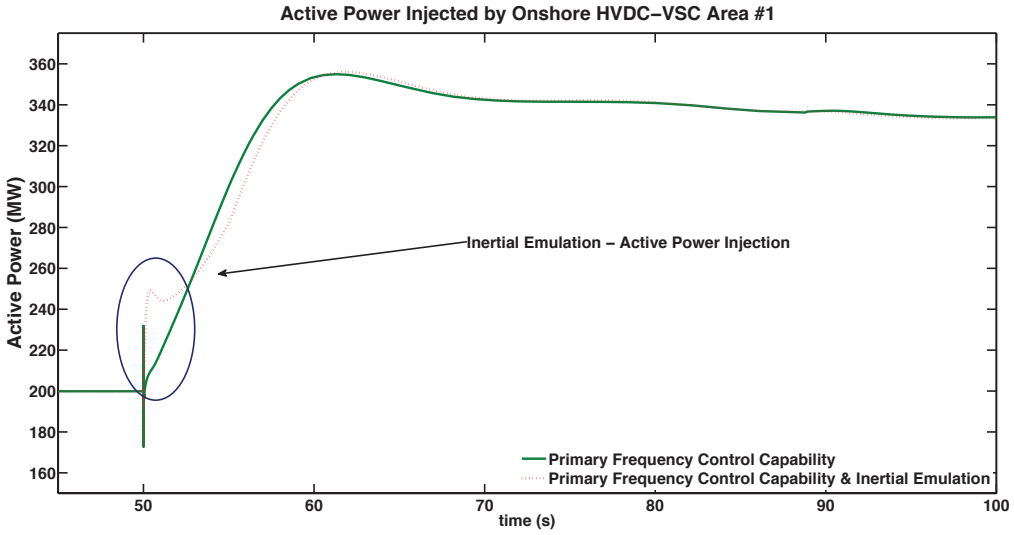

Figure 5.7: Active power delivery towards mainland AC Area ♯1

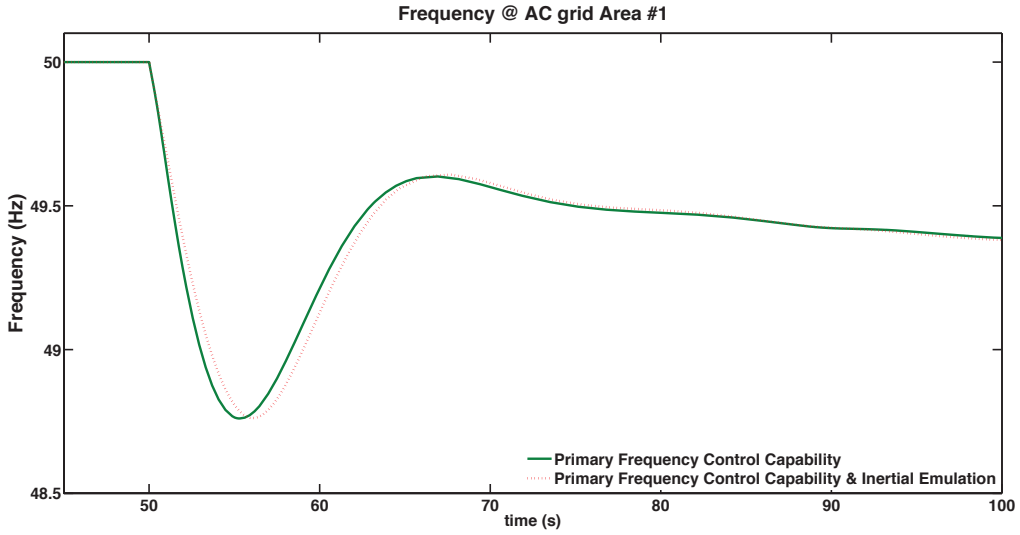

Figure 5.8: Mainland AC Area ♯1 frequency

5.2.4 Multi-terminal DC grid Frequency Support After the Sudden Disconnection of an Offshore WF

The results presented in the previous subsections illustrate the effectiveness of the control strategies for the MTDC system regarding its response to a disturbance taking place in the mainland AC grids. However, an event consisting on the sud-

den disconnection of an offshore HVDC-VSC may also significantly affect frequency behaviour of the mainland AC grids by affecting its active generation/load power balance. Therefore, this section aims at assessing the performance of the developed primary frequency regulation scheme on dealing with a frequency disturbance from a sudden reduction of in-feed into the MTDC grid. To do so and without the sake of generality, the offshore WF ♯1 has been suddenly disconnected from the DC grid. Additionally, to guarantee no interference on the results analyses, the inertial emulation capability has been de-activated on the offshore WF ♯2. As it can be observed in Figure 5.9 and Figure 5.10, for the case where primary frequency control capability is disabled, the DC voltage/active power droop control is responsible by setting the DC voltage and consequently the active power sharing between the onshore converters. Additionally, the remaining connected offshore WF (offshore WF ♯2) is not able to deploy its reserve margin. However, when the primary frequency control capability is enabled,offshore WF ♯2 deploys its reserve margin, thus contributing to a significant reduction in the frequency deviations observed in the onshore AC grids. It is also important to highlight that according to the results presented in the Figure 5.10, the inclusion of primary frequency control capability is responsible for the offshore WF ♯2 active power increase that is further shared among the onshore HVDC-VSC.

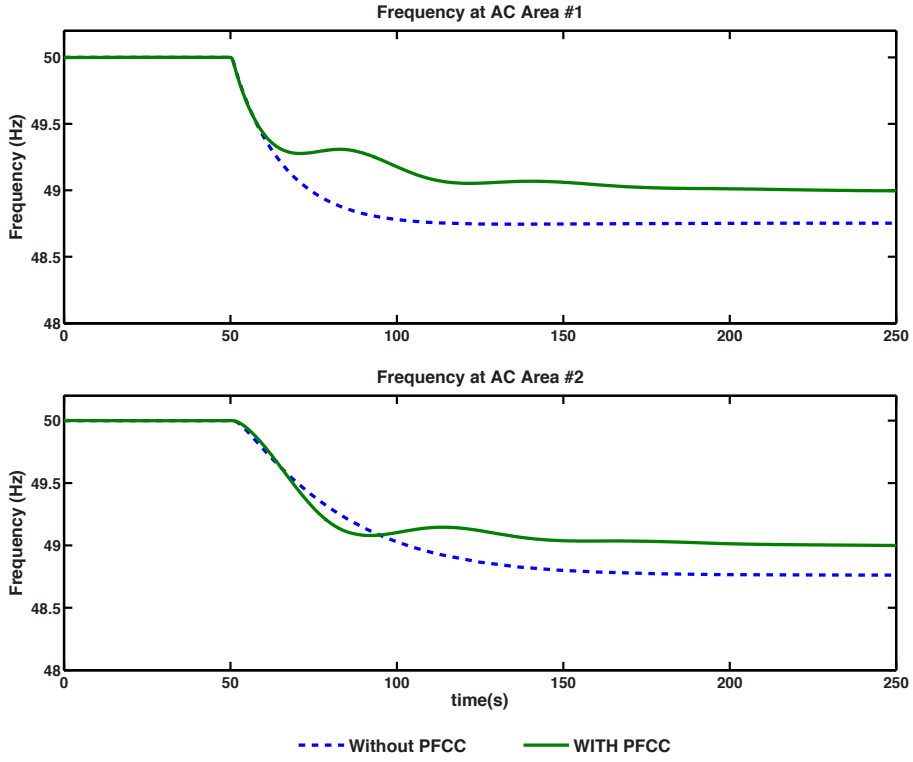

Figure 5.9: Frequency on AC mainland Areas

5.3 Evaluation of the Control Strategies for AC Fault Ride-through Capability in MTDC Grids

5.3.1 Case Study

In order to evaluate the performance and effectiveness of the proposed control strategies(Section 4.4) for the assuring the AC of FRT capability in MTDC grids, a set of simulations were performed. The base case considered for the assessment of the effectiveness of the FRT service has been simulated adopting the previously presented H topology DC grid (see Figure 5.1), with two offshore WF injecting 200 MW to the DC grid . The active power/DC voltage droop control for normal operation has been set and the power sharing of 50 % has been considered among the onshore HVDC-VSC. To evaluate the performance of the several FRT control approaches, it has became crucial to implement not only PMSG-based WF, but also DFIG-based WF. This necessity is related with the substantial difference that can be found on

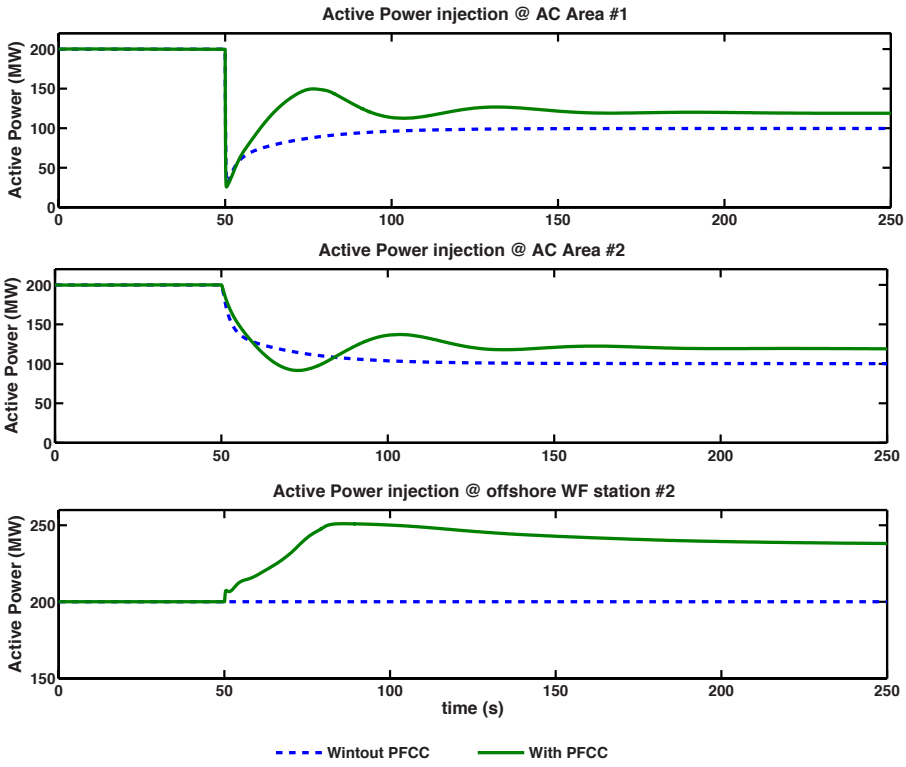

Figure 5.10: Active power flow on the DC grids terminals

both technologies when responding to voltage or frequency deviations, which are the basis of the proposed control strategies (in Section 4.5.1 and Section 4.5.2).

DFIG fast active power reduction response based on the frequency variation as well as on AC voltage variation schemes (which are presented in Section 5.3.3), that differs from the PMSG response. The data for the PMSG and DFIG WT are highlighted in the Appendix A.

The AC mainland grid voltage sag was achieved by simulating a symmetrical fault in the mainland AC grid ♯1, near the associated onshore HVDC-VSC. The close distance fault has been chosen in order to give origin to a severe AC voltage sag at onshore HVDC-VSC terminals, allowing to fully evaluate the performance of the proposed control strategies in a stressful situation. To perform a comparative analyses among the proposed FRT control methods, the same symmetrical fault has been considered for all the cases, being located in the mainland AC Area ♯1 grid.

Section 5.3.2 is presents the evaluation of onshore-based strategies for FRT compliance. Section 5.3.3 presents the evaluation of offshore-based strategies for FRT compliance. In all set of simulations performed hereafter, a current limit of (1.2 p.u.) has been set on the HVDC-VSC.

Not withstanding, before going into FRT DC voltage rise control strategies and the evaluation of its performance, a set of simulation over the DC grid facing the proposed AC-side fault without any DC voltage control mechanism has been simulated, allowing to assess and evaluate the phenomena that arise from the fault occurrence. The results for this set of simulation are presented in Figure 5.11 where active power and DC voltage are illustrated in the MTDC grid terminals.

From the results, it can be observed that during the fault event (triggered at $t = 1s$ and cleared at $t = 1.5s$) the active power flow towards the onshore HVDC-VSC Area ♯1 suffers a severe reduction due to current limiters installed at HVDC-VSC. The offshore WF do not sense the fault occurrence thus, do not change their active power injection. Additionally, the onshore HVDC-VSC Area ♯1 increases its active power delivery from the DC grid towards the correspondent AC mainland grid (Area ♯2). This active power flow increase has its origin due to the DC voltage rise within the DC grid. In fact, on the affected onshore HVDC-VSC and offshore HVDC-VSC, the DC voltage profile rises to values above the maximum admissible over voltage (considered to be 20 % above nominal value). The onshore HVDC-VSC Area ♯2 increases the active power delivered on the attempt of controlling the DC voltage according to the DC voltage/active power droop control rule. It is important to stress that, as illustrated by the results, if no DC voltage control mechanism is set on the DC grid, it cannot remain connected to the AC mainland grid during a fault event due to the high DC voltage rise. The proposed control strategies that are evaluated in the next sections, aim at controlling the DC voltage rise magnitude through the promotion of active power equilibrium within the DC grid during the AC-side onshore fault event.

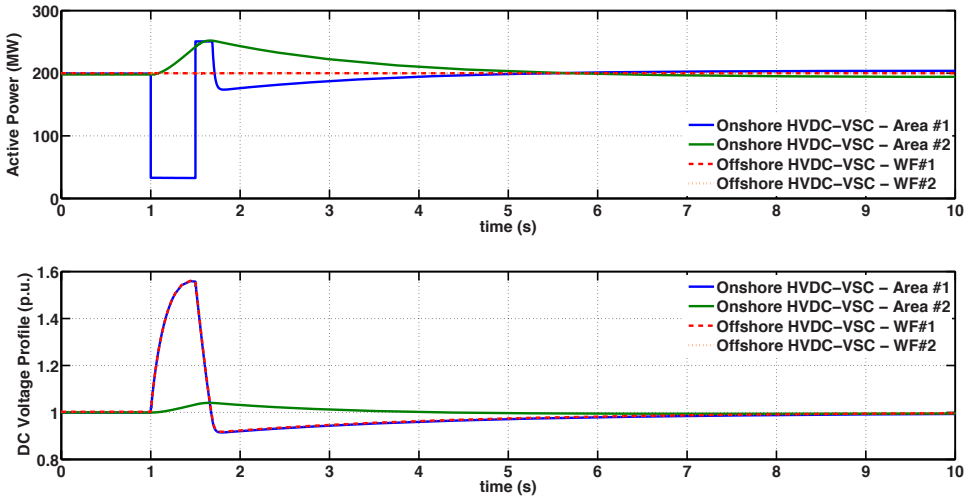

Figure 5.11: Active power flow and DC Voltage on the DC grids terminals during AC-side fault event - without DC voltage control strategies

5.3.2 Evaluation of the Control Strategies for the DC Voltage Rise Control at Onshore HVDC-VSC level

This section aims at evaluating the performance of the whole MTDC grid on withstanding AC-side voltage sags, having installed the onshore-based FRT control strategy to contain the DC voltage rise within the DC grid, presented in Section 4.4.4. The onshore-based DC voltage rise control strategy consists on endowing onshore HVDC-VSC with an active power dissipation device, named as chopper. The chopper is an electronic interfaced resistance that is interconnected in parallel to the MTDC grid terminal and dissipates active power. For this specific case, the active power dissipation has been set to be proportional to the DC overvoltage magnitude. It is expected that the active dissipation impacts on promoting the active power equilibrium within the DC grid, mitigating the DC voltage rise. The simulation results obtained within this case constitutes also a base case for comparison purpose since it is aimed at avoiding the adoption of this control solution through the use of alternatives that exploit fast active power control at the WT-level.

For this simulation set, two chopper devices were included in the previously presented H-topology grid case, one at each DC grid onshore HVDC-VSC terminal. The chopper were set to operate whenever the DC voltage is over 1.1 p.u. (V_{trig}=0.1 p.u. -

see Figure 4.10). The results achieved are presented in Figure 5.12.

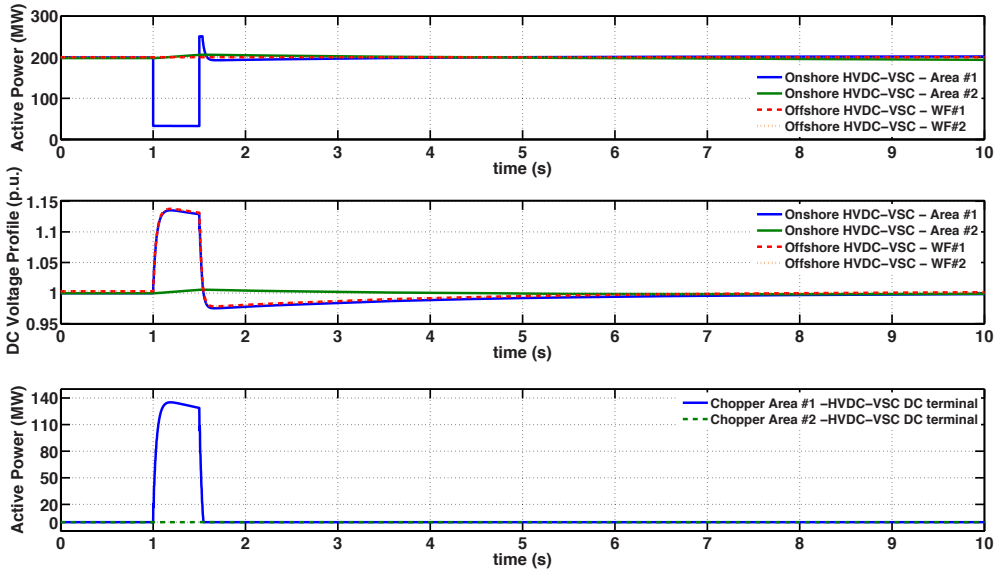

Figure 5.12: Active power flow and DC Voltage on the DC grids terminals during AC-side fault event - onshore DC voltage control strategy

From the results depicted in Figure 5.12 it can be observed the reduction of the active power injection was verified at the onshore HVDC-VSC Area ♯1 due to the AC-side voltage sag. However, the Area ♯2 does not increase its active power flow similarly to the previously presented results (where no DC voltage control strategies were applied). Regarding the DC voltage, it can be observed that its magnitude is considerably smaller in comparison with the previous case. Also, it is below the pre-defined maximum admissible DC voltage value of 1.2 p.u. Analysing the active power dissipation on chopper resistors, it is noticeable that the onshore HVDC-VSC Area ♯1 chopper dissipates a significant amount of power, almost coping to all non-injected power resulting from the fault event in Area ♯1.The additional power dissipation in the DC chopper os therefore responsible to mitigate the DC voltage rise effect, while assuring the necessary condition to provide the FRT capability in the MTDC grid. In fact, the chopper resistor cannot make a perfect active power equilibrium by dissipating all the non-delivered active power since, a dead-band block disables its operation below 10% overvoltage(due to the consideration of triggering voltage of 1.1 p.u. to allow power fluctuations due to wind resource increase

or DC grid power sharing re-dispatch). Additionally, the lack of integral control-loop disables the chopper controller on offsetting the permanent error.

Regarding the chopper located at the onshore HVDC-VSC Area ♯2, no active power dissipation has been performed due to the negligible DC voltage rise in the associated DC terminal. In fact, the small DC voltage rise at the onshore HVDC-VSC Area ♯2 is related with the onshore Area ♯2 HVDC-VSC active power/DC voltage droop control which leads also a small increase in the active power injection into Area ♯2 (in the attempt of controlling the associated DC voltage), while marginally contributing to the power equilibrium within the DC grid.

As general conclusion, it is possible to state that, the adoption of chopper resistors at the onshore HVDC-VSC grid terminals is able to deal with the DC voltage rise effect by reducing the power imbalance in the DC grid. However, according to the results, an enormous chopper is required to guarantee the over 100MW (about 140MW for the studied case) power dissipation.

5.3.3 Evaluation of the Control Strategies for the DC Voltage Rise Control at Offshore HVDC-VSC level

The classical solution based on the instillation of chopper resistors at onshore HVDC-VSC DC-side terminal, although effective, requires significant investment in additional hardware. In order to overcome this situation, other solutions, exploiting the capability of fast active power control at the WT-level are extensively tested in order to demonstrate its feasibility. According to presented in Section 4.4.5, two strategies for active power reduction were considered, both exploiting the DC voltage rise effect during the fault event. From hereafter, the control strategies are identified as:

- Case A - AC offshore voltage reduction based on the DC voltage rise;
- Case B - AC offshore frequency increase based on the DC voltage rise.

For both cases, two set of simulations were conducted. One considering that offshore WF are equipped with PMSG-based WT, name as Case 1, and other considering that offshore WF are equipped with DFIG-based WF, named as Case 2.

In order to properly evaluate the behaviour of the control strategies, at this stage, both offshore WF are assumed to be equipped with the same WT technology (DFIG or PMSG). However, in Section 5.3.4, after having evaluated the control strategies, additional simulations are included, mixing wind turbine technologies as well as offshore-based DC overvoltage control strategies. The objective of performing such studies relies on the evaluation of the robustness of the proposed control strategies.

Case A

To evaluate the performance of the DC grid voltage rise control based on the AC offshore voltage control as the triggering signal during a mainland AC-side fault for active power reduction at WT level (Case A), a set of simulations were performed. Therefore this study assumes that offshore HVDC-VSC with the control strategy proposed in Section 4.5.1. The results for this set of simulations are presented in Figure 5.13, Figure 5.14 and Figure 5.15.

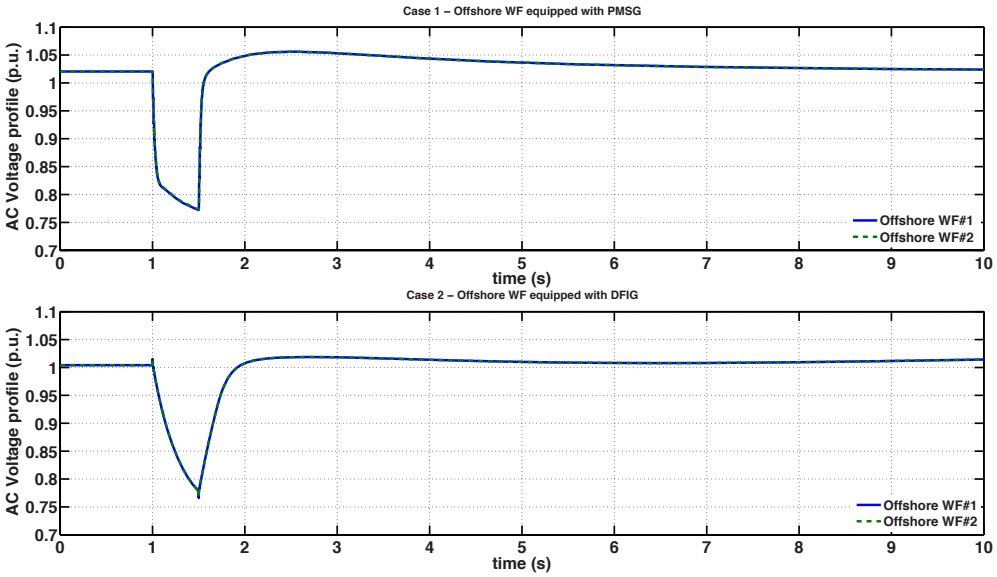

Figure 5.13: AC voltage profile at offshore HVDC-VSC - Case A

According to the results illustrated in Figure 5.13, it can be observed that the AC offshore voltage reduction based on the DC voltage is successfully achieved through the adoption of the Case A FRT control strategy. It is also observable that the response of the voltage reduction differs depending on the adopted WT

technology. In fact, the same pattern is also observable on the DC voltage illustrate on Figure 5.14. Also, it is observable that the control approach was able to mitigate the voltage rise, which is sustained below the maximum admissible value (1.2 p.u.). This behaviour indicates that an active power injection reduction was successfully achieved at offshore WF level. It is now important to analyse the effect of the offshore AC grid voltage on the WT power output and consequently on the mitigation of the DC voltage rise effect, in order to assure the FRT compliance for the MTDC grid.

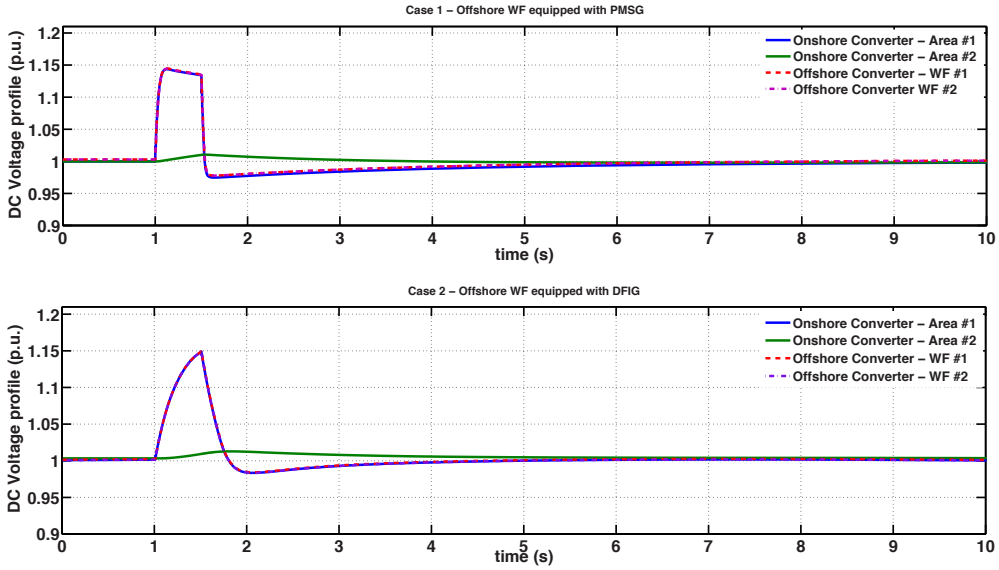

Figure 5.14: DC voltage profile at MTDC grid terminals for Case A

The active power flow on each MTDC grid terminals are depicted on Figure 5.15. It is observable that the active power flow reduction has been performed for the both WF technologies. The results related with PMSG-based WF present a faster and smoother response which is associated to the active power dissipation promoted by the WT electronically interfaced chopper resistors. The results related to DFIG-based WF have a slower characteristic associated to the intrinsic generator response during an AC voltage reduction. It is noticeable that after fault clearance, the active power recovery is achieved being slower in DFIG case in comparison to the PMSG-based case. Nevertheless, the generators are able to fully recover to the pre-disturbance active power generation. This indicated that at the generator side, the active power/speed stability was guaranteed.

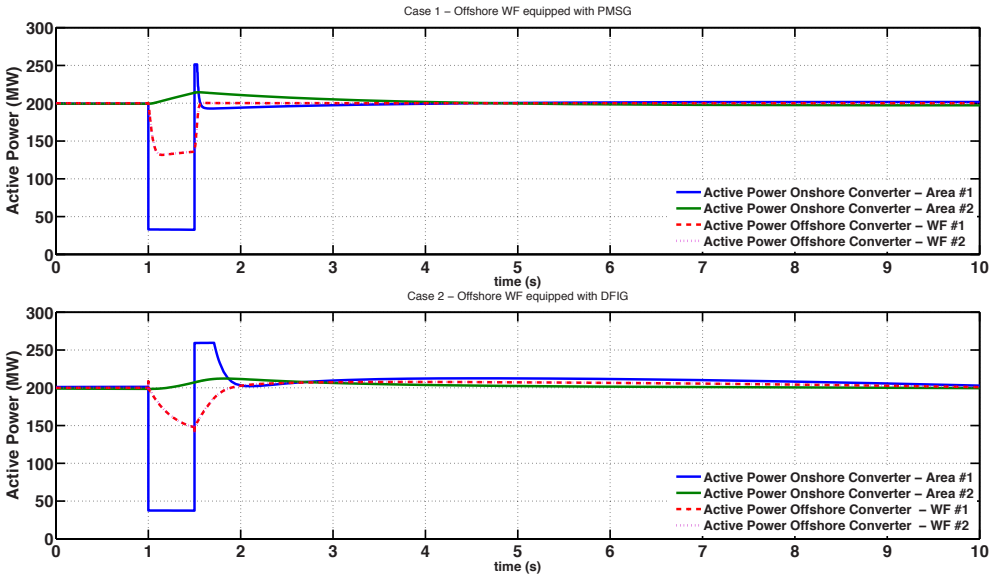

Figure 5.15: Active power flows at the DC grid terminals for Case A

During the simulation, the WT major variables were also monitored. For the PMSG-based WF, the active power dissipation at WT-level while for the DFIG-based WF, the generator speed as well as the electrical torque. These results are illustrated on Figure 5.16. From the results it can be inspected that the active power reduction previously observed at the PMSG-based offshore WF is attained by an active power dissipation at the DC chopper resistors (bearing in mind that the generator is fully decoupled from the grid by the converter, thus does not experience any disturbance) and according to the results illustrated in Figure 5.16, around 65-70 MW is dissipated at each WF. Regarding the results for the DFIG-based WF, the same figure shows that the active power reduction is achieved by an electric torque reduction, which leads a transitory generator speed increase followed by an oscillatory behaviour that is fully damped by the DFIG speed controller set at the RSC.

Regarding WF equipped with DFIG, it might be expected that the offshore AC voltage sag might result on stressful currents for the offshore HVDC-VSC station. In a later stage, and as a demonstration of the robustness of the proposed solution, this issue is properly addressed.

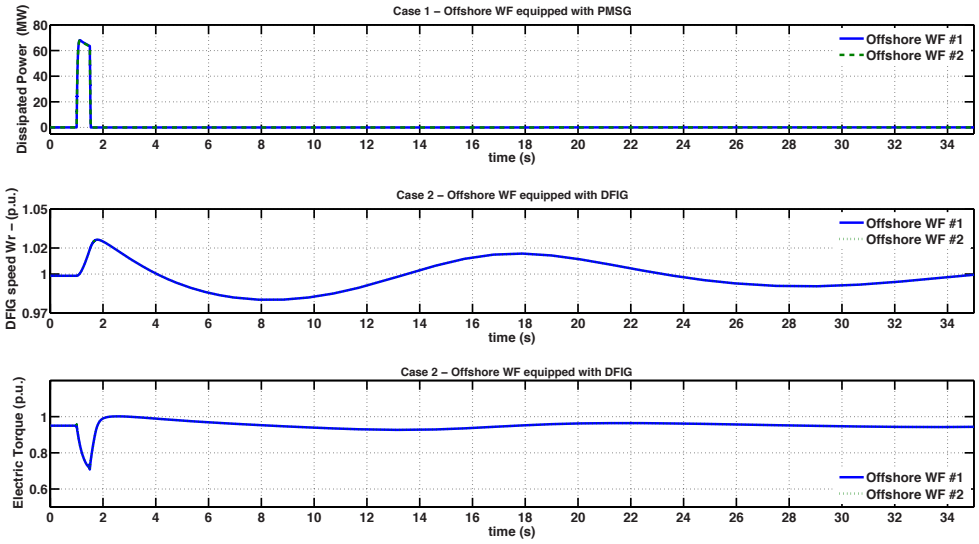

Figure 5.16: Dissipated power at PMSG-based WF, speed and electrical torque at DFIG-based WF - Case A

Case B

To evaluate the performance of the DC grid considering the DC voltage rise control based on the AC offshore frequency control during mainland AC-side fault event (Case B), a set of simulations were performed, endowing offshore HVDC-VSC with the control strategy proposed in Section 4.5.2. The results for this set of simulations are presented in Figure 5.17 , Figure 5.18 and Figure 5.19.

The results illustrated in Figure 5.17 show that the frequency increase based on the DC voltage rise was successfully achieved on both cases. However, a slight difference in the frequency pattern is observed depending to the WT technology which equips the offshore WF. Additionally, the same figure presents the results of the dissipated power for the PMSG-based offshore WF and the electric torque reduction for DFIG-based offshore WF. As explained on Section 4.5.2, the active power reduction on DFIG-based WF for the Case B control strategy is achieved through the electrical torque reduction allowing generator speed increase and kinetic energy storage ♯2. Regarding the PMSG-based active power injection reduction (achieved through the chopper active power dissipation) was achieved based on the

proportional control as a function of the frequency (overfrequency) deviation.

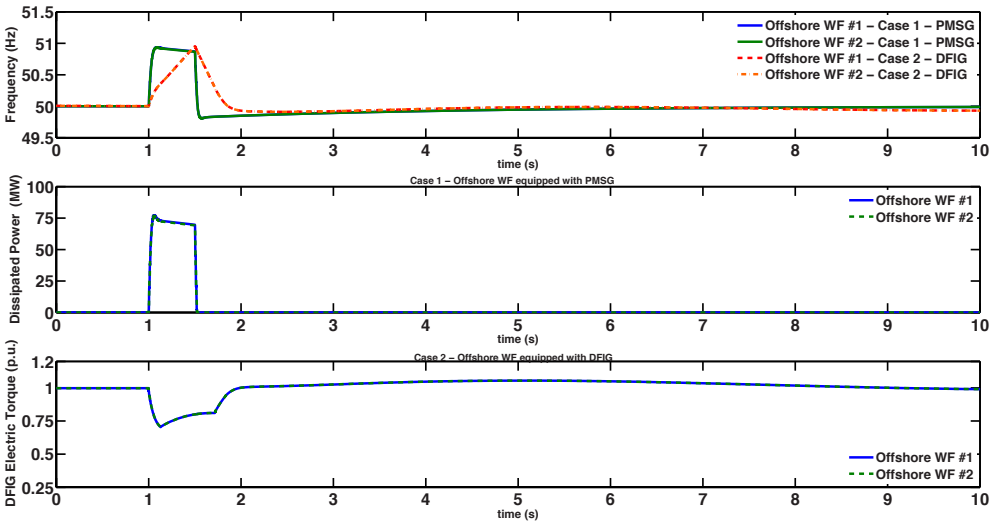

Figure 5.17: AC offshore frequency, dissipated power and electric torque for Case B

The results illustrating the DC voltage behaviour on each DC grid terminals are depicted in Figure 5.18. The DC voltage rise control strategy based on the AC offshore frequency increase is able to cope with the fast active power reduction at WT to mitigate the DC voltage rise. For both WT technologies the DC voltage was kept below the maximum admissible value (1.2 p.u.). Once again, the difference in the voltage raise and decay pattern is related with the nature of the power reduction at WT-level. PMSG-based WT have the electronically interfaced DC chopper at the back-to-back converter DC link, presenting a faster response. The active power reduction on the DFIG-based WF has an electrical and mechanic characteristic, presenting a slower response. Nevertheless, the impacts on the DC voltage maximum value are very small.

Regarding the active power flow in each MTDC grid terminals, the results are illustrated in Figure 5.19. It is observable that the control strategy is able to induce an active power injection reduction on both WT technologies. Again, the response differs from PMSG and DFIG WF. Nevertheless, the most differentiate factor consists on the DFIG-based WF recovery (after fault clearance) which has a slower response towards the pre-disturbance active power. In fact, between fault clearance and $t = 4s$, there is a small power gap which is not observed in PMSG-based offshore

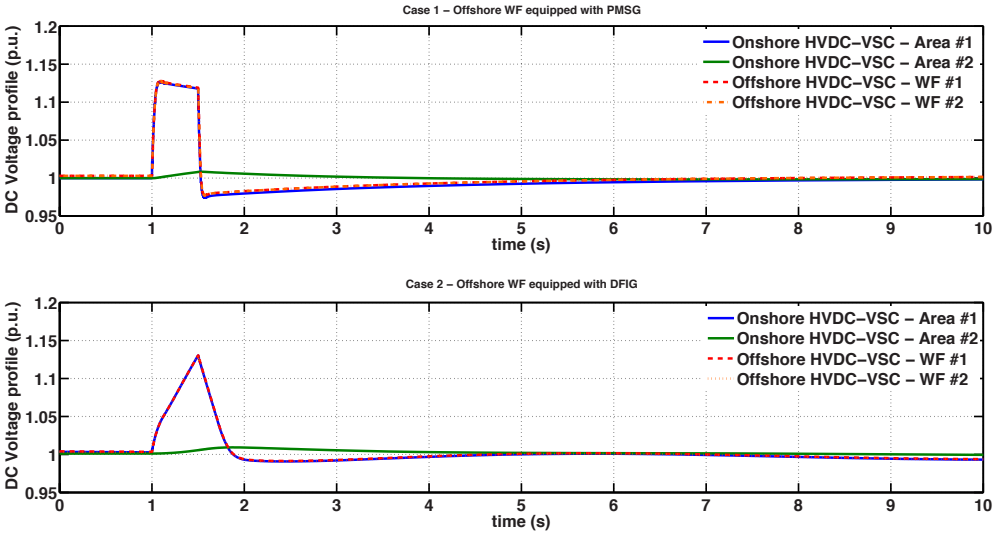

Figure 5.18: DC voltage profile at MTDC grid terminals for Case B

WF. However after $t = 4s$ the DFIG-based WF is fully recovered and injects the pre-disturbance power.

These set of simulations allowed to assess the effectiveness of both DC voltage rise control strategies for PMSG and DFIG WT technologies. Not withstanding, a more detailed analyses is performed in next section where DC grid topology, mixed WF technology and different control approaches including control parameters variations are considered, aiming at putting in evidence the robustness of the proposed control approaches.

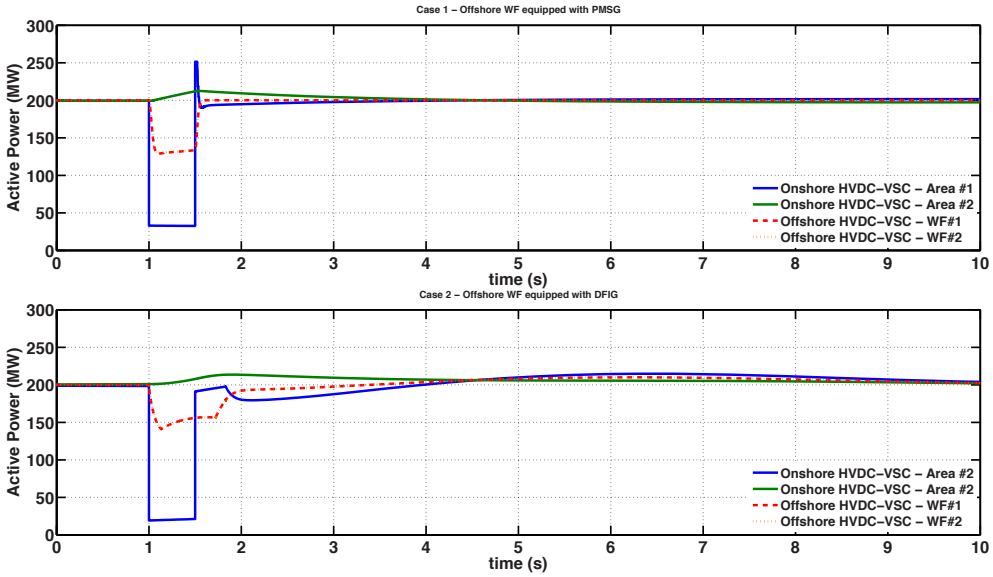

Figure 5.19: Active power flows at the DC grid terminals for Case B

5.3.4 Sensitivity Analyses

An additional set of simulations were performed to evaluate the performance of the proposed control strategies for situations were different WT technologies are integrated in the same DC grid an possibly following different control strategies while actively participating on the fulfilment of MTDC grid FRT capability. Additionally, the DC grid topology has been changed to a meshed DC grid aiming at evaluating the extendibility of the proposed control strategies for different DC grid topologies. The illustration of the simulation test bench is depicted in Figure 5.20. It consists of a meshed DC grid connecting two offshore WF (being WF ♯1 equipped with PMSG and WF ♯2 equipped with DFIG), injecting 200 MW each, and two mainland HVDC-VSC connected to the same mainland AC grid but, in different locations. The AC fault event was considered to be a symmetrical fault, located close to the onshore HVDC-VSC Area ♯1. For this particular case, the AC grid system is interconnected thus, the fault event has impact on both onshore HVDC-VSC. Despite for this specific case, the AC grid is composed for a single Area, for the sake of generality, the converters' name were kept as Area ♯1 and Area ♯2, as depicted in Figure 5.20.

The sensitivity analysis simulations have been performed in two Configurations, mainly differing on the adopted control approach for DC voltage rise installed at

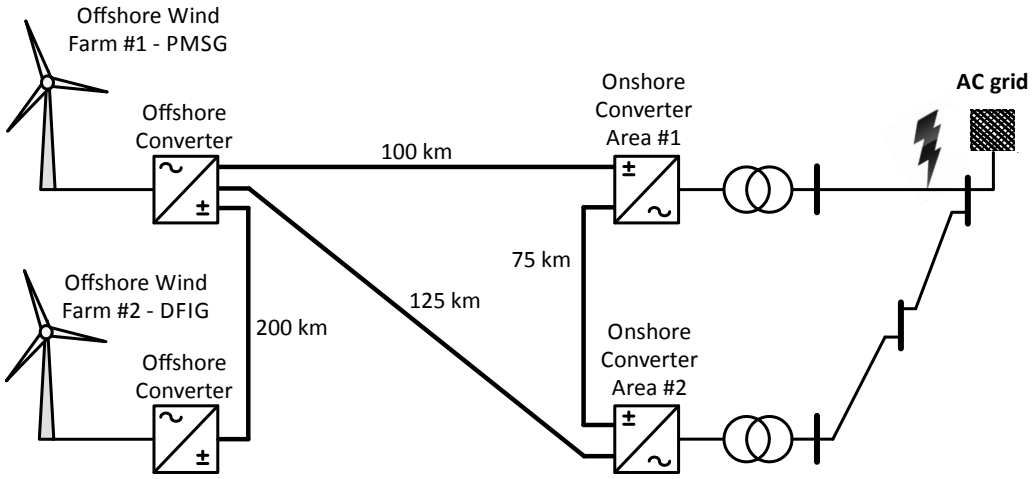

Figure 5.20: Meshed DC grid topology adopted for the FRT sensitivity analysis

offshore HVDC-VSC. The summary of the control approaches set in each offshore HVDC-VSC are presented in Table 5.1.

Table 5.1: FRT control setup for Configuration 1 and 2

	FRT control strategy at WF 1 (equipped with PMSG)	FRT control strategy at WF 2 (equipped with DFIG)
Configuration 1	AC voltage decrease proportional to the DC voltage increase	AC frequency increase proportional to the DC voltage increase
Configuration 2	AC frequency increase proportional to the DC voltage increase	AC voltage decrease proportional to the DC voltage increase

Configuration 1

The sensitivity tests based on the Configuration 1 setup were performed for two set of gains (combinations of $K_{DC/AC}$ and $K_{DC/f}$) . The gains values are presented on Table 5.2.

Where $K_{DC/AC}$ is the proportional gain for the DC voltage /AC offshore voltage control and $K_{DC/f}$ is the proportional gain adopted on the DC voltage /AC offshore frequency control. The rationale of changing the gain values aimed at creating di-

Table 5.2: DC voltage /AC offshore voltage ($K_{DC/AC}$) and DC voltage /AC offshore frequency control ($K_{DC/f}$) FRT control gain values for each analysed case

	WF ♯1	**WF ♯2**
	$K_{DC/AC}$ (pu volt/pu volt)	$K_{DC/f}$ (pu volt/ Hertz)
Case A	-2	5
Case B	-4	2.5

versity on the control parameters, allowing to evaluate the performance of the FRT control strategies as well as the DC grid performance during and aftermath the fault event. The results for these set of simulation are presented in Figure 5.21 and Figure 5.22.

The results depicted in Figure 5.21 show that the mainland AC-side voltage drop (resulting from the fault event) has been replicated at both offshore WF. As an AC voltage decrease in WF ♯1 and as an AC frequency increase in WF♯2. The combination of the applied control strategies for fast active power, successfully assures the DC grid voltage rise control achieved through active power injection reduction, as illustrated in Figure 5.22. The DC voltage was kept around 1.15 p.u. (below the maximum admissible value of 1.2 p.u.). In the same figure, it can also be observed that both onshore HVDC-VSC are affected by the reduction of the injected active power during the fault event. This fact is related with the configuration of the mainland AC grid. In fact, the fault event was set near the converter ♯1, leading to a higher AC voltage sag and consequently a higher reduction on injected active power. Additionally, in line to the control strategy set on offshore HVDC-VSC and at WT level, both offshore WF were able to reduce the injected active power during the fault event. Aftermath fault event, both WF recovers the pre-disturbance active power. However, the DFIG-based WF (♯2) WF presented a small overshoot response in comparison to the PMSG-based WF (♯1). As previously addressed, this fact is related to the DFIG natural response and the associated speed controller installed at the RSC-level.

The results for the Case B simulations are depicted on Figure 5.23 and Figure 5.24. In this case, the $K_{DC/AC}$ has doubled it value while $K_{DC/f}$ assumes the half in comparison to Case A, according to the gain values shown on Table 5.2.

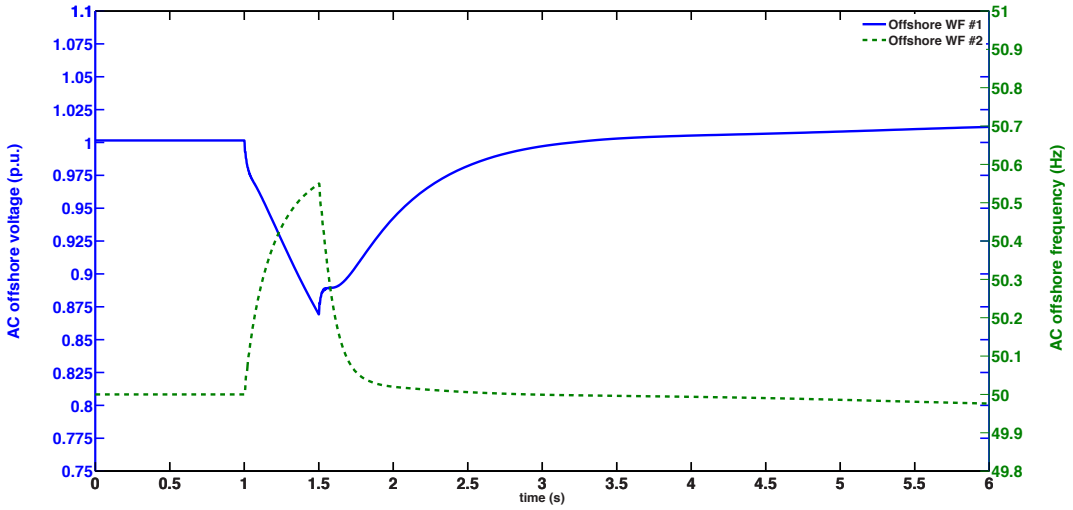

Figure 5.21: AC voltage and frequency on offshore WF ♯1 and ♯2 - Case A

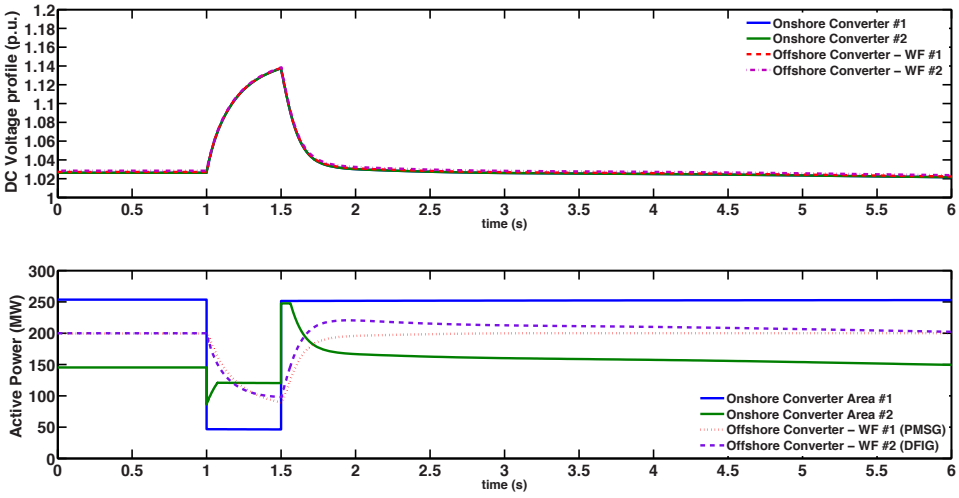

Figure 5.22: AC voltage and Active power on MTDC grid terminals - Case A

The offshore AC voltage profile at WF ♯1 and the offshore frequency at WF ♯2, are depicted on Figure 5.23.

A greater AC offshore voltage drop and a smaller AC offshore frequency increase have been verified, being consistent with the changes applied to the gain values. Additionally, the active power reduction (depicted in Figure 5.24) is consistent with this pattern being smaller at the WF ♯2 where the gain $K_{DC/f}$ has been reduced to

half and bigger ar the WF ♯1 where the gain $K_{DC/AC}$ has been increased to double.

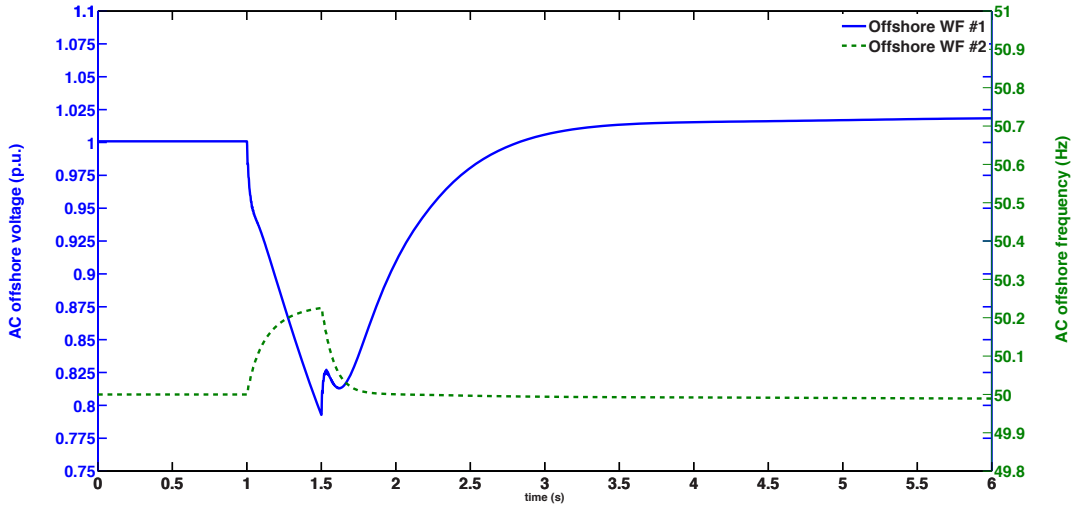

Figure 5.23: AC voltage and frequency on offshore WF ♯1 and ♯2 - Case B

The DC voltage profile and active power flow at the MTDC grid terminals are depicted in Figure 5.23. The DC voltage profile is kept below the maximum admissible value and it is smaller than the homologous achieved on Case A simulation (about 1.12 p.u. in contrast to 1.15 p.u. achieved for the Case A gains Configuration). Regarding the active power, as expected, the PMSG-based WF dissipates more active power due to the increased AC voltage reduction imposed on WF ♯1. In fact, the active power reduction at WF ♯1 almost reaches 100% during the fault event. Regarding the DFIG-based WF (WF ♯2) the active power reduction comes smaller due to the smaller frequency deviation defined by the applied control rule.

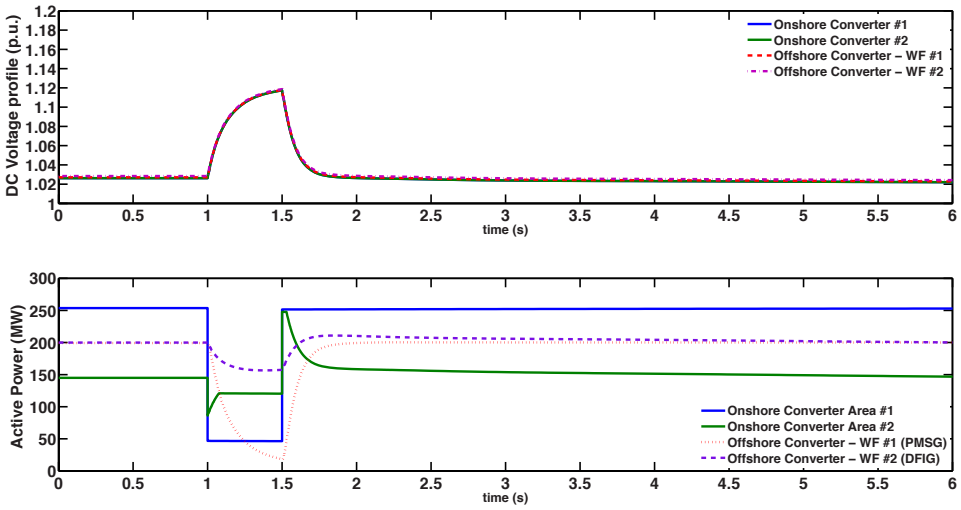

Figure 5.24: AC voltage and Active power on MTDC grid terminals - Case B

Configuration 2

In order to complement the simulations performed on Configuration 1, a new set of simulation named as Configuration 2 has been performed. In this set of simulations, the MTDC grid topology has been kept the same, being the layout illustrated on Figure 5.20. However, for this set of simulations, the WF ♯1, composed by PMSG, is set to participate in the FRT regulation strategy based on AC frequency increase proportional to the DC voltage increase ($K_{DC/f}$), while WF ♯2, fully composed by DFIG, is set with FRT control based on the offshore AC voltage decrease proportional to the DC grid voltage increase (through the adoption of $K_{DC/AC}$ gain). The sensitivity tests based on the Configuration 2 setup were performed for three set of gains through tree cases, Case A, Case B and case C. The gain values are presented on Table 5.3.

The rationale of these set of simulations consisted on evaluating the DFIG generator behaviour for three different $K_{DC/AC}$ gains, thus allowing to evaluate the response of the whole MTDC grid for different power reduction scenarios. It is important also to highlight stress analysis in terms of the current output at the offshore HVDC-VSC, which is equal to the total current output of the DFIG. Regarding the WF ♯1 control parameters, the $K_{DC/f}$ gain was kept constant, allowing to evaluate the impacts of the other WF on the DC grid operation. The results for these set of

Table 5.3: DC voltage /AC offshore voltage ($K_{DC/AC}$) and DC voltage /AC offshore frequency control ($K_{DC/f}$) FRT control gain values for cases A, B and C

	WF ♯1	**WF ♯2**
	$K_{DC/f}$ (pu volt/ Hertz)	$K_{DC/AC}$ (pu volt/pu volt)
Case A	7.5	-1.5
Case B	7.5	-3.0
Case C	7.5	-4.5

simulations are presented on Figure 5.25 and Figure 5.26.

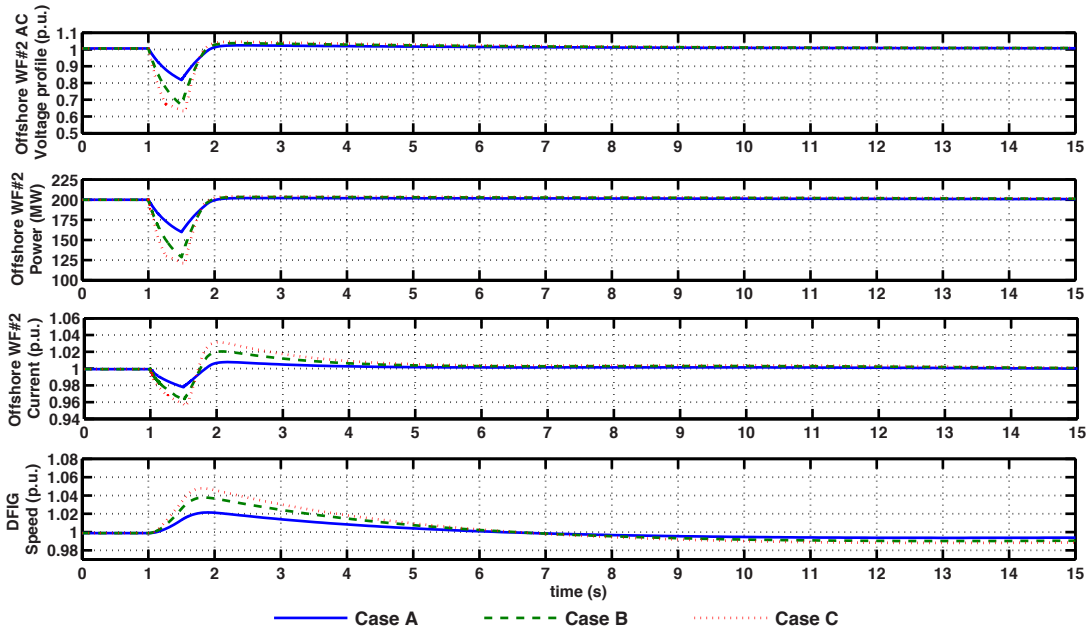

Figure 5.25: Main results for the DFIG-based WF - Case B

The most important results for the DFIG-equipped WF (offshore WF ♯2) are illustrated in Figure 5.25. According to the results, it is possible to observe that the adoption of different $K_{DC/AC}$ gains has a direct impact on the AC offshore WF ♯2 voltage profile. The highest the gain value (in absolute value), the highest is the AC voltage reduction. The AC voltage reduction has impact on the generated active power reduction, as well as the resulting DC voltage rise during the fault. Also in the same figure, it is depicted the current flow incoming to the associated offshore

HVDC-VSC since it has an associated maximum current limit. During the fault event, the injected current becomes slightly reduced while after fault clearance, a small current increase is observable. The current increase can be a crucial factor namely to the offshore HVDC-VSC. However, the over current magnitude (3% in the worst case) is smaller than the HVDC-VSC maximum current capability which was considered to be 10% greater than the nominal current. Finally, the same figure depicts the DFIG rotational speed and allows to observe that the active power reduction leads to a small generator speed increase which is controlled back to the nominal value after the fault clearance.

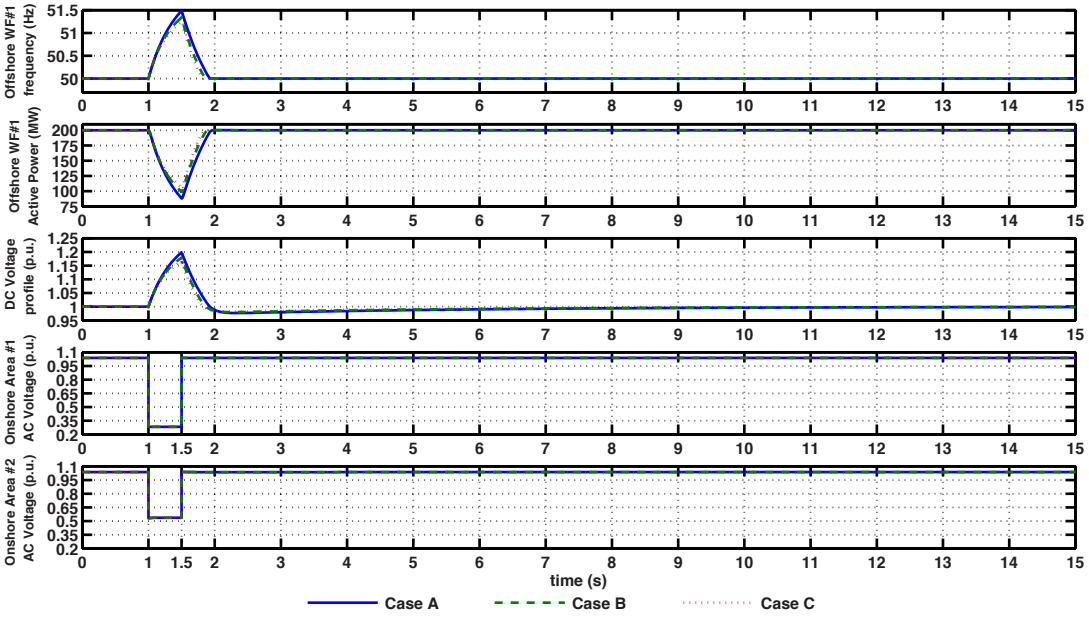

Figure 5.26: Main results for the PMSG-based WF and DC grid - Case B

The results depicted in Figure 5.26 illustrates the main results for the PMSG-based WF (WF ♯1) and for the MTDC grid. The frequency increase has been successfully achieved for the three simulation cases. Despite maintaining the $K_{DC/f}$ gain values, the frequency increase presented different magnitudes. This fact is related to the DC voltage at the associated MTDC grid terminal. According to the results depicted in the same figure, the DC voltage is different for each simulated case. The reason associated to that is related with the offshore WF power reduction during the fault event for each analysed case. For the Case A, the active power

reduction was smaller, thus leading to higher DC voltages. For the case C where the active power reduction was greater, the DC overvoltage becomes smaller. The aforementioned differences on the frequency deviation at the offshore WF ♯1 led to different active power reductions as illustrated in the same figure. Finally, the same figure illustrates the AC voltage profile at each onshore HVDC-VSC. It is observable that onshore Area ♯1 HVDC-VSC, the one electrically closer to the fault, suffers a higher AC voltage sag in comparison to the onshore Area ♯2 HVDC-VSC.

Performance of FRT Control Schemes in the Presence of Frequency Time Constant

The offshore grid frequency based control strategy for fast active power reduction at WT level may have a direct impact from the time constant associated to the frequency control loop. Thus, a set of simulation has been performed considering different time constant associated to the offshore frequency control loop to test the efficiency of the proposed fast DC voltage rise control based on AC offshore frequency control. The time constant has been modelled by a first order transfer function and the constant time, named as T_d has assumed three values, 25ms , 50 ms and 100 ms. The simulation tests were based on the MTDC grid test bench illustrated on the Figure 5.20 (WF ♯1 equipped with PMSG and WF ♯2 equipped with DFIG) being both offshore WF set to operate with frequency-based control (as function of the DC voltage) as the strategy for the DC voltage rise control during the provision of FRT functionality. The results achieved are depicted in Figure 5.27 and Figure 5.28.

From the DFIG result analysis (depicted on Figure 5.27), it is possible to verify that the introduction of the time constant does not have a significant impact on the WF operation during the DC voltage rise control and also after fault clearance. In fact the results for $t_d = 25ms$ and $t_d = 50ms$ are almost identical, being the main difference consisting on a small temporal shift. For $t_d = 100ms$, the same temporal shift tendency is observed. Additionally, a slight increase on AC frequency and generator speed is observed. These facts give origin to small decrease on the generated power and current.

Regarding the results related to the PMSG-based offshore WF and the DC grid, which results are illustrated in Figure 5.28, it is possible to verify that the previously

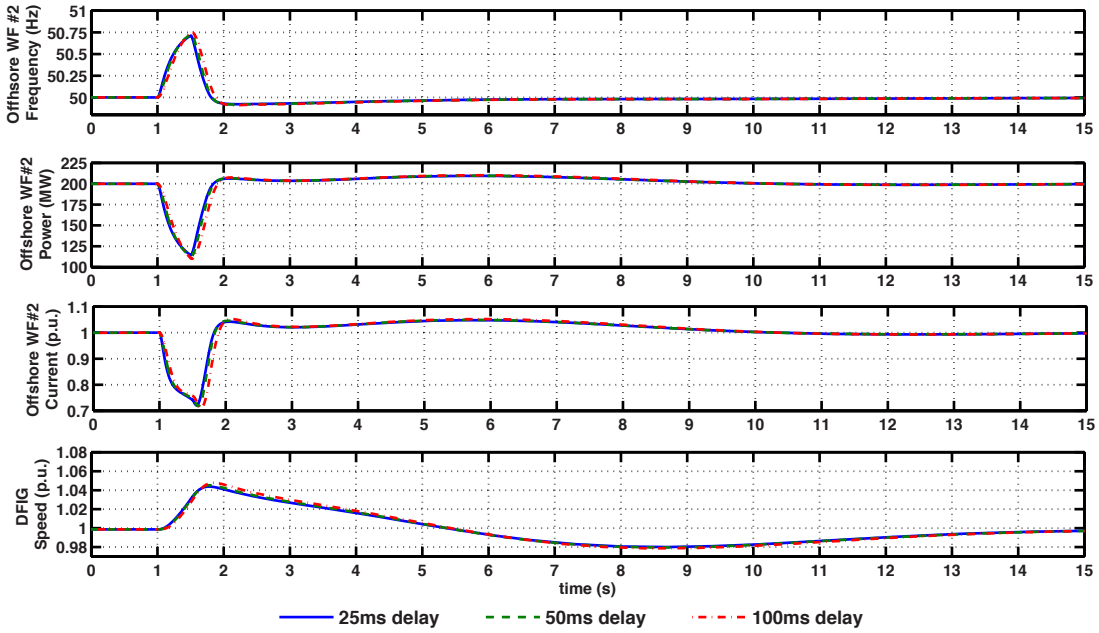

Figure 5.27: Main results for the DFIG-based WF - Frequency time constant presence

mentioned temporal shift is also observable as well as the small frequency increase at WF ♯1, which leads to smaller active power injection during the fault event. Regarding the DC voltage at the MTDC terminals, the inclusion of the time constant does not affect the DC voltage with temporal shifts, contrariwise the impact of time constant inclusion can be observed on the DC grid voltage which increases with the increase of time constant. For the specific case of $t_d = 100ms$, the DC voltage profile slightly overpasses the maximum admissible value of 1.2. p.u., indicating that higher time constant values may lead to the failure of the fast active power control mechanisms on maintaining the DC voltage below the maximum admissible value.

5.3.5 Operation of the DC Grids Following the Disconnection of an Onshore HVDC-VSC

This section aims at evaluating the performance of the DC grid facing the disconnection of an onshore HVDC-VSC and consequently loosing some active power evacuation capability. The control functionalities proposed in Section 4.6 were implemented at onshore and offshore HVDC-VSC as well as at WT level. Without

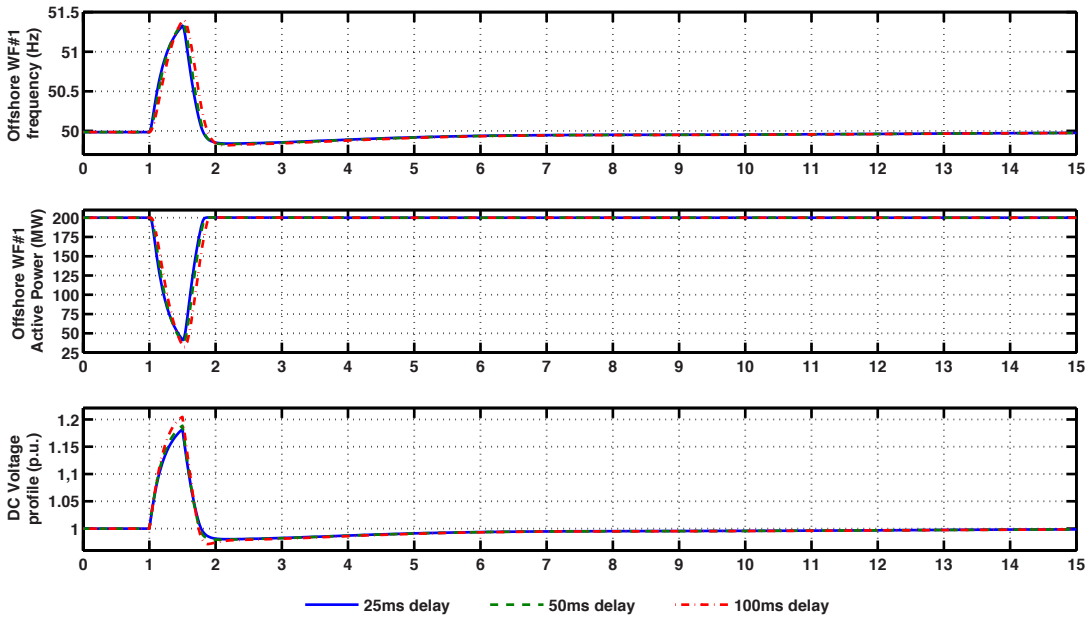

Figure 5.28: Main results for the PMSG-based WF and DC grid - Frequency time constant presence

lake of completeness, the offshore WF were equipped with PMSG generators with frequency response capabilities similar to the proposed in Section 4.6. However, the objective now consists on reducing active power injection proportionally to the offshore frequency increase. Nevertheless, the same controller is able to deal with positive and negative frequency deviations, giving origin to the correct pitch angle value to generate more or less power according to the frequency deviation.

The network topology chosen for this set of simulations was the previously presented H topology MTDC grid. The simulation consisted on the loss of the onshore Area ♯1 HVDC-VSC, as depicted in the Figure 5.29.

With the objective of evaluating the performance of power reduction mechanisms as a consequence of the DC voltage rise mitigation control, two set of simulations were performed. The first, named as Case A, consisted on the adoption of AC offshore frequency-dependent pitch control (identically to the approach implemented on Section **??**) and aimed at achieving the active power reduction based on the WT pitch angle increase (the opposite behaviour to the primary frequency control tests). The second approach, named as Case B, derives from the Case A plus the inclusion

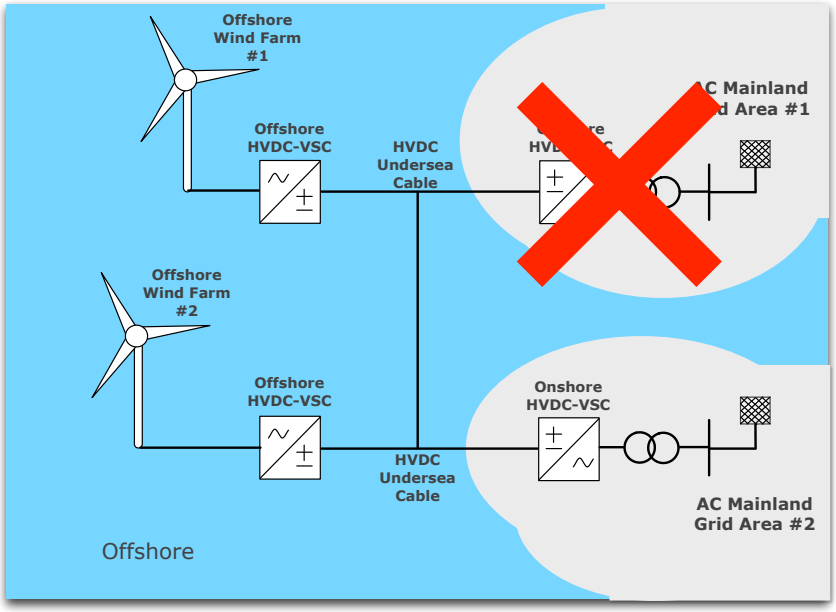

Figure 5.29: MTDC grid case used to simulate the loss of onshore HVDC-VSC

of chopper resistors at onshore HVDC-VSC DC terminals. The results for both cases are presented in Figure 5.30 Figure 5.31, Figure 5.32, Figure 5.33 and Figure 5.34.

The frequency variation at offshore WF has been achieved as illustrated on Figure 5.30. For the Case A, a highly oscillatory behaviour can be observed. For the Case B, the inclusion of onshore chopper resistors smooths the frequency variation response in the moments subsequent to the onshore HVDC-VSC disconnection.

The DC voltage profile results at the MTDC grid terminals are illustrated in the Figure 5.31. For the Case A, the high oscillatory behaviour is also present in the DC voltage response. The control strategy adopted on the Case A, does not cope with the requirements regarding the DC overvoltage magnitude. In fact, the maximum admissible DC voltage value of 1.2 p.u. is overpassed, reaching almost 1.3 p.u. The inability on quickly controlling the DC voltage rise with the Case A control approach is related to the intrinsic response time inherent to the WT blades' pitch angle adjustment time-constant.

For the Case B, the DC voltage rise does not overpasses the maximum admissible value (of 1.2 p.u.). Indeed, a smooth DC voltage behaviour is observed in the mo-

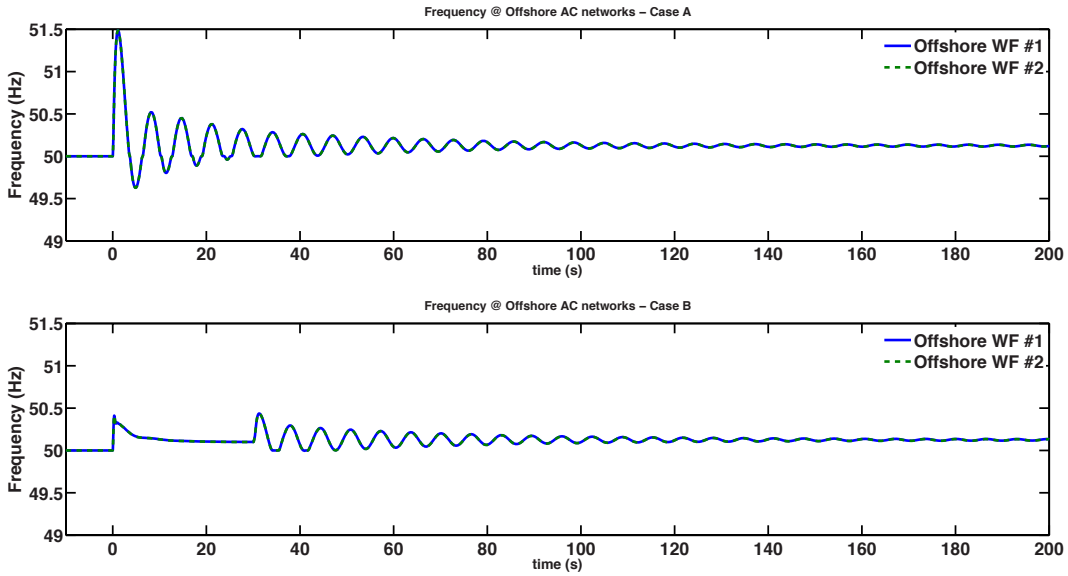

Figure 5.30: Offshore WF frequency after loss of onshore HVDC-VSC - Case A and Case B

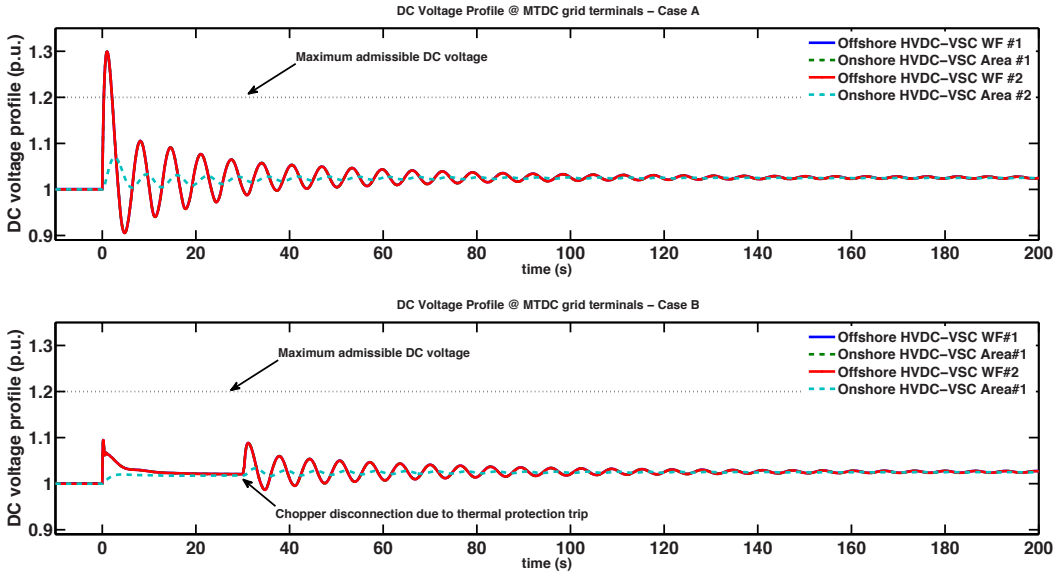

Figure 5.31: DC voltage profile at MTDC grid terminals after loss of onshore HVDC-VSC - Case A and Case B

ments subsequent to the onshore HVDC-VSC disconnection, followed by a small oscillatory response. The oscillatory response begins after the disconnection of the

DC choppers resistor. The chopper is disconnected since it is assumed that the maximum energy dissipation capacity has been achieved.

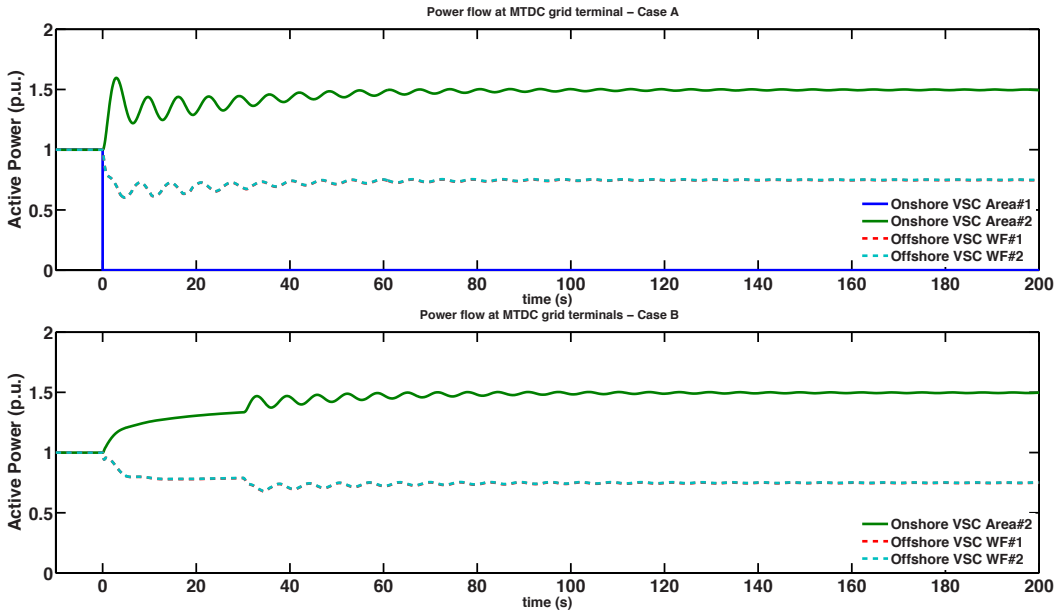

Figure 5.32: Active power flow at MTDC grid terminals after loss of onshore HVDC-VSC - Case A and Case B

The active power flow at each DC grid terminal has also been monitored and the results are depicted in Figure 5.32. From a comparative perspective, it is also noticeable in the powerflow behaviour, that the Case A approach leads to higher oscillatory behaviour in comparison to Case B. It is also possible to observe that the healthy onshore HVDC-VSC (Area ♯2), is able to deliver some of the non-delivered power due to the Area ♯1 onshore HVDC-VSC disconnection (about 50%). Since the Area ♯2 HVDC-VSC reaches it maximum power limit, the remaining non-delivered power does not have any additional pathway to be evacuated from the DC grid, thus, the offshore WF reduced their power injection towards the DC grid power equilibrium.

A detailed perspective of the active power generation at offshore WF for each analysed case are depicted in Figure 5.33. In the Case A, the offshore WF present

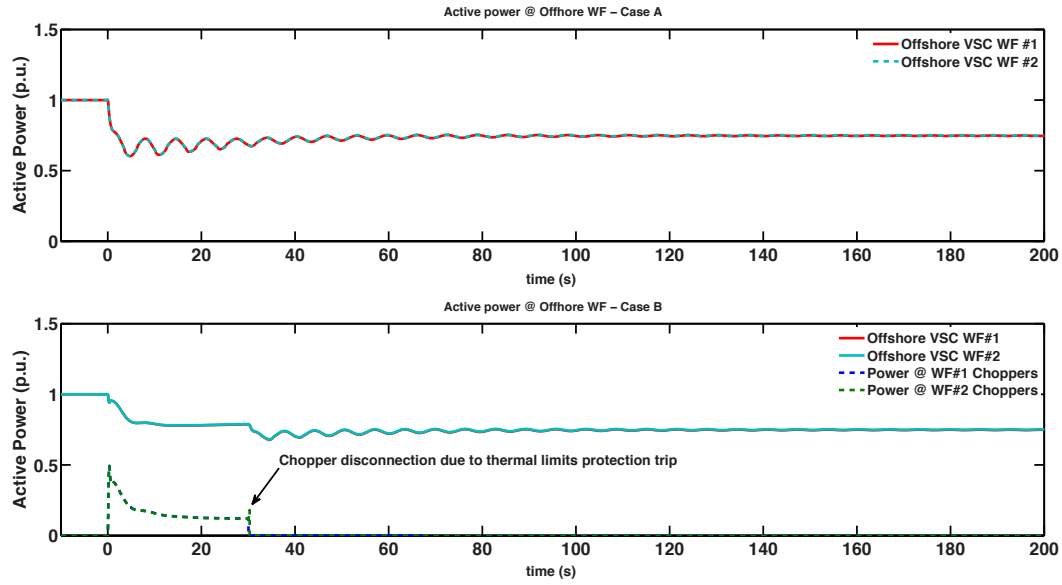

Figure 5.33: Active power at offshore WF-level after loss of onshore HVDC-VSC - Case A and Case B

a quick power reduction, followed by an oscillatory behaviour that leads to a constant active power generation value (new value for the offshore WF active power generation). For the Case B, the results show that the offshore WF does not have an abrupt active power reduction (in comparison to Case A). On contrary it slowly reduces the power injection towards a new (lower) value for the active power generation. In fact, the same figure shows that for the Case B, the chopper responds with a quicker power dissipation following the disconnection fo the onshore HVDC-VSC. However, with the time evolution, the chopper dissipation becomes reduced due to: (1) offshore WF active power reduction (on both WF) and (2) onshore Area ♯2 active power increase. Both reasons lead to a smaller DC voltage rise, requiring less active power dissipation at choppers.

Finally, WT blades' pitch angle position has also been monitored. The results are depicted in Figure 5.34. The aforementioned oscillatory behaviour is noticed for both cases with a larger emphasis on Case A. The adoption of pitch control approach for fast active power reduction does not produce satisfactory results regarding the DC voltage rise control. Additionally, from a mechanical point of view it is hardly

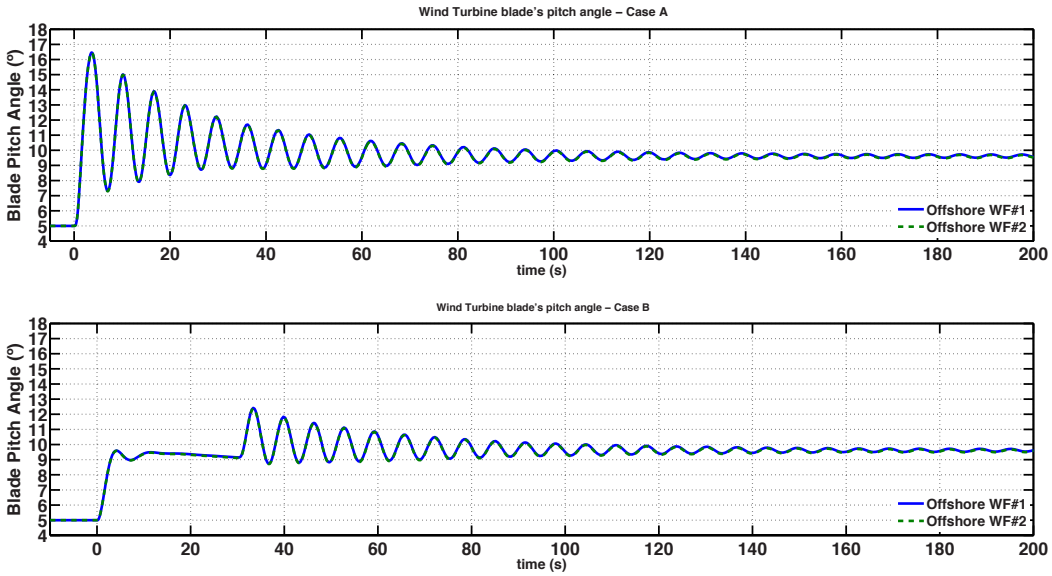

Figure 5.34: Offshore WF blades' pitch angle after loss of onshore HVDC-VSC - Case A and Case B

harmful for the WT components since it introduces a severe pitch angle rate-of-change on the moments subsequent to the onshore HVDC-VSC disconnection and a severe set of adjustment cycles towards the achievement of the optimal position. The introduction of chopper resistors perform as a buffer for whole MTDC system, including the WT pitch angle controller that benefices by presenting smaller rate-of-change as well as oscillations magnitude.

5.4 Summary

The set of simulations performed in this chapter allowed on assessing the performance and robustness of control strategies proposed in Chapter 4. Section 5.2 aimed at assessing and evaluating the performance of the proposed control schemes for providing primary frequency regulation, and inertia emulation. The results achieved demonstrated that the cascaded control scheme for primary frequency regulation allows MTDC grids with offshore WF to actively participate in this service exploiting a communication-free approach. Also, the proposed control scheme is able to achieve inter-AC mainland Area frequency support. This functionality is achieved

by the reduction of the active power injection towards the healthy Area mainland AC Areas and simultaneously channelling it toward the affected mainland AC Area.

The control schemes for DC voltage rise control during mainland AC fault events have also been evaluated. A introductory assessment has been performed, consisting on testing the control strategies proposed in Chapter 4. The capability of providing adequate DC voltage rise control for different WT technologies has been evaluated. The results shown that the fast active power reduction for DC voltage-rise mitigation can be successfully achieved by:

- The adoption of onshore chopper;
- The adoption of DC rise voltage control strategies for the fast reduction of offshore power injection.

Regarding the offshore-based DC voltage rise control, two strategies were tested considering the proposed control schemes:

- AC offshore voltage reduction based on the DC voltage rise;
- AC offshore frequency increase based on the DC voltage rise.

The offshore-based DC voltage rise mitigation control were tested with offshore WF composed by DFIG and PMSG wind turbines. Both control approaches were able to provide an effective active power reduction, guaranteeing a satisfactory DC voltage rise control for both adopted WT technologies.

Afterwards a set of simulation has also been performed to evaluate the robustness of the proposed control schemes under a scenarios. In order to include diversity in the analyses, in these scenarios were now considered a meshed topology DC grid. The evaluation of mixing the control schemes and offshore WT technologies were simultaneously evaluated. Additionally, sensitivity analysis tests have been performed, allowing to verify that the proposed control schemes are able to guarantee the DC voltage regulation during a mainland AC fault event for different DC grid topology, mixed WF technologies within a DC grid, different set of control parameters and even on the presence of moderate time constants associated to the control

deployment.

Finally, the operation of the DC grid after the sudden disconnection of an onshore HVDC-VSC has been investigated, resorting the control approach presented in Section 4.6. The assessment led on concluding that the pitch control mechanism is necessary to guarantee the long-term operation of the DC grid. However, presented to be ineffective on controlling the DC voltage on the moments subsequent to the onshore HVDC-VSC disconnection. The adoption of an hybrid control scheme, relying on choppers (for fast active power dissipation purpose) together with the WT pitch control (for permanent active power reduction), produced very satisfactory results, guaranteeing the DC voltage control as well as the permanent active power generation reduction.

6

Conclusions and Future Work

6.1 Final Remarks

During the last years, several plans for offshore grid development (particularly in Europe) have been under discussion as a result of the need to create conditions for the integration of large amounts of offshore wind power, providing additional transmission system security and building the adequate conditions for bulk power transmission in order to create a single European electricity market. From the system operation perspective, technical constraints justify the need for adopting High Voltage Direct Current (HVDC) technology with Voltage Source Converters (VSC) for offshore grid development rather than conventional AC connections. Additionally, reliability and flexibility of operation is pushing for the development of the MTDC grid concept, which is in line with the envisioned plans for the development of the pan-European Transmission System.

A fully operational MTDC grid can be regarded as a large (virtual) power plant with multiple injection points. Given the key role MTDC grids are expected to play in the future, their contribution for the provision of advanced services to TSO such as the participation on primary frequency regulation (including inertial emulation capabilities) and Fault Ride Through (FRT) capability in case of mainland AC grid faults is addressed in this Dissertation. The development of the necessary control functionalities for the provision of the referred services was then developed within

a communication-free framework. Both cost, reliability and security issues will preclude the development of a communication-based solution that should be able to process and communicate real-time information, regarding the core application oriented to frequency control purposes. Therefore, the development of local controllers (to be located at each onshore and offshore converter stations and at the WT level), was undertaken in order to implement at the MTDC grid level the ability to appropriately react to specific mainland AC grid disturbances.

In order to identify the most appropriate control strategies to provide the previously mentioned services from MTDC grids (including the offshore wind farms and the MTDC grid converter stations), it was required to understand of the main dynamic phenomena that characterize the behaviour of their main components (DC grid itself, converter stations and offshore WF), addressing thereafter the resulting interaction with mainland AC grids. Therefore, dynamic modelling of components and simulation tools development was of paramount importance in order to demonstrate the effectiveness of advanced control functionalities for the MTDC grid and to evaluate its impacts on mainland grids.

In mainland AC grids, system frequency is a natural indicator of the imbalance between load and generation and is the main variable used to design well-known control loops for power/frequency regulation. Being MTDC grids a key future development, it is also expected that they should be able to provide similar functionalities currently available in conventional generation units and also incorporated in the most recent onshore WF. Making use of simulation platform that was initially developed, innovative control solutions were conceived in order to enable offshore WF to participate in primary frequency regulation of the mainland AC grid (and also emulating inertial behaviour). As previously mentioned, an approach based on the development of local control schemes to be installed at HVDC-VSC was envisioned. The use of power electronic interfaces in the MTDC grid fully decouples offshore WF from onshore AC grid. Therefore, in order to enable offshore WF contributing to mainland grid AC frequency regulation services, it is necessary to explicitly transpose onshore AC grid frequency variations in a cascading control structure based on the following principles: at the onshore HVDC-VSC, the MTDC grid voltage is

controlled proportionally to the mainland grid frequency variations, while at the offshore converter level, the WF grid frequency is controlled proportionally to the DC grid voltage variations. Then, supplementary control loops can be applied at each turbine level, similarly to the solutions used for onshore wind turbine applications regarding their participation on frequency regulation services. This solution exploits the concept of WT de-load to provide a reserve margin at the WT level for its participation in primary frequency regulation. Exploiting the same control solution, inertial emulation is also possible to be achieved exploiting the fast control of WT power output proportionally to the offshore grid rate of change of frequency. The envisioned control scheme has been implemented over the developed simulation platform. The results show that offshore WF can actively participate on the primary frequency regulation following a load/generation disturbance located at mainland AC grid. The frequency-responsive control schemed housed at onshore HVDC-VSC is able to reproduce AC mainland frequency disturbances as proportional DC voltage variations which are spread over the DC grid. At the offshore-side, the offshore HVDC-VSC are able to reproduce a proportional AC offshore disturbance based on the DC voltage variations. Then, offshore WT with capability of performing primary frequency regulation, are able to deploy the previously de-load reserve margin. Additionally it was possible to verify that the design of the proposed control schemes are able to effectively promote inter AC mainland Area frequency support. For the analysed case, the onshore HVDC-VSC corresponding to the non-disturbed AC mainland area was able to reduce its power extraction (from the DC grid towards the associated AC mainland grid), creating the conditions for redirecting this power towards the onshore HVDC-VSC corresponding to the affected AC area.

The inertia emulation is a service that nowadays is included in some commercial WT or onshore application. The replication of this concept for the offshore WF has been also tested in this thesis. A simulation case based on the developed frequency regulation control scheme was adopted to assess the effectiveness of the provision. The results showed that an effective active power surplus was achieved at WT-level. Also, the power was correctly delivered to the affected AC mainland grid, contributing to the reduction of the onshore frequency rate of decay. In addition, it was verified that the developed control scheme is able to cope with fast phenomena such

as the provision of inertial response.

The investigation performed on the topic of FRT is of extreme importance for the reliable interconnection of a large amount of offshore wind power. As explained in the beginning of this thesis, large-scale undervoltage generation tripping could culminate in severe dynamic instability on the mainland AC systems. Despite HVDC-VSC technology having capability on remaining connected to the AC system during low voltage sags, the literature review enabled identifying a common challenge inherent to the deployment of this capability, such as the occurrence of DC voltage rise due to power mismatch in the DC grid.

The literature review puts in evidence that some authors assume the adoption of communication links for fast control within HVDC links. However, this solution may not comply with the restricted time-frame required to mitigate the DC voltage rise in case of mainland AC faults. Additionally, the specificity of MTDC grids increases the challenge for the implementation of communication networks for fast control actions. In general, a communication-based solution demands some coordination regarding the decision making process for the definition and assignment of power in-feed reductions in the MTDC nodes required to control the DC voltage rise. In this specific case, communication delays or failures may cause unacceptable DC overvoltages, precluding the successful implementation of FRT capability. To overcome the bottlenecks of communication-based solutions, a new control philosophy to assure FRT compliance in MTDC grids was identified and extensively tested thorough numerical simulation: the implementation of a decentralized control structure fully based on local controllers to be housed at HVDC-VSC stations and at the offshore wind turbines. The local control solutions aims at mitigating the DC voltage rise based on the fast control of wind turbine power output which is achieved through offshore grid voltage or frequency control strategies. The feasibility of the proposed control concepts are extensively demonstrated considering the most typical wind turbine technologies currently available: Doubly Fed Induction Generators (DFIG) and synchronous generators connected to the grid through a full converter.

Following the use of the proposed control strategies under different circumstances, it is also demonstrated that the reduction of active power injection can be achieve at offshore-level, avoiding the installation of additional equipment such

Table 6.1: Qualitative analysis of the fast power reduction control mechanism

	Onshore Dc chopper	Offshore Voltage based	Offshore Frequency based
"Distributed control approach"	NO	YES	YES
Estimated cost	HIGH	LOW	LOW
Control level required	LOW	HIGH	HIGH
Capability to deal with offshore AC faults	NO	YES	NO

as DC chopper resistors at onshore HVDC-VSC. To assess the performance of the DC voltage rise control strategies, a set of simulations were performed under varied characteristics such as: meshed DC grid, different set and combination of control parameters, mixing of different WT technologies (DFIG and PMSG). The results showed that the developed strategies were able to cope with the diversity induced in all the cases. The DC voltage rise has always been controlled through the active power injection reduction performed at offshore WF-level. Nevertheless, the fast characteristic inherent to the fulfilment of the DC voltage rise control, brings up the need of assessing the impacts of delays on the process of providing an effective DC voltage rise regulation. The tests conducted allowed to verify that for the specific case, the control schemes for offshore-located DC voltage rise control were able to avoid the DC voltage overpassing the maximum magnitude up to a time constant of 100 ms. It is then important to guarantee that for real-world implementation, the whole cascading control scheme has a sufficient response time below this critical value.

The aspects related to the operation of the DC grid following the disconnection of a onshore HVDC-VSC have also been addressed. In fact, the disconnection of an onshore HVDC-VSC is a situation that can occur due to an external condition such as a permanent fault in a AC mainland grid. From the stability perspective it is desirable that the DC grid and offshore WF remain operating as well as the non-affect AC mainland area remain connected to the DC grid, avoiding load/generation imbalance. However, it is necessary to guarantee that the proper conditions to operate the DC grid exist following to the disconnection of a onshore HVDC-VSC. From the

simulations performed, it has been verified that following the disconnection of an onshore HVDC-VSC, the loss of some power extraction capability culminates in a DC voltage rise phenomena. The proposed control strategies for FRT compliance are able to cope with this effect in the moments subsequent to the HVDC-VSC. However the disconnection of a converter may take longer than required given the expected duration of the fault event. Thus, a hybrid control scheme was implemented, comprising the functionalities of the DC voltage rise control for FRT capability with the primary frequency control through the WT pitch-angle adjustment. On the moment subsequent to the onshore HVDC-VSC, the fast DC voltage rise control is able to promote the DC power equilibrium. Simultaneously, but with a larger deployment time, the pitch-angle control is able to semi-permanently reduce the active power injection on the offshore WF, maintaining the generated power adequate to the DC grid capacity of delivery to mainland grid, mitigating the DC voltage rise.

As previously stated, the onshore HVDC-VSC can be disconnected due to fault events. These events can have their origin at AC or DC side. The control strategies developed in this theses intended to deal with onshore HVDC-VSC disconnection due to AC mainland side events. The DC-side fault was out of the scope of this thesis and would require a different approach from the modelling perspective.

6.2 Answering the Research Question

The research process of this thesis started with the objective of seeking for the answer of three research questions formulated at the beginning of the research process of this thesis and presented in Chapter 1. The research questions and respective answers are presented next.

- **RQ 1:** *What are the impacts on AC system dynamics from the integration of offshore wind power interconnected by MTDC grids?*
  From the literature review, it was ascertained that the integration of offshore wind power provided by means of HVDC technology (point-to-point or via DC grid) has the associated effect of decoupling among the AC-sides. The adoption of DC decouples the AC voltages and frequency. Consequently, the offshore WF, located several kilometres from the mainland grid are not able to directly

sense or detect mainland AC voltage or frequency variations. the literature proposes the adoption of communications or cascaded control schemes to be applied to point-to-point connections. However, no exploitation of the DC grid connections were found in the literature. Nonetheless, regarding the dynamic aspects of AC mainland grids with the presence of large amount of wind power connected through DC grids, this thesis anticipates problems related to: lack of primary frequency support, reduction of inertia, lack of capability to withstand to voltage sags and possible lack of capability to operate following the disconnection of an onshore HVDC-VSC. Thus, this inabilities may preclude the reduction of AC system stability margins.

- **RQ 2:** *Is there the possibility of allowing offshore WF (connected through a MTDC grid) on participating in AC primary frequency control in a communication-free framework?*

  Yes. The work performed in this thesis, related to the provision of primary frequency regulation culminates in the identification of a cascaded control scheme based on local controllers to be housed on the HVDC-VSC and offshore WT aiming at endowing the whole system with the characteristics for the provision of such services. The simulation results inherent to the deployment of these control scheme highlight that previously de-loaded offshore WF are able to contribute towards AC mainland grid frequency regulation, In addition, the interconnected AC area(s) are able to provide inter-AC area frequency support (through the DC grid infrastructure). The control scheme is then able to provide an effective contribution by mitigating problems overcoming from the adoption of the HVDC technology.

- **RQ 3:** *How can the DC voltage be controlled in a MTDC with offshore incoming wind power during a mainland AC grid fault event?*

  The literature reports the DC voltage rise as the major problem related to the capability of a DC link or grid on withstanding mainland AC-side voltage sags. The literature also reports that the DC voltage rise appearance is related to the loss of active power delivery at the onshore HVDC-VSC (associated to the faulted area) due to maximum current limitation. To overcome this effect,

an effective power equillibrium (re-dispatch, reduction or dissipation) must be promoted within the DC grid. This thesis has assessed the time for the effective deployment of the control having in consideration the studied base case and came up with a value of tens of miliseconds. Three communication-free control approaches were proposed being:

- Onshore-based DC voltage rise control;
- Offshore-based DC voltage rise control through AC offshore voltage control;
- Offshore-based DC voltage rise control through AC offshore frequency control.

As previously mentioned, the three DC voltage rise control approaches are able to cope with the requirements of fast power control, culminating in the avoidance of overpassing the maximum admissible value and guaranteeing the conditions for assuring the requirements for FRT capability.

6.3 Future Work

The work conducted in this thesis intended to research control schemes to allow offshore WF and the MTDC on actively participating in regulation services to the AC grid, mitigating the impacts that naturally arise from the adoption of HVDC technology.

Beyond the contributions brought by this thesis, additional developments over the MTDC grids and offshore WF control are required in order to improve its operation flexibility while providing additional services to the mainland AC grids. As a suggestion, some of the topics not tackled in this thesis but envisioned by its relevance, for a successful deployment of MTDC grids and offshore WF integration are:

- Contribution to Small Signal Stability damping from MTDC grids;
- Fault detection in DC grids;
- Fault elimination in DC grids - DC breakers;

- Active support to AC mainland grids black-start functionality from offshore WF and DC grid;
- Operation and voltage support during AC-side asymmetrical fault events.

Additionally, a next step in the continuation of the developed work consists on evaluating the performance of the proposed control schemes on a real environment through scaled models. In order to achieve this, a laboratory scaled MTDC grid model should be endowed with the control strategies proposed in this thesis. Some authors, mainly in Europe, have already published scientific papers presenting results from tests conducted on MTDC grid mock-up laboratory test facilities [85], [100]. In addition to the HVDC-VSC and the DC grid, it is also possible to enrich the simulation test-bed with scaled-size DFIG and PMSG and also Real-time Digital Simulators like RTDS [101] [102] or OPAL-RT [103], in a hardware-in-the-loop set-up, allowing interactions between the real measurements and the models programmed inside the simulator, in real-time. Recognizing that digital simulations provide invaluable knowledge regarding MTDC grid operation and control, the establishment of such test-bed is a key development regarding the need of a deeper understanding of the MTDC system operation and control as well as the need of providing demonstration facilities for such complex systems incorporating the developed advanced control mechanisms. Therefore, a reduced scale laboratory test rig may allow the demonstration of key finding developments such as frequency control functionalities, FRT functionality and the operation of the DC grid following the disconnection of an onshore HVDC-VSC.

Following the theoretical/conceptual background developments presented in this thesis, extensive laboratory tests should be performed in order to actively test and demonstrate the performance and effectiveness of the proposed architectures, control mechanisms and operation functionalities. This natural step, regarding the maturity of the concepts involved in this research, would enable the validation and tuning of proposed control philosophies. For these purposes the development of laboratory mock-up is essential, since it will be a key tool to demonstrate the envisioned MTDC system operation and provides the pilot conditions for future research activities concerning the pan-European electric power system.

References

[1] EREC Statistics, "http://www.erec.org/statistics". xxi, 1, 2

[2] EWEA, "Wind in power - 2011 european statistics", Tech. Rep., The European Wind Energy Association, 2012. xxi, 10, 11

[3] EWEA, "Wind energy factsheets", Tech. Rep., The European Wind Energy Association, 2010. xxi, 12

[4] D. Gautam, L. Goel, R. Ayyanar, V. Vittal, and T. Harbour, "Control strategy to mitigate the impact of reduced inertia due to doubly fed induction generators on large power systems", *Power Systems, IEEE Transactions on*, vol. 26, no. 1, pp. 214–224, 2011. xxi, 17, 18

[5] A.H. Kasem, E.F. El-Saadany, H.H. El-Tamaly, and M.A.A. Wahab, "An improved fault ride-through strategy for doubly fed induction generator-based wind turbines", *Renewable Power Generation, IET*, vol. 2, no. 4, pp. 201 –214, december 2008. xxi, 25, 26, 31

[6] Gil-Soo Jang Seong-Joo Lim Seok-Jin Lee Chan-Ki Kim, Vijay K. Sood, *HVDC Transmission: Power Conversion Applications in Power Systems*, vol. 1, John Wiley & Sons, 1 edition, April 2009, ISBN:978-0470822953. xxi, 34, 35, 41, 134

[7] "", "Clean power from deserts - the desertec concept for energy, water and climate security", Tech. Rep., Desertec Fundation, 2009. xxi, 38

[8] Oriol Gomis-Bellmunt, Jun Liang, Janaka Ekanayake, Rosemary King, and Nicholas Jenkins, "Topologies of multiterminal hvdc-vsc transmission for large offshore wind farms", *Electric Power Systems Research*, vol. 81, no. 2, pp. 271 – 281, 2011. xxi, 39, 40, 93

[9] N. Flourentzou, V.G. Agelidis, and G.D. Demetriades, "Vsc-based hvdc power transmission systems: An overview", *Power Electronics, IEEE Transactions on*, vol. 24, no. 3, pp. 592 –602, march 2009. xxii, 44, 45, 46, 48, 49

[10] Zhixin Miao, Lingling Fan, D. Osborn, and S. Yuvarajan, "Wind farms with hvdc delivery in inertial response and primary frequency control", *Energy Conversion, IEEE Transactions on*, vol. 25, no. 4, pp. 1171 –1178, dec. 2010. xxii, 51

[11] Rogerio G. Almeida, "Contributions for the evaluation of the double fed wind generators capability to provide ancillary services", Phd thesis, Faculty of Engineering of Porto University, 2006. xxii, xxiii, 74, 76, 77, 86, 120, 122

[12] Kundur. Prabha, *Power System Stability and Control*, McGraw-Hill, Inc., 1994. xxii, 20, 66, 82, 87, 90

[13] ENTSO-E, "Draft network code for requirements for grid connection applicable to all generators", Tech. Rep., European Network of Transmission System Operators for Electricity, 2012. xxvii, 121, 122

[14] European Commission, "Analysis of options beyond 20% ghg emission reductions:member state results", Tech. Rep., European Commission, 2012. 1

[15] European Commission, "A roadmap for moving to a competitive low carbon economy in 2050", Tech. Rep., European Commission, 2011. 1

[16] Commission of the European Communities, "Offshore wind energy: Action needed to deliver on the energy policy objectives for 2020 and beyond", Tech. Rep., European Commission, 2008. 3

[17] ENTSO-E, "Offshore grid development in the north seas entso-e views", Tech. Rep., European Network of Transmission System Operators for Electricity, 2011. 3

[18] John K. Kaldellis and D. Zafirakis, "The wind energy (r)evolution: A short review of a long history", *Renewable Energy*, vol. 36, no. 7, pp. 1887 – 1901, 2011. 9, 10

[19] Niels I. Meyer, "Danish wind power development", *Energy for Sustainable Development*, vol. 2, no. 1, pp. 18 – 25, 1995. 10

[20] Paul Gipe, "Wind energy comes of age california and denmark", *Energy Policy*, vol. 19, no. 8, pp. 756 – 767, 1991. 10

[21] "A strategy for competitive, sustainable and secure energy", Tech. Rep., European Comission, 2010. 13

[22] Ana Estanqueiro, Rui Castro, Pedro Flores, João Ricardo, Medeiros Pinto, Reis Rodrigues, and J. Peças Lopes, "How to prepare a power system for 15% wind energy penetration: the portuguese case study", *Wind Energy*, vol. 11, no. 1, pp. 75–84, 2008. 13

[23] G. Lalor, A. Mullane, and M. O'Malley, "Frequency control and wind turbine technologies", *Power Systems, IEEE Transactions on*, vol. 20, no. 4, pp. 1905 – 1913, nov. 2005. 13, 15, 123

[24] J.G. Slootweg and W.L. Kling, "The impact of large scale wind power generation on power system oscillations", *Electric Power Systems Research*, vol. 67, no. 1, pp. 9 – 20, 2003. 13

[25] Le-Ren Chang-Chien and Yao-Ching Yin, "Strategies for operating wind power in a similar manner of conventional power plant", *Energy Conversion, IEEE Transactions on*, vol. 24, no. 4, pp. 926 –934, dec. 2009. 13, 20

[26] M. Kayikci and J.V. Milanovic, "Dynamic contribution of dfig-based wind plants to system frequency disturbances", *Power Systems, IEEE Transactions on*, vol. 24, no. 2, pp. 859 –867, may 2009. 13, 31

[27] M.P. Palsson, T. Toftevaag, K. Uhlen, and J. O G Tande, "Large-scale wind power integration and voltage stability limits in regional networks", in *Power Engineering Society Summer Meeting, 2002 IEEE*, 2002, vol. 2, pp. 762–769 vol.2. 13

[28] D. Bryans L. Jenkins-N. O'Malley M. Watson R. Milborrow-D. Fox, B. Flynn, *Wind Power Integration: Connection and System Operational Aspects*, IET, 2007. 13

[29] G. Lalor, J. Ritchie, S. Rourke, D. Flynn, and M.J. O'Malley, "Dynamic frequency control with increasing wind generation", in *Power Engineering Society General Meeting, 2004. IEEE*, june 2004, pp. 1715 –1720 Vol.2. 14, 120

[30] N.R. Ullah, T. Thiringer, and D. Karlsson, "Temporary primary frequency control support by variable speed wind turbines – potential and applications", *Power Systems, IEEE Transactions on*, vol. 23, no. 2, pp. 601 –612, may 2008. 15, 20, 121

[31] J. Morren, S.W.H. de Haan, W.L. Kling, and J.A. Ferreira, "Wind turbines emulating inertia and supporting primary frequency control", *Power Systems, IEEE Transactions on*, vol. 21, no. 1, pp. 433 – 434, feb. 2006. 15, 19, 21

[32] YajvenderPal Verma and Ashwani Kumar, "Load frequency control in deregulated power system with wind integrated system using fuzzy controller", *Frontiers in Energy*, vol. 7, no. 2, pp. 245–254, 2013. 15

[33] J. Ekanayake and N. Jenkins, "Comparison of the response of doubly fed and fixed-speed induction generator wind turbines to changes in network frequency", *Energy Conversion, IEEE Transactions on*, vol. 19, no. 4, pp. 800–802, 2004. 15

[34] Ye Wang, G. Delille, H. Bayem, X. Guillaud, and B. Francois, "High wind power penetration in isolated power systems – assessment of wind inertial and primary frequency responses", *Power Systems, IEEE Transactions on*, vol. 28, no. 3, pp. 2412–2420, 2013. 15

[35] G. Diaz, P.G. Casielles, and C. Viescas, "Proposal for optimising the provision of inertial response reserve of variable-speed wind generators", *Renewable Power Generation, IET*, vol. 7, no. 3, pp. –, 2013. 15

[36] R.G. de Almeida and J.A.P. Lopes, "Participation of doubly fed induction wind generators in system frequency regulation", *Power Systems, IEEE Transactions on*, vol. 22, no. 3, pp. 944 –950, aug. 2007. 15, 17, 31, 120, 121

[37] N. Jenkins L. Holdsworth, J. B. Ekanayake, "Power system frequency response from fixed speed and doubly fed induction generator based wind turbines", *Wind Energy*, vol. 7, pp. 21–35, 2004. 16, 52

[38] S. El Itani and G. Joos, "Comparison of inertial response implementations in dfig-based wind turbines", in *Electrical and Computer Engineering (CCECE), 2011 24th Canadian Conference on*, 2011, pp. 000900–000903. 17

[39] Panayiotis Moutis, Stavros A. Papathanassiou, and Nikos D. Hatziargyriou, "Improved load-frequency control contribution of variable speed variable pitch wind generators", *Renewable Energy*, vol. 48, no. 0, pp. 514 – 523, 2012. 18

[40] N.A. Janssens, G. Lambin, and N. Bragard, "Active power control strategies of dfig wind turbines", in *Power Tech, 2007 IEEE Lausanne*, july 2007, pp. 516 –521. 18

[41] Ping-Kwan Keung, Pei Li, H. Banakar, and Boon Teck Ooi, "Kinetic energy of wind-turbine generators for system frequency support", *Power Systems, IEEE Transactions on*, vol. 24, no. 1, pp. 279 –287, feb. 2009. 21

[42] Portuguese Legistlation, "Ordinance n. 596/2010", 30^{th} July 2010. 22

[43] C. Wessels and F.W. Fuchs, "High voltage ride through with facts for dfig based wind turbines", in *Power Electronics and Applications, 2009. EPE '09. 13th European Conference on*, 2009, pp. 1–10. 24

[44] M. Fischer and M. Schellschmidt, "Fault ride through performance of wind energy converters with facts capabilities in response to up-to-date german grid connection requirements", in *Power Systems Conference and Exposition (PSCE), 2011 IEEE/PES*, 2011, pp. 1–6. 24

[45] C. Wessels, F. Gebhardt, and F.W. Fuchs, "Fault ride-through of a dfig wind turbine using a dynamic voltage restorer during symmetrical and asymmetrical

grid faults", *Power Electronics, IEEE Transactions on*, vol. 26, no. 3, pp. 807–815, 2011. 24

[46] J. Morren and S.W.H. de Haan, "Ridethrough of wind turbines with doubly-fed induction generator during a voltage dip", *Energy Conversion, IEEE Transactions on*, vol. 20, no. 2, pp. 435 – 441, june 2005. 24, 25

[47] S.M. Muyeen, R. Takahashi, T. Murata, and J. Tamura, "A variable speed wind turbine control strategy to meet wind farm grid code requirements", *Power Systems, IEEE Transactions on*, vol. 25, no. 1, pp. 331 –340, feb. 2010. 26, 27, 28, 79

[48] J.F. Conroy and R. Watson, "Low-voltage ride-through of a full converter wind turbine with permanent magnet generator", *Renewable Power Generation, IET*, vol. 1, no. 3, pp. 182 –189, september 2007. 27

[49] Siegfried Heier, *Grid Integration of Wind Energy Conversion Systems*, Wiley, 2nd edition, April 2006, ISBN: 978-0-470-86899-7. 28

[50] N. Amutha and B. Kalyan Kumar, "Improving fault ride-through capability of wind generation system using dvr", *International Journal of Electrical Power & Energy Systems*, vol. 46, no. 0, pp. 326 – 333, 2013. 28

[51] F. Blaabjerg, F. Iov, T. Terekes, R. Teodorescu, and K. Ma, "Power electronics - key technology for renewable energy systems", in *Power Electronics, Drive Systems and Technologies Conference (PEDSTC), 2011 2nd*, feb. 2011, pp. 445 –466. 29, 30

[52] F. O. Resende and J.A. Peas Lopes, "Evaluating the performance of external fault ride-through solutions used in wind farms with fixed speed induction generators when facing unbalanced faults", in *PowerTech, 2009 IEEE Bucharest*, 2009, pp. 1–6. 30

[53] Fujin Deng and Zhe Chen, "An offshore wind farm with dc grid connection and its performance under power system transients", in *Power and Energy Society General Meeting, 2011 IEEE*, july 2011, pp. 1 –8. 36

[54] K. Bell, D. Cirio, A.M. Denis, L. He, C.C. Liu, G. Migliavacca, C. Moreira, and P. Panciatici, "Economic and technical criteria for designing future offshore hvdc grids", in *Innovative Smart Grid Technologies Conference Europe (ISGT Europe), 2010 IEEE PES*, oct. 2010, pp. 1 –8. 36

[55] N.M. Kirby, Lie Xu, M. Luckett, and W. Siepmann, "Hvdc transmission for large offshore wind farms", *Power Engineering Journal*, vol. 16, no. 3, pp. 135 –141, june 2002. 36

[56] The Crown State, "Offshore wind cost reduction - pathways study", Tech. Rep., The Crown State, 2012. 36

[57] N.M. Macleod, S. Chackravorty, and B.T. Barrett, "Design studies for the 3150 mw, 600 kv uhvdc bipole 2 of the rio madeira long distance transmission project in brazil", in *Cigr*, 2010. 36

[58] A. Kumar, M. Lagerkvist, M. Eklund, and Y QingYun, "Three gorges - changzhou hvdc : Ready to bring bulk power to eas", in *The 4th International Conference on Power Transmission & Distribution Technology*, 2003. 36

[59] Patrik Buijs, David Bekaert, Stijn Cole, Dirk Van Hertem, and Ronnie Belmans, "Transmission investment problems in europe: Going beyond standard solutions", *Energy Policy*, vol. 39, no. 3, pp. 1794 – 1801, 2011. 36

[60] H. Weber, "Topology and control of overlay grids using dc transmission", Tech. Rep., Steinbeis GmbH & Co. KG fr Technologietransfer, 2012. 36, 37

[61] H. Ergun, J. Beerten, and D. Van Hertem, "Building a new overlay grid for europe", in *Power and Energy Society General Meeting, 2012 IEEE*, 2012, pp. 1–8. 37

[62] Dirk Van Hertem and Mehrdad Ghandhari, "Multi-terminal {VSC} {HVDC} for the european supergrid: Obstacles", *Renewable and Sustainable Energy Reviews*, vol. 14, no. 9, pp. 3156 – 3163, 2010. 37

[63] J. Decker and P. Kreutzkamp, "Offshore electricity grid infrastructure in europe - a techno-economic assessment", Tech. Rep., 3E (coordinator), dena, EWEA, ForWind, IEO, NTUA, Senergy, SINTEF, 2011. 37

[64] P. Lundberg, M. Callavik, M. Bahrman, and P. Sandeberg, "Platforms for change: High-voltage dc converters and cable technologies for offshore renewable integration and dc grid expansions", *Power and Energy Magazine, IEEE*, vol. 10, no. 6, pp. 30 –38, nov. 2012. 38, 39

[65] "", "Integrating wind - developing europes power market for the large-scale integration of wind power", Tech. Rep., TradeWind European Project, 2009. 40

[66] The North Seas Countries Offshore Grid Initiative, "Working group 1 grid configuration the north seas countries offshore grid initiative - initial findings", Tech. Rep., Benelux, 2012. 40, 41

[67] Oriol Gomis-Bellmunt, Jun Liang, Janaka Ekanayake, and Nicholas Jenkins, "Voltage current characteristics of multiterminal hvdc-vsc for offshore wind farms", *Electric Power Systems Research*, vol. 81, no. 2, pp. 440 – 450, 2011. 42, 67, 93, 94

[68] C. Meyer, M. Hoing, A. Peterson, and R.W. De Doncker, "Control and design of dc grids for offshore wind farms", *Industry Applications, IEEE Transactions on*, vol. 43, no. 6, pp. 1475 –1482, nov.-dec. 2007. 42

[69] K. Friedrich, "Modern hvdc plus application of vsc in modular multilevel converter topology", in *Industrial Electronics (ISIE), 2010 IEEE International Symposium on*, july 2010, pp. 3807 –3810. 42

[70] G. Asplund, "Application of hvdc light to power system enhancement", in *Power Engineering Society Winter Meeting, 2000. IEEE*, 2000, vol. 4, pp. 2498–2503 vol.4. 42

[71] B.R. Andersen, L. Xu, P.J. Horton, and P. Cartwright, "Topologies for vsc transmission", *Power Engineering Journal*, vol. 16, no. 3, pp. 142 –150, june 2002. 43, 44, 45, 47

[72] Risheng Li, S. Bozhko, and G. Asher, "Frequency control design for offshore wind farm grid with lcc-hvdc link connection", *Power Electronics, IEEE Transactions on*, vol. 23, no. 3, pp. 1085 –1092, may 2008. 50, 51

[73] Yao. L.-Ran. L. Li.R., Bozhko. S.V.. Asher. G.M., "Offshore grid frequency control design for line-commutated converters high-voltage direct-current link connected wind farms", *IET Renewable Power Generation*, vol. 1, 2007. 52

[74] Sanjay K Chaudhary, *Control and Protection of Wind Power Plants with VSC-HVDC Connection*, PhD thesis, The Faculty of Engineering, Science, and Medicine, Aalborg University, 2011. 52

[75] N. R. Chaudhuri, R. Majumder, and B. Chaudhuri, "System frequency support through multi-terminal dc (mtdc) grids", *Power Systems, IEEE Transactions on*, vol. PP, no. 99, pp. 1, 2012. 53

[76] J. Zhu, C.D. Booth, G.P. Adam, A.J. Roscoe, and C.G. Bright, "Inertia emulation control strategy for vsc-hvdc transmission systems", *Power Systems, IEEE Transactions on*, vol. 28, no. 2, pp. 1277–1287, 2013. 54

[77] O. Gomis-Bellmunt, A. Junyent-Ferre, A. Sumper, and J. Bergas-Jane, "Control of a wind farm based on synchronous generators with a central hvdc-vsc converter", *Power Systems, IEEE Transactions on*, vol. 26, no. 3, pp. 1632–1640, 2011. 54

[78] F. Deng and Zhe Chen, "Operation and control of a dc-grid offshore wind farm under dc transmission system faults", *Power Delivery, IEEE Transactions on*, vol. 28, no. 3, pp. 1356–1363, 2013. 54

[79] G. Ramtharan, A. Arulampalam, J.B. Ekanayake, F.M. Hughes, and N. Jenkins, "Fault ride through of fully rated converter wind turbines with ac and dc transmission", *Renewable Power Generation, IET*, vol. 3, no. 4, pp. 426 –438, december 2009. 54, 57, 134, 135, 136, 137

[80] C. Feltes, H. Wrede, F.W. Koch, and I. Erlich, "Enhanced fault ride-through method for wind farms connected to the grid through vsc-based hvdc transmission", *Power Systems, IEEE Transactions on*, vol. 24, no. 3, pp. 1537 –1546, aug. 2009. 56, 64, 67, 136, 137

[81] T.D. Vrionis, X.I. Koutiva, N.A. Vovos, and G.B. Giannakopoulos, "Control of an hvdc link connecting a wind farm to the grid for fault ride-through enhancement", *Power Systems, IEEE Transactions on*, vol. 22, no. 4, pp. 2039 –2047, nov. 2007. 57

[82] Weixing Lu and Boon-Teck Ooi, "Dc overvoltage control during loss of converter in multiterminal voltage-source converter-based hvdc (m-vsc-hvdc)", *Power Delivery, IEEE Transactions on*, vol. 18, no. 3, pp. 915 – 920, july 2003. 59

[83] Federico Milano, *Power System Modelling and Scripting*, Springer, 2010. 65

[84] Jef Beerten and Ronnie Belmans, "Modeling and control of multi-terminal vsc hvdc systems", *Energy Procedia*, vol. 24, no. 0, pp. 123 – 130, 2012, ¡ce:title¿Selected papers from Deep Sea Offshore Wind R&D Conference, Trondheim, Norway, 19-20 January 2012¡/ce:title¿. 66

[85] Jun Liang, Tianjun Jing, O. Gomis-Bellmunt, J. Ekanayake, and N. Jenkins, "Operation and control of multiterminal hvdc transmission for offshore wind farms", *Power Delivery, IEEE Transactions on*, vol. 26, no. 4, pp. 2596–2604, 2011. 66, 67, 69, 93, 94, 201

[86] Carlos Coelho Leal Moreira, *Identification and Development of Microgrids Emergency Control Procedures*, PhD thesis, Faculty of Engineering of University of Porto, 2008. 66

[87] S. Cole, J. Beerten, and R. Belmans, "Generalized dynamic vsc mtdc model for power system stability studies", *Power Systems, IEEE Transactions on*, vol. 25, no. 3, pp. 1655 –1662, aug. 2010. 71

[88] Enercon, "Enercon product overview", Tech. Rep., Enercon-Gmbh. 75

[89] Van-Tung Phan and Hong-Hee Lee, "Performance enhancement of stand-alone dfig systems with control of rotor and load side converters using resonant controllers", *Industry Applications, IEEE Transactions on*, vol. 48, no. 1, pp. 199–210, 2012. 83

[90] S.K. Salman and A. L J Teo, "Windmill modeling consideration and factors influencing the stability of a grid-connected wind power-based embedded generator", *Power Systems, IEEE Transactions on*, vol. 18, no. 2, pp. 793–802, 2003. 83, 84

[91] E. Rezaei, A. Tabesh, and M. Ebrahimi, "Dynamic model and control of dfig wind energy systems based on power transfer matrix", *Power Delivery, IEEE Transactions on*, vol. 27, no. 3, pp. 1485–1493, 2012. 83

[92] ENTSO-E, "Entso-e operation handbook", Tech. Rep., European Network of Transmission System Operators for Electricity, 2004. 119

[93] K. Samarakoon, J. Ekanayake, and N. Jenkins, "Investigation of domestic load control to provide primary frequency response using smart meters", *Smart Grid, IEEE Transactions on*, vol. 3, no. 1, pp. 282–292, 2012. 119

[94] A. Molina-Garcia, F. Bouffard, and D.S. Kirschen, "Decentralized demand-side contribution to primary frequency control", *Power Systems, IEEE Transactions on*, vol. 26, no. 1, pp. 411–419, 2011. 119

[95] M. El Mokadem, V. Courtecuisse, C. Saudemont, B. Robyns, and J. Deuse, "Experimental study of variable speed wind generator contribution to primary frequency control", *Renewable Energy*, vol. 34, no. 3, pp. 833 – 844, 2009. 120

[96] I. Erlich and M. Wilch, "Primary frequency control by wind turbines", in *Power and Energy Society General Meeting, 2010 IEEE*, 2010, pp. 1–8. 121

[97] Jing Dai, Y. Phulpin, A. Sarlette, and D. Ernst, "Impact of delays on a consensus-based primary frequency control scheme for ac systems connected by a multi-terminal hvdc grid", in *Bulk Power System Dynamics and Control (iREP) - VIII (iREP), 2010 iREP Symposium*, 2010, pp. 1–9. 123

[98] Allen-Bradley, "Powerflex dynamic braking resistor calculator", Tech. Rep., Allen-Bradley. Rockwell Software, 2011. 136

[99] Lihui Yang, Zhao Xu, J. Ostergaard, Zhao Yang Dong, and Kit Po Wong, "Advanced control strategy of dfig wind turbines for power system fault ride

through", *Power Systems, IEEE Transactions on*, vol. 27, no. 2, pp. 713–722, 2012. 143

[100] A. Egea-Alvarez, F. Bianchi, A. Junyent-Ferre, G. Gross, and O. Gomis-Bellmunt, "Voltage control of multiterminal vsc-hvdc transmission systems for offshore wind power plants: Design and implementation in a scaled platform", *Industrial Electronics, IEEE Transactions on*, vol. 60, no. 6, pp. 2381–2391, 2013. 201

[101] Zhang Jian, Xue Ancheng, Chen Jinmei, Bi Tianshu, Wang Ningbo, and Ma Yanhong, "An adaptive lvrt control for dfig wind power system", in *Control Conference (CCC), 2012 31st Chinese*, 2012, pp. 6747–6751. 201

[102] Chulsang Hwang, Gyeong-Hun Kim, Namwon Kim, Sang-Yong Kim, Hyo-Guen Lee, Hyo-Rong Seo, Minwon Park, In-Keun Yu, Jung-Do Park, Dong-Young Yi, and Sangjin Lee, "Controller-hardware-in-the loop simulation-based transient analysis of pmsg type wind power generation system", in *Electrical Machines and Systems (ICEMS), 2010 International Conference on*, 2010, pp. 669–673. 201

[103] J.-N. Paquin, J. Moyen, G. Dumur, and V. Lapointe, "Real-time and off-line simulation of a detailed wind farm model connected to a multi-bus network", in *Electrical Power Conference, 2007. EPC 2007. IEEE Canada*, 2007, pp. 145–152. 201

Appendix A

Parameters of the MTDC Grid model

This appendix present the set of parameter adopted in the MTDC model introduced in Chapter 3.

The AC synchronous generator data are available on Table A.1.

Table A.1: Synchronous Generator data

Synchronous Generator	
Apparent Power (S)	5000 MVA
Inertia (H)	10 s
Xd	2.040 (p.u. machine base)
X'd	0.266 (p.u. machine base)
X"d	0.193 (p.u. machine base)
Xq	1.960 (p.u. machine base)
X'q	0.262 (p.u. machine base)
X"q	0.193 (p.u. machine base)
Xs	0.192 (p.u. machine base)

The data of the turbine governor associated to the synchronous generator are expresses on Table A.2.

The PMSG Wind Turbine data are presented on Table A.3.

The HVDC-VSC data are presented on Table A.4.

Table A.2: Turbine Governor data

Turbine Governor	
Droop	0.05 Hz (Hz(p.u.)/V(p.u))
Time Constant (T)	1.5 s

Table A.3: PMSG Wind Turbine data

Wind Turbine (with PMSG)	
Rated Power (Prat)	2.5 MW
Nominal Voltage (V)	690
Rotor radius	42 m
Inertia (J)	$3 \times 10^6 (\text{kg}.m^2)$
Rotation speed (wn)	16 rpm
Ld	0.0016 (H)
Lq	0.0011 (H)

Table A.4: HVDC-VSC data

Onshore HVDC-VSC	
Operating Voltage	±150 kV
Maximum Power	250 MVA
Droop K_{pv}	0.05 (MW(p.u.)/V(p.u.))
Droop K_{fv}	0.1 (Hz(p.u.)/V(p.u))
Offshore HVDC-VSC	
Operating Voltage	±150 kV
Maximum Power	250 MVA
Droop K_f	0.2 (V(p.u.)/Hz(p.u.))

The DC grid parameters are presented on Table A.5.

The DFIG Wind Turbine data are presented on Table A.6.

Table A.5: DC grid parameters

DC grid parameters	
DC Cable Resistance	0.0139 Ω/km
DC Cable Inductance	0.159 mH/Km
DC Cable Capacitance	0.231 $\mu F/km$
HVDC-VSC capacitor bank	75 $\mu F/pole$

Table A.6: DFIG Wind Turbine data

Wind Turbine (with DFIG)	
Rated Power (Prat)	2.0 MW
Nominal Voltage (V)	690 V
Rotor radius	42 m
Inertia (H_t)	3.5s
Rotation speed (wn)	1650 rpm
Rs	0.00706 p.u.
Rr	0.005 p.u.
Ls	0.171 p.u.
Lr	0.516 p.u.
Lm	3.5 p.u.